

ISSN 1916-9671(Print)
ISSN 1916-968X(Online)

INTERNATIONAL JOURNAL OF BIOLOGY

Vol. 1, No. 2
July 2009



Canadian Center of Science and Education

Editorial Board

Abdul Khaliq Naveed	National University of Science & Technology, Pakistan
Amara Naksathit	Mahidol University, Thailand
Anne Brown	Canadian Center of Science and Education, Canada
Billy Sinclair	University of Cumbria, UK
Da Jia	UT Southwestern, USA
Florent Engelmann	Institut de Recherche pour le Développement, France
Ignacy Kitowski	Maria Curie-Sklodowska University, Poland
Mark Andrew Skidmore	The University of Liverpool, UK
Mike Gormally	National University of Ireland, Ireland
Mike Watson	University of Southern Queensland, Australia
Muhammad Ishtiaq	University of Azad Jammu & Kashmir, Pakistan
Naowarat Cheeptham	Thompson Rivers University, Canada
Nikolas Zagris	University of Patras, Greece
Olga Kukal	Queen's University, Canada
Olga Pantos	University of Queensland, Australia
Paramita Basu	Indian Institute of Technology Kanpur, India
Patrick Marcel Schaeffer	James Cook University, Australia
Peer Schenk	The University of Queensland, Australia
Risto Penttinen	University of Turku, Finland
S Craig Roberts	University of Liverpool, UK
Salil Kumar Bose	Nanyang Technological University, Singapore
Shree R. Singh	National Cancer Institute, USA
Stuart Craig Smith	Deakin University, Australia
Zaini Mohd Zain	University Technology MARA, Malaysia



Contents

Philippine Panay Island Bushy-tailed Cloud Rat (<i>Crateromys heaneyi</i>): A Preliminary Behavioural Study of Captive Cloud Rats <i>Root-Gutteridge, H.A.J. & Chatterjee, H.J.</i>	3
Purification and Characterization of Cold-Adapted Metalloprotease from Deep Sea Water Lactic Acid Bacteria <i>Enterococcus Faecalis</i> TN-9 <i>Qingzhu Yuan, Atsushi Hayashi, Yoshihisa Kitamura, Takashi Shimada, Ren Na & Xiao Jin</i>	12
Model Stability Analysis of Marine Ecosystem <i>Yuejian Jie & Yuan Yuan</i>	22
Preliminary Study on Mitochondrial DNA Cytochrome <i>B</i> Sequences and Genetic Relationship of Three Asian Arowana <i>Scleropages Formosus</i> <i>Yinchang Hu, Xidong Mu, Xuejie Wang, Chao Liu, Peixin Wang & Jianren Luo</i>	28
Genetic Variation of Six <i>Azadirachta excelsa</i> (Jacks) Jacobs Populations <i>Hazandy Abdul-Hamid</i>	33
Investigation and Application Progress of Vero Cell Serum-free Culture <i>Tian Chen & Keping Chen</i>	41
Purification and Characterization of the Lipase from Marine <i>Vibrio fischeri</i> <i>P. Ranjitha, E. S. Karthy & A. Mohankumar</i>	48
Cloning and Analysis of DNA Sequence of Gene <i>CylA</i> of Enterococci Inducing Sheeps Encephalitis <i>Guijun Ma, Sujuan Han, Genqiang Yan & Xia Zhou</i>	57
Biology of <i>Macrolophus caliginosus</i> (Heteroptera: Miridae) Predator of <i>Trialeurodes vaporariorum</i> (Homoptera: Aleyrodidae) <i>Mohd Rasdi, Z., Fauziah, I., Wan Mohamad, W.A.K, Syed Abdul Rahman, S.R, Che Salmah, M.R. & Kamaruzaman, J.</i>	63
Molecular Cloning and Characterization of a Putative <i>BnHEC3</i> Gene in Oilseed Rape (<i>Brassica Napus</i>) <i>Xiaoli Tan, Lili Zhang & Zongwei Xia</i>	71
A New Species of <i>Aspergillus</i> <i>Zongzhou Zhang</i>	78
Transcription and Expression of Major VP Gene of <i>Bombyx Mori</i> Parvo-like Virus <i>Jinsong Cheng, Qin Yao, Meng Lv, Chen Sun, Yuanqing He & Keping Chen</i>	81
Effects of Waterlogging on Growth and Physiology of <i>Hopea odorata</i> Roxb <i>Hazandy Abdul-Hamid, Nor Aini Ab. Shukor, Sapari Mat, Abdul Latib Senin & Kamaruzaman Jusoff</i>	87
Preliminary Study on the Mechanism for Adaptation of <i>Stipagrostis Pennata</i> to Desert <i>Baohua Gong, Jianbo Zhu, Hongying Zhao & Yuxing Zhang</i>	94
Isolation and Characterization of a Silkworm cDNA Encoding a Protein Homologous to the 14kDa Protein of Bovine Ubiquinol-cytochrome C Reductase <i>Guangwei Xing, Jinghong Xing & Suhua Wang</i>	101



Contents

Expression of Cocoonase in Silkworm (<i>Bombyx mori</i>) Cells by Using a Recombinant Baculovirus and Its Bioactivity Assay	107
<i>Jianjun Yang, Wenbing Wang, Bing Li, Yudan Wu, Huiling Wu & Weide Shen</i>	
IGF-1 Gene Polymorphism and Weight-Related Analysis	113
<i>Wei Li, Fangqun Li & Daquan Li</i>	
Bioinformatics of NS3 Gene and Inverted Terminal repeats (ITR) of <i>Bombyx Mori</i> Parvo-like Virus (China Zhenjiang Isolate)	119
<i>Chen Sun, Qin Yao, Huijuan Yin, Yuanqing He & Keping Chen</i>	



Philippine Panay Island Bushy-tailed Cloud Rat (*Crateromys heaneyi*): A Preliminary Behavioural Study of Captive Cloud Rats

Root-Gutteridge, H.A.J. & Chatterjee, H.J. (Corresponding author)

Research Department of Genetics, Evolution and Environment

Darwin Building, University College London

Gower Street, WC1E 6BT, London, UK

Tel: 44-207-679-4113 E-mail: h.chatterjee@ucl.ac.uk

Abstract

Panay Island bushy-tailed cloud rats *Crateromys heaneyi* are nocturnal, arboreal, probably herbivorous Philippine rodents. Apart from limited morphological data, there is very little reported information about them. The aim of this study was to gather preliminary data with a view to developing an ethogram for these taxa, based on a captive population housed at ZSL London Zoo. Cloud rats are probably not social rodents and are likely to live in pairs or solitarily in the wild when not raising offspring. They are intolerant of intruders in their territory and will fight to the death when stressed. They spend the majority of their time resting, climbing and feeding. Cloud rats are fastidious in their habits; defecating and urinating away from their nest boxes and food at a particular constant site and cleaning themselves methodically after every meal. There are significant gaps in our knowledge of these mammals, which are listed as endangered on the IUCN Red List.

Keywords: Cloud rats, Ethogram, Behavioural profile, Endangered, Captive population

1. Introduction

Cloud rats, or cloud runners as they are also called, are medium sized, soft-furred, nocturnal, arboreal rodents, found exclusively in the Philippine Islands at 10° north latitude and 125°45' east longitude. The Panay Island bushy-tailed cloud rat (*Crateromys heaneyi*) is the most recent to be identified and London Zoo has the only breeding colony outside of the Philippines. Classified by the IUCN as endangered, the Zoo's protective attitude prevented any invasive or disturbing means of observing behaviour. Almost nothing is known of the genus' behaviour or ecology and the study was intended to function as a preliminary observation on which more intensive studies could be based. Behavioural studies have not been undertaken and at London Zoo the cloud rats are kept according to the principles that govern the captivity of other nocturnal rats. There has been no proper survey of population size or range for any species of cloud rat and the threat of extinction has only been estimated (Heaney et al., 1998, 2005; Musser et al., 1981, 1985; Gonzales and Kennedy, 1996; Nowak and Paradiso, 1983).

All assumptions of behaviour are based on anecdotal evidence gathered by Musser et al. (1985) from Philippine Island hunters. Detailed descriptions of their teeth by Gonzales and Kennedy (1996) indicate herbivory. The cloud rats scurry around the tops of oak and pine trees at altitudes of up to 400m and are seen as glimpses amongst the clouds (Heaney et al, 1998; Oliver et al., 2001). They have yet to have more than one offspring per pregnancy in captivity which is unusual amongst rodents (London Zoo, 2005).

Humans threaten wild cloud rats as they hunt them for meat and pelts, furthermore deforestation has seen a 20% reduction in forest cover between 1950 and 1980. As there is no accurate estimate of population sizes, the probable effect of such habitat loss can only be estimated (Heaney et al., 2005; IUCN, 2006; Heideman et al., 1987; Kummer, 1991).

This behavioural study aimed to build upon existing knowledge to improve captive care. Small mammals are notoriously sensitive to stress and with almost no data about their lives in the wild, it is very difficult to assess the requirements of cloud rats in captivity.

2. Materials and Methods

All methods were designed to minimise stress and disruption to the cloud rats.

2.1 Captive Habitat Conditions and Group Composition

London Zoo houses ten cloud rats in four enclosures (Table 1). The largest enclosure (Enclosure 1) housed a family group; the remaining three enclosures were smaller and housed a breeding pair (Enclosure 2) and single individuals (Enclosures 3 and 4). Each had a layer of woodchips on the base with a number of thick branches acting as climbing poles; this was the only enrichment. The enclosures' building was renovated and their move to new accommodation ended the data collection.

2.2 Observational Data Collection Methods

In October 2005, 60 hours and 8 minutes of observation were undertaken based on the protocol used by London Zoo for all its ethograms. Behavioural categories were added following a brief pilot survey lasting 3 days to include cloud rat specific activities. Instantaneous and one-zero samplings at two-minute intervals were combined to record 20-minute periods of the behaviour of a single focal animal. Data could not be collected by the use of cameras, infra red or changes in photoperiod as the Zoo did not permit any invasive methods. The cloud rats' light sensitivity only allowed observation of activity from 10.45am to 4pm. Table 2 outlines the key behaviours and the definitions were subsequently used as variables for data collection. The duration of time when no cloud rats were visible was recorded as negative data.

Diet sheets were provided by London Zoo and food intake details were recorded over two weeks of London Zoo's normal husbandry routine. Likely calorie intake was estimated from food provided by the keepers and the remains measured the next day. Biographical details (Table 3) were estimated from London Zoo's brief biographical record sheets.

3. Results

Preliminary observations based on the above protocol suggest that the captive cloud rat population at London Zoo spend most of their visible waking time climbing, feeding and resting (Figures 1 - 4). Other activities such as grooming and playing account for significantly less total activity time (Table 4). Their waking time is predominately spent in repose and the only possible activities in the nest boxes are self grooming, allogrooming and resting. This suggests that the cloud rats are either a) generally inactive or b) inactive in captivity. Data for cloud rats in enclosures 2, 3 and 4 were limited and focus here is towards the family group in enclosure 1.

The data suggest that there was little correlation between age and time spent in company outside the nest box with all of the cloud rats spending at least 200 minutes outside of the nest box with another cloud rat. Proximity was usually 0.5-0.75m apart (Table 4). How significant the results are for behaviour is not known as the cloud rats had little choice in proximity due to the enclosure size (Figure 5).

Biographical data is summarised in Table 3. The second youngest specimen at London Zoo, aged some 2 months when the study started, appeared to have a light coloured soft natal coat which was shed at age approximately 10 weeks to be replaced by a darker adult coat. The diet data was analysed and showed distinct food preferences on the part of the cloud rats: Fruit was always favoured while seeds, nuts, rodent pellets and bread were most commonly rejected (Figure 6). The average calorie intake was calculated to be 176.985 calories per day per cloud rat (Calorie King, 2006; Zoo Plus, 2006).

4. Discussion

London Zoo's captive breeding program is part of an international effort to prevent the extinction of threatened species. As far as possible, the effects of enforced time limits were curbed and the resulting data were tested and shown to be statistically significant under Dytham's rule (1999); even rough estimates of likely gestation time and age of sexual maturation are an important advance.

4.1 Negative Data

There were more negative data when no observations of cloud rat activity were recorded than positive data when there were observations (4680 minutes compared to 1600); this was probably because the cloud rats spent most of their time in nest boxes. The family group was the most active and had the largest enclosure so it seems more likely that the cloud rats were idle because of lack of stimulation. The cloud rats were sensitive to light and would not emerge in either artificial or natural light conditions in any of the enclosures.

4.2 Feeding and Play Behaviour

The cloud rats showed a preference for fruit and with the high metabolic demand of a small homeothermic body it is likely that they preferentially feed on the high-energy sugary food. The calorie intake was higher than would normally be predicted (Barnett, 1963), but there was a nursing female who would have an elevated calorie intake. Spatial constrictions did not permit whole group feeding so no conclusions about sociality and food can be made and this is a distinct limit to the research (Montgomery and Gurnell, 1985). As the family only spent 1% of their time allogrooming, close social bonds cemented by altruistic behaviour are unlikely (Figure 3), but the juveniles did follow the adults across branches in play behaviour that could teach agility and territorial boundaries.

4.3 Escape and Reintroduction

In the final week of the study, the juvenile male CRJ1 showed increasingly distinctive behaviour typified by standing on the nest box on the uppermost ledge and clawing / chewing at the ceiling. This formed a hole through which CRJ1, CRJ2 and CRJ3 escaped. Following a temporary separation of approximately 72 hours, they were reintroduced to their family group in the new enclosure. This presented antagonistic behaviour within the group resulting in some physical injury to the two offspring males (CRJ1 and CRJ3) one of which was killed. It may be that cloud rats are territorial and once the males have left the natal group they are not accepted back, which is true in rats (Barnett, 1963). Why the cloud rats had not previously reacted in this way is not known, but juvenile mice produce urine that has a distinctive smell which reduces the aggressiveness shown by elders towards them (Poole, 1985). The cloud rats were often sociable in pairs and were observed feeding or playing in groups of two or three. There was some correlation between age, sex and sociability.

5. Conclusion

This preliminary study has presented novel findings regarding the captive behaviour of the world's only breeding population of cloud rats. Observations made over a longer time period are required. The most important future research would be a simple continuation of the ethogram over a greater range of daily times and also for a longer length of observation, ideally including nest box cameras and infra red. A continuation of the present study was not possible due to concerns expressed by London Zoo regarding within group aggression and stress induced by on-site observers; infra-red cameras and nest box cameras would help alleviate these stresses. Dietary changes, increasing male aggression with age, offspring dispersal, the effect on behaviour of changes in temperature, and daylight length and intensity, would be interesting subjects for further study. Critically, further field studies of *C. heaneyi* and other cloud rats are required to understand their behaviour in the wild. This is particularly important in light of the significant extinction risk facing these enigmatic Philippine rodents.

Acknowledgements

We are extremely grateful to Andy Hartley of the Zoological Society of London, Marie Whatmough and all the small mammal keepers of London Zoo, Lawrence Heaney of the Chicago Field Museum, for whom the Panay Island bushy-tailed cloud rat is named and William Oliver, the Director of the Philippines Biodiversity Conservation Programme.

References

- Barnett, S. (1963). *The Rat*. Chicago & London: University of Chicago Press.
- Calorie King. (2006). Calorie king food search: world's biggest database. [Online] Available: <http://www.calorieking.com/> (January 26, 2009)
- Dytham, C. (1999). *Choosing and using statistics: a biologist's guide*. Blackwell Science.
- Gonzales, P.C. & Kennedy, R.S. (1996). A new species of *Crateromys* (Rodentia: Muridae) from Panay, Philippines. *Journal of Mammalogy*, 77, 1, 25-39.
- Heaney, L.R., Balete, D.S., Dolar, M.L., Alcala, A.C., Dans, A.T.L., Gonzales, P.C., Ingle, N.R., Lepiten, M.V., Oliver, W.L.R., Ong, P.S., Rickart, E.A., Tabaranza, Jr. B.R. & Uzzurum, R.C.B. (1998). *A synopsis of the mammalian fauna of the Philippine Islands*. Fieldiana Zoology new series, 88, 1-61.
- Heaney, L.R., Walsh, Jr. J.S. & Townsend Peterson, A. (2005). The roles of geological history and colonisation abilities in genetic differentiation between mammalian populations in the Philippine archipelago. *Journal of Biogeography*, 32, 229-247.
- Heideman, P.D., Heaney, L.R., Thomas, R.L. & Erickson, K.R. (1987). Patterns of faunal diversity and species abundance of non-volant small mammals on Negros Island, Philippines. *Journal of Mammalogy*, 68, 884-888.
- IUCN. (2006). IUCN red list of threatened species. [Online] Available: <http://www.iucnredlist.org> (January 26, 2009)

- Krebs, J.R. & Davies, N.B. (1987). *An introduction to behavioural ecology*. Blackwell Scientific Publications 2nd edition.
- Kummer, D.M. (1991). *Deforestation in the postwar Philippines*. University of Chicago Geography Research paper 234:39-76.
- London Zoo. (2005). *Biographical Records for the Captive Cloud Rats*. Unpubl. material.
- Montgomery, W.I & Gurnell J. (1985). The behaviour of Apodemus. In J.R. Flowerdew, J.Gurnell, & J.H.W. Gipps (Eds.), *The Ecology of Woodland Rodents, Bank Voles and Wood Mice* (p 89-115). Zoological Society of London Symposia 55: Oxford, Clarendon Press.
- Musser, G.G. & Gordon, L.K. (1981). A new species of Crateromys (Muridae) from the Philippines. *Journal of Mammalogy*, 62, 513-525.
- Musser, G.G., Heaney, L.R. & Rabor, D.S. (1985). Philippine rats: a new species of Crateromys from Dinagat Island. *American Museum Novitates*, 2821, 1-25.
- Nowak, R.M. & Paradiso, J.L. (1983). *Walker's mammals of the world*. 4th Ed. Baltimore and London: Hopkins University Press.
- Oliver, W.L.R., Lindsay, N. & Kloes, H. (2001). Philippine cloud rats' conservation programme – a report on progress to June 2001. Unpubl. Courtesy of William Oliver, FFI-Philippines Programme, Manila, Philippines.
- Poole, T.B. (1985). *Social behaviour in mammals*. 1st Ed. Blackie, USA: Chapman and Hall, New York.
- Zoo Plus UK. (2006). Nutrition analysis of Eukanuba dog food. [Online] Available: <http://www.zooplus.co.uk> (26 January, 2009)

Table 1. Captive habitat conditions and group composition

Enclosure	Description of Enclosure	Captive Population
1	2 x 2 x 2m Concrete enclosure with one glass wall exposed to the public Reverse lighting conditions 2 nest boxes	CRA1: Adult male (2 years of age) CRA2: Adult female (2 years of age) CRJ1: Juvenile male (8 months) CRJ2: Juvenile female (5 months) CRJ3: Juvenile male (2 months) CRJ4: Juvenile female (< 5 days old)
2	1 x 1 x 1m Concrete enclosure with one glass wall exposed to the public Reverse lighting conditions 1 nest box	CRA3: Adult male (age unknown) CRA4: Adult female (age unknown)
3	1m depth x 1m width x 2m height Wire cage enclosure, closed to the public Normal lighting conditions 1 nest box	CRA5: Adult male (age unknown)
4	1m depth x 1m width x 2m height Wire cage enclosure, closed to the public Normal lighting conditions 1 nest box	CRA6: Adult female (age unknown)

Table 2. Definitions of the behaviours

Activity	Definition
Feed	Inactive: feeding at rest or if combined with foraging feeding during movement.
Forage	Active: searching for food, not eating it
Rest	Inactive: sitting or lying down without other activity.
Play	Active: usually walk / climb behaviour with another cloud rat as in “follow my leader” game or wrestling.
Walk / climb	Active: movement that was not part of a game with another cloud rat or in search of food.
Groom self	Active: grooming self always done in sitting position and involved a small amount of gymnastic movement.
Groom other	Active: grooming another cloud rat, sometimes moving around or over the other individual to do so. Also known as allogrooming.
Neighbour ID	The identity of the nearest neighbour (if any) to the focal animal.
Distance to nearest neighbour	The estimated distance between the focal animal and its nearest (if any) neighbour.
Hide	Any period when the cloud rat was not visible during the observation time, not definitely at rest but due to the arrangement of the enclosure, usually resting, feeding or grooming were the only activities possible.
Other	Any behaviour that is not covered by the above. Described further in notes; included mating behaviour, creating a hole in the ceiling and other social activities.

Table 3. Life history data for *C. heaneyi* and *P. pallidus*

	<i>C. heaneyi</i>	<i>P. pallidus</i>
Average female sexual maturity	10 months	8 months
Average male sexual maturity	10 months	12-18 months
Gestation time parameters	1-2 months	69-95 days
Birth interval	2-5 months	8 months
Number offspring per pregnancy	1	1
Weight of young at birth	124g	100-150g
Estimated weaning age	2 months	5 months
Oestrus cycle	Unknown	10-15 days
Lifespan	Unknown	13-15 years in captivity

C. heaneyi values calculated from data given by London Zookeepers (2006).

P. pallidus values from Minnesota Zoo website (2006).

Table 4. Total behaviour times for individuals and total behaviour times overall (positive and negative data)

(time in minutes)

ID	Feed	Forage	Rest	Play	Climb	Groom				PositiveNegative			
						Groom self	Other	Hide	Other	ID	Distance	Data	Data
CRA1	78	96	116	12	174	54	2	170	0		0.707	340	468
CRA2	154	86	32	42	174	44	2	66	0		0.455	360	468
CRA3	10	10	4	2	28	0	0	8	60	B	2.75	80	380
CRA4	12	10	58	2	26	0	0	2	10	A	2.75	80	380
CRA5	0	0	40	0	0	0	N/A	0	0	N/A	N/A	40	310
CRA6	0	0	0	0	0	0	N/A	0	0	N/A	N/A	0	310
CRJ1													
	182	74	202	46	94	50	8	130	0		0.647	480	468
CRJ2	104	88	50	42	230	52	2	92	4		0.5	340	468
CRJ3	86	58	60	50	116	16	6	54	0		0.278	240	468
CRJ4	0	0	0	0	0	0	0	0	0		0	0	468
TOTAL	532	422	562	209	842	216	20	522	74			1600	4188

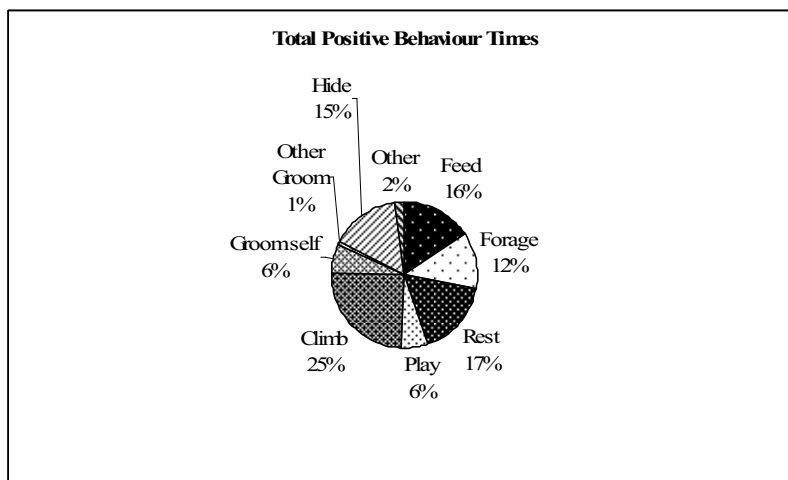


Figure 1. Pie chart showing % behaviour times for all study individuals.

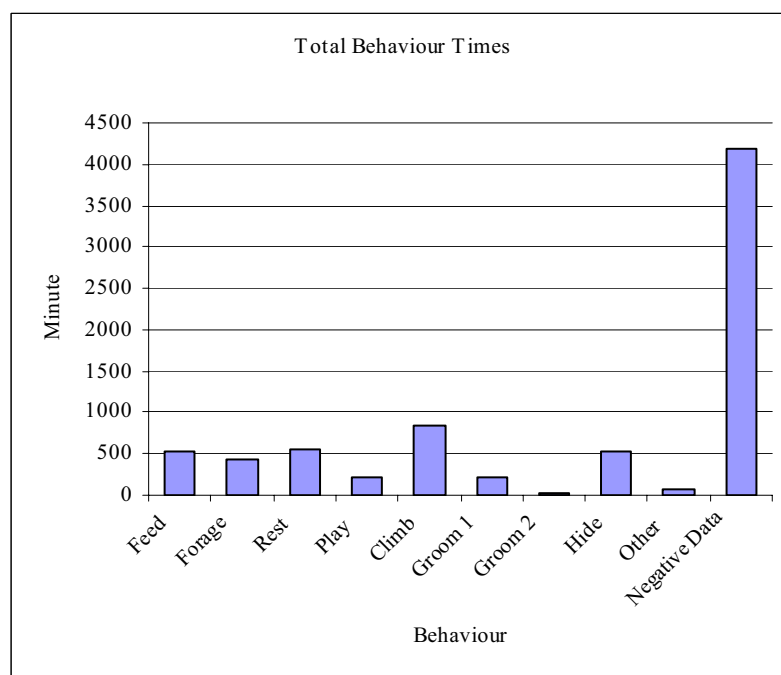


Figure 2. Time spent by individuals in different types of behaviour.

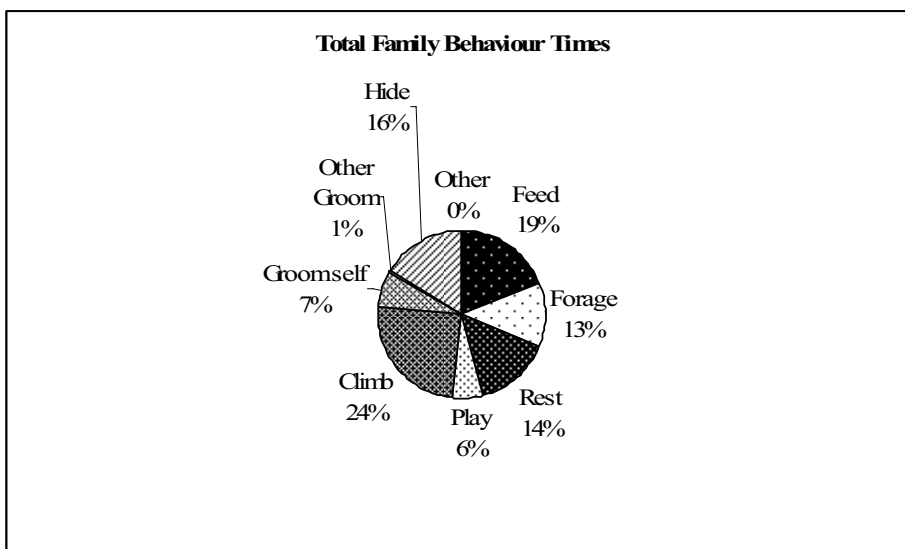


Figure 3. Pie chart showing % behaviour times for the family group.

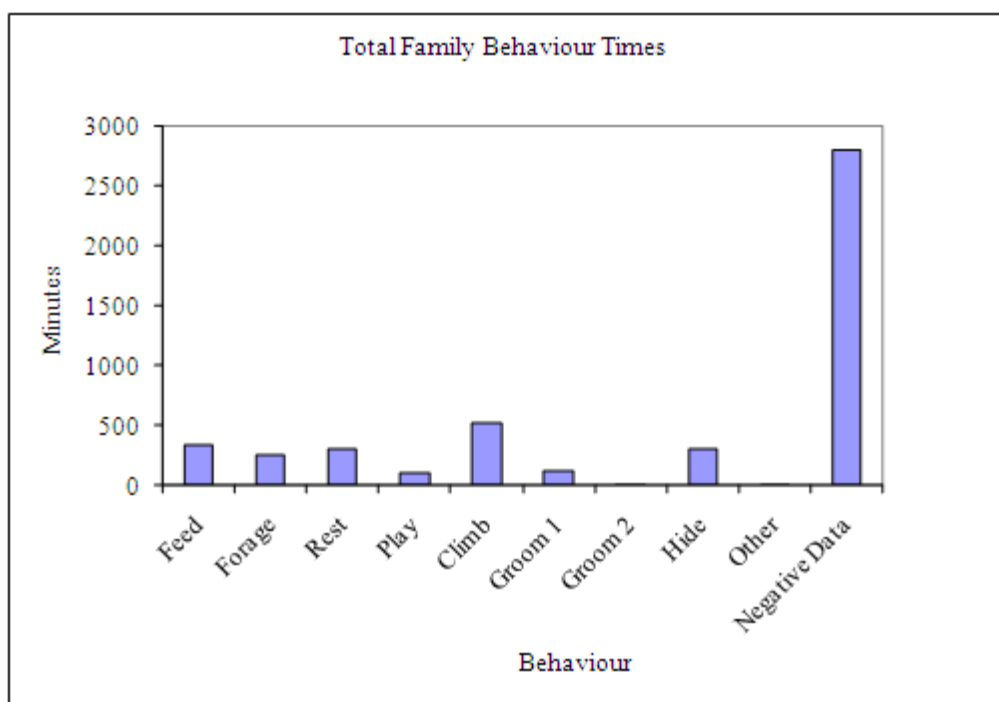


Figure 4. Time spent by the family group in different types of behaviour.

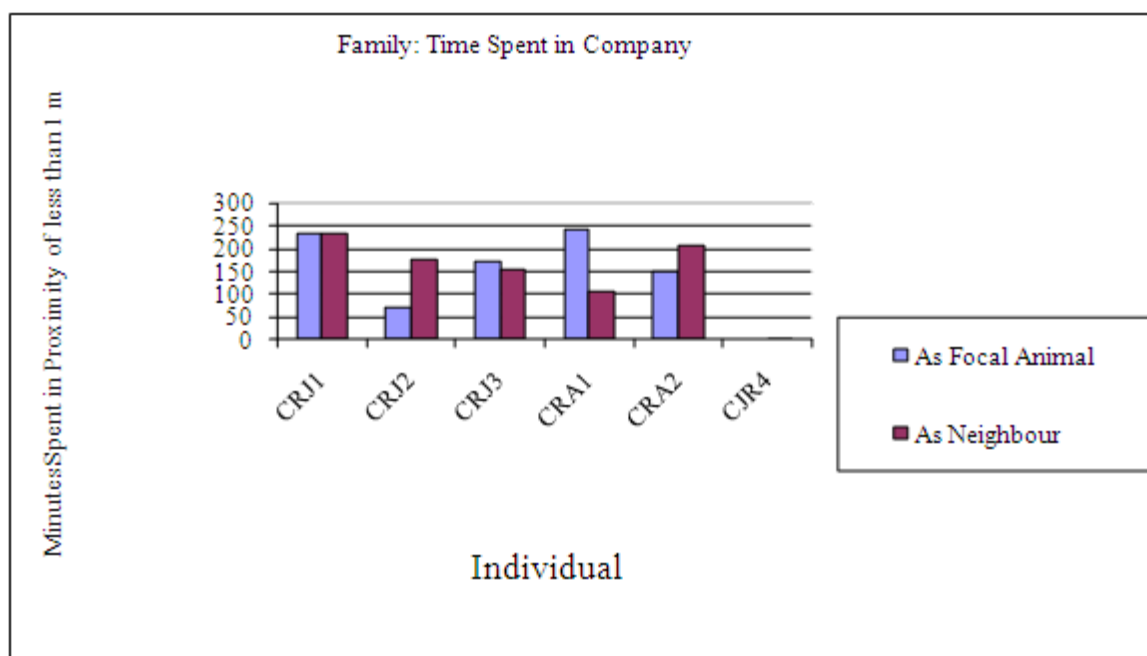


Figure 5. Time spent by the focal animal within <1m to its nearest neighbour.

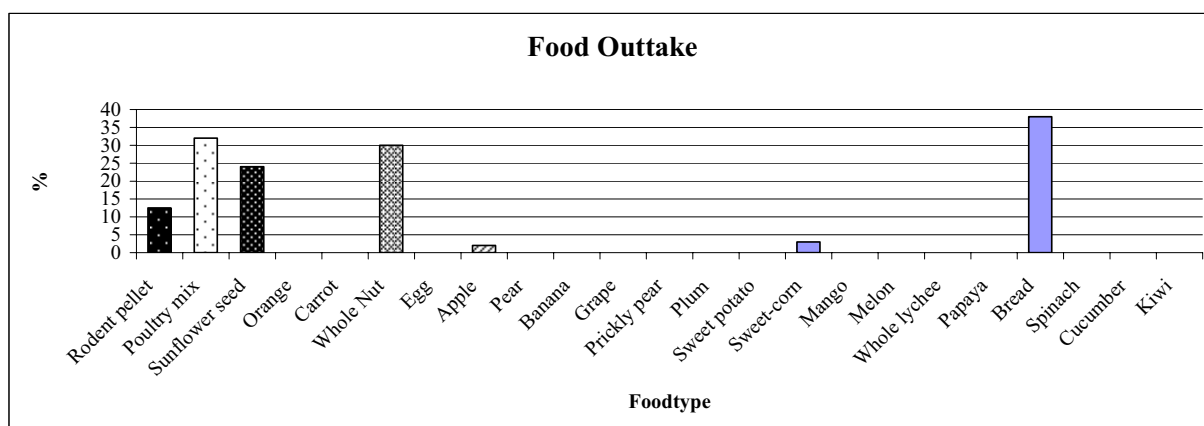


Figure 6. Percentage of uneaten food removed from enclosures. Figures are collated from across the whole study period.



Purification and Characterization of Cold-Adapted Metalloprotease from Deep Sea Water Lactic Acid Bacteria *Enterococcus Faecalis* TN-9

Qingzhu Yuan (Corresponding author) & Atsushi Hayashi

Central Research Laboratories, Nichinichi Pharmaceutical Co., Ltd.

Mie 518-1417, Japan

Tel: 81-595-48-0201 E-mail: yqz5012001@yahoo.com.cn

Yoshihisa Kitamura & Takashi Shimada

Central Research Laboratories, Nichinichi Pharmaceutical Co., Ltd.

Mie 518-1417, Japan

China-Japan Collaborating Centre for Probiotics Research

Nanjing Medical University

Nanjing, Jiangsu 210029, China

Ren Na

Development & Service Centre of Cow Industrialization

Xilinhaote, Inner Mongolia 026000, China

Xiao Jin

Animal Hygiene Supervision Place of Inner Mongolia

Huhehaote, Inner Mongolia 010015, China

Abstract

This paper investigated a 3-step purification and characterization of a protease from *Enterococcus faecalis* TN-9, a bathypelagic lactic acid bacteria. The purification procedure includes precipitation with $(\text{NH}_4)_2\text{SO}_4$, then ion-exchange chromatography with DEAE-Sephadex A-25 and DEAE Cellulofine A-500. Native PAGE analysis indicates a single protease band. The molecular weight is 30 kDa by SDS-PAGE analysis, and 69 kDa by gel chromatography analysis. It proves that the optimal temperature for protease reaction is 30 °C, and the optimal pH is 7.5-8.0. The reaction is stable while pH is 6.0-9.5 and temperature is under 45 °C. The relative activity is 6.1% at 0 °C. The enzyme is totally deactivated with heat treatment at 60 °C or over. The protease is partially inhibited by EDTA-2Na, Hg^{2+} , Cu^{2+} , Ni^{2+} , Ag^{2+} , Co^{2+} and Pepstatin A. Zn^{2+} shows obvious activation to the protease. K_m and V_{max} of purified protease acting on azocasein are 0.098 % and 72 mg/(h·mg) respectively. This protease is one of gelatinase with N-terminal sequence of VGSEVTLKNS, and shows characteristics of a cold-adapted metalloprotease.

Keywords: Deep sea water, Lactic acid bacteria, Cold-adapted enzyme, Metalloprotease, Azocasein

1. Introduction

The cold-adapted enzymes from cold-adapted organisms or other microbial life in extreme environments have been widely studied in recent years. Reports are often on cold-adapted enzymes from marine microorganism. Shi et al (2005, p. 258-263; 2006, p. 72-75) separated and purified a strain of cold-adapted enzyme from a psychrophilic bacteria *Bacillus cereus* SYP-A2-3 acquired from samples collected from glacier. Nushin Aghajari et al (2003, p. 636-647) and Denner E B et al (2001, p. 44-53) isolated a strain of psychrophilic bacteria from samples of Antarctic and studied on the cold-adapted metalloprotease. Miyamoto K et al (2002, p. 416-421) acquired and purified two types of cold-adapted

metalloprotease (MprI and MprII) from marine microorganism *Alteromonas* sp. strain O-7. However, we have not found any report on the cold-adapted protease isolated from marine lactic acid bacteria.

Study described in this paper isolated 25 strains of lactic acid bacterium from deep sea water at Toyama Bay of Japanese Sea. Among them *Enterococcus faecalis* strain TN-9 (Atsushi Hayashi, 2007, p. 58-64) shows liquefying gelatin, fermented and solidified litmus milk, β -galactosidase activity and other characteristics. Oral administration has been proved safe by sub-acute toxicity study of this bacteria strain in rats (Chie Motonaga, 2007, p. 191-196). Therefore, *E. faecalis* TN-9 is expected promising in the research and development of health foods containing lactic acid bacteria. Based on above-mentioned results, the study in this paper isolated, purified and characterized the protease from lactic acid bacteria *E. faecalis* TN-9.

2. Materials and methods

2.1 Materials and equipments

Bacteria stain: lactic acid bacteria *E. faecalis* strain TN-9, stored and provided by Nichinichi Pharmaceutical Co., Ltd; Lactobacilli MRS Broth from USA; Hinute SMP provided by Fuji Oil Co. of Japan; Azocasein from Sigma of USA; DEAE-Sephadex A-25 from Pharmacia of Sweden; DEAE-Cellulofine A-500 and Toyopearl HW-55s provided by Chisso of Japan; standard protein provided by Wako of Japan; and other commonly used reagents made in Japan. Key instruments: U-2000 spectrophotometer from Hitachi of Japan and KUBOTA 7780 centrifuger from Kubota of Japan.

2.2 Methodology

2.2.1 Culture of strain and collection of culture media

(1) Culture medium

Take MRS agar plate as solid culture media. Liquid culture media is a mixture of A, B and C, where A is composed of 1.5 g Hinute SMP, 2.4 g D-Glucose, 0.2 g NaCl and 70 ml distilled water; B is composed of 18.0 g K_2HPO_4 and 100 ml distilled water; C is composed of 0.05 g $FeSO_4 \cdot 7H_2O$, 0.58 g $MgSO_4 \cdot 7H_2O$, 0.03 g $MnSO_4 \cdot 5H_2O$, 0.10 g $ZnSO_4 \cdot 7H_2O$ and 100 ml distilled water. Begin by formulating A and B, in turn autoclaving at 121 °C for 15 min, then sterilize C by sterilizing filter (DISMIC-25CS/0.45 μm , made in Toyo of Japan), finally mix A, B and C at the ratio of 7:2:1 in aseptic environment, ready for culture of strain.

(2) Culture of strain and collection of culture media

On the MRS medium, cut marker lines on the -80 °C stored bacteria strain, culture the slides at 30 °C for 48 h. Select and inoculate the independent bacterial colonies into 50 ml the above-mentioned liquid medium. After static culture at 30 °C for 18 h, transfer it into 800 ml the same liquid medium to have the second static culture at 30 °C for 18 h. Centrifuge at 4 °C (12,000 $\times g$, 10 min) to collect supernatant as crude enzyme solution for isolating and purifying protease.

2.2.2 Determination of protease activity

Protease activity is measured by the TCA-azocasein assay based on the methods proposed by Hagihara B et al (1958, p. 185-194) and Thomas J B et al (1986, p. 139-145). 100 μl protease solution with specific concentration is added into 400 μl 1.25% (w/v) phosphate-buffered saline (100 mM Na-K phosphate buffer with pH of 7.5, called buffer A); react at 30 °C for 10 min (shaking at 170 times per minute) in water bath; adding 1 ml 10 % (w/v) trichloroacetic acid (TCA) to stop the reaction; centrifuge (16,000 $\times g$, 20 min, 10 °C) the resulting product to remove undigested azocasein. The absorbance (A335) of the obtained supernatant is measured at 335 nm with a spectrophotometer (Hitachi, U-2000). Protease activity is calculated from the amount of L-tyrosine, which is achieved from A335. One unit of protease activity is defined as the amount of enzyme for 1 μg of L-tyrosine which is released from the substrate per minute under the above conditions.

2.2.3 Determination of protein

Protein is measured by the Lowry process (Lowry O H, 1951, 265-275), with bovine serum albumin (Sigma of USA) as criterion.

2.2.4 Polyacrylamide gel electrophoresis (PAGE)

Referring to the method proposed by Reisfeld R A et al (1962, p. 281-283), Native-PAGE is carried out under the following conditions: 2.5% (w/v) stacking gel, 7.5% (w/v) separation gel (pH 4.0), alanine-acetic acid (pH 4.5) as electrolyte bath, anode/cathode reversely-connected NA-1311 Electrolyte Bath (NIHON EIDO Co. Ltd. Tokyo), and electrophoresis at a constant current of 2.5 mA for 3.5 h per column. Referring to the method proposed by Weber K and Osborn M (1969, p. 4406-4412), SDS-PAGE is carried out under following conditions: 7.5% (w/v) polyacrylamide gel and 0.10% (w/v) SDS-0.10 M phosphate buffer (pH 7.2) as electrolyte bath, electrophoresis at a constant current of 6.0 mA for 3 h per column. Use BSA (79,000), Aldolase (42,000), Carbonic Anhydrase (30,000), Trypsin Inhibitor (20,000) and Lysozyme (14,000, from Wako of Japan) as reference standards for molecular weight. Stain for 1 h with 0.25% (w/v)

Coomassie Brilliant Blue R-250 solved in the mixture of ethanol, acetic acid and deionized water at the ratio of 9:2:9; destain for 1 h with the mixture of ethanol, acetic acid and deionized water at the ratio of 25:8:65, further with the mixture of ethanol, acetic acid and deionized water at the ratio of 10:15:175.

2.2.5 Gel chromatography

Gel chromatography is carried out at 20 ml/h by using Toyopearl HW-55s column (25×900 mm) and buffer A containing 0.2 M NaCl as eluent. Reagents and kits for molecular weight measurement: Ferritin (440 kDa), Catalase (240 kDa), γ -globulin (160 kDa), Bovine serum albumin (67 kDa) and Ovalbumin (43 kDa, from Wako of Japan).

2.2.6 Isolation and purification of enzyme

Collect supernatant as crude enzyme by centrifuging 3,200 ml culture medium at 12,000×g, 4 °C for 10 min. Slowly add $(\text{HN}_4)_2\text{SO}_4$ powder of saturation 0-60% (w/v); stir and sediment for 30 min. Centrifuge the mixture and have the sediment resolved in 40 ml 100 mM Tris-HCl buffer (buffer B, pH 7.5). The resulting filtrate from semi-permeable membrane is forced through buffer B-balanced DEAE-Sephadex A-25 column (26×180 mm); uncombined protein is then removed by washing with 450mL buffer B; obtained product is finally eluted with 720 ml buffer B at 50 ml/h (elution gradient is 0→2.5 M NaCl). Determine protease activity and protein amount of each fraction (6.0 ml/tube), collect the fractions with high protease activity, apply buffer A-balanced DEAE-Cellulofine A-500 column (26×180 mm) after dialysis by buffer A for 24 h (change buffer at the 3rd hour and the 9th hour from the beginning of dialysis), remove other proteins by rinsing with 450mL buffer A, then elute with 720 ml buffer A at 40 ml/h (elution gradient is 0→2.0 M NaCl). Determine protease activity and protein amount of each fraction (3.0 ml/tube); collect the fractions with high protease activity. The purified enzyme is obtained by dialysis with buffer A for 24 h.

2.2.7 Determination of subunit molecular weight

Using SDS-PAGE, find subunit molecular weight from R_f -Log M_r chart, wherein R_f represents relative mobility of standard protein with certain molecular weight (M_r) under SDS-PAGE condition.

2.2.8 Determination of optimal reaction temperature and optimal pH

The optimal reaction temperature and optimal pH are found from relative activities of enzyme at different temperature (0-80 °C) and in different buffers of different pH, buffers such as 100 mM acetate solution (pH 3.2-5.5), 100 mM phosphoric acid solution (pH 4.8-9.0), 100 mM Tris-HCl solution (pH 7.5-9.5), 100 mM carbonic acid solution (pH 9.0-12.0), relative activities of enzyme in turn is measured by Azocasein Method with the highest enzyme activity being defined as 100%.

2.2.9 Thermal stability and pH stability

Investigate the thermal stability after holding at 20-80 °C for 10 min and then quick-cooling in ice bath, as well as pH stability after storing respectively in the above buffers (pH 3.2-12.0) and then dialyzing at 4 °C overnight, by measuring the residual activity of enzyme according to the above-mentioned procedure.

2.2.10 Determination of kinetic constants

Use buffer A to formulate azocasein substrates with different concentrations of 0.02%, 0.04%, 0.08%, 0.16%, 0.32%, 0.64%, 1.25%, 2.50%, wherein the amount of enzyme is 1.5 g. Based on Lineweaver-Burk plotting method, K_m and V_{max} are obtained from the enzyme activity of each substrate.

2.2.11 Effects of inhibitor, metal ions and denaturant on enzyme activity

Solve inhibitor, metal ions and denaturant respectively in deionized water to obtain concentrated solutions; add the concentrated solutions in 0.5 ml purified enzyme solution (1.0 unit) to formulate the specimen with final concentrations of 1.0 mM and 0.1 mM, keep them at 25 °C for 30 min. Effects of inhibitor, metal ions and denaturant on enzyme activity are investigated by determination of residual enzyme activities of the obtained specimen according to the above-mentioned procedure with the enzyme-free system as blank control and pure enzyme solution as 100%.

2.2.12 Activation experiment on deactivated protease

Add 0.5ml 2.0 mM EDTA-2Na solution in 0.5 ml purified enzyme solution, keep it at 25 °C for 30 min; then add various 2.0 mM metallic salt solutions at the amount of 0.5 ml, keep it at 25 °C for 30 min. Effects of various metallic ions on activation of EDTA-2Na-deactivated protease are investigated by determination of the residual enzyme activities of the specimen according to the above-mentioned procedure with EDTA-2Na-free system and the metallic salt-free system as blank controls respectively.

2.2.13 NH_2 -terminal amino-acid sequence analysis

NH_2 -terminal amino-acid sequence analysis is carried out by SHIMADZU PPSQ-10 protein sequence analyzer (Shimadzu of Japan) after electro blotting the purified enzyme based on the method proposed by Matsudaira P (1987, p. 10035-10038).

3. Results and discussions

3.1 Purification of protease

After purifying the crude enzyme by ammonium sulfate precipitation (Fraction 2) and two-step anion-exchange chromatography with DEAE-Sephadex A-25 (Figure 1, Fraction 3) and DEAE-Cellulofine A-500 (Figure 2), The specific enzyme activity of the obtained specimen is increased from 25 U/mg to 12,300 U/mg. The purification fold is 492, and the recovery rate reaches 23% (Table 1).

From the purification procedure, we can see that ammonium sulfate precipitation is a simple and effective means for initial fractionation of proteins. 80% protease is recovered and the specific enzyme activity is increased by 120 folds. This is because that ammonium sulfate doesn't affect the enzyme activity; and not only is Hinute SMP-mainly-contained culture medium suitable for *E. faecalis* TN-9 to develop and produce large amount of protease, but also its residual protein is easy to be removed by ammonium sulfate precipitation process, making it easy for further purification.

Native PAGE analysis shows only one protease band, indicating lack of isozyme in purified protease specimen (Figure 3A); SDS-PAGE analysis also shows only one protease band, indicating an electrophoresis grade for the purification of protease. The subunit molecular weight is calculated as 30 kDa. Molecular weight measured by gel chromatography analysis is 69 kDa, indicating that the natural state of protease is a dimer consisting of two subunits. Mäkinen et al (1989, p. 3325-3334) isolated and purified a protease with molecular weight of 31.5 kDa from *Streptococcus faecalis* (OG1-10) and proved it to be a new neutral endoprotease (Gelatinase, EC3.4.24.4).

During purification and while using Tris-HCl buffer (100 mM, pH 7.5), protease is absorbed to DEAE series anion exchange resin adhesive, then eluted with NaCl solution. However, protease can not be absorbed to DEAE series anion exchange resin adhesive nor CM resin adhesive while using phosphoric acid buffer (100 mM, pH 6.0-7.5) instead. In addition, during PAGE analysis, protease does not show any movement in alanine-acetic acid solution (pH 4.5) in anode/cathode normal-connected NA-1311 Electrolyte Bath; on the other hand, protease moves towards cathode when anode and cathode are reversely connected. This is explained that the protease shows electronegative in Tris-HCl buffer with pH higher than 7.0, neutral in phosphoric acid buffer with pH of 7.0, and electropositive in alanine-acetic acid buffer with pH of 4.5. Therefore, the isoelectric point of this protease should be between pH 4.5-pH7.0.

3.2 Study on the properties of protease

3.2.1 Optimal reaction temperature and optimal pH of the enzyme

The optimal reaction temperature and optimal pH of the purified protease are 30 °C (Figure 4A) and 7.5-8.0 (Figure 4C) respectively. The optimal pH of gelatinase isolated from *S. faecalis* (Strain OG1-10) reported by Mäkinen (1989, p. 3325-3334) is 6-8.

3.2.2 Thermal stability and pH stability of the enzyme

The relative activity of this purified protease is 6.1% at 0 °C (Figure 4A), and 65.1% at 15 °C; while that of cold-adapted protease isolated from psychrophile bacteria *Bacillus cereus* SYP-A2-3 from glacier is about 6.0% at 0 °C, and 60% at 25 °C. It indicates that this protease, with larger low temperature enzyme activity, shows characteristics of cold-adapted enzyme (Shi, Jinsong, 2005, p. 258-263; 2006, p. 72-75). The activity of this purified protease maintains 100% after heat treatment at 45 °C for 10 min, drops sharply from 50 °C, and is completely inactivated over 60 °C (Figure 4B). This indicates that this protease is unstable to heat. The residual activity is over 89% with pH in the range of 6.0-9.5, and maintains over 70% in phosphoric acid buffer even with pH decreased to 4.8 (Figure 4D), demonstrating that this protease is more stable in phosphoric acid buffer.

3.2.3 Determination of kinetic constants

Based on Lineweaver-Burk plotting method, K_m and V_{max} are respectively found to be 0.098% and 72 mg/(h·mg) from the relation between enzyme activity and concentration of azocasein substrate.

3.2.4 Effects of inhibitor, metal ions and denaturant on enzyme activity

As illustrated in Table 2, the purified protease is partially inhibited by β -mercaptoethanol, Pepstatin A, Chymostatin, DTT and EDTA-2Na, where the inhibiting rate of EDTA-2Na is highest, up to 42%. It is not inhibited by PMSF, TLCK and Leupiptin, inhibited to certain extend by Hg^{2+} , Cu^{2+} , Ag^+ , Ni^{2+} and Co^{2+} . However, Zn^{2+} , Fe^{3+} , Mn^{2+} , Mg^{2+} , Fe^{2+} and IAA increase enzyme activity (Table 3). In addition, EDTA-2Na-deactivated enzyme (apoenzyme) can be activated by Zn^{2+} , indicating that Zn^{2+} is the main metal ion to catalyze chemical reactions begins with the binding of the substrate to the active site on the enzyme. Meanwhile, the protease is inhibited by the inhibitor of aspartic acid Pepstatin A, suggesting that aspartic acid is abundant at the active site on the enzyme and active in catalyzing chemical reactions.

3.2.5 NH_2 -terminal amino-acid sequence analysis

10 NH₂-terminal amino-acid starting with V (Val) sequence (VGSEVTLKNS) are proved. By using FASTA sequence similarity analysis with NCBI database, the analysis are in accordance with that of gelatinase (EC 3.4.24.4) isolated from *S. faecalis* (Strain OG1-10) (Pirkko-Liisa, Mäkinen, 1989, p. 3325-3334) and Coccolysin (EC 3.4.24.30) (Pirkko-Liisa, Mäkinen, 1994, p. 981-985). It suggests that the metalloprotease isolated from *E. faecalis* TN-9 is a gelatinase. In 1994, Mäkinen et al isolated and purified Coccolysin (EC3.4.24.30) from *E. faecalis* (OG1-10) and concluded that Coccolysin is one of Gelatinase based on amino-acid sequence analysis. Although Pirkko-Liisa, Mäkinen et al (1989, p. 3325-3334; 1994, p. 981-985) isolated and determined gelatinase (EC 3.4.24.4) and coccolysin (EC 3.4.24.30) sequentially, the study on the characteristics of cold-adapted metalloprotease isolated from *E. faecalis* hasn't been reported so far.

4. Conclusion

This paper illustrated the purification process and common characteristics of extracellular protease isolated from lactic acid bacteria *E. faecalis* TN-9 from deep sea water. The electrophoresis-grade metalloprotease acquired by 3-step purification process has a specific activity 12,300 U/mg, a recovery rate 23%, a subunit molecular weight 30 kDa and Native molecular weight 69 kDa and an isoelectric point is between pH 4.5 and pH 7.0. These properties indicate that the protease is a metalloprotease with Zn²⁺-dependent active site. The protease has 10 N-terminal sequence (VGSEVTLKNS) the same as Gelatinase (EC3.4.24.4) and Coccolysin, indicating the isolated protease is one of Gelatinase for classification point of view. The purified protease has a relative activity 6.1% at 0 °C, a maximum relative activity at 30 °C and between pH 7.5 and pH 8.0. The activation protease is in the most stable state between pH 6.0 and pH 9.5 and at temperature below 45 °C, drops sharply above 50 °C, is completely inactivated above 60 °C. Meanwhile, phosphoric acid buffer is more beneficial to the storage and activation of this protease. Km and Vmax of purified protease acting on azocasein are 0.098 % and 72 mg/(h·mg) respectively.

The purified metalloprotease exhibits certain features of cold-adapted enzyme, especially in low-temperature catalyst and thermal instability. Therefore it is concluded as a cold-adapted metalloprotease. It is shown by an incomplete literature search that this is the first report on the characteristics of cold-adapted metalloprotease isolated from lactic acid bacterium in deep sea so far. Atsushi Hayashi et al (2007, p. 58-64) believes that *E. faecalis* TN-9 most likely comes from muddy cold seabed or excrement of psychrophilic fish at the bottom of deep sea. Our study further validates the conclusion. Cold-adapted enzymes in many research reports come from psychrophilic bacteria in extreme cold environments such as glacier, marine environment and alike. Most psychrophilic bacteria secrete cold-adapted enzymes. Gerday C et al (2000, p. 103-107) believes that as dominating species of cold ecosystem, cold-adapted microorganisms live widely in polar region, glacier, ice sea, deep sea and other year-around cold environments. Cold-adapted microorganisms can produce some efficient cold-adapted enzymes to maintain normal metabolism and other complex functions.

Application of cold-adapted protease isolated from bacteria has bright future in food industry. It can improve the quality, stability and solubility of food. It could be produced in industrial scale, serving as an inexpensive and abundant enzyme source. It is generally toxic free, capable of processing food at low temperature and is generally free of side effect as the enzymes deactivate rapidly at moderate temperature (Ryoma Miyake, 2007, p. 4849-4856; Wang, Yujing, 2004, p. 8-15; Nakagawa T, 2004, p. 383-387; Gu, Jing, 2002). The purified cold-adapted protease studied in this paper has a maximum activity at 30 °C, and is deactivated at 60 °C within only 10 min, therefore meets the enzyme-processing requirements for food at low temperature. In addition, the safety of the oral administration of *E. faecalis* TN-9 has been proved. Not only can the purified enzyme from culture media be applied to food industry, but also is the culture media itself and bacterium strain applied in food industry directly. In all, the application of lactic acid bacteria *E. faecalis* TN-9 and the cold-adapted metalloprotease from it has promising future in food industry.

References

- Atsushi Hayashi, Takashi Shimada, Hiroyasu Onaka & Tamotsu Furumai. (2007). Isolation and phenotypic characterization of enterococci from the deep-seawater samples collected in Toyama Bay. *Japanese Journal of Lactic Acid Bacteria*, 18(2), 58-64.
- Chie Motonaga, Atsushi Hayashi, Masatoshi Kondoh, Mariko Okamori, Takashi Shimada & Tamotsu Furumai. (2007). Toxicological studies on *Enterococcus faecalis* TN-9 isolated from Deep-seawater. *Pharmacometrics*, 73(1/2), 191-196.
- Denner E B, Mark B, Busse H J, Turkiewicz M & Lubitz W. (2001). *Psychrobacter proteolyticus* sp. nov., a psychrotrophic, halotolerant bacterium isolated from the Antarctic krill *Euphausia superba* Dana, excreting a cold-adapted metalloprotease. *Syst Appl Microbiol.*, 4(1), 44-53.
- Gerday C, Aittaleb M, Bentahir M, Chessa J P, Claverie P, Collins T, D'Amico S, Dumont J, Garsoux G, Georgette D, Hoyoux A, Lonhienne T, Meuwis M A & Feller G. (2000). Cold-adapted enzymes: from fundamentals to biotechnology. *Trends Biotechnol*, 18(3), 103-107.
- Hagihara B, Matsubara H, Nakai M & Okunuki K. (1958). Crystalline bacterial proteinase I, preparation of crystalline

protease of bacillus subtilis. *J. Biochem.*, 45(3), 185-194.

Jing, Gu, Feng, Jing, Kong, Jian & Ma, Guirong. (2002). Research progress on metalloproteinases from microorganisms. *Progress in Biotechnology*, 22(1).

Lowry O H, Rosebrough N J, Farr A L & Randall R J. (1951). Protein measurement with the Folin phenol reagent. *J. Biol. Chem.*, 193, 265-275.

Matsudaira P. (1987). Sequence from picomole quantities of proteins electroblotted onto polyvinylidene difluoride membranes. *J Biol Chem*, 262, 10035-10038.

Miyamoto K, Tsujibo H, Nukui E, Itoh H, Kaidzu Y & Inamori Y. (2002). Isolation and characterization of the genes encoding two metalloproteases (MprI and MprII) from a marine bacterium, *Alteromonas* sp. strain O-7. *Biosci Biotechnol Biochem.*, 66(2), 416-421.

Nakagawa T, Nagaoka T, Taniguchi S, Miyaji T & Tomizuka N. (2004). Isolation and characterization of psychrophilic yeasts producing cold-adapted pectinolytic enzymes. *Lett Appl Microbiol.*, 38(5), 383-7.

Nushin Aghajari, Filip Van Petegem, Vincent Villeret, Jean-Pierre Chessa, Charles Gerday, Richard Haser & Jozef Van Beeumen. (2003). Crystal structures of a psychrophilic metalloprotease reveal new insights into catalysis by cold-adapted proteases. *Proteins*, 50(4), 636-647.

Pirkko-Liisa Mäkinen & Kauko K Mäkinen. (1994). The enterococcus faecalis extracellular metallendopeptidase (EC3.4.24.30; coccolysin) inactivates human endothelin at bonds involving hydrophobic amino acid residues. *Biochem.. Biophys. Res. Commun.*, 200(2), 981-985.

Pirkko-Liisa Mäkinen, Don B Clewell, Florence An & Kauko K Mäkinen. (1989). Purification and substrate specificity of a strongly hydrophobic extracellular metalloendopeptidase ("Gelatinase") from streptococcus faecalis (Strain 0G1-10). *J. Biol. Chem.*, 264(6), 3325-3334.

Reisfeld R A, Lewis U J & Williams D E. (1962). Disk electrophoresis of basic proteins and peptides on polyacrylamide gels. *Nature*, 195: 281-283.

Ryoma Miyake, Jun Kawamoto, Yunlin Wei, Masanari Kitagawa, Ikunoshin Kato, Tatsuo Kurihara & Nobuyoshi Esaki. (2007). Construction of a low-temperature protein expression system using a cold-adapted bacterium, *Shewanella* sp. Strain Ac10, as the host. *Applied and Environmental Microbiology*, 73 (15), 4849-4856.

Shi, Jinsong, Wu, Qifan, Xu, Zhenghong & Tao, Wenyi. (2005). Identification of psychrotrophs SYP-A2-3 producing cold-adapted protease from the No. 1 Glacier of China and study on its fermentation conditions. *Acta Microbiol Sin.*, 45(2), 258-263.

Shi, Jinsong, Xu, Zhenghong, Wu, Qifan & Tao, Wenyi. (2006). Purification and characterization of cold-adapted protease produced by psychrotroph of glacier environment. *Chin J Appl Environ Biol.*, 12(1), 72-75.

Thomas J B, Gary W S & James H H. (1986). Activation of intracellular serine protease in bacillus subtilis cells during sporulation. *J. Bacteriol.*, 165(1), 139-145.

Wang, Yujing, Zhang, Manping, Sun, Mi, Wang, Yuejun, Xie, Hongguo & Chen, Chunguang. (2004). The chemical characteristics of marine low-temperature alkaline protease (YS-80-122). *Transactions of Oceanology and Limnology*, 1, 8-15.

Weber K & Osborn M. (1969). The reliability of molecular weight determination by dodecyl sulfate-polyacrylamide gel electrophoresis. *J. Biol. Chem.*, 244, 4406-4412.

Table 1. Summary of purification of protease

Purification steps	Total activity (U)	Total protein (mg)	Specific activity (U/mg)	Purification (fold)	Recovery (%)
Culture supernatant	3.5×10^5	14,265	25	1	100
Ammonium sulfate	2.8	95	2,950	118	80
DEAE-Sephadex A-25	0.8	12.8	6,250	250	23
DEAE-Cellulofin A-500	0.8	6.5	12,300	492	23

Table 2. Effects of inhibitor, denaturant and reducing agent on the activity of protease

Compound	Concentration	Relative activity (%)
Inhibitor		
None	0	100
PMSF	10 µg/ml	105
TLCK	10 µg/ml	100
Leupiptin	10 µg/ml	100
PCMB	10 µg/ml	105
ICH ₂ COOH	1.0 mM	98
EDTA-2Na	0.1 mM	58
Pepstatin A	10 µg/ml	81
n-Octyl alcohol	1.0 mM	99
Chymostatin	10 µg/ml	91
IAA	10 µg/ml	124
AEBSF	10 µg/ml	100
Phosphoramidon	10 µg/ml	119
Antipain	10 µg/ml	100
BHH	10µg/ml	100
Denaturant and reducing agents		
None	0	100
SDS	1.0 mM	102
Urea	1.0 mM	101
DTT	10 µg/ml	96
β-mercaptoethanol	1.0 mM	68

Table 3. Effects of metal ions on the activity of protease

Metal ion	Relative activity (%)	
	Concentration	
	1.0 mM	0.1 mM
None	100	100
Zn ²⁺	116	109
Fe ³⁺	112	100
Mn ²⁺	107	103
Mg ²⁺	106	100
Fe ²⁺	104	100
Co ²⁺	78	88
Ni ²⁺	74	82
Ag ⁺	72	82
Cu ²⁺	27	51
Hg ²⁺	8	10

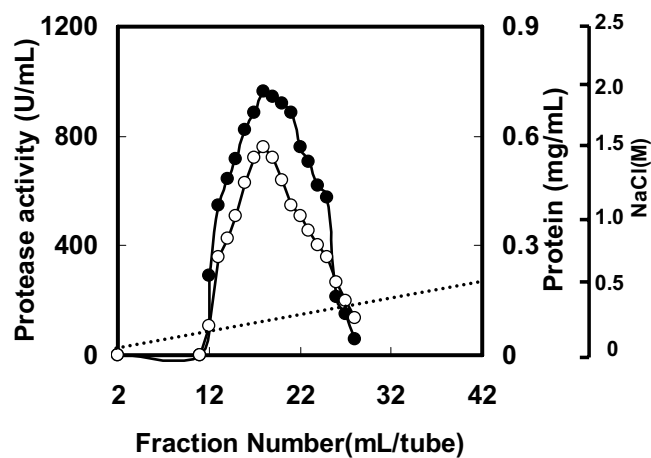


Figure 1. Column chromatography of protease on DEAE-Sephadex A-25

The enzyme solution (Fraction 2) was applied to a column (26×180 mm) of DEAE-Sephadex A-25 equilibrated with buffer A. The column was washed with 450 ml buffer A, then proteins were eluted with a linear gradient of 0 to 2.5 M NaCl solved in 720 ml buffer A. Fractions of 6.0 ml were collected at flow rate of 60 ml/h. Protein concentration and protease activities were assayed.

● represents enzyme activity; ○ represents protein concentration; ··· represents NaCl.

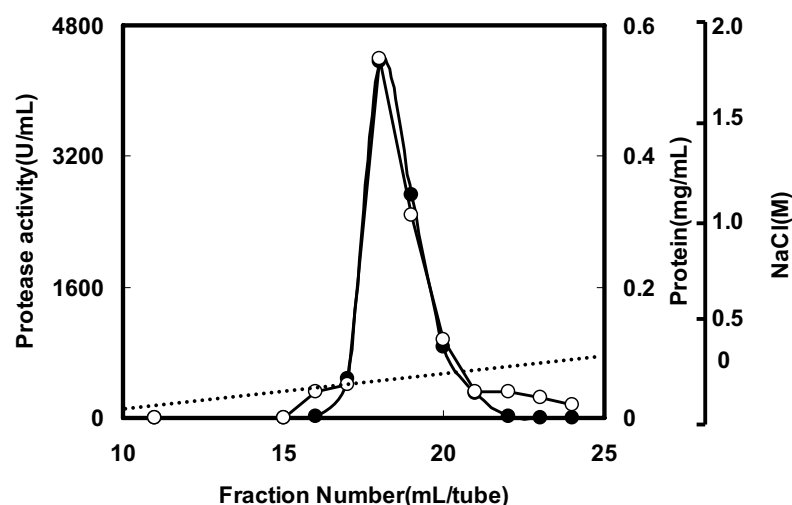


Figure 2. Column chromatography of protease on DEAE-Cellulofine A-500

The enzyme solution (Fraction 3) was applied to a column (26×180 mm) of DEAE-Cellulofine A-500 equilibrated with buffer A. The column was washed with 450 ml buffer A, then proteins were eluted with a linear gradient of 0 to 2.0 M NaCl solved in 720 ml buffer A. Fractions of 3.0 ml were collected at flow rate of 40 ml/h. Protein concentration and protease activities were assayed.

● represents enzyme activity; ○ represents protein concentration; ··· represents NaCl.

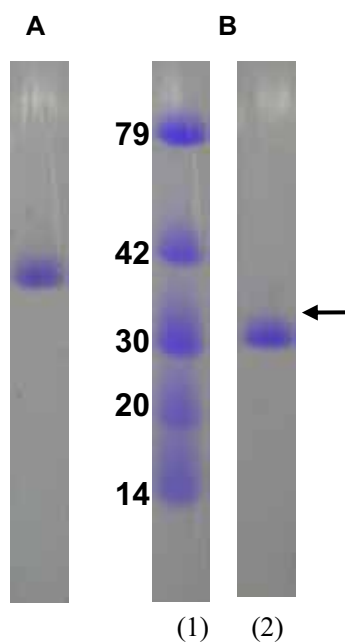


Figure 3. Native PAGE (A) and SDS-PAGE (B) of protease.

A: Native PAGE, the purified enzyme (5.0 μ g) was run on a 7.5% (w/v) gel with pH 4.0 at 2.5 mA/tube for 3.5 h in a running buffer (pH 4.5) of β -alanine-acetic acid.

B: SDS-PAGE, the purified enzyme (5.0 μ g) denatured with SDS was run on a 7.5% (w/v) gel containing 0.10% (w/v) SDS at 6.0 mA/tube for 3.0 h in a running buffer (pH 7.2) of 0.10% (w/v) SDS-0.10 M sodium phosphate.

The gels were stained with 0.25% (w/v) Coomassie Brilliant Blue R-250 in a solvent mixture of ethanol, acetic acid and water at the ratio of 9:2:9.

B(1): molecular weight markers: Lysozyme (14,000), trypsin inhibitor (20,000), carbonic anhydrase (30,000), aldolase (42,000) and bovine serum albumin (79,000).

B(2): purified enzyme.

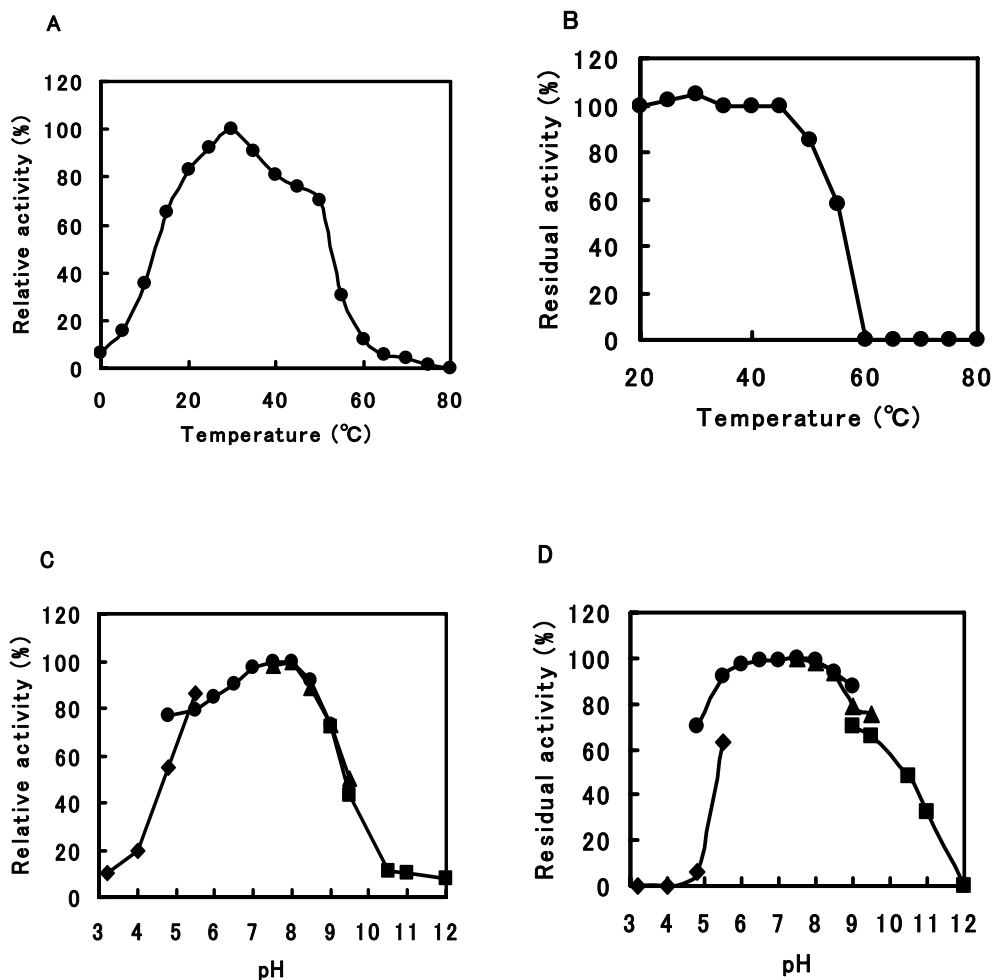


Figure 4. Effects of temperature on activity (A) and stability (B), and effects of pH on activity (C) and stability (D) At the amount of 1.25 % (w/v), Azocasein assay was used for characterization of the protease.

A: Protease activity was measured at 0-80 °C with pH of 7.5 for 10 min.

B: After heat treatment at various temperatures (20-80 °C) with pH of 7.5 for 10 min.

C: The buffer used was: (◆) 100 mM Ac (pH 3.2-5.5); (●) 100 mM Na₂HPO₄/KH₂PO₄ (pH 4.8-9.0); (▲) 100 mM Tris/HCl (pH 7.5-9.5) and (■) 100 mM NaCO₃/NaHCO₃ (9.0-12.0). Maximal activity of protease was defined as 100%. Enzyme assay was carried out at 30 °C for 10 min.

D: pH of the purified protease was adjusted in different buffers: (◆) 100 mM Ac (pH 3.2-5.5); (●) 100 mM Na₂HPO₄/KH₂PO₄ (pH 4.8-9.0); (▲) 100 mM Tris/HCl (pH 7.5-9.5) and (■) 100 mM NaCO₃/NaHCO₃ (pH 9.0-12.0) buffer. The enzyme was incubated at 4°C overnight, then the residual activity of protease was measured at pH 7.5 for 10 min.



Model Stability Analysis of Marine Ecosystem

Yuejian Jie & Yuan Yuan

College of Sciences, China Agriculture University, Beijing 100094, China

E-mail: jieyj@cau.edu.cn

Abstract

Based on a number of actual factors interfering with the research, according to the original Lotka-Volterra model and actual situation of marine ecosystem, a modified Lotka-Volterra model was applied to obtain realistic data with attempts to discuss the stability, limit cycle and ecological significance of the modified model.

Keywords: Population, Predatory model, Limit cycle

1. Introduction

Population dynamics is the dominant branch of ecology, that studies environmental conditions, interactions between individuals, interactions with other species, and trend of evolvement and development, reveals the variations of biological population, utilizes resource properly and promotes ecological balance through mathematical modeling, which showed that math has been deeply applied in ecology so far and become a systematic and in-depth branch. Currently, ecological mathematical models applied as an important method to study ecology, have played a vital role in elucidating ecological phenomena, depicting ecological processes of energy information and value orientation, deciphering inherent law of ecosystem, forecasting biological trend, adjusting controllable ecosystem directionally, optimizing administrative ecosystem and so on. Mathematical models are used not only as one of the basal theories for qualitative and quantitative analysis of ecosystem, but also a way to solve the practical issues of ecology, get optimal management of agriculture, forest, animal husbandry and fishery ecosystem and improve ecological benefits.

2. Original model and its modification

2.1 Model establishment

Assumed $x(t)$ and $y(t)$ as the size of prey and predator respectively, the only factor inhibiting population proliferation resulted from the pressure of predators, while the increment limitation of predators depend on the size of preys. If such, without preys, the population size of predators increased exponentially at a rate of α ; Whereas without predators, the population size of preys died exponentially at a rate of β . Therefore, coefficient α and β were intrinsic growth rate of preys and intrinsic death rate of predators respectively.

Assumed $\varphi(x)$ as nutrition function of predators, in which K was applied as the increment of predators and $(1-k)\varphi(x)$ as the activity of maintaining metabolism and hunting, herein, predator-prey dynamic system equation was expressed as follows:

$$\begin{cases} dx/dt = \alpha x - \varphi(x)y \\ dy/dt = y(k\varphi(x) - m) \end{cases}$$

However, the Lotka-Volterra model in general cannot be applied to most ecological systems due to the strict limitations imposed by the necessary assumptions. This study shows that modification of the model can be made by considering the biological or ecological implications.

Volterra model is simple and not adapt to many practical predator-prey system. In the present paper, there are still limitations existed in our marine predator-prey ecosystem between grampus and cod. For example, in the original model, without predators (grampus), the numbers of preys(cod) could increase unlimitedly, however, it is not really the case in practice due to any population is confined to resources(food, environment etc.) and thus has a limited size. On the other hand, total numbers of predators (grampus) eating preys(cod) per time unit with the increasing size of preys could increase to infinity, and this also is impossible due to pure physiological limitations.

Considering interfering factors, when dealing with our marine predator-prey ecosystem between grampus and cod,

intraspecific competition or density dependence of preys and predators was introduced into Volterra model, and thus the modified model was expressed as follows:

$$\begin{cases} dx/dt = \alpha x - \beta xy - \gamma x^3 \\ dy/dt = k\beta xy - my \end{cases} \quad (2.0)$$

Where $\gamma > 0$, γx^3 described intraspecific competition.

Considering density dependence of predators population, interfering factors affecting functional response, namely mechanical effects of nutrition relationship between preys and predators on regulating numbers of predators population were further introduced, and thus Π functional response was added to the modified model.

Herein the modified model with Π functional response was expressed as follows:

$$\begin{cases} dx/dt = x(g(x) - ay/1 + wx) \\ dy/dt = y(-d + eax/1 + wx) \end{cases} \quad (2.1)$$

Where $g(x)$ was density dependence of preys without predators, a, d, e, w were positive parameters, and $ax/1 + wx$ was Π functional response of predators population.

2.2 Stability analysis and limit cycle discussion of the modified model

2.2.1 Stability and limit cycle of the modified model of preys intraspecific competition

Obviously, limit cycle of preys population size was $\bar{x} = \alpha/\gamma$ without predators, point (x^*, y^*) was the only nontrivial equilibrium point of the modified equation, and herein we had

$$x^* = m/k\beta, y^* = (\alpha k^2 \beta^2 - \gamma m^2)/k^2 \beta^3$$

When one condition was met: $(x^*)^2 \leq \bar{x}(m^2/k^2 \beta^2 \leq \alpha/\gamma)$, y^* would be certain to be positive and thus the positive equilibrium point existed.

The increment of the studied population of predators(grampus) and preys(cod) was all limited by density,so the equilibrium point was partly and progressively stable.

When $\gamma m(\gamma + 4\beta k) < 4\alpha k\beta$, point (x^*, y^*) was the focus. Therefore, the modified model has whole stability.

As far as the function $V(x, y) = x^*(x/x^* - \ln(x/x^*) - 1) + y^*(y/y^* - \ln(y/y^*) - 1)/k$ was concerned, for any $z > 0$, the inequation $z - 1 \geq \ln z$ existed (equal when $z = 1$). It could be easily observed that in the positive quadrant of plane (x, y) , $V(x, y) \geq 0$ existed everywhere. Only at the point of (x^*, y^*) where function V had continuous partial derivatives and trajectory derivative met $dV/dt = -\gamma(x - x^*)^2 \leq 0, V = 0$ existed.

Obviously, when $\gamma \neq 0$, derivative dV/dt was zero only at the point of $x = x^*$. Point (x^*, y^*) is the only invariant sets of the beeline. Therefore, it could be speculated that the point was progressively stable and the stability region superposed the positive quadrant of plane (x, y) . So no limit cycle existed in the positive quadrant, namely that point (x^*, y^*) is the stable focus, and thus in any region of the positive quadrant, the structure was stable.

Ecological significance: through the systematic analysis of the modified model, results showed that intrinsic growth rate decreased with the increasing of its size without predators, from positive values to negative ones; There was intraspecific competition in the preys population due to the limited resource, and thus even if without predators, the size of preys could not increased infinitely and approached to a stable state of $x = \alpha/\gamma$; With the increasing of preys size, intrinsic growth rate increased, from negative values(food deficiency) to positive ones; Finally, as the time went by, the number of preys and predators approached to stable at the point (x^*, y^*) .

2.2.2 Stability and limit cycle of the modified model of Π functional response

Supposed that there was a positive equilibrium point (x^*, y^*) in the modified model and $x^* > 0, y^* < 0$ were met with the following equation groups:

$$g(x^*) - \frac{ay^*}{1 + wx^*} = 0, \quad -d + \frac{eax^*}{1 + wx^*} = 0. \quad (2.2)$$

Therefore, $x^* = \frac{d}{ea - wd}$, $y^* = \frac{1}{a}g(x^*)(1 + wx^*)$ could be speculated. This equilibrium position existed only at

the condition of $ea > wd$, $g(x^*) > 0$. In brief, $s = \frac{1}{(1 + wx)(1 + wx^*)}$. Equation (2.2) introduced into (2.1), the

following equation was obtained:

$$\begin{cases} dx/dt = x(g(x) - g(x^*) - \frac{ay}{1 + wx} + \frac{ay^*}{1 + wx^*}) \\ dy/dt = y(\frac{eax}{1 + wx} - \frac{eax^*}{1 + wx^*}) \end{cases} \quad (2.3)$$

Function Liapunov was made as follows:

$$V = x - x^* - x^* \ln \frac{x}{x^*} + c(y - y^* - y^* \ln \frac{y}{y^*}),$$

Where C was constant, and to be determined. Along with the solution of equation (2.3), we had

$$dV/dt = (x - x^*)[g(x) - g(x^*) + awy^*s(x - x^*)] - a(1 + wx^*)(x - x^*)s(y - y^*) + cea(x - x^*)s(y - y^*),$$

If we assumed that $c = \frac{1}{e}(1 + wx^*)$, we had

$$dV/dt = (x - x^*)[g(x) - g(x^*) + awy^*s(x - x^*)] \quad (2.4)$$

Under the condition of theorem, for all $x > 0, y > 0$ and $x \neq x^*$, equation (2.12) was negative; Only at the condition of $x = x^*$, equation (2.4) was zero. Therefore, there was only one equilibrium position and consequently, the modified model of Π functional response was totally stable.

Ecological significance: Stability and limit cycle of the model means that the ecosystem of predators (grampus) and preys(cod) was stable, and coexisted in a long term. Their size tended to a periodic oscillation finally. Predators continuously improved their own capability, namely searching, catching and chasing in order to make their preying strategies of arresting and hunting get improvement; Preys persistently promoted their own ability, namely protective coloration, mimesis, warning coloration, resisting and evading in order to make their anti-arresting strategies of suspended animation and hiding get improvement. Density of the two populations increased/decreased at the same time, or increased/decreased alternatively, moving in cycles, which made them coevolution.

3. Numerical simulation

3.1 Numerical simulation by MatLab

Through numerical analysis of equation (2.0) by MatLab, we assumed that $\alpha = -0.15, \beta = 2.5, \gamma = 0.1, k = 0.2, m = 0.008$, namely equilibrium point (0.016, 0.0131), and we have

<Figure 1>

<Figure 2>

As seen from figures, X decreased with the increasing of X, and approached to stable at the equilibrium point (0.016, 0.0131).

Conclusions: Intraspecific competition predator-prey system established by the modification of Lotka-Volterra model was a stable ecosystem. However, the number of predators (grampus) and preys(cod) failed to approach to stable at the point (x^*, y^*) as time went by in practical but tended to a periodic oscillation. The modified model was not completely coincidence with practice and need further modification considering other interfering factors.

Through numerical analysis of equation (2.1) by MatLab, we assumed that $a = 0.5, d = 0.25, e = 0.1, w = 0.05$, which satisfied the following constraint $a_2 + 2a_3 > 0$, and we had

<Figure 3>

<Figure 4>

<Figure 5>

As seen from figures, we could also speculate that the values of X and Y approached to a periodic oscillation within their range as time went by and limit cycle existed in the model where values of X and Y were ranged as follows:

$$\{(x, y) \mid 0 \leq x \leq 6.5, 0.5 \leq y \leq 7.7\}$$

Conclusions: Through comparison analysis of object data and model data, equation tended to stable finally, and values of (x, y) tended to limit cycle and periodic oscillation which was coincidence with practice, and thus the model is practical.

3.2 Discussions about limitations of the model

For the modified model, basically in agreement with practice, but there are still some insufficiency and issues tough to deal with.

Firstly, marine ecosystem has its mobility. In the present paper, data was collected from the records of grampus and cod number in a certain sea area at a certain period, and could solve such issues with regard to the possibilities of immigration and emigration among the fish population.

Secondly, grampus as a carnivore would prey on other fishes when preys (cod) was in a extremely low scale. However, in the present model, assumption that grampus only preyed on cods, not totally in agreement with practice, and thus would affect the veracity of the model.

Finally, some factors as intervening marine ecosystem, grampus battue, deep sea fishing of cods and marine pollution imposed by human being would all affect the veracity of the model to some extent.

References

- Chen, L.S. (1998). *Models and studies of mathematical ecology*. Beijing: Science press.
- Gao, L.Q., Hethcote, H.W. (1992). Disease transmission models with density-dependent demographics. *J. Math.Biol.*, 30:717-731.
- Hadeler, K.P., Freedman, H.I. (1989). Predator-prey populations with parasitic infection. *J.Math.Biol*, 27:609-631.
- Mena-Lorca, J., Hethcote, H.W. (1991). Parasitism: a cryptic determinant of animal community structure. *Trends Ecol.Evol.*, 6:250-254.
- Shen, G.Y., Shi, B.Z. (2005). *Marine ecology (second edition)*. Beijing: Science press.
- Venturino, E. (1994). The influence of diseases on Lotka-Volterra systems. *J.Math*, 24:381-402.
- Wang, S.Q., Wang, W.X., & Xu, H.G. (2004). *Stable theories and methods of mathematical ecology (first edition)*. Beijing: Science press.

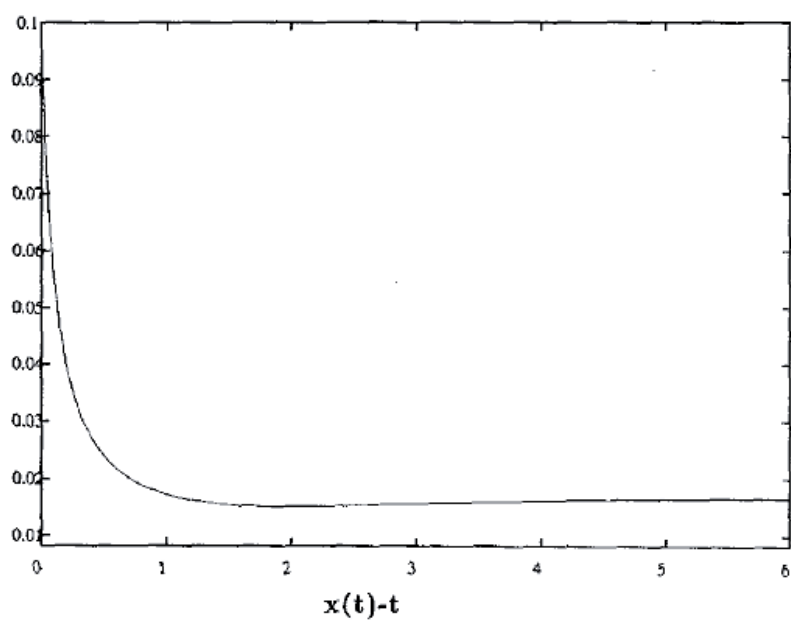


Figure 1.

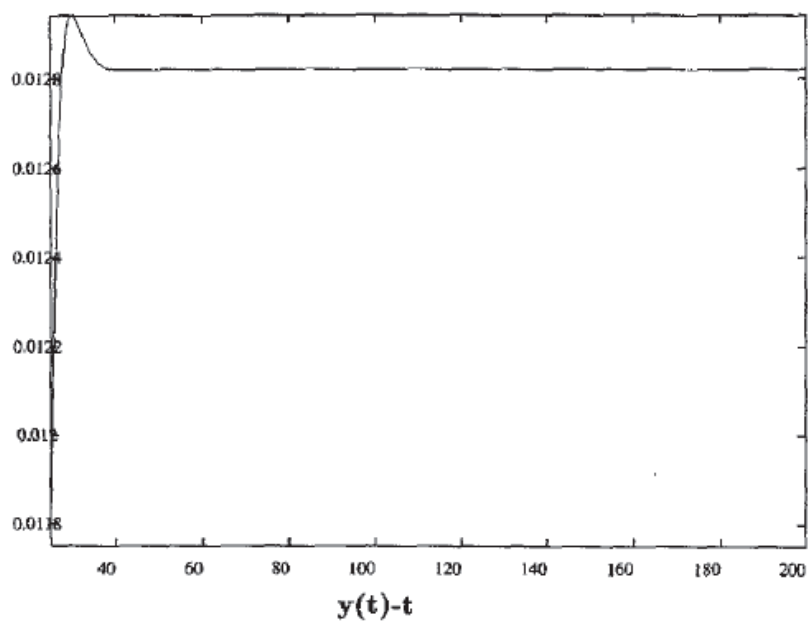
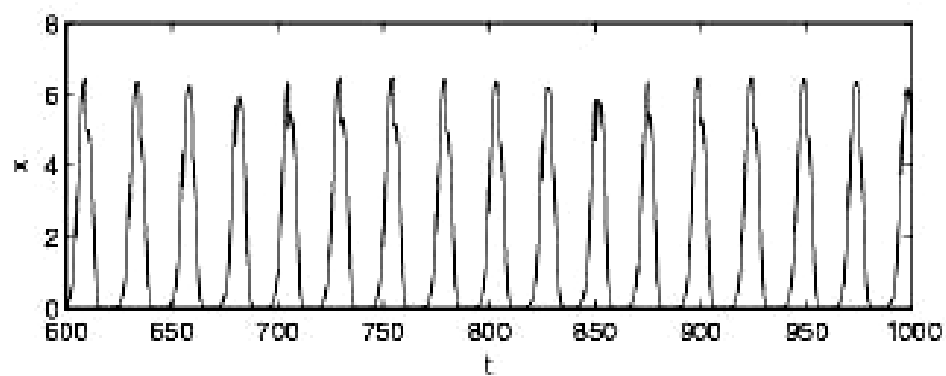
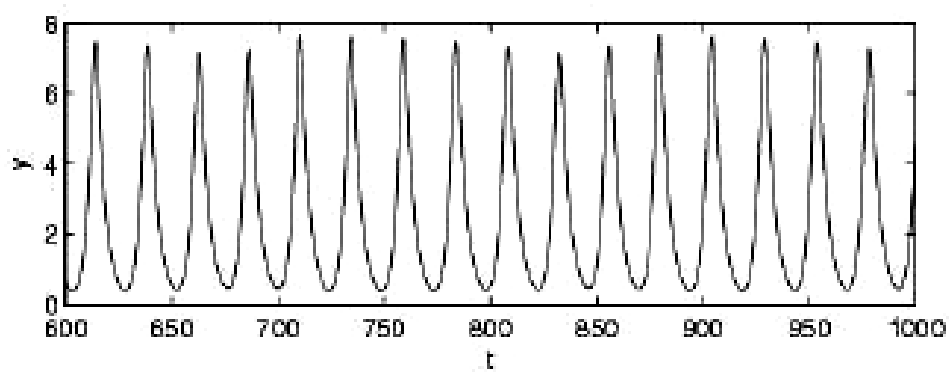


Figure 2.



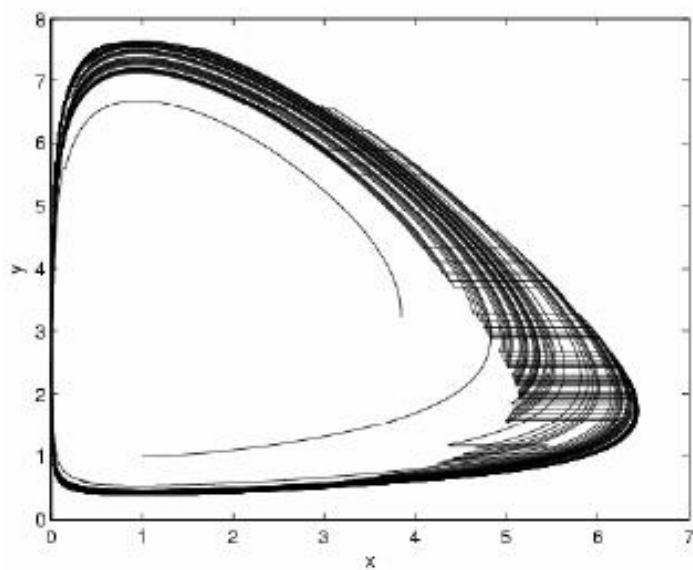
$X(t) \sim t$

Figure 3.



$Y(t) \sim t$

Figure 4.



Phrase map of $X(t)$ and $Y(t)$

Figure 5.



Preliminary Study on Mitochondrial DNA Cytochrome *B* Sequences and Genetic Relationship of Three Asian Arowana *Scleropages Formosus*

Yinchang Hu

Pearl River Fisheries Research Institute, Chinese Fishery Academy of Sciences

Xilang, Fangcun district, Guangzhou 510380, China

Tel: 86-20-8161-6088 E-mail: huyc2@163.com

Xidong Mu

Pearl River Fisheries Research Institute, Chinese Fishery Academy of Sciences

Xilang, Fangcun district, Guangzhou 510380, China

Tel: 86-20-2217-5232 E-mail: muxd1019@126.com

Xuejie Wang

Guangzhou tiny-lake aquatic organism technology co., ltd

Xilang, Fangcun district, Guangzhou 510380, China

Tel: 86-20-81617952 E-mail: aqwang@163.com

Chao Liu

Guang zhou tiny-lake aquatic organism technology co., ltd

Xilang, Fangcun district, Guangzhou 510380, China

Tel: 86-20-81617952 E-mail: truman.liu@tom.com

Peixin Wang

Pearl River Fisheries Research Institute, Chinese Fishery Academy of Sciences

Xilang, Fangcun district, Guangzhou 510380, China

Tel: 86-20-8161-6127 E-mail: wpx@126.com

Jianren Luo

Pearl River Fisheries Research Institute, Chinese Fishery Academy of Sciences

Xilang, Fangcun district, Guangzhou, 510380, China

Tel: 86-20-8161-6133 E-mail: fishlo@163.net

The research is financed by The People's Republic of China Ministry of Agriculture Affairs State(948), Science Research Institute fund of scientific research operational fee technical Program from Chinese Academy of Fishery Sciences Research InstituteNo. 2130108, Technology fund of Pearl River Fisheries Research InstituteNo.2003-3-5, Science and Technology Developing Fisheries Program of liwan district Guangdong Province. No. 20082109029

Abstract

Mitochondrial DNA cytochrome *b* (*cytb*) gene complete sequences of golden arowana, red arowana and green arowana of *Scleropages formosus* were amplified with PCR technique and sequenced. The sequence length was 1141bp for three Asian arowanas which had 5 nucleotide sites substituted, among of them 4 base substitutions were transition and only 1 was transversion, all of the base substitution happened in the third locus of the codon which only 1 site caused amino acid variation. A global deficit of guanosines (G:13.7%) and approximately equal frequencies of the other three nucleotides (A: 27.8 %, C: 34.6 %, T: 23.9%) and G+C content (48.3%) was quite constant among sequences. The genetic distance of mtDNA *cytb* gene sequences was 0.0026-0.0035 between green arowana and the other two Asian arowana, which indicated that Asian arowana perhaps did not evolve to the level of specie. Phylogenetic trees were constructed with NJ method and MP method using arithmetic average method. The results showed that red arowana clustered with golden arowana, after clustering with green arowana.

Keywords: *Scleropages formosus*, Cytochrome**b**, Genetic relationship

1. Introduction

Asian arowana (*Scleropages formosus*) is known as dragonfish, Asia Bonytongue, kelisa or bajurantai. There are considered "lucky" by many people, particularly those from Asian cultures. Due to its popularity and great demand, Asian arowanas have been fiercely hunted in its native habitat for profits, causing declination of the population of these fishes in the wild. Arowanas have been classified as an endangered species, threatened with extinction in CITES appendix I since 1980 (Joseph, 1986, p73) and have listed as endangered by the 2006 IUCN Red List (Kottelat, 1996). There are a number of breeders registered CITES in Asia so that the specimens what they produce can be imported into several nations. Other nations restrict or prohibit possession of Asian arowanas. The Asian arowana consists of geographically isolated strains distributed in Southeast Asia. The green, gold strains of Asian arowana have lower commercial value than the red one (Kottelat, 1993). More work is needed to understand genetic relationship in arowanas.

Mitochondrial DNA analysis has become a widely used technique for many applications in population or evolutionary studies (Avice, 1986, p1192; Fumihito et al, 1995, p11053; Randi et al, 2000, p1103). The cytochrome *b* gene (*cytb*) from mitochondrial genome contains species-specific information and has been used in phylogeny (Irwin, 1991, p128). In the study, mtDNA *cytb* sequences of three Asian arowana were obtained and compared with each other for further clarifying phylogenetic relationship among Asian arowanas, with a view to raise awareness of resources.

2. Material and methods

2.1 Samples and DNA isolation

Fin clips of three Asian arowanas samples from Guangzhou tiny-lake aquatic organism technology co., Ltd housed which were originated from Malaysia collected in 2001, were collected, and kept in absolute ethanol. Genomic DNA was extracted from Fin clip of each fish using a Blood & Cell Culture DNA Kit (Tiangen, Beijing, China).

2.2 PCR protocol

PCR was performed in a final volume of 20 μ l using a Cyclor machine. The reaction mix contained 10 \times PCR buffer 2.0 μ l, MgCl₂ (25mmol/L) 1.6 μ l, dNTPs (10 mmol/L each) 0.4 μ l, each primer (20 μ mol /L) 0.5 μ l, Taq DNA polymerase (5U/Ml) 0.3U, and DNA template 50ng. The primers used for the amplification were *cytb1* (5'-TGCGACTAAACATAAATGTTTAG-3') and *cytb2* (5'-TGTATGGAAA TTGCAGTTATG-3'). Amplification was carried out using 2 min of initial denaturation followed by 30 cycles of 50s of denaturation at 94°C, 50s annealing at 52°C and 60s extension at 72°C with a final extension period of 5 min at 72°C. After the electrophoretic run, DNA molecules were visualized under UV light and analyzed. The amplified products were sequenced directly with an ABI DNA Sequencer. Sequencing reactions were carried out as recommended by the manufacturer.

2.3 Sequences and alignment

DNA sequences were initially automatically aligned using Clustal X vers. 1.8 (Thompson, 1997, p4876), followed by manual editing. Phylogenetic analysis of the aligned sequences was performed with the Molecular Evolutionary Genetics Analysis (MEGA) program vers. 3.0 (Kumar, 2001). Distance analysis was conducted using the Neighbor-joining (NJ) option employing the p-distance with gap data treated as pairwise deletions. MP analysis was conducted using heuristic searches, 1000 bootstrap replicates, and 100 randomly added trees of sequences to search for the most parsimonious trees.

3. Results

3.1 Sequence characteristics and variation

1141bp length for the entire *cytb* were sequenced for three Asian arowana (Figure 1). All sequences were submitted to GenBank (accession to GenBank: Gold Arowana, EU594546, Red Arowana EU594545, Green Arowana EU594547).

Base composition in three sequences was similar to that of previously reported fish cytochrome *b* sequences (Rafael, 1998, p1365; Jerome, 1998, p100; Johanna, 2007, p43): low G content (mean: 13.7%) and almost equal A, C, and T contents (mean: 27.8, 34.6, and 23.9%, respectively). This pattern was mainly due to third codon positions (mean G content at third codon positions: 4.1%) and to a lesser extent to second codon positions (mean G content at second codon positions: 13.2%), whereas base composition in first codon positions was balanced (mean T, C, A, and G contents at first codon positions: 22.3, 27.6, 26.4, and 23.7%, respectively) (Table1.). Base composition was quite homogeneous among sequences: G+C content 48.3%.

Among 1141 nucleotide sites, 5 nucleotide sites substituted, among of them 4 base substitutions were transition and only one was transversion, all of the base substitution happened in the third locus of the codon which only 1 site caused amino acid variation, suggesting that these sites may be prone to saturation.

3.2 Phylogenetic Relationships

Genetic distances within and between stocks based on *cytb* are shown in Table 2. For *cytb*, the results indicate that genetic distances within populations were below 0.1%. Based on the *cytb* sequences, the MP and NJ trees of three Asian arowanas were constructed. The MP and NJ tree had the same (Figure2). The results showed that these two methods were effective in common laboratories.

4. Discussion

1141bp length for the entire *cytb* genes were sequenced of three Asian arowana, containing the start codon ATG, with T for the stop codon which is not a complete stop codon in the transcription process to be added after the formation of polyA stop codon. This study showed that genetic distance among three Asian arowanas between 0.26% ~ 0.35%. Billington (1991, p80) reported intraspecific divergence at the 10% of the general level. Nei (1990, p873) that the same individuals are generally 0.1% to 5% of the divergence. According to both differences in the degree of *cytb* gene, the study concluded that three Asian arowanas differentiation between the subspecies may have already reached the level Consistent with the morphological.

Since Muller first found and named in 1933, the taxonomic classification of *Scleropages formosus* has undergone not any changes. *Scleropages formosus* refers to several varieties of freshwater fish in the genus. The present study demonstrates that the classification of subspecies is consistent with the genetic clusters in *Scleropages formosus*. Geological evidence showed that continental Southeast Asian terranes could be classified into two categories, based on their Late Palaeozoic tectonic history (Hutchison, 1993, p883). It is believed that different strains of arowana inhabit separate regions of Southeast Asia and were connected through freshwater habitats during the Pleistocene era (Goh, 1999), implying that freshwater fishes could not have migrated between the two supercontinents after 160 MYA. The fossil records of *Scleropages* which should be considered in evaluating the migrational history of the Asian arowana. Freshwater beds of Eocene times (35–57 MYA) in central Sumatra yielded fossils that could be attributed to the genus *Scleropages*. The Indian subcontinent became connected to Eurasia by the late Early Eocene (Jaeger, 1989, p316; Metcalfe, 1999, p9) implying an ancestor of the Asian arowana originated when Laurasia and Gondwanaland were still connected and that it dispersed via fresh water habitats from Gondwanaland to Laurasia. The morphological similarity of all *Scleropages* species shows that little evolutionary change has taken place recently for these ancient fish (Kumazawa, 2000, p1869). The morphological similarity of all *Scleropages* species shows that little evolutionary change has taken place recently for these ancient fish. Genetic studies also have confirmed these. Yue (2000, p1007; 2000, p89; 2002, p1025; 2003, p951; 2006, p627) successfully examined genetic diversity and population structure of *Scleropages formosus* originating from the south-east Asian region using RAPD and AFLP, and reported the identification of a sex-associated AFLP marker and a strain-specific RAPD marker in the Asian arowana using pooled DNA samples. The two markers were successfully converted into STS markers and are applicable for rapid sexing of the green strain or for differentiation of the Indonesian golden strain from blood red and green varieties respectively. Tang (2004, p81) supported the view that green arowana is the outgroup among the arowana strains using microsatellite and mtDNA. At the same time, the results showed the correlation between molecular marker diversity and geographic region that several of arowana strains diverged from late Pliocene to middle Pleistocene. The isolated strains evolved at intraspecific level. As noted above, genetic estimates of divergences suggest an early divergence between Asian arowanas taxa occurred from the late Pliocene to middle Pleistocene. However, it should also be greater use of molecular markers, such as D-loop, COI to verify this inference, etc.

References

- Avice, J.C. (1989). Gene trees and organismal histories: a phylogenetic approach to population biology. *Evolution*, 43: 1192-1208.
- Billington N, & Hebert PDN. (1991). Mitochondrial DNA diversity in fishes and its implications for introductions. *Can J Fish Aquat Sci*, 48(sup.): 80-94.
- Dawes J, Lim LL, Cheong L. (1999). *The Dragon Fish*. Kingdom Books England.

- Fumihito A, Miyake T, & Sumi SI. (1995). The genetic link between the Chinese bamboo partridge (*Bambusicola thoracica*) and the chicken and junglefowls of the genus *Gallus*. *Proceedings of the National Academy of Science of the United States of America*, 92(24):11053-11056.
- Goh, W., & Chua, J. (1994). *The Asian arowana. Dragon Fish Industry*. Singapore: E-Publishing Inc. pp.17-24
- Hutchison, C.S. (1993). Gondwana and Cathaysian blocks, Palaeotethys sutures and Cenozoic tectonics in Southeast Asia. *Geologische Rundschau*, 82: 388-405.
- Irwin DM, Kocher TD, & Wilson AC. (1991). Evolution of cytochrome b gene of mammals. *J Mol Evol*, 32:128-14
- Jerome B, Nicolas G, & Miguel B. (1998). Molecular Phylogeny of Cyprinidae inferred from cytochrome b DNA Sequences. *Molecular phylogenetics and evolution*, 9(1): 100-108
- Johanna J, Christo V, & Jon-Arne S. (2007). Four genes, morphology and ecology: distinguishing a new species of *Acesta* (Mollusca; Bivalvia) from the Gulf of Mexico. *Mar Biol*, 152:43-55.
- Joseph J, Evans D, & Broad S. (1986). International trade in Asian Bonytongues. *Traffic Bulletin*, 3, 73-76.
- Kottelat M, Whitten AJ, & Kartikasari SN. (1993). *Freshwater Fishes of Western Indonesia and Sulawesi*. Periplus Editions (HK) Ltd, Indonesia.
- Kottelat, M. (1996). *Scleropages formosus*. (2006). IUCN Red List of Threatened Species. IUCN 2006.
- Kumar S, Tamura K, & Nei M. (2001). MEGA (Molecular evolutionary genetics analysis), Version 3.0. Tempe: Arizona State University.
- Kumazawa Y, & Mutsumi N. (2000). Molecular Phylogeny of Osteoglossoids: A New Model for Gondwanian Origin and Plate Tectonic Transportation of the Asian Arowana. *Mol. Biol. Evol*, 17(12): 1869-1878
- Jaeger, J.J., v. courtillot, & p. tapponnier. (1989). Paleontological view of the ages of the Deccan Traps, the Cretaceous/Tertiary boundary, and the India-Asia collision. *Geology*, 17:316-319.
- Metcalfe, I. (1999). Gondwana dispersion and Asian accretion: an overview. Pp. 9-28.
- Nei M, & Miller JC. (1990). A simple method for estimating average number of nucleotide substitution within and between populations from restriction data. *Genetics*, 125:873-879.
- Randi V, Lucchini T, & Armijo P. (2000). Mitochondrial DNA phylogeny and speciation in the Tragopans. *Auk*, 117(4):1003-1015.
- Rafael Z, & Ignacio D. (1998). Phylogenetic relationships of Iberian cyprinids: systematic and biogeographical implications. *Proc. R. Soc. Lond. B*, 265:1365-1372.
- Tang PY, & Sivananthan J. (2004). Pillay SO, et al. Genetic Structure and Biogeography of Asian Arowana (*Scleropages formosus*) Determined by Microsatellite and Mitochondrial DNA analysis. *Asian Fisheries Science*, 17:81-92.
- Thompson J D, Gibson T J, & Plewnia F. (1997). The Clustal_X windows interface: Flexible strategies for multiple sequences alignment aided by quality analysis tools. *Nuc Aci Res*, 25: 4876-4882.
- Yue GH, Li Y, & Chen F. (2002). Comparison of three DNA markers systems for assessing genetic diversity in Asian arowana. *Electrophoresis*, 23:1025-1032.
- Yue GH, Chen F & Orban L. (2000). Rapid isolation and characterization of microsatellites from the genome of Asian arowana (*Scleropages formosus*, Osteoglossidae, Pisces). *Mol Ecol*, 9:1007-1009.
- Yue, G.H., Li, Y., & Chen, F. (2000). Monitoring the genetic diversity of three Asian arowana (*Scleropages formosus*) stocks using AFLP and microsatellites. *Aquaculture*, 237, 89-102
- Yue, G.H, Ong, D, & Wong, CC. (2003). A strain-specific and a sex-associated STS marker for Asian arowana (*Scleropages formosus*, Osteoglossidae). *Aquaculture Research*, 34 (11): 951-957.
- Yue, G.H., Zhu, Z.Y., & Lin, L.C. (2006). Novel polymorphic microsatellites for studying genetic diversity of red Asian Arowanas. *Conservation Genetics*, 7, 627-629.

Notes

Note 1. This is an example.

Note 2. This is an example for note 2

Note 3. This is an example for note 3

Table 1. Nucleotide composition for cytochrome*b* gene sequences(1141bp) of Asian arowana

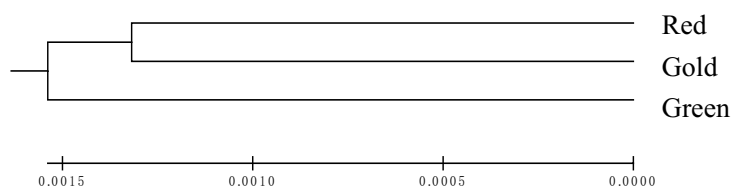
Nucleotide composition	T(%)	C(%)	A(%)	G(%)	A+T(%)	G+C(%)
Green arowana	23.9	34.6	27.8	13.7	51.7	48.3
Red arowana	24.0	34.5	27.8	13.7	51.8	48.2
Gold arowana	23.9	34.6	27.8	13.7	51.7	48.3
Average	24.0	34.6	27.8	13.7	51.8	48.2

Table 2. Genetic distance among three Asian arowanas

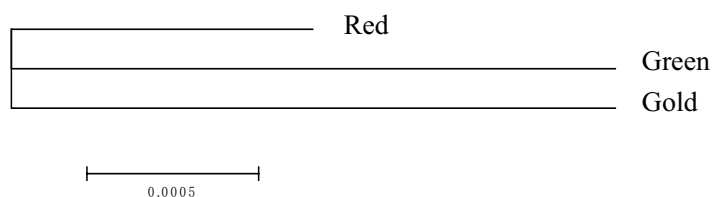
	Red arowana	Green arowana	Gold arowana
Red arowana	-		
Green arowana	0.0026	-	
Gold arowana	0.0026	0.0035	-



Figure 1. Agarose gel electrophoresis of *Cytb* gene PCR products
 1: Green Arowana; 2: Gold Arowana; 3: Red Arowana; 4: Blank; M:marker



a.



b.

Figure 2. Phylogenetic trees of the three Asian arowanas based on the *cytb* sequences
 a. MP b. NJ trees



Genetic Variation of Six *Azadirachta excelsa* (Jacks) Jacobs Populations

Hazandy Abdul-Hamid

Institute of Tropical Forestry and Forest Products

Universiti Putra Malaysia, 43400 Serdang, Selangor, Malaysia

Tel: 603-8946-7585 E-mail: hazandy@gmail.com; hazandy@putra.upm.edu.my

The research is financed by Universiti Putra Malaysia seed money.

Abstract

The study of the extent and pattern of genetic variation of six populations of *Azadirachta excelsa* (Jacks) Jacobs, i.e. Manong (Perak), Pokok Sena (Kedah), Sik (Kedah), FRIM (Selangor), Merchang (Terengganu) and Sg. Caru (Pahang) was carried out using starch gel electrophoresis. The analysis on eleven enzyme systems was found to be coded by 25 and 26 loci. The mean of observed heterozygosity ranged from 0.08 to 0.11 and the percentage of proportion of polymorphic loci varied from 61.54% to 73.08%. The extents of genetic identities ranged from 0.81 to 0.98.

Keywords: *Azadirachta excelsa*, Isozyme, Observed heterozygosities, Polymorphic loci

1. Introduction

The ecosystem of tropical rainforest of Malaysia is extremely complex and rich with tree species. In Peninsular Malaysia alone, the flora is estimated to comprise of 7,500 species of seed plants of which 4,100 are woody species (Whitmore 1975). However, its species richness may be threatened due to rapid destruction of the forest. Globally, an estimation of indiscriminate deforestation of tropical forest at 10.4 million hectares a year in the period of 2000-2005 (FAO 2005) has caused the genetic erosion of many valuable forestry species. In Malaysia alone the rate of change in total deforestation is about 85.7% between 2000-2005 and 1990-2000 period (FAO 2005). This has resulted in the disappearance of many valuable genetic traits that gives cause for much apprehension. Forest plantation is one of the approaches which is not only catering the problem of timber shortage but can also be served as a conservation mean.

In Malaysia, most of plantation forestry involved exotic species such as *Acacia mangium*, *Tectona grandis*, *Khaya ivorensis* and *Pinus caribaea* but no major successful outputs were recorded to date. However, the approach of establishing plantation forestry should not be stopped with that hiccup. The idea by shifting the attention to the fast growing indigenous is highly acceptable because these species are readily available at vast in our region and well adapted to our physical and biological environment. The cost of establishing and managing plantations can be reduced by this movement and conservation works can also be done at the same time. Nevertheless, careful plans should be initiated first together with extensive and thorough researches to avoid any unnecessary outcome. One of the important scientific information that should be gathered is about genetic variation of selected indigenous species. However, the knowledge about genetic traits of promising indigenous species is still lacking. This information is actually needed which is can help forest managers to identify the appropriate indigenous species for plantation and conservation purposes.

In this study, we used *Azadirachta excelsa* which is said to be one of the fast growing indigenous species. *A. excelsa* has the potentials to be considered as a plantation species to this region. *A. excelsa* is a tree of lowland monsoon forests from sea level up to an altitude of approximately 300 m and is of scattered distribution. It inhabits a vast region in Southeast Asia extends from Peninsular Malaysia, Sumatra, Borneo to northward in Myanmar, the Philippines, Papua New Guinea and the Aru Islands (Schmutterer and Doll 1993). It is a multipurpose valuable species that has been reported to produce good quality timber for use in construction, panelling, partitioning, flooring, plywood manufacture and packing cases, house and boat building, cigar boxes, shop fitting and production of piano (Jacobs 1960, Burgess 1966, Wong 1976, Corner 1988 and Schmutterer and Doll 1993). The young shoots can be eaten as vegetables or salad while the intensely bitter old leaves have been used in traditional medicines for the treatment of dysentery and diarrhea

(Anon 1995). In addition, chemicals such as azadirachtin and marragin extracted from seed kernels and leaves were more efficacious as an insecticide and growth regulator (Schumutterer 1989, Ermel *et al.* 1991, Mordue and Blackwell 1993).

Isozyme analysis has been used widely to detect the genetic variation of plant species especially using starch gel electrophoresis procedure. With the fast technology advancements, several other reliable markers have been introduced such as RAPD, RFLP, AFLP and SSR. However, isozyme technique still stands by its own advantages such as cheap, fast and not affected by environmental changes. This analysis is one of the multiple forms of an enzyme that produce similar or identical catalytic activities (Feret and Bergmann 1976) and the assessment of single genetic markers is reliable when compared with morphological markers such as colour, tree form and size.

The objective of this study was to assess the amount and distribution of genetic variation of six populations of *A. excelsa* in Peninsular Malaysia by means of isozymes analysis.

2. Materials and methods

2.1 Plant materials

Thirty matured leaves of *A. excelsa* were collected randomly from six populations namely Manong (Perak), Pokok Sena and Sik (Kedah), Bukit Lagong Forest Reserve of Forest Research Institute of Malaysia (Selangor), Merchang (Terengganu) and Sg. Caru (Pahang). Populations from Manong, Pokok Sena and Sik were collected from natural forest stands while populations from FRIM and Sg. Caru were from artificial stands. Seedlings of Merchang, Terengganu origin were obtained from a trial plot established at Pasoh (Negeri Sembilan).

2.2 Sample preparation

0.6 g of each leaf sample was homogenised with liquid nitrogen before adding to 1200 µl of leaf extraction buffer. The samples were then centrifuged at 10 000 rpm for 5 minutes. Supernatant was removed and stored at -70 °C before being used.

2.3 Isozymes analysis

Starch gel was prepared using 10.5 % of potato hydrolysed starch. The resulting homogenate was absorbed onto filter paper (Whatman No. 3) and being inserted gently onto the slice gel. This gel was placed between two electrodes containing 500 ml of electrode buffer. Both the gel and bridge wicks were covered with a polythene sheet to prevent the gel from drying up during the electrophoretic run. Eleven enzymatic proteins were used to stain and they were Alcohol dehydrogenase (ADH), Esterase (EST), Glutamate oxaloacetate transaminase (GOT), α-Glycerophosphate dehydrogenase (α-GPDH), Isocitrate dehydrogenase (IDH), NADP Nothing dehydrogenase (NDH), 6-Phosphogluconic dehydrogenase (6-PGD), Phosphoglucose Isomerase (PGI), Phosphoglucose mutase (PGM), Shikimate dehydrogenase (SDH and Tetrazolium oxidase (TO).

3. Results

Genetic variation was assessed based on allelic frequencies, observed and expected heterozygosities. It was found that they were coded by 25 and 26 loci. Generally for all loci were polymorphic except 4 loci namely 6-Pgd-1, Pgi-1, To-1 and To-3 where they were monomorphic (Table 1). The mean of observed heterozygosity was found to vary from 0.0800 to 0.1115 while the expected heterozygosity ranged from 0.1474 to 0.1902. The observed heterozygosities were found to show lower values than the expected heterozygosity. The percentage of polymorphic loci among population produced varied from 62% to 73% with the highest polymorphic loci proportion achieved by Manong population and the lowest by Sg. Caru population (Table 2).

Table 3 shows the Nei's coefficient of genetic identities for all possible combinations among six populations of *A. excelsa*. Genetic identities ranged from 0.815 to 0.984 with the mean of 0.889. The combination of Pokok Sena (Kedah) - Sik (Kedah) gave the highest value of genetic identity which is 0.984 and the combination of FRIM (Selangor) - Sik (Kedah) gave the lowest value of genetic identity with 0.815 (Figure 1).

4. Discussion

4.1 The extent of intraspecific variation

The results obtained in this study especially on the range of observed heterozygosity is similar to the ones obtained by Kueh (unpublished). In fact the value of heterozygosities are comparatively similar to Nor Aini and John Keen (2003) on *Acacia crassicarpa* and Moran *et al.* (1989) on *Pinus radiata* but are lower than values obtained in other indigenous species like *Shorea acuminata* by Kong (unpublished), *S. curtisii* by Daim (unpublished) and *S. leprosula* by Daisy (unpublished). However, these values are noted to fall within the range suggested by Hamrick and Loveless (1986) and Loveless and Hamrick (1987) for tropical trees, i.e. between 0.00 to 0.216.

The polymorphic loci among populations produced an average of 67.5%, which is higher than Kueh (unpublished) on the same species and other *Acacia* species (Nor Aini and John Keen 2003) but is lower than *Shorea* species (Table 4).

The results produced were also higher than the one reported for tropical trees i.e. 11.1% to 54.2% according to Loveless and Hamrick (1987) and is also higher than the Australian tree species according to Moran (1992).

Generally, this species showed low values for both heterozygosities and proportion of polymorphic loci. This could be due to the limited gene exchange within and between populations as seedlings from these populations were raised under uniform environments. Furthermore the limited gene exchange could be due to seeds and seedlings from similar mother trees as a result of their poor occurrence in their natural population. This is evident from population Sik (Kedah), where the seeds and seedlings collected for a provenance trial were actually from only 14 mother trees that were separated 10 m away (Jusoh *pers. comm.*).

Population from Manong (Perak) exhibited low level heterozygosity, i.e. 0.105 although it possessed the highest level of proportion polymorphic loci i.e. 73% (Table 2). Low level of heterozygosity inferred that there is a possibility of related mating between few mother trees. On the other hand, the highest proportion of polymorphic loci of 73% suggests this population has undergone competition and selection within species in the natural stand. Polymorphism is required as part of the adaptive strategies of population in a heterogeneous environment of the forest (Feret and Bergman 1976).

Also, the overall low heterozygosity in these populations indicated that these populations undergo genetic drift where isolation with a small population size often increased the possibility of genetic drift which will reduce the genetic variability as a result of bottlenecks. This phenomenon has been well discussed by other researchers such as Hamrick (1983), Kimberly and Constance (1991) and Liengsiri *et al.* (1995).

Based from both criteria, Manong (Perak) is the most potential population to be conserve or to be sources for future plantation programme purposes. However, values on polymorphism tend to fluctuate depending on the enzyme systems used. Variability could also be increased further if genetic variation is assessed directly from actual mother trees from natural population.

4.2 Genetic identity between population

The mean genetic identity found in this study (0.889) was found to be slightly higher than the one recorded by Kueh (unpublished) on the same species, i.e. 0.820. Figure 1 shows a dendrogram constructed based on genetic identities using un-weighted group analysis (UPGMA). These populations were clustered into two main groups suggesting that they are closely related genetically and may share a common ancestor.

The dendrogram also suggest a clear linkage with the historical and geographical factors. FRIM (Selangor) and Manong (Perak) populations were found to cluster closely together because based on the history, population from FRIM is originated from Perak according to Abd-Ghani (*pers. comm.*). Moreover, the results of clusteration showed a clear association with geographic linkages. Populations from Pokok Sena (Kedah) and Sik (Kedah) might be related to each other because they are from the same geographic region. Pokok Sena area is located not far away from Sik area which is about 110 km away from each other (Jusoh *pers. comm.*). Similar reason can be true also to explain the phylogenetic relationship between Merchang (Terengganu) and Sg. Caru (Pahang) populations. According to Yeh and O'Malley (1980), if geographic distance between population decreases, the genetic similarity between them increases.

5. Acknowledgements

I wish to express our deepest gratitude and thanks to Prof. Dr. Nor Aini Ab Shukor and Assoc. Prof. Dr. Kamis Awang for their invaluable suggestions and comments. My special thanks also extended to Mr. Abdul Latib, Mr. Salim Ahmad and Mr. Zakaria Taha for their assistance and co-operation during sample and information collection of the project.

References

- Anon, (1995). Sentang - the plantation tree. Utusan Pusaka, STIDC, Sarawak Vol 2: 14p.
- Burgess, P.F. (1966). Timber of Sabah. Sabah Forest Record No. 6. Forest Department, Sabah, 394-398.
- Corner, E.J.H. (1988). Wayside tree of Malaya. Vol 2. Malayan Nature Society, Kuala Lumpur. pp 492.
- Daim, B. unpublished. Allozyme variation of *Shorea curtisii* Dyer ex King and *Shorea leprosula* Miq. Bac. Forestry Sc. Thesis. UPM, Serdang, pp 75.
- Daisy, A. unpublished. Isozyme variation of *Shorea curontisii* Dyer ex king, *Shorea leprosula* Miq and *S. parvifolia* Dyer. Bac. Forestry Sc. Thesis. UPM, Serdang, 97-99.
- Ermel, K., H.O. Kalisowski, and H. Schmutterer. (1991). Isolierung und charakterisierung einer neuen, die Insektenmetamorphose storenden substanz aus samenkernen des marrangobaumes, *Azadirachta excelsa* (Jack). *Journal of Applied Entomology*, 112: 512-519.
- Feret, P.P and F. Bergmann. (1976). Gel electrophoresis of proteins and enzymes. In Miksche, J.P (ed). *Moderns methods in forest genetics*. Springer, Berlin Heidelberg, New York, 49-77.

Food and Agriculture Organization. (2005). Global Forest Resources Assessment.

Hamidi, A.H., unpublished. Isoenzyme variation of *Acacia mangium* Wild. Bac. Forestry Sc. Thesis. UPM, Serdang, pp 65.

Hamrick, J.L. (1983). The distribution of genetic variation within and among natural populations. In : Genetics and conservation. CM Shonewald-Cox, S.M. Chambers, B. Macbryde and L. Thomas (Eds). Benjamin/Cummings, Menlo Park, New Jersey, 335-348.

Hamrick, J.L. and M.D. Loveless. (1986). Isozyme variation in tropical trees: procedures and preliminary results. *Biotropica*, 18(3): 201-207.

Jacobs, M. (1960). The genetic identity for *Melia excelsa* Jack. Gard. Bull. 18(1) : 71-75. King, J.E. and Dancik B.P. (1983). Inheritance and linkage of isozymes in white spruce (*Pinus glauca*). *Canadian Journal of Genetics and Cytology*, 25 : 430-436.

Kong, T.F. (1993). Isozyme variation of *Shorea acuminata* Dyer and *Shorea parvifolia* Dyer. Bac. Forestry Sc. Thesis. UPM Serdang. pp 75-77.

Kueh, J.H. (1995). Isozyme variation and RAPD analysis of *Azadirachta excelsa* (Jack) Jacobs. Bac. Forestry Sc. Thesis. 114pp.

Liengsiri, C., F.C. Yeh and T.J.B. Boyle. (1995). Isozyme analysis of a tropical forest tree, *Pterocarpus macrocarpus* Kurz in Thailand. *Forest Ecology and Management.*, 74 : 13-22.

Loveless, M.D. and J.L. Hamrick. (1984). Ecological determinants of genetic structure in plant populations. *Annual Review of Ecology and Systematics*, 15: 65-95.

Moran, G.F. (1992). Patterns of genetic diversity in Australian tree species. *New Forests*, 6: 49-66.

Mordue (Luntz), A.J. and A. Blackwell. (1993). Azadirachtin : an update. *Journal of Insect Physiology* 39(11): 903-924.

Nor Aini Ab. Shukor and John Keen Chubo. (2003). Genetic variation in isozyme of *Acacia crassicaarpa* A. Cunn Ex Benth. *Journal of Tropical Forest Science*, 15(1):74-81

Schmutterer, H. (1989). Erste untersuchungen zur insektiziden wirkung methanolischer blatt-und rindenextrakte aus dem philippinischen niembaum *Azadirachta integrifoliola* Merr. Im vergleich zu extrakten aus *Azadirachta indica* A. Juss und *Melia azedarach* L. *Journal of Applied Entomology*, 108: 483-489.

Schmutterer, H. and M. Doll. (1993). The marrango or Phillipine neem tree, *Azadirachta excelsa* (= *A. integrifoliola*) : A new source of insecticide with growth regulating properties. *Phytoparasitica*, 21(1): 79-86.

Wong, T.M. (1976). Wood structure of the lesser known timbers of Peninsular Malaysia: Malaysian Forest Record No 28. pp 80-81.

Yeh, F.C. and D.M. O'Malley. (1980). Enzyme variation in natural populations of Douglas fir (*Pseudotsuga menziesii* (Mirb.) Franco) from British Columbia. I. Genetic variation patterns in coastal populations. *Silvae Genetica*, 29: 83-92.

Table 1. Allelic Frequencies of 25 and 26 loci in 6 populations of *A. excelsa*.

Locus	Allele	Population					
		Manong	Pokok Sena	Sik	FRIM	Merchang	Sg. Caru
Adh-1	F	0.0333	0.0833	0.1500	-	-	-
	M	0.9333	0.8333	0.7833	0.9667	1.0000	1.0000
	S	0.0334	0.0834	0.0667	0.0333	-	-
Adh-2	F	-	-	0.0833	0.0500	-	-
	M	1.0000	1.0000	0.7500	0.9167	1.0000	0.9333
	S	-	-	0.1667	0.0333	-	0.0667
Adh-3	F	0.8500	-	-	0.7833	-	-
	M	0.0833	-	0.1000	0.1000	-	-
	S	0.0667	1.0000	0.9000	0.1167	1.0000	1.0000
Est-1	F	-	-	-	-	-	0.0333
	S	1.0000	1.0000	1.0000	1.0000	1.0000	0.9667
Est-2	F	0.1833	0.3500	0.3667	0.2333	0.1500	0.2167
	S	0.8167	0.6500	0.6333	0.7667	0.8500	0.7833
Est-3	F	-	0.0167	-	-	0.0667	-
	S	1.0000	0.9833	1.0000	1.0000	0.9333	1.0000
Got-1	F	0.1500	0.1667	0.1833	0.0500	0.1000	0.0833
	S	0.8500	0.8333	0.8167	0.9500	0.9000	0.9167
Got-2	F	0.2167	0.1833	0.1500	0.0833	0.2333	0.2167
	M	0.7833	0.7000	0.7500	0.8833	0.7667	0.7833
	S	-	0.1167	0.1000	0.0334	-	-
Got-3	F	0.8500	0.6833	0.8000	-	-	-
	M	0.1500	0.1167	0.1000	0.0667	0.0167	-
	S	-	0.2000	0.1000	0.9333	0.9833	1.0000
α Gpdh-1	F	0.2000	0.1167	0.0833	0.1833	0.1667	0.1500
	S	0.8000	0.8833	0.9167	0.8167	0.8333	0.8500

Table 1 (continued)

Locus	Allele	Population					
		Manong	Pokok Sena	Sik	FRIM	Merchang	Sg. Caru
Idh-1	F	0.9667	0.9333	1.0000	1.0000	1.0000	0.9833
	S	0.0333	0.0667	-	-	-	0.0167
Idh-2	F	0.0333	0.0167	0.0167	0.0833	0.0667	-
	M	0.0500	0.0167	0.0333	0.0500	0.8333	-
	S	0.9167	0.9667	0.9500	0.8667	0.0500	1.0000
Idh-3	F	0.2000	0.0833	0.0833	0.1333	0.1333	0.0500
	M	0.6000	0.8333	0.7833	0.7833	0.7500	0.8333
	S	0.2000	0.0834	0.1334	0.0834	0.1167	0.1167
Ndh-1	F	0.0500	0.0667	-	0.4667	0.0833	0.1500
	S	0.9500	0.9333	1.0000	0.5333	0.9167	0.8500
6 Pgd-1	F	1.0000	-	1.0000	1.0000	-	1.0000
6 Pgd-2	F	0.9667	0.0833	0.0667	1.0000	0.0667	0.1167
	M	0.0333	0.9167	0.9333	-	0.8833	0.8500
	S	-	-	-	-	0.0500	0.0333
6 Pgd-3	F	0.9833	1.0000	1.0000	0.3667	0.9667	1.0000
	M	0.0167	-	-	0.5833	0.0333	-
	S	-	-	-	0.0500	-	-
Pgi-1	F	1.0000	1.0000	1.0000	1.0000	1.0000	1.0000
Pgi-2	F	0.1167	0.0667	0.0333	0.0167	0.0833	0.0333
	M	0.1333	0.0333	0.1167	0.0167	0.0667	0.0667
	S	0.7500	0.9000	0.8500	0.9666	0.8500	0.9000
Pgi-3	F	0.6500	0.5167	0.6333	0.8333	0.6667	0.7167
	M	0.2500	0.4500	0.3000	0.1167	0.3167	0.2000
	S	0.1000	0.0333	0.0667	0.0500	0.0166	0.0833
Pgm-1	F	0.2167	0.1000	0.0500	0.3167	0.0833	0.1333
	S	0.7833	0.9000	0.9500	0.6833	0.9167	0.8667

Table 1 (continued)

Locus	Allele	Population					
		Manong	Pokok Sena	Sik	FRIM	Merchang	Sg. Caru
Pgm-2	F	0.0833	0.1167	0.1500	0.1333	0.1833	0.0833
	S	0.9167	0.8833	0.8500	0.8667	0.8167	0.9167
Sdh-1	F	0.0333	1.0000	0.9833	0.1833	0.0833	0.1500
	M	0.1333	-	0.0167	0.0833	0.1000	0.1167
	S	0.8334	-	-	0.7334	0.8167	0.7333
To-1	F	1.0000	1.0000	1.0000	1.0000	1.0000	1.0000
To-2	F	0.9167	0.8667	0.8667	0.8833	0.9500	0.8333
	M	0.0500	0.0333	0.0500	0.0500	0.0333	0.0167
	S	0.0333	0.1000	0.0833	0.0667	0.0167	0.1500
To-3	F	1.0000	1.0000	1.0000	1.0000	1.0000	1.0000

Table 2. Mean observed (Ho) and expected heterozygosity (He) and percentage of polymorphic loci of *A. excelsa*.

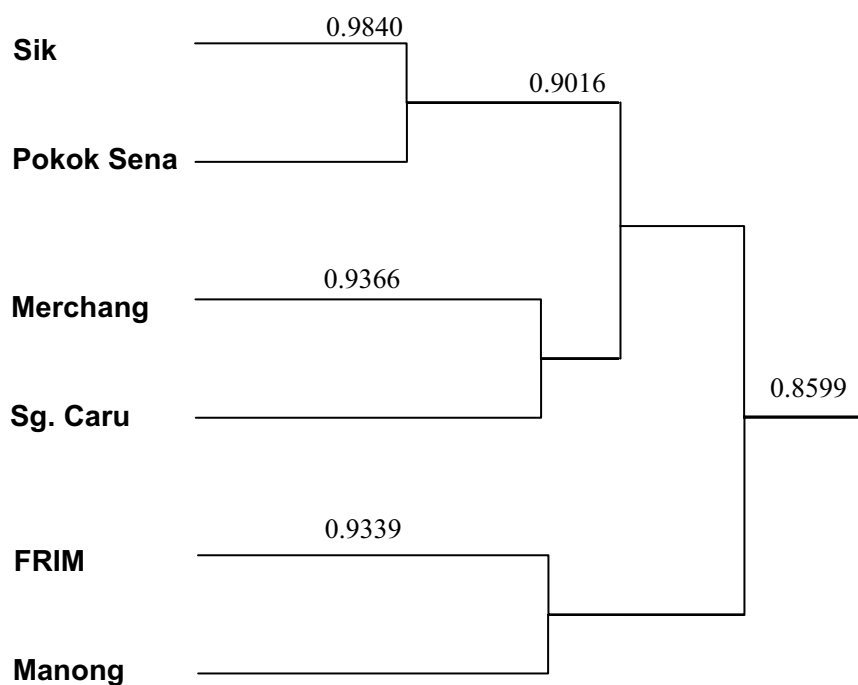
	Population					
	Manong	Pokok Sena	Sik	FRIM	Merchang	Sg. Caru
Ho	0.1051	0.0999	0.1115	0.0846	0.0800	0.0846
He	0.1719	0.1721	0.1759	0.1902	0.1579	0.1474
Proportion Polymorphic Loci (%)	73	68	65	69	68	62

Table 3. Nei's coefficients of genetic identity among six natural populations of *A. excelsa*

	Sik	Pokok Sena	FRIM	Merchang	Sg. Caru
Manong	0.852	0.894	0.934	0.824	0.886
Sik		0.984	0.815	0.861	0.915
Pokok Sena			0.852	0.888	0.943
FRIM				0.845	0.911
Merchang					0.937

Table 4. The mean heterozygosity and percentage of proportion polymorphic loci.

Species	H	P (%)	References
<i>Acacia crassicaarpa</i>	0.086	58.7	Nor Aini and John (2003)
<i>Azadirachta excelsa</i>	0.086	60.8	Kueh (unpublished)
<i>A. excelsa</i>	0.094	67.5	Present study
<i>Shorea acuminata</i>	0.604	100	Kong (unpublished)
<i>S. curtisii</i>	0.480	72.2	Daim (unpublished)
<i>S. leprosula</i>	0.457	93.3	Daisy (unpublished)
<i>S. parvifolia</i>	0.535	95.2	Kong (unpublished)

Figure 1. Dendrogram of Six Populations of *A. excelsa* using Un-Weighted Pair Group Cluster Analysis of Identity Coefficients



Investigation and Application Progress of Vero Cell Serum-free Culture

Tian Chen & Keping Chen

School of life science, Jiangsu University, Jiangsu 212003, China

E-mail: chenlpwx@163.com

Abstract

Serum-free culture is now becoming the general trend of biological production. Its application in Vero cell culture is significant. In the present paper, we reviewed factors affecting Vero cell serum-free culture and several culture techniques. In light of these reviews, we outlined its extensive application prospect.

Keywords: Vero cell, Vaccine, Serum-free, Microcarrier

1. Background of Vero cell serum-free culture

Vero cells are considered as a substrate for the production of viral vaccines. Vero cells were first separated from a normal adult African green monkey kidney cell line by Yasumura of Chiba University, Japan in 1962. This cell line presents several advantages over primary and diploid cell substrates. ① Vero cells are easily available, grow fast and require no rigor culture conditions which can support various virus proliferations; ② Vero cells have been extensively characterized to evaluate their oncogenic potential. Several studies have shown that this cell line is free from oncogenic property and is not presenting any threat to human health when used as a substrate for biological production authorized by the World Health Organization (WHO); ③ Vero cells can be used in microcarrier and suspension cultures for large scale production in bioreactors. Moreover, virus titer achieved is higher than that reached using other types of cell substrates. These properties greatly facilitate the transfer of vaccine-producing capability to developing countries, which is an important goal of WHO.

Cell cultures have been used extensively in the manufacture of biologicals for diagnostics, therapeutics and vaccines. The production of vaccines by animal cell culture was one of the earliest commercial applications of in vitro animal cell technology, and despite the recent spotlight accorded recombinant protein products, vaccines remain the most significant application of cell culture in terms of product numbers and social impact. Product safety is of paramount concern since the majority of viral vaccines are for use in healthy paediatrics. Cell substrate, production cultures, culture conditions, production media, detachment agents, etc. are major issues of safety considerations (Rourou, 2007). One of the important points of safety concerns relates to the composition of culture medium. All classical vaccine production processes make use of animal derived substances: serum, trypsin, lactalbumin, etc. Animal sera are required for vigorous growth of animal cells used as substrate for virus propagation. Serum was shown to have several essential functions in culture. It is a source of nutrients, hormones, growth factors and protease inhibitors. Furthermore, serum facilitates the attachment and spreading of cells, and provides nonspecific protection against mechanical damage and shear forces. In addition, it is able to bind to toxic compounds. However, besides these growth-promoting properties, serum has some major disadvantages. It is undefined with respect to its chemical composition. It can be a source of adventitious agents and their by-products. Serum also presents a variable performance of cell growth and has a substantial cost. Therefore, the benefits of in vitro culture of animal cell lines in the absence of serum are widely acknowledged. The removal of serum components and the elimination of other animal-derived raw materials are proving more challenging. Processes for serum free culture of several cell types expressing r-DNA derived proteins and monoclonal antibodies (MAbs) have been developed and established for large scale production since the beginning of the 1990s. However, the picture is different for existing conventional biotechnology products such as viral vaccines, the scientific challenge is probably greater because diploid cell lines or even continuous cell lines (CCLs) such as Vero cells may require additional growth and attachment factors that CCLs growing in suspension culture do not need. Serum free culture applied in production area would give greater application potential and broad market prospect Vero cells. Serum free culture of Vero cells has been an important focus on produce and research currently or for the future.

2. Studies on serum free culture of Vero cells

2.1 Serum free medium

Medium is the most direct and paramount environmental factor affecting growth metabolism, proliferation and survival of cells in vitro. Hence, the key point of serum free culture is the optimization and development of serum free medium. For many years, whether small scale laboratory or large scale medium producer, whether for scientific research or mass production, more and more attention have been paid to the studies and researches on the serum free medium of Vero cells and thus corresponding improvements have been continuously made.

2.1.1 Independent development

There are two ways to develop serum free medium: one is to design and assay brand-new medium suitable for cell proliferation. In the method, components were gradually changed one by one according to the known formula of certain cell lines until attaining optimized in line with particular requirement. A detailed growth curve and clonal growth should be undertaken at the expense of time and labor; The other is to add several possible conducive components to assure the normal growth with reference to available formula and gained experience, and on this basis, eliminate toxic or void components and optimize several components to advisable concentration. Numerous statistic methods are applied in the method due to the complicated constitute of medium and many affecting factors. Mass production mainly relied on the serum free medium formula developed in the combination of certain cell lines and produce technology by research department of biological pharmacy enterprises, and contract production of medium manufacturer; Small scale production relied on medium formula confirmed by research institutions and produce enterprises and adding several serum substitute to the commercial synthetic medium, which was an economic way at low cost. Currently, based on commercial medium such as DMEM, F-12, M199, RPMI 1640, etc., serum free medium of Vero cells used either or in the combination of them, added some trace elements, growth factor, hormone, transport protein and adhesion factor, increased or decreased amino acid and the concentration of lipids and its precursor. Statistic method and software were applied to optimize the ration of each component and make the good use of them.

Gao and Wei (Hong-liang and Wei, 2001) have found that amino acids are very important nutrients in mammalian cell cultivation, 12 amino acids (Gln, Arg, His, Leu, Thr, Ile, Lys, Ser, Tyr, Phe, Val and Met) were consumed, and 4 amino acids (Glu, Asp, Ala and Pro) were produced during the growth of Vero cells. Amino acid Gln and Ser should be first added into the serum free medium because Sebastien (Sebastien Quesney, 2001) have pointed out that they are the first deficient components in the medium and possibly main factors inducing cell apoptosis. Adhesion factor added are mainly components of intercellular substance and serum, such as fibronectin, collagen, and laminin. When studies of cell biology came into molecular domain, it was noted that sequence Arg-Gly-Asp (RGD) in previous extracellular matrix proteins mediated cell attachment by interacting with proteins of the integrin family of cell surface receptors. RGD promoted the attachment of Vero cells to polystyrene and cellulose acetate (Andrew Wierzbza, 1995). Vero cells in the prepared serum- and protein- free medium by adding yeast extract and soy hydrolysate into basic medium grew well (Zhenglun and Xianping, 2007), for these hydrolysates contained low relative molecular mass peptides, which could afford physical protection and promote cell attachment. However, recent research has noted that great discrepancy existed in batches of these hydrolysates, which could be the new uncertain components of serum free medium (Genzel, 2006). Consequently, seeking for new, more efficient and definite additive is urgent for preparing serum free medium at present or in the future. In order to cut down cost and mass production, cheaper additive or nutrient substitutes are considered, such as chelating agents or citrates to simulate the function of transport protein, surfactants to protect fluid mapper shear for protein.

2.1.2 Commercial product

Due to high specificity of serum free medium, commercial serum free medium suitable for other cell lines is not desirable for Vero cells, which has been confirmed by experiments. Currently, routine Vero cell commercial serum free medium are products of high quality, specially designed for Vero cells. These products get improvements continuously in quality and quantity. ① The most typical medium among numerous products is VP-SFM (virus production-serum free media), produced by the largest cell culture product manufacturer (GIBCO/Invitrogen). It is a serum free medium with ultra-low protein. Microprotein in VP-SFM derived from recombinant protein. Transferrin was already replaced by a kind of ion chelate, and albumin was replaced by dipeptide or tripeptide from plants. The only necessary addition is L-glutamine, with a concentration of 2~6mM according to the relative cell lines. Vero cells are not necessary to adapt to VP-SFM. Cell density could attain 1.8×10^5 cells/cm² when static incubation in 75cm² spinner flasks. Just as its name implies, VP-SFM is kind of medium particular for the application of virus propagation. Many reports of VP-SFM used for producing virus are available (Frazzati-Gallina, 2001; Toriniwa, 2007). ② OptiPro SFM is another serum free medium of GIBCO/Invitrogen for Vero cells, with uncertain chemical components and no peptides from plants, animals or synthetical protein, excluding Vero cells, and is also suitable for kidney derived cells such as MDBK, BHK-21, PK-15 and so on with respect to virus producing. For attachment dependent cells, it is unnecessary to add some attachment protein or pretreatment with culture surface. ③ EX-CELL™ VERO produced by JRH, is a kind of serum

free medium specially designed for the high density growth of Vero cells, supporting attachment and suspension culture. It contains no animal components and hydrolysates from plants, with low level of recombinant protein and no phenol red or PluronicF68. When EX-CELLTMVERO transferred from serum containing medium, cells need a short period to accommodate, compared to other similar products, the particular dominance is the high density growth supporting spinner flask static culture and microcarrier culture in bioreactor. Cell density could attain 2×10^5 cells/cm² when static incubation in 75cm² spinner flasks and 1.9×10^6 cells/ml in bioreactor with microcarrier Cytodex-1. In serum free culture, cell density and virus titers was identical to the level in serum containing culture (Kolell, 2005).

Except the above-mentioned mediums, commercial serum free mediums for Vero cells include MD Cell DMEM (Biowest), MP-VeroTM SFM (MP), Plus VEROceso Bioengineering Co., Hsinchu, Taiwan(CESCO), ICN-VERO(ICN), PEEK-1(Biochrom) and so on. But reports on them are less available.

Main issues existed in the commercial serum free medium are as follows: They could only be available in the form of liquid; They are expensive with unknown components due to severe commercial security; They are only suitable for laboratory or small scale investigation, and not acceptable due to its high cost in industrial mass production.

2.2 Serum free culture

2.2.1 Culture mode

① Attachment culture

Vero cells, as well as other many cell lines with great application value in industry (including BHK, CHO and 293 cells), are all attachment dependent. Vero cells have experienced a development process from experimental spinner bottles to small industrial scale roller bottles, however, such culture system afford a limited growth area, and is not suitable for large scale culture. Microcarrier culture developed in 1967 solved such problem well. Microcarrier means beads with the diameter of 60~250μm and attachment dependent cells could adhere to its surface, and suspended to grow together with microcarrier in bioreactor. This technology greatly increased surface area of cell growth. Taking microcarrier Cytodex-3 for example, surface area afforded by per 1g is 4600cm², equal to that of 3~4 roller bottles. Moreover, this technology has some dominant advantages: highlight homogenous culture together with the advantages of suspension and attachment, easy to control culture conditions and has a systematic and automatic culture process. In the microcarrier culture of Vero cells with serum free medium, researchers ameliorated attachment effects of cells through the adhesion factor afforded by the culture medium, and on the other hand ameliorated bulk characters of cell adhesion substrates. Earlier microcarrier adopted synthetic polymers such as PVB and PS-TC, and some reports indicated that Vero cells under the condition of serum free were quickly adsorbed and extended. In recent years, many researchers attempted to use natural polymers and their derivatives such as glutin, collagen, fibrin, chitin and etc to prepare microcarrier.

Microcarrier applied extensively is solid ones, including solid sphere and macroporous microcarrier. Solid microcarriers facilitate cells to attach and spread in the bead surface, are conducive to beads to beads inoculation technology in the process of cell infection and amplification imposed by virus, and thus are extensively applied in Vero cell culture, especially for Cytodex series, mainly two types available in the market, namely Cytodex-1 and Cytodex-3. Cytodex-1 is used more in the serum free culture of Vero cells because Cytodex-3 is made of collagen which could possibly induce some animal source. When compared to Cytodex 1, Cytodex 3 allowed a 30%-lower cell concentration and the earlier stationary phase to be obtained, which was probably related to the lower surface area per bead mass of Cytodex 3 microcarriers(de Souza, 2005).

In the condition of low level serum, after Vero cells adsorbed in microcarrier Cytodex-1 for 6 hours, a higher cell density level that was equal to 5×10^6 cells/mL was reached with a higher attachment rate of 83% (Rourou, 2007). Baxter Company has had the case of 6000L Vero cell culture to produce influenza virus. Microcarrier technology maintained a high cell population density, but serum free condition facilitates cell apoptosis. Some modifications for Vero cell serum free microcarrier culture includes batch stirring, which facilitate cell attachment(Toriniwa, 2007); Pretreatment with microcarrier, includes changing charge distribution in the surface of microcarrier, which make its surface conducive to cell attachment; Specific trypsin inhibitor was used to terminate protease effects(trypsin could hinder the proliferation of cell in microcarrier) (Genzel, 2006); The addition of shear protectants such as Pluronic F-68 to protein free media is often needed to protect cells against shear forces (could affect downstream process); Silicone pipeline is used in the small bioreactor to eliminate the air bubble when aeration and attenuate cell injury.

② Suspension culture

Due to the high cost of microcarrier, and attempts to continuous high density cell culture, serum free suspension culture of Vero cells has attracted many researchers' attention. The big difference of medium between suspension and attachment culture is Pluronic-F68 or tween-80 with protection effect for fluid mapper shear instead of some attachment factors. As far as suspension is concerned, domestication is crucial, where cells incubated in serum containing medium are transferred into serum free medium. Domestication of serum free medium suspension culture is main optimization

of serum free medium, which is a project with huge workload. Based on this, changing the growth manner of Vero cells, increasing cell density are conducive to produce vaccine efficiently, extend produce scale and reduce cost. For serum free suspension culture, cells almost need no adaptation period and cell density could reach $0.5-1.0 \times 10^7$ cells/ml which was far higher than normal attachment culture (5-10 fold). Vero cells in the condition of serum free suspension culture is easy to form all kinds of cell-aggregates of various sizes and adhere to container-wall. Cells in the inner of cell-aggregates were prone to necrosis, and without proper control, culture failure could immediately occur. Marcelo Daelli(Daelli, 2007) was successfully obtained Vero cells by domestication which could single grow in the high density serum free culture not to form mass in USA in 2007. This cell line was preserved by German Collection of Microorganisms and Cell Cultures (DSMZ). The formation of cell-aggregates in suspension culture offers a number of advantages: The cells within the aggregates are at tissue-like densities offering protection against physical stress and possibly helping each other metabolically; The cells are more in vivo-like environment than as monolayers or in single cell suspension cultures; It is easy to change medium with retention because of the fast sedimentation rate of the aggregates. Vero cells were cultured by combing five commercially available base media at different ratios to investigate the effects of serum free medium culture on cell-aggregates. Results showed that cell-aggregates and growth rate by combing different combination of five media varied, and cell density after aggregate could usually reach 10^6 cells/ml. With the entire serum free medium attempted, a long lag period of between 20 to 30 days was required before the cell concentration reached levels over 10^6 cells/ml even though these cells had been adapted to an serum free medium in anchorage-dependent cultures. Serum free suspension culture of Vero cells are not mature and hard to spread. Some researchers inferred that suspension cell could result in block, and protective agents added were mostly abluents which could interfere with downstream process. If cells were not adapted to the serum free medium well, cells grew quite slowly, which could directly ruin the production of virus. Although many disadvantages above, we could speculate that this technology, due to its profound application potential, would be new research direction of large scale culture of Vero cells.

2.2.2 Culture technology

Whether attachment or suspension, Vero cell culture could be classified into 3 types as follows:

① Batch culture

In batch mode of operation, the medium was not changed during the whole period of culture and virus was added when cell growth attained a certain stage. The entire virus production was harvested when the viral titer was highest. In order to guarantee the growth of virus, Vero cells were usually incubated in serum free medium for several generations to adapt to the medium without serum.

② Fed-batch culture

Fed-batch mode of operation was mainly applied for serum free medium suspension culture of Vero cells, as well as microcarrier. 1/3 or 2/3 of the total volume of culture was replaced every day, according to the continuous expenditure and demand of nutrients in Vero cells, which facilitated a high cell density.

③Perfusion culture

In perfusion mode of operation, one volume of culture per day was changed by continuous flow medium supplied by a peristaltic pump. This technology could eliminate the toxic metabolites efficiently and promptly, maintain an excellent nutritional status for cells, and thus was desirable for high density culture.

Serum free medium culture of Vero cells are generally classified into the biomass production phase (cell growth phase before virus inoculation) and sometimes also for the virus production phase (period after virus inoculation up to the harvest of virus suspension). According to special requirement of cells and virus during its growth period, different or same substrates or technology were applied. At the first stage, add little serum medium, and eliminate serum containing medium by rinse until cell density attained desired degree. Then add serum free medium for the grown of second stage(Frazzati-Gallina, 2001); Or fed-batch culture was applied at the first stage, and perfusion culture followed at the second stage, which could attain higher cell density and virus titers compared to the traditional batch culture(Rourou, 2007). This process combination could not only decrease production cost, but also enhance process yield.

3. Application of serum free medium culture of Vero cells

Vero cells derived from the African green monkey have been approved for viral vaccine production under specified regulatory guidelines, and are currently used for the production of rabies (Frazzati-Gallina, 2001) and polio vaccines. Moreover, Vero cells have been employed to produce bovine vesicular stomatitis virus, herpes simplex virus, influenza virus, and reovirus (Butler, 2000). The use of these cells also allows large-scale production of vaccines using microcarriers and culture in a bioreactor. For several new eruptible diseases, Vero cells were used as first cell line to produce vaccines. For SARS attracted more attention in past several years, inactivated vaccine have been developed by using Vero cells, and after preclinical investigation, will be undertaken phase 1 clinical trial. As for avian influenza

H5N1 focused by many researchers, some companies have claimed that H5N1 vaccine derived from Vero cells was of good safety and immunogenicity, and would be undertaken phase 3 clinical trial. Some vaccines were described in detail as follows:

3.1 Rabies

The rabies vaccines recommended by WHO include those produced in Vero cells, available since the 80s was the most successful. The authors concluded that the results obtained in the present study showed that the new Vero-cell human rabies vaccine, produced by Instituto Butantan, using serum-free medium, was safe and immunogenic. Experimental results showed that dominant commercial serum free medium was properly suitable for cells of virus propagation. Merten have studied that virus was propagated by static culture in spinner flask with serum free medium MDSS2 and attained similar results of cell proliferation with serum containing medium, but higher and earlier the highest virus titers, and 1.5-fold virus production rate. Rabies vaccine cultured in microcarrier Cytodex-3 with serum free medium culture of Vero cells, also attained a higher virus titers. Rabies virus strain production in Vero cells grown on Cytodex 1 in a 2 L stirred tank bioreactor and in a medium free of components of human or animal origin (VP-SFM) is described. Cell banking procedure in VP-SFM supplemented with an animal components free mixture was reported and cell growth after revitalization was assessed. Vero cells exhibited growth performances (specific growth rate and cell division number) similar to that obtained a higher cell density level maximal virus titer in serum containing medium (Rourou, 2007).

3.2 Polio vaccines

There was case that polio vaccines were produced by fixed perfusion culture of Vero cells in a large scale of 1000L abroad. Earlier studies indicated that there was no significant difference in static culture between using serum- free or containing medium, and even a higher production rate in serum-free than serum-containing medium. With respect to titers, virus production existed subtle difference using these two mediums.(Cinatl J Jr, 1993), and in general, titers in serum containing medium was little higher. The main difference between two mediums is the rather important difference between virus titers, which is probably due to the different components (age of culture, origin of clones, passage history) of these two mediums which resulted in varied cell physiology and cell metabolism (O.-W. Merten, 1999). This difference could be omitted by subsequent optimization of mediums.

3.3 Influenza vaccines

Influenza virus was produce by using chicken embryo for a long time. Since Vero cells were involved in the production of influenza virus, tests have confirmed that almost all virus strains tested in chicken embryos could grow and attain high titers in Vero cells. Although titers were lower than that in chicken embryos, virus yield increased greatly in Vero cells. Several researches found that virus titers in mass production were identical to or higher than in cell monolayer culture, which indicated that the technology of virus production by using Vero cells could be enlarged with no influence on production rate. It is anticipated that scale of producing vaccines in this serum free medium system could attain 1200L. Bacter Company has developed a total virus inactivated influenza vaccine by using Vero cells with serum free medium, which was undertaken phase II/III clinical trial in Europe at present.

3.4 Enterovirus 71 (EV71) vaccines

EV71 is a human enterovirus belonging to the Enterovirus genus of the Picornavirus family. At the beginning of 2008, EV71 infection has caused a few outbreaks of hand-foot-and-mouth disease (HFMD) associated with severe neurological diseases in young children in Anhui and Beijing of China. At present, there are no antiviral agents against such virus, and hence developing effective vaccines is the best approach to prevent infection and control the disease. Recent researches have described two VP1 subunit vaccines of EV71, one administered as a DNA vaccine and another as a recombinant protein vaccine, which elicited a neutralization antibody response in both ICR and BALB/c mice. These findings provide direct evidence that VP1 of EV71 contains neutralizing epitopes independent of the other viral capsid proteins, and pave the way for the potential use of VP1 as the backbone antigen for developing subunit vaccines against EV71(Wu CN, 2002). Serum free culture increased cell death rate after infection, reduced the virus specific productivity, but resulted in elicitation of higher neutralizing titers in immunized mice as compared to that parallel obtained in serum-containing cultures. The enhanced immunogenicity of EV71 virions produced in serum-free microcarrier Vero cell culture was in agreement with the result reported for rabies virus vaccine production (Chia-Chyi Liu, 2007). The enhanced immunogenicity of the inactivated virions produced in serum-free cultures is possible that the virions produced in serum-free culture may give better antigen stability as reported for reovirus.

In recent years, in the area of pharmaceutical engineering vaccines, medImmune Vaccines has engineered a live, attenuated chimeric virus that could prevent infections caused by parainfluenza virus type 3 (PIV3) and respiratory syncytial virus (RSV), causative agents of acute respiratory diseases in infants and young children. Researchers have exerted the development of a serum-free Vero cell culture production platform for this virus vaccine candidate. This improved serum-free process achieved comparable virus titers to the serum-supplemented process, and demonstrated

consistent results upon scale-up: Vero cultures in roller bottles, spinner flasks and bioreactors reproducibly generated maximum infectious virus titers of $8 \log_{10}$ TCID₅₀/ml. As it could be speculated, this platform of producing chimeric virus would have great developing potential.

4. Outlook

For the issues of cost control and virus yield in large scale culture of cells and vaccines production, we inferred that there were lots of potential to be further developed in serum free medium culture of Vero cells: ① Considering from Vero cell itself, cell strains of attachment and anti-apoptosis were incubated in the combination of molecular biology and genetic engineering technology, which could greatly ameliorate growth metabolism in serum free condition, and enhance cell resistance ability against harsh environment. For example, genes of adhesion protein, such as vitronectin, introduced into cells, could facilitate cell attachment and extension after the expression of protein; Anti-apoptosis gene Bcl-2, transferred into Vero cells, could effectively inhibit cell apoptosis after expression of protein or high expression of telomerase. ② Considering from the perspective of mass production, it could facilitate cell growth of high density and hence enhance the production capacity of bioreactors by good combination of serum free medium and bioreactor, and optimization of cell culture processes.

Based on the great application value and prospect of Vero cells, the increment of vaccines requirement in the biological product market, technology of serum free medium culture of Vero cells would be continuously developed.

References

- Andrew, W., & Udo, R. (1995). Production and properties of a bifunctional fusion protein that mediates attachment of vero cells to cellulosic matrices. *Biotechnology and Bioengineering*, 47 (2): 147-154.
- Butler, M. (2000). Application of a serum-free medium for the growth of VERO cells and the production of reovirus. *Biotechnol. Prog.*, (16): 854-858.
- Cinatl, J.J., & Rabenau, H. (1993). Protein-free culture of Vero cells: a substrate for replication of human pathogenic viruses. *Cell Biol Int.*, 17 (9): 885-895.
- Costa, & Wagner, A. (2007). Immunogenicity and safety of a new Vero cell rabies vaccine produced using serum-free medium. *Vaccine*, 25: 8140-8145.
- Daelli, & Marcelo (2007). Vero cell line adapted to grow in suspension.
- Frazzati, G., & Neuza M. (2001). Higher production of rabies virus in serum-free medium cell cultures on microcarriers. *Journal of Biotechnology*, 92: 67-72.
- Gao, H.L., & Wei, C. (2001). Amino Acid Metabolism of Vero Cells in Batch Culture. *The Chinese Journal of Process Engineering*, 1 (2): 177-180.
- Gao, Z.L., & Zhang, X.P. (2007). Culture of Vero Cells in Serum free and Protein free Medium. *Chin J Biologica*, 20 (9): 688-690.
- Genzel, Y. (2006). Serum-free influenza virus production avoiding washing steps and medium exchange in large-scale microcarrier culture. *Vaccine*, 24 (2006): 3261-3272.
- Inn, H., Yuk, G., & Lin, B. (2006). A serum-free Vero production platform for a chimeric virus vaccine candidate. *Cytotechnology*, (51): 183-192.
- Kolell, K., & Padilla, Z. (2005). Virus Production in Vero Cells Using a Serum-Free Medium, JRH. *Biosciences*.
- Litwin, & Jack (1992). The growth of Vero cells in suspension as cell-aggregates in serum-free media. *Cytotechnology*, 10 : 169-174.
- Liu, C.C., & Lian, W.C. (2007). High immunogenic enterovirus 71 strain and its production using serum-free microcarrier Vero cell culture. *Vaccine*, 25 (2007): 19-24.
- Merten, O.W., & Kallel, H. (1999). The new medium MDSS2N, free of any animal protein supports cell growth and production of various viruses. *Cytotechnology*, 30: 191-201.
- Rourou, & Samia (2007). A microcarrier cell culture process for propagating rabies virus in Vero cells grown in a stirred bioreactor under fully animal component free conditions. *Vaccine*, 25: 3879-3889.
- Sebastien, Q., Jacqueline, M., & Annie, M. (2001). Characterization of Vero cell growth and death in bioreactor with serum-containing and serum-free media. *Cytotechnology*, 35: 115-125.
- Souza, D., & Marta, C.O. (2005). Influence of Culture Conditions on Vero Cell Propagation on Non-Porous Microcarriers. *Brazilian archives of biology and technology*.
- Toriniwa, & Hiroko (2007). Japanese encephalitis virus production in Vero cells with serum-free medium using a novel oscillating bioreactor. *Biologicals*: 1-6.

- Wierzbna, A., & Reichl, U. (1995). Production and properties of a bifunctional fusion protein that mediates attachment of vero cells to cellulosic matrices. *Biotechnol Bioeng*, Jul 20 (47): 147-154.
- Wu, C.N., Lin, Y.C., & Fann, C. (2002). Protection against lethal enterovirus 71 infection in newborn mice by passive immunization with subunit VP1 vaccines and inactivated virus. *Vaccine*, 20: 895-904.



Purification and Characterization of the Lipase from Marine *Vibrio fischeri*

P. Ranjitha (Corresponding author)

Research Department of Microbiology, Sengunthar Arts and Science College

Tiruchengode 637 205, Tamilnadu, India

E-mail: ranjithaponn@gmail.com

E. S. Karthy

Research Department of Microbiology, Sengunthar Arts and Science College

Tiruchengode 637 205, Tamilnadu, India

A. Mohankumar

Research Department of Microbiology, Sengunthar Arts and Science College

Tiruchengode 637 205, Tamilnadu, India

Abstract

Lipolytic enzymes from marine microbes have been the focus of intense and growing research. The bioluminescence bacterium *Vibrio fischeri* was produced lipase enzyme when the medium contained specific substrate. The lipase was purified from the concentrated culture supernatant. The most active fractions were obtained using the technique of precipitation with ammonium sulphate. The precipitated fraction was purified by desalting and ion exchange chromatography. The purified active fraction exhibiting final specific activity of 121U/mg and characterized; the optimum pH was likely between 7 to 8, the optimum temperature was 30°C and about 80 % of activity at 5°C. The enzyme was very stable at the pH 8, at the temperature 30°C. The enzyme was monomeric protein having molecular mass of 57 KDa estimated by native PAGE assay.

Keywords: *Vibrio fischeri*, Lipolytic enzymes, Extracellular, Lipase

1. Introduction

Marine microorganisms which are salt tolerant, provide an interesting alternative for therapeutic purposes. Marine microorganisms have a diverse range of enzymatic activity and are capable of catalyzing various biochemical reactions with novel enzymes. Especially, halophilic microorganisms possess many hydrolytic enzymes and are capable of functioning under conditions that lead to precipitation or denaturation of most proteins. Further it is believed that sea water, which is saline in nature and chemically closer to the human blood plasma, could provide microbial products, in particular the enzymes, that could be safer having no or less toxicity or side effects when used for therapeutic applications to humans (Sabu, 2003).

The *Photobacterium (Vibrio) fischeri* group consists of rod-shaped cells with a light yellow, cell-associated pigment and a tuft of sheathed flagella (Hendrie et al., 1970). The species is restricted to the marine environment and has a specific requirement for sodium ion for growth (Reichelt and Baumann, 1973). It occurs both free living in sea water (Ruby and Nealson, 1976) and as the specific luminous symbiont of the monacanthid fish and squid.

Lipases, triacylglycerol hydrolases, catalyse both the hydrolysis and synthesis of esters formed from glycerol and long chain fatty acids. These enzymes exhibit broad substrate specificity and degrade tweens, phospholipids often with positional, stereo and chain length selectivity (Jaeger et al., 1994). Lipases have been recognized as very useful biocatalysts because of their wide ranging versatility in industrial applications such as food technology, detergent,

chemical industry and biomedical sciences (Jaeger and Reetz, 1998; Jaeger et al., 1999; Ghanem et al., 2000; Gupta et al., 2004). Information of lipolytic enzymes produced by marine *Vibrio* spp is particularly limited. Therefore, the objective of this study is to focus on the lipase production of *V. fischeri* isolated from squid and on the purification and partial characterization of its lipase.

2. Experiments

2.1 Bacteria and growth conditions

The squids (*Sepia* sp.) were collected and cooled to about 8°C before opening the mantle cavity along the ventrum. The following two methods were used to obtain samples of symbiotic luminescent bacteria. Light organ fluid containing bacteria was obtained from pore that leads into channels with in the organ tissue. Whole light organs were removed by dissection and homogenized in 700µl of sterile seawater (Ruby and Nagai, 1992). Material obtained in either of these ways was serially diluted in seawater complete (SWC) broth and the samples were spreaded on SWC (0.38M NaCl, 0.02M MgCl₂.6H₂O, 0.025M MgSO₄.7H₂O, 8mM KCl, 0.5% peptone, 0.3% yeast extract, 2% agar and 0.3% glycerol) agar plates and identified the luminous bacteria based on the work of Reichelt and Baumann (1973) and VHA (*Vibrio* Hareyi Agar) differential media (Harris et al., 1996).

2.2 Screening of Lipase Enzyme

2.2.1 ZoBell 2216E modified media

All strains were precultivated on the solid maintenance SWC medium. For detection of lipolytic activity the following basal medium (Zobell 2216E, slightly modified) was used. It contains 10g of peptone, 1g of yeast extract, 0.05g of CaCl₂, 15 g of bacto agar made to 1 L with aged seawater, pH was adjusted to 7.6. The media supplements with either of 1% tweens (20, 80) or 0.25% Triacylglycerols (tributyrin, triolein) were then poured into petri dishes, after solidification of these media inoculated and incubated at 30°C for 10 days. The total diameter, minus the diameter of the colony was considered to be proportional to the lipolytic activity rate. After 1-10 day incubation the halos, clear (on tributyrin, triolein) or turbid (on all other substrates) were measured.

2.2.2 Spirit Blue Agar

Broth culture was streaked on the spirit blue agar plates with substrate (Tweens or Triacylglycerol). Then the plates were incubated at different temperature 6°C, 17°C, 30°C for up to 15 days. The plates were observed after 6 hrs and every 12 hrs for the clearing of the blue or deep blue color around each streak. Lipolytic activities at different hours were compared by measuring the width (millimeter) of areas of cleaning or area of deep blue color around the colonies.

2.2.3 Rhodamine B Agar

A plate assay to detect bacterial lipase in a medium containing olive oil or triglycerol and the florescent dye rhodamine B. Growth medium was adjusted to pH 7.0, autoclaved and cooled about 60°C. Then 1% of olive oil, 10 ml of rhodamine B solution (0.001% w/v) was added with vigorous stirring and emulsified by mixing for 1 min with an homogenizer. 20 ml of medium was poured into each petri dish. The overnight culture was spotted in the centre of the plate and incubated for 48 hrs. The plates were incubated for 16 hrs at 30°C. Lipase production was monitored by irradiating plates with UV light at 350nm. After 16 hrs of incubation bacterial colonies began to show an orange fluorescence, with continuing incubation time orange fluorescent halos were formed around the colonies.

2.3 Enzyme Production and Preparation of Cell Free Filtrate

150µl of culture was inoculated into 200ml of sea water medium with substrate and incubated at 30°C for 3 days. The portion was centrifuged at 20,000 xg at 4°C for 30 min. The supernatant was filtered using 0.45 µm cellulose acetate filter units. The cell free filtrate was used as the crude enzyme in the purification experiments.

2.4 Purification of extracellular lipase

2.4.1 Ammonium Sulfate Fractionation and Dialysis Against Buffer (Desalting)

Solid ammonium sulphate was added to the fraction 1 at 20% saturation and allowed to stand for 30 min. The precipitate obtained was separated by centrifugation (Fraction II) and the resulting supernatant was further treated with solid ammonium sulphate at 40% saturation. The precipitate obtained was collected by centrifugation (Fraction III). The supernatant was similarly treated with ammonium sulphate at 60 and 80% saturation and the precipitates obtained were termed as fractions IV, V respectively. All the precipitates (II-V) were resuspended in a minimal amount of buffer (0.1M Tris-HCl, pH 7.0) and dialyzed against the same buffer by using successive large volume of buffer. The process was continued till the last trace of ammonium sulphate was removed. The desalted fractions were used for further process. All the concentrated fractions (II-V) were subjected to protein and enzyme activity assay to choose the fraction containing maximum activity.

2.4.2 Ion-exchange chromatography (DEAE-Cellulose Column)

The dialyzed sample was removed from the tubing and filtered through a 0.45µm filter. Then applied to a column previously equilibrated with 0.01M Tris HCl buffer (pH 7.2) slowly percolating large volume of buffer through packed material. A sample of desalted enzyme preparation was loaded onto the column. The elution of the pure lipolytic enzyme accomplished with 15 column volume gradient of NaCl obtained by 270 ml of 0.6M NaCl in 0.01 M Tris HCl buffer (pH 7.2). Flow rate was controlled at 0.5 ml/ min by 5 ml of fractions collected and analyzed for protein and enzyme activity. After assaying the fractions for lipase activity, fractions collected from DEAE-cellulose chromatography were impregnated on to a small disc (5mm) of filter paper and placed on top of chromogenic substrate plates. The plates were incubated at 30°C for 15-30 min. Those with highest activity were pooled together and used for further enzyme characterization.

2.5 Enzyme Activity Assay

Enzyme assay used for the determination of lipase activity upon emulsified substrates and Tween solutions. The final concentration of oil was 10%, gum arabic 8%, Triacylglycerols (TAGs) 10-50mM, Tweens 0.8-20% (v/v). The mixture of the substrate and buffer (final volume 8ml) was adjusted to pH 8.0 by 1N NaOH and the pH was maintained for 3 min by titration with 50mM NaOH solution (blank). Then 1 ml of the lipase solution in the buffer was added and the lipolytic reaction was observed for 40 min by titration as mentioned above. Enzyme activity is expressed as U/ml and one unit (U) of activity is defined as µmols of free fatty acids liberated /min/ml by the enzyme solution under assay conditions.

2.6 Protein Mass Determination (Native PAGE)

In order to study the undenatured protein profile of lipase enzyme from *V. fischeri* in cell free broth, performed electrophoresis by the method described by Lammeli et al., (1970) with some modifications (Vorderwulbecke et al., 1992). Gel was casted by using discontinuous buffer system having 10% resolving gel and 5% stacking gel. For measurement of molecular mass of protein, commercial broad range molecular mass standard proteins were used. Protein bands were located by coomassie blue staining and molecular mass was determined using TotalLab v2.01 software.

2.7 Characterization of Lipase Enzyme

2.7.1 pH stability

Enzyme solutions at a concentration of 70mg/ml were adjusted to various pH ranging from pH 2 to 11 with either 0.1N NaOH or 0.1 N HCl and aliquots were incubated at 30°C for 4 hrs. Then aliquot was removed and assayed for activity.

2.7.2 pH optimum

Enzyme assays were conducted at various pH in an emulsified reaction mixture containing 0.4 ml of oil or Tween or TAG, 4ml 50mM Tris, 0.1 ml enzyme. The pH was maintained by pH stat with 0.02 NaOH. After incubation of the reaction mixture for 40 min at 30°C, it was titrated to pH 9. The quantity of free fatty acids released was calculated from the total quantity of base used. Control reaction mixture contained heat inactivated enzyme.

2.7.3 Temperature stability

The solution of enzyme at concentration of 45mg/ml was adjusted to pH 7.0 with 0.02 NaOH and aliquots were incubated at temperatures ranging from 5°C to 65°C for 4 hrs. Then the aliquots were assayed for activity.

2.7.4 Temperature optimum

Enzyme activity was determined at various temperatures ranging from 5°C to 65°C. The reaction mixtures (except enzyme) were held at the respective temperature for 5 min before the addition of the enzyme.

2.7.5 Substrate and Enzyme Kinetics

The lipase enzyme was incubated with various concentrations of substrates and the final substrate concentration ranged from 1 to 10 mM of tributyrin, triolein. Different concentrations of enzymes also studied in the concentration of 5, 10, 15 and 20 microlitres.

2.7.6 Enzyme Stability on metal ions and other chemicals

Enzymes were preincubated for 1 h at 30°C (pH 7.0) and in 0.1M Tris-HCl buffer with various ions and other chemicals (one at a time). Assay was performed with the mixture, which did not contain CaCl₂ (except in test sample). The ions used were included NaCl (10mM), BaCl₂ (0.001M), MgCl₂ (0.001M), KCl (2mM), FeSO₄ (0.001M), CaCl₂ (0.001M), SrCl₂ (0.001M), NaF (2mM), MnCl₂ (2mM), CuO₂ (2mM). Other chemicals tested were ethylene diamine tetra acetic acid (0.5% EDTA), the ammonic detergent, sodium dodecyl sulphate (0.5% SDS).

2.7.7 Enzyme Stability During Storage

Enzyme solutions from 2 days culture were stored at -20, 1, 8, and 20°C. Formaldehyde was added to a final concentration of 0.04% to prevent bacterial growth. 30 ml of a 2 days culture of lipase solution was sterilized by membrane filtration (0.22µm, Millipore corp.). The lipase activity in the stored samples was determined periodically by the pH stat technique and expressed as percent initial activity.

3. Results and Discussion

3.1 Bacteria and growth condition

V. fischeri encountered 100% of luminous bacteria. Total viable luminous count range was varied from 4 to 18 CFU/ml. The habitats of this squid species must receive a significant input of cells of symbiotic *V. fischeri* (Lee and Ruby, 1994). The luminous *V. fischeri* isolate was motile Gram negative rods. They produced yellow colonies on SWC agar plates. They were halophiles, unable to grow in the absence of NaCl. The colony morphology of the luminous *V. fischeri* strains tested on VHA was small (2 to 5mm) dark blue green colonies. Harris et al., (1996) reported that the VHA media displays great potential as primary isolation medium and offers significant advantages over thiosulfate-citrate- bile salts- sucrose agar.

3.2 Screening of Lipase Enzyme

In ZoBell modified media, the *V. fischeri* was showed 40 mm of halos after 10 days incubation indicates that the strain *V. fischeri* showed significant lipase activity. In fact it actively splits tributyrin and tween 80 than triolein as good substrates. Bruni et al., (1982) reported that the most strains of *Pseudomonas* sp. NCMB 1082 was split all tweens, tributyrin, but not triolein, 9 strains showed good activity on water soluble tweens, 4 on tween 85. In spirit blue agar, the width of hydrolysis areas were measured to observe the lipase activity of luminous *V. fischeri* bacteria at different temperatures. At 30°C, the lipase activity of strain was appeared after 7 hrs with a large discoloration area or dark blue halos and the widest area observed after 1 day. At 17°C, the activity began after 12 hrs, the size of halos increase after 3 days but the area of hydrolysis was smaller than that at 30°C. Apparently low activity was observed at 6°C. More or less similar mm of halos as that in ZoBell modified agar was observed in spirit blue agar with the substrate (tweens, triacylglycerol) at 30°C. The higher activity at 30°C may be attributed to maximum growth of the organism and subsequently increased lipase secretion. Similar results were observed by Makhzoum et al., (1995) during their study of lipase production by *P. fluorescens*. In Rhodamine B agar, the strains of *V. fischeri* showed 12mm of orange halos around the bacterial colonies at the 10 day incubation. Kouker and Jaeger (1987) detected a plate assay for bacterial lipase in a medium containing triacylglycerol and the fluorescent dye rhodamine B. Substrate hydrolyses causes the formation of orange fluorescence halos around bacterial colonies visible upon UV irradiation.

3.3 Purification of Lipase Enzyme

Highest yield was obtained in the medium after 3 days at 30°C. To minimize the loss of enzyme activity, the purification procedures were performed at 4°C. Results of several trials indicated that 60% saturation of the supernatant fluid with ammonium sulfate precipitated the largest amount of lipase. After dialysis, the specific activity of lipase containing dialysate was increased than that in culture supernatant fluid. In DEAE – cellulose chromatography, lipolytic fraction could be eluted with 0.6M NaCl (pH 7.0). Hundred lipolytic fractions on the top of chromogenic substrate plates showed yellow zone around the disc, those highest activity was observed in between the fractions of 40-46, similar result was observed in titrimetric assay. DEAE-cellulose column chromatogram is shown in Figure 5. The purified lipase was exhibiting final specific activity of 121U/mg and also showed single band in native PAGE. Nawani and Kaur (2000) have been used phenyl sepharose chromatography as a single step process that yielded a high active and pure lipase. Low yield of purified enzymes can be attributed to loss during ammonium sulphate precipitation as well as tight binding of lipase to hydrophobic column as a significant amount of lipase activity never eluted from the column. Like most of *Bacillus* lipases, the lipase from *Bacillus* J33 does not form aggregates (Lesuisse et al., 1993; Schmidt-Dannert et al., 1994). On the CM-cellulose column, the highest lipase activity was eluted very early in fractions 6 to 20 and about 93% of its activity was recovered. Active fractions were applied to the DEAE-cellulose and the lipase activity was highest between 0.23 and 0.35 M NaCl in fractions 21 to 32 and the recovery was 45%. The purified lipase showed only one protein band on SDS-PAGE (Abdou, 2003).

3.4 Molecular Mass

The lipase from *V. fischeri* was showed molecular mass of 57 KDa was calculated by Rf value. The crude lipase (culture supernatant) was showed multiprotein bands, indicates the impurities of other proteins (Fig 6). Lipases from *P. fluorescens* had a molecular mass of 55, 52, 32 KDa (Bazoglu, 1984; Kumura et al., 1993; Stepaniak and Fox, 1985). The lipase molecular mass was estimated to be 52 KDa (Abdou, 2003). Matsumae and Shibatani (1994) found that the molecular mass for *S. marcescens* lipase was 62 KDa, while that of *S. graminisii* was 57 KDa (Abdou, 1997). The lipase from a bacterium (*Pseudomonas aeruginosa* YS-7) showed the molecular size of 40 KDa hydrolysed a variety of fatty acid esters (Shabtai and Mishne, 1992).

3.5 Characterization of Lipase

3.5.1 pH stability

The purified lipase showed maximum stability at pH 8. Under the pH 5 the lipase lost about 40% of its activity after holding at 4 hrs. The stability range was 7 to 9. Similar results were observed by Matsumae and Shibatani (1994). *Serratia marcescens* Sr41 8000 lipase was stable between pH 6 to 9, also that of *Serratia grimisii* was stable over the pH range of 7 to 9 (Abdou, 1997). Other lipase showed stability with in the pH range of 5.5 to 9 (Fox and Stepaniak, 1983; Kumura et al., 1993).

3.5.2 Optimum pH

The optimum pH was likely between 7 and 8. The pH activity curve (Fig 1) showed that the enzyme reached about 100% of its maximum activity at pH 8. Abdou (1997) reported that the purified lipase from *Serratia grimisii* exhibited an optimum pH over the range 8 to 9, while that from *S. marcescens* Sr41 8000 showed maximum activity at about pH 8 (Matsumae and Shibatani, 1994). Previous investigation (Fox and Stepaniak, 1983) showed that the optimum pH for lipases from different psychrotrophs was 8.

3.5.3 Thermal Stability

The lipase of *V. fischeri* showed 80% stability at 35°C, but the least residual activities was at 5, 10 and 50°C. No activity was observed in 60, 65°C and above. Petersen and Daniel (2006) determined the effects of temperature and pH on the activity of purified lipase was 6-9.5 and 15-60°C respectively. The maximal activity was recorded at 40°C and at pH 8.

3.5.4 Optimum Temperature

The effect of temperature on the lipase activity (Fig 2) showed that optimum temperature for the enzyme activity occurred at 30°C and about 80% of its maximum activity occurred at 5°C. This high activity at low temperature was observed by some workers. Fox and Stepaniak (1983) found that purified lipase of *P. fluorescens* strain AFT 36 exhibited about 15% of its maximum activity at 4°C, Stepaniak et al., (1987) reported that *P. fluorescens* P1 lipase showed about 30% at 4°C.

3.5.5 Enzyme and Substrate Kinetics

The lipase activity was reached at maximum in between the 1 to 2 mM tributyrin concentration. The 50% of the activity was inhibited by 7 mM of tributyrin. This results was supported by Abdou (2003), he reported that the enzyme was inhibited by a concentration more than 6.25 mM. A linear relationship was also evident when enzyme activity was measured as a function of protein concentration. The same direct proportionality was found when crude extract were used as the source of enzyme (Oterholm et al., 1970).

3.5.6 Effect of Metal Ions, Chelator and Other Chemicals on Lipase

Figure 3 shows the results on the effect of various inhibitors on the activity of the lipase. Except NaCl, CaCl₂, which were showed no effect on enzyme activity. All other ions tested in the present study showed inhibition with relative degree of variation. Evidently even the low concentration of NAF and CuO₂ highly retarded the lipase activity. The ion chelator, EDTA and anionic detergent SDS, retarded lipase activity. The inhibitory action of former was stronger than that of latter. Action of these two compounds could be attributed to their effect in creating the imbalance of ions in the reaction mixture by absorption or release, respectively. Benjamin and Pandey (2000) reported that the chelator, EDTA and anionic detergent SDS effect 75% of lipase activity and the effect of EDTA is higher than the latter. In this study 80% of activity inhibited by SDS and no lipase activity was observed in the presence of EDTA.

3.5.7 Enzyme Stability During Storage

Figure 4 shows the lipase activity in the time of storage at different temperatures. Frozen storage did not affect the enzyme activity to any greater extent. The lipase enzyme stability suggests that the differences are due to a real decrease in enzyme production, rather than to an accelerated destruction of enzyme at higher temperatures. An explanation might be that the enzyme systems involved in lipase formation are repressed at higher temperatures, thus resulting in a lower productivity (Andersson, 1980).

4. Conclusions

V. fischeri is the bioluminous bacteria secreting extracellular lipase has been purified and characterized. The lipase hydrolytic activity upon tributyrin (C4) was found to be higher than upon triolein (C16). This higher effect of lipase was due to the different chain length of substrates. The characteristics such as pH stability in the alkaline range and high hydrolytic reaction on tweens and triacylglycerols will be useful for further research. Further study will focus on cloning and molecular characterization of the *V. fischeri* lipase coding gene.

References

- Abdou, A. M. (1997). Studies on some gram negative proteolytic and lipolytic microorganisms in milk and milk product. Ph.D., Diss., Zagazig Univ. (Benha branch), *Kaliobyia*. Egypt.
- Abdou, A. M. (2003). Purification and partial characterization of psychrotrophic *Serratia marcescens* lipase. *J. Dairy Sci*, 86: 127-132.
- Andersson, R. E. (1980). Microbial lipolysis at low temperature. *App. Env. Microbiol*, 39: 36-40.
- Benjamin, S. & Pandey, A. (2000). Isolation and characterization of three distinct forms of lipases from *Candida rugosa* produced in solid state fermentation. *Brazilian Archives of Biology and Technology*, 43: 453-460.
- Bozoglu, F. (1984). Isolation and characterization of an extracellular heat-stable lipase produced by *Pseudomonas fluorescens*. *Agric. Food. Chem.*, 32: 2-6.
- Bruni, V., Maugeri, T. & Alonzo, V. (1982). Lipolytic activity of marine bacteria influence of NaCl and MgCl₂. *Marine Biology*, 67:113-119.
- Fox, P. F. & Stepaniak, L. (1983). Isolation and some properties of extracellular heat- stable lipases from *Pseudomonas fluorescens*. Strain APT. 36. *J. Dairy Res.*, 50: 77-89.
- Ghanem, E. H., Al-Sayeed, H. A. & Saleh, K. M. (2000). An alkalophilic thermostable lipase produced by new isolate of *Bacillus alcalophilus*. *World Journal of Microbiology and Biotechnology*, 16: 459-464.
- Gupta, R., Gupta, N. & Rath, P. (2004). Bacterial lipases: an overview of production, purification and biochemical properties. *Appl. Microbiol. Biotechnol.* 64: 763-781.
- Harris, L., Owens, L. & Smith, S. (1996). A selective and differential medium for *Vibrio harveyi*. *Appl. Environ. Microbiol*, 62(9): 3548-3550.
- Hendrie, M. S., Hodgkiss, W. & Shewan, J. M. (1970). The identification, taxonomy and classification of luminous bacteria. *J. Gen. Microbiol*, 64: 151-169.
- Jaeger, K. E. & Reetz, M. T. (1998). Microbial lipases form versatile tools for biotechnology. *Trends in Biotechno*, 16: 396-403.
- Jaeger, K. E., Dijkstra, B. W. & Reetz, M. T. (1999). Bacterial biocatalysts: molecular biology, three-dimensional structure and biotechnological applications of lipases. *Ann. Rev. Microbiol.* 53: 315-35.
- Jaeger, K. E., Ransac, S., Dijkstra, B. W., Colson, C., Van Henvel. & Misset M. O. (1994). Bacterial lipases. *FEMS Microbiol. Rev.* 15: 29-63.
- Kouker, G. & Jaeger, K. E. (1987). Specific and sensitive plate assay for bacterial lipases. *App. Environ. Microbiol*, 53: 211-213.
- Kumura, H., Mikawa, K. & Sceito, Z. (1993). Purification and characterization of lipase from *Pseudomonas fluorescens*. *Milchwissenschaft*, 48:431-434.
- Lee, K. H. & Ruby, E. G. (1994). Effect of squid host on the abundance and distribution of symbiotic *V. fischeri* in nature. *App. Environ. Microbiolog.* 60. 1565-1571.
- Lesuisse, E., Schanck, K. & Colson, C. (1993). Purification and preliminary characterization of the extracellular lipase of *Bacillus subtilis* 168, an extremely basic pH tolerant enzyme. *Eur. J. Biochem.* 216:155-160.
- Makhzoum, A., Knapp, J. S. & Ownsce, R. K. (1995). Factors affecting growth and extracellular lipase production by *Pseudomonas fluorescens*. 2D. *Food Microbiol*, 12: 277-299.
- Matsumae, H. & Shibatani, T. (1994). Purification and characterization of lipase from *Serratia marcescens* Sr41 8000 responsible for asymmetric hydrolysis of 3- phenylglycidic acid esters. *J. Ferment. Bioeng*, 77:152-158.
- Nawani, N. & Kaur, J. (2000). Purification, characterization and thermostability of lipase from a thermophilic *Bacillus* sp. *Molecular and Cellular Biochemistry*, 206: 91-96.
- Oterholm, A., Ordal, Z. J. & Witter, L. D. (1970). Purification and properties of a glycerol ester hydrolase (lipase) from *Propionibacterium shermanii*. *App. Microbiol.* 20:16-22.
- Petersen, M. & Daniel, R. (2006). Purification and characterization of an extracellular lipase from *Clostridium tetanomorphum*. *World Journal of Microbiology and Biotech.* 22:431-35.
- Reichelt, J. L. & Baumann, P. (1973). Taxonomy of the marine, luminous bacteria. *Arch. Microbiol.* 94: 283-330.
- Ruby, E. G. & Nagai, M. J. M. (1992). A squid that glows in the night: development of an animal bacterial animal mutualism. *J. Bacteriol*, 174: 4865-4870.

Ruby, E. G. & Nealson, K. H. (1976). Symbiotic association of *Photobacterium fischeri* with the marine luminous fish *Monocentris japonica*: a model of symbiosis based on bacterial studies. *Biol. Bull.* 151: 574-586.

Sabu, A. (2003). Sources, properties and applications of microbial therapeutic enzymes. *Indian J. Biotechnol.* 2: 334-341.

Schmidt-Dannert, C., Sztajer, H., Stocklein, S., Menge, V. & Schmid, K. D. (1994). Screening, purification and properties of a thermophilic lipase from *Bacillus thermocatenulatus*. *Biochem. Biophys. Acta*, 1214:1249-1259.

Shabtai, Y. & Mishne, N.D. (1992). Production, purification and properties of lipase from a bacterium (*Pseudomonas aeruginosa* YS-7) capable of growing in water-restricted environments. *App. Environ. Microbial*, 59:174-180.

Stepaniak, L., Brikeland, J.E., Sorhavy, T. & Vagias, G. (1987). Isolation and partial characterization of heat stable proteinase, lipase and phospholipase C from *Pseudomonas fluorescens*. *Milchwissenschaft*. 12: 75-79.

Stepaniak, L., and Fox, P. F. (1985). Isolation and characterization of heat stable proteinases from *Pseudomonas fluorescens* strain AFT 21. *J. Dairy Res.*, 52: 77-89.

Vorderwulbecke, T., Kieslich, K. & Erdman, H. (1992). Comparison of lipases by different assays. *Enzyme Microb. Technol*, 14: 631-639.

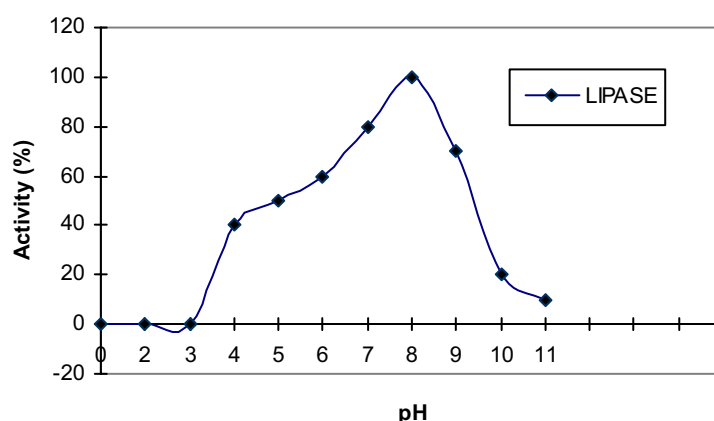


Figure 1. Effect of pH on the Lipase Enzyme from *Vibrio fischeri*

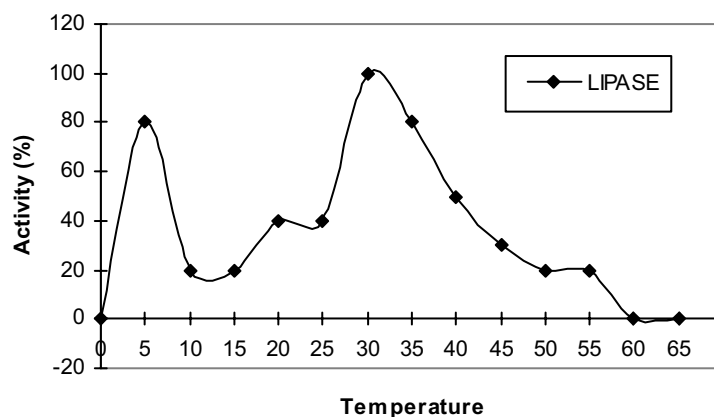


Figure 2. Effect of Temperature on the Lipase Enzyme from *Vibrio fischeri*

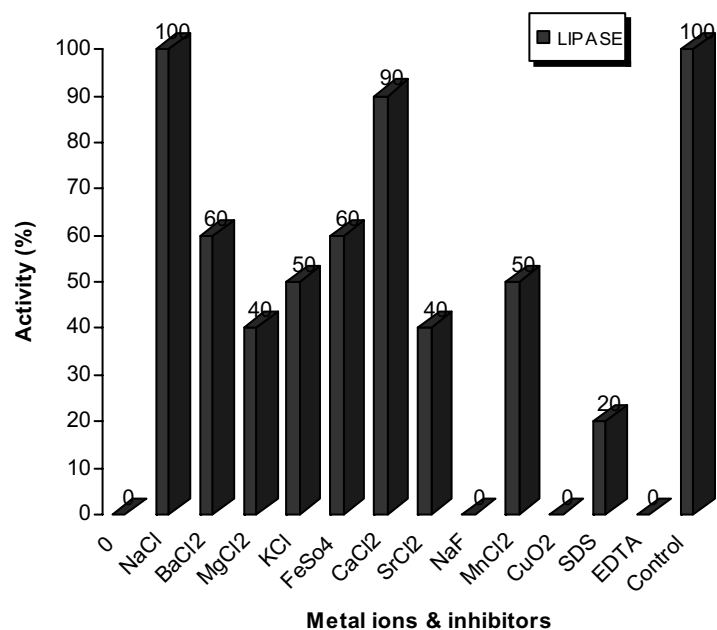
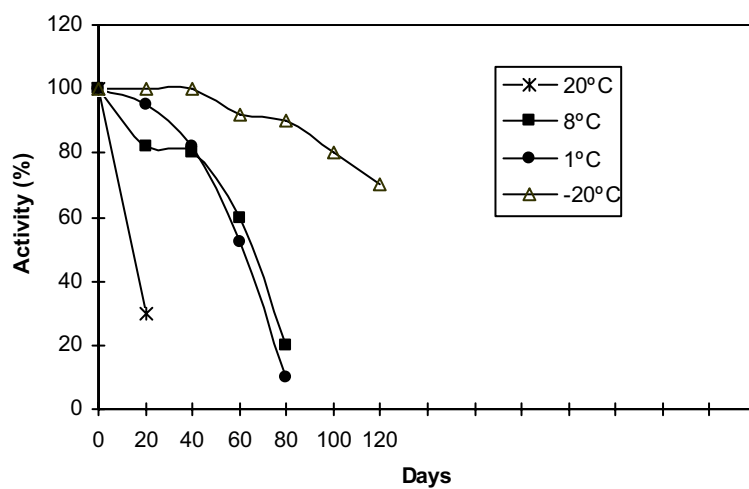


Figure 3. Effect of inhibitors on lipase enzyme

Figure 4. Storage Stability of *Vibrio fischeri* Lipase at Different Temperature

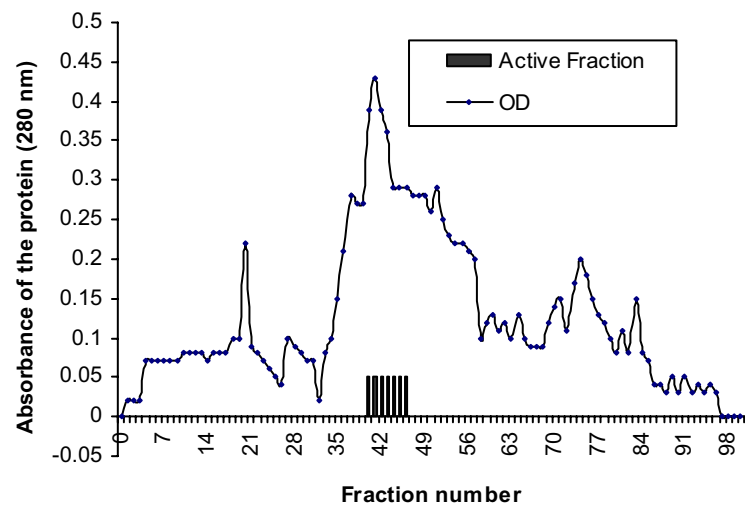


Figure 5. Elution Profile of Lipase from the DEAE-Cellulose Column

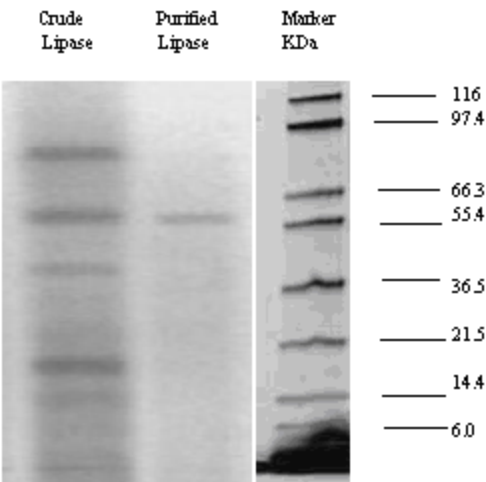


Figure 6. Molecular Mass of Crude and Purified *V. fischeri* Lipase



Cloning and Analysis of DNA Sequence of Gene CylA of Enterococci Inducing Sheeps Encephalitis

Guijun Ma, Sujuan Han, Genqiang Yan & Xia Zhou

College of Animal Sciences and Technology

ShiHeZi University/Laboratory of Xin jiang Endemic and Ethnic Diseases

Shihezi 832003, China

E-mail: shzmgj@163.com

Abstract

A DNA fragment was amplified from the chromosomal DNA of Enterococci Inducing Sheeps Encephalitis by PCR and then was cloned into pMD19-T Vector. The cloned fragment was sequenced. Comparing the DNA sequence of the amplified fragment with the published sequence of gene CylA showed that they were 99.3% homologous.

Keywords: Enterococci inducing sheeps encephalitis, CylA cloning, DNA sequence

Enterococci are Gram-positive commensal bacteria inhabiting the alimentary canals of humans and animals. Recently, excessive employment of broad-spectrum antibiotics has created resistant strains. Enterococci infection has become an intractable problem in clinical treatment due to enterococci possessing intrinsic and acquired resistance (Wang Yan-hong & Zhang Kou-xing 2005). This problem is now a hotspot within the study of enterococci.

In 2002 Nathan Shankar et al. (Nathan, Shankar & Arto S. Baghdayan 2002) found a pathogenicity island in vancomycin-resistance *Enterococcus faecalis*. The virulence factors in *E. faecalis*, including a structurally novel toxin, the cytolysin, a surface protein, Esp, and an aggregation substance, which resided in this pathogenicity island. Expression of cytolysin (cyl), which is known to contribute to enterococcal virulence and have the ability to lyse erythrocyte, to kill leucocyte and to damage cordis cell (M.C.Booth et al. 1996, Y.Ike, H.Hashimoto & D.B.Clewell 1987, Qiang Hua, Lin Jian-yin & Jiang Ming-sen 2001). Some investigators reported it also poisoned neutrophils, aematoblast and spermatozoa cells (Yang Jin-song & bao You-di.1997, Haas & Wgilmore 1999). In our study the cylA gene fragment was amplified from the chromosomal DNA of enterococci inducing sheeps encephalitis by PCR and then was cloned into pMD19-T Vector. Then it was sequenced and found homologous with the published sequence of gene CylA. This study provides groundwork for studying the enterococcal molecular biology characteristics, expression of gene Cyl and biological activity of productions.

1. Materials and methods

1.1 Bacterial strain and Vector

The EA strain of enterococci Inducing Sheeps Encephalitis is conserved by our laboratory. Its serotype is lancefield group D (Qi Ya-yin, Yan Gen-qiang & Wang Jing-mei 2005). Vector pMD19-T obtained from Takara.

1.2 Chemicals.

Restriction endonucleases (HindIII, EcoR I) and T4 DNA ligase were also from Takara. QIAquick Gel Extraction Kit, Taq DNA polymerase and dNTP were purchased from Shanghai Sangon Biological Engineering Technology & Services Co.

1.3 Preparation of Genomic DNA from EA strain.

1.3.1 Inoculate 2ml of LB containing the ampicillin with a single colony of EA strain. Incubate the culture overnight at 37°C with vigorous shaking.

1.3.2 Pour 1.5ml of the culture into a microfuge tube. Centrifuge at maximum speed for 30 seconds at 4°C in a microfuge.

1.3.3 Resuspend the bacterial pellet in 50μL proteinase K (100μg/ml), then incubate the tube for 1 hour at 37°C.

1.3.4 Add 200μL lysis solution (Tris-HCl 40mmol/L, Natrium Acetate 20mmol/L, EDTA 1mmol/L, SDS 1%), vigorous

blow by tip.

1.3.5 Then add 60µL 5mol/L NaCl, Centrifuge the bacterial lysate at 12000r/m for 10minutes after full mix. This step eliminates residua of albumen compounds and cell-wall components.

1.3.6 Transfer the aqueous phase to a fresh centrifuge tube and add an equal volume of phenol equilibrated 0.1mol/L Tris-Cl (Ph8.0).Gently mix the two phases by turning the tube end-over-end for ten minutes.

1.3.7 Separate the two phases by centrifugation at 12000r/m for 3 minutes at room temperature. Then a fresh centrifuge tube was used to collect the viscous aqueous phase.

1.3.8 Repeat the extraction twice and pool the aqueous phase.

1.3.9 Precipitate the DNA by adding an equal volume of isopropanol. Collect the precipitated DNA by centrifugation at 15000rpm for 15 minutes at 4°C.

1.3.10 Carefully remove the isopropanol. Rinse the pellet of DNA with 1 ml of 70% ethanol. Remove the 70% ethanol, and allow the pellets to dry in air for 15-20 minutes at room temperature.

1.3.11 Dissolve the nucleic acids in 50µL of TE (Ph8.0) containing 20µg/ml DNase-free RNase A. Store the DNA solution at -20°C.

1.4 PCR primers and PCR amplification

Both of the oligonucleotide primers chosen for amplification of *cylA* gene were selected from the published sequences with the assistance of the Primer Design software, P-I(5'GAC TCG GGG ATT GAT AGG C 3')and P-II(5'GCT GCT AAA GCT GCG CTT AC 3'),and the PCR product is 689bp.The oligonucleotides were synthesized by Shanghai Sangon. The reaction mixtures contained 1×PCR buffer,2 mM MgCl₂, 200 µM each dNTP, 400 nM each primer and 0.25 U Taq DNA polymerase, 5µL DNA template. The final reaction volume was 50µL. Samples were amplified on a DNA thermal cycler by heating for 5 min at 95°C for 60 s,58°C for 60 s and 72°C for 60 s,and a final step of 72°C for 10 min. PCR products were analysed by gel electrophoresis in 1%(w/v) agarose gel.

1.5 Recovery and Purification of DNA fragments

Recovery and Purification of DNA fractionated on agarose gels using QIAquick Gel Extraction Kit.

1.6 Joined the target DNA

The pMD19-T vector used in this experiment was purchased from Takara. The steps was followed the explanation. Place Confected DNA solution in sterile microfuge tubes in final volume 5µL mixtures, which contain: pMD19-T Simple Vector 1µL, Control Insert 1µL, Target DNA 3µL. Then add an equal volume Ligation Mix. Incubate the reaction mixtures overnight at 16°C.

1.7 Preparation and Transformation of Competent *E.coli*

E.coli used in this experiment was engineering bacterial Top 10. Preparation of competent *E.coli* using Calcium Chloride(Liu Jin-yuan,Chang Zhi-jie & Zhao Guang-rong 2002). Add 10µL of DNA joined productions to polypropylene tube which contains 100µL of suspension of competent cells. Mix the contents of the tube by swirling gently. Store the tube on ice for 30 minutes. Transfer the tube to a rack placed in a preheated 42°C circulating water bath. Store the tubes in the rack for exactly 90 seconds. Rapidly transfer the tubes to an ice bath. Allow the cells to chill for 1-2minutes. Add 890µL of LB medium to the tube. Incubate the culture for 60min at 37°C with vigorous shaking. Transfer the appropriate volume of transformed competent cells onto agar LB medium containing the amp, X-Gal, IPTG. Store the plate at room temperature until the liquid has been absorbed. Invert the plate and incubate at 37°C for 16 hours.

1.8 Colony PCR and Plasmid DNA Enzyme Cutting

The white colony was picked out, which was used as the PCR template for the identification of target DNA fragment. Plasmid DNA was isolated from small-scale white colony bacterial cultures by treatment with alkali and SDS and by digesting them with restriction enzymes whose sites flank the insert in the multiple cloning site. Enzyme cutting system contained plasmid DNA 10µL,EcoR I 1µL, Hind III 1µL, 10×Buffer 1µL, add ddH₂O to 20µL.Incubated the mixtures for 3~6 hours in a preheated 37°C circulating water bath.

1.9 DNA Sequencing

Selected positive colonies were punctured in the microfuge tubes containing LB solid medium. The sequencing of target DNA was undertaken by the Shanghai Sangon Sequence Sequence Dep.

2. Results

2.1 PCR Amplification the Gene of *CylA*

PCR products were analysed by gel electrophoresis in 1% (w/v) agarose gel as shown in Figure1. The amplification

products were aggregated among the 600bp and 750bp. That result was consistent with the target DNA fragment.

2.2 Colony PCR

Picked a number of white and blue colonies by transformation with the ligation reaction. Confirmed the presence of the amplified fragment by colony PCR. Consequently, white colony is positive clone and blue colony is negative clone, shown in Figure 2. Therefore, the white colony was positive cloning recombinant.

2.3 Identification by Enzyme Cutting of Plasmid DNA

Isolating the plasmid DNA and digesting them with restriction enzymes (EcoR I , Hind III), the cut-off fragment was around 750bp as shown in Figure 3. The enzymes cutting sites in the pMD19-T vector flank the insert about 30bp, respectively, and add the target DNA 689bp, which is consistent with above consequence.

2.4 Sequencing

The sequencing of the target DNA which was inserted into the pMD19-T vector was undertaken by using currency primer M13. Comparing the DNA sequence of the amplified fragment with the published sequence of gene CylA showed that they were 99.3% homologous with only six mutated nucleotides. The mutated nucleotides were matched with the corresponding site nucleotide in Genebank, respectively. The results are shown in the Figure 4.

3. Discussion

The *E. faecalis* cytolysin has been demonstrated to contribute to the virulence of enterococcal disease in a number of animal models, as well as in humans. Studies about cytolysin in China are fewer than those of foreign countries and have been limited to the strains from nosocomial infections. In this study the *cylA* gene fragment was amplified from the chromosomal DNA of *Enterococcus* Inducing Sheep's Encephalitis by PCR and cloned into pMD19-T Vector. Then sequencing and homologous comparison with the published sequence of gene CylA showed that they were 99.3% homologous with only six mutated nucleotides. The six mutated nucleotides were matched with the corresponding site nucleotide in Genebank, respectively. Taq DNA polymerase lacked 3'-5' exonuclease proofreading activities, sequence apparatus and software sometimes occurred fault or leak read, that both cases perhaps led to the mutation. This experiment supported the observation that the genes of the enterococcal cytolysin were consistent regardless whether the strains came from different regions and infections, human or animal. So we can further investigate the expression of gene Cyl and biological activity of productions.

Although scientists have been paying more attention to the antimicrobial resistance mechanisms of enterococcus and have one large numbers of studies, the study of the enterococcal pathogenesis is just begun. A number of studies over the years have addressed the issue of enterococcal virulence and the identification of enterococcal virulence factors (P.M.Tendolkar, A.S.Baghdayan & N.Shankar 2003). Most prominent among these virulence determinants have been the surface adhesions Esp and aggregation substance (AS), collagen-binding protein Ace, secreted toxin cytolysin, secreted proteases gelatinase (gelE) and endocarditis antigen (efaA) et al. (BRADLEY, D. JETT, MARK & M. HUYCKE 1994, P.M.Tendolkar, A.S.Baghdayan & N.Shankar 2003). All these virulence determinants may contribute to the pathogenesis of enterococcal infection through a number of mechanisms; gelE, esp and *cylA* may play a crucial role in the pathogenic process (Roberta et al. 2004, H.A.Elsner et al. 2000, Ma Li-yan et al. 2005). The enterococcal cytolysin is a novel toxin that consists of two nonidentical, post-translationally modified subunits that interact to cause lysis of erythrocytes and other eukaryotic cells, and cytolysin is lethal for a wide range of Gram-positive bacteria (PHILLIP, S. COBURN, YNN & E. HANCOCK 1999). Cytolysin is a crucial virulence factor for enterococcal infection and can aggravate the degree of enterococcal infection (Haas & Wgilmore 1999). In some reports, genes of the cytolysin and the resistance may be presence some relation (L.De, Vuyst, M.R.F. Moreno & H. Revets 2002, Colmar & Homud. T 1987). The relations of those virulence factors and the mechanism of those pathogenic substances in enterococcal infection, remain to be explored. Therefore we identified the gene of the *cylA* by cloning and sequencing. In future research will involve cloning and expression of cytolysin protein and, according to that preparation, developing the antiserum for immunology detection, studying the enterococcal pathogenesis and developing the generic engineering bacterium.

References

- BRADLEY, D. JETT, MARK & M. HUYCKE. (1994). Virulence of Enterococci. *CLINICAL MICROBIOLOGY REVIEWS*, Oct, 462-478.
- Colmar & Homud. T. (1987). *Enterococcus faecalis* hemolysin-bacteriocin plasmids belong to the same incompatibility group. *Appl Environ Microbiol*, 53, 567.
- Haas & Wgilmore. (1999). Molecular nature of a novel bacterial toxin: the cytolysin of *Enterococcus ecalis*. *Med Microbiol Immunol*, 187:183-190.
- H.A.Elsner, I.Sobottka, D. Mack & M.Claussen. (2000). Virulence Factors of *Enterococcus faecalis* and *Enterococcus faecium* Blood Culture Isolates. *Eur J Clin Microbiol Infect Dis*, 19 :39-42.

- L. De, Vuyst, M.R.F. Moreno & H. Revets. (2002). Screening for enterocins and detection of hemolysin and vancomycin resistance in enterococci of different origins, *Int. Food Microbiol*, 2635, 1-20.
- Liu, Jin-yuan, Chang, Zhi-jie & Zhao, Guang-rong. (2002). *Experimental Protocols for Molecular Biology*, Tsinghua university press, 1-2.
- Ma, Li-yan, Xu, Shu-zhen & Ma, Ji-ping. (2005). Advance in Study of Enterococcal Pathogenesis. *Chinese Journal of Nosocomiology*, 15 (3), 356-360.
- Ma, Li-yan, Xu, Shu-zhen, Ma, Ji-ping. (2005). Detection of partial virulence determinants and phenotypes in Enterococci. *Chinese Journal of Laboratory Medicine*, 28(5), 529-532.
- M. C. Booth, C. P. Bogie, H. G. Sahl, K. L. Hatter & M. S. Gimore,. (1996). Structural analysis and proteolytic activation of *Enterococcus faecalis* cytolysin, a novel lantibiotic. *Mol. Microbio*, 21, 1175-1184.
- Nathan, Shankar & Arto S. Baghdayan. (2002). Modulation of virulence within a pathogenicity island in vancomycin-resistant *Enterococcus faecalis*. *Nature*, 417:746-750.
- PHILLIP, S. COBURN, YNN & E. HANCOCK. (1999). A Novel Means of Self-Protection, Unrelated to Toxin Activation, Confers Immunity to the Bactericidal Effects of the *Enterococcus faecalis* Cytolysin. *INFECTION AND IMMUNITY*, July, 3339-3347.
- P. M. Tendolkar, A. S. Baghdayan & N. Shankar. (2003). Pathogenic enterococci: new developments in the 21st century. *CMLS, Cell. Mol. Life Sci*, 60, 2622-2636.
- Qiang, Hua, Lin, Jian-yin & Jiang, Ming-sen. (2001). The Relationship between Hemolysin and Virulence of Enterococci. *Chinese Journal of Zoonoses*, 17(6), 68-70.
- Qi, Ya-yin, Yan, Gen-qiang & Wang, Jing-mei. (2005). Isolation and Identification of *Enterococcus Faecalis* in Lambs with Meningitis. *Journal of Shihezi University (Natural Science)*, 23(2), 200-202.
- Roberta, Creti, Monica, Imperi & Lucia, Bertuccini. (2004). Survey for virulence determinants among *Enterococcus faecalis* isolated from different Sources. *Journal of Medical Microbiology*, 53, 13-20.
- Wang, Yan-hong & Zhang, Kou-xing. (2005). Advance in Study of Enterococcal Infection. *Section of Respiratory System Foreign Medical Sciences*, 25(1), 38-40.
- Yang, Jin-song & Bao, You-di. (1997). Studies of Pathogenicity of Enterococci. *Chinese Journal of Zoonoses*, 13(6), 33-35.
- Y. Ike, H. Hashimoto & D. B. Clewell. (1987). High incidence of hemolysin production by *Enterococcus (Streptococcus) faecalis* strains associated with human parenteral infections. *Clin Microbiol*, 25, 1524-1528.

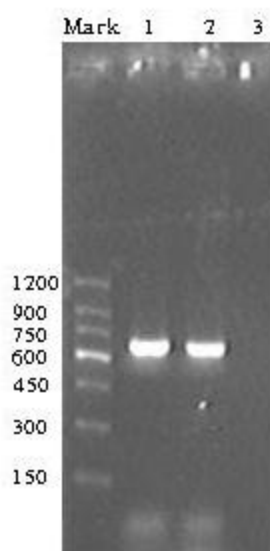


Figure 1. Electrophoretogram of EA CylA PCR products
Lane M: DNA Mark; Lane 1,2: PCR product 689bp; Lane 3: negative control

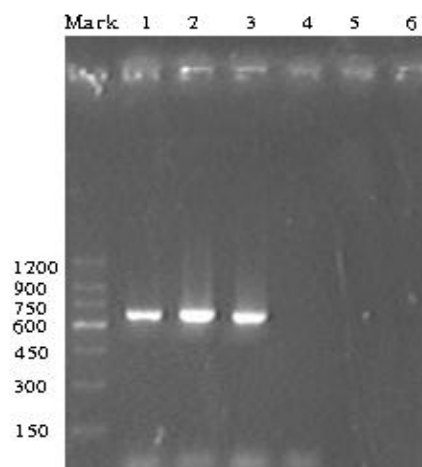


Figure 2. Identification of recombinant plasmid by PCR. Lane 1,2,3:PCR products of white colony; Lane4,5,6:PCR products of blue colony

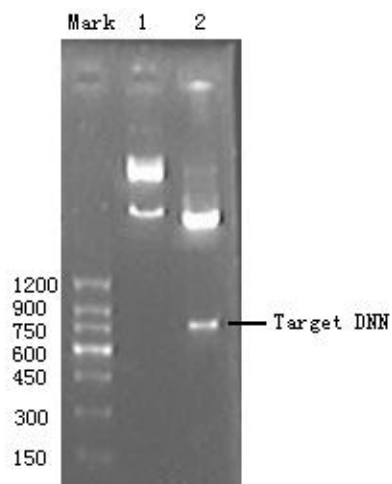


Figure 3. Restriction enzyme analysis of recombinant plasmid. Lane Mark: DNA Mark;
Lane 1: The results of cloning plasmid extraction; Lane2: enzyme cutting results

```

CylA-P GACTCGGGGATTGATAGGCTTCATCCTAATCTTCAAGACAATAACCTAAGATTAAAAAC
CylA-S GACTCGGGGATTGATAGGCTTCATCCTAATCTTCAAGACAATAACCTAAGATTAAAAAC
*****
CylA-P TATGTTAATGATATTGAGTTAGATGAATATGGTCATGGTACACAAGTTGCTGGAGTAATA
CylA-S TATGTTAATGATATTGAGTTAGATGAATATGGTCATGGTACACAAGTTGCTGGAGTAATA
*****
CylA-P GACACGATTGCTCCAAGAGTGAATTTAAATTCCTTACAAGGTGATGGATGGGACAGATGGA
CylA-S GACACGATTGCTCCAAGAGTAAATTTAAATTCCTTAAGGTGATGGATGGGACAGATGGA
*****
CylA-P AACTCTATAAATATGCTTAAAGCTATAGTTGATGCTACAAATGATCAAGTAGATATAATA
CylA-S AACTCTATAAATATGCTTAAAGCTATAGTTGATGCTACAAATGATCAAGTAGATATAATA
*****
CylA-P AATGTGAGTCTTGGATCATATAAAAAATATGGAAATAGATGACGAAAGATTTACTGTAGAA
CylA-S AATGTGAGTCTTGGATCATATAAAAAATATGGAAATAGACGACGAAAGATTTACTGTAGAA
*****
CylA-P GCATTGAGAAAGTTGTTAACTATGCAAGAAAAAATAACATTCTAATTGTTGCATCAGCA
CylA-S GCATTGAGAAAGCTGTTAACTATGCAAGAAAAAATAACATTCTAATTGTTGCATCAGCA
*****
CylA-P GGAAATGAGTCGCGTGATATAAGCACTGGTAATGAAAAACATATACCAGGAGGACTAGAG
CylA-S GGAAATGAGTCGCGTGATATAAGCACTGGTAATGAAAAACATATACCAGGAGGACTAGAG
*****
CylA-P TCTGTAATTACCGTCGGAGCTACAAAAAGAGTGGTGATATTGCTGACTATTCTAATTAT
CylA-S TCTGTAATTACCGTCGGAGCTACAAAAAGAGTGGTGATATTGCTGACTATTCTAATTAT
*****
CylA-P GGGTCTAATGTATCTATATATGGTCCCGCAGGAGGATATGGTGACAATTACAAAATAACA
CylA-S GGGTCTAATGTATCTATATATGGTCCGTCAGGAGGATATGGTGACAATTACAAAATAACA
*****
CylA-P GGACAAATTGATGCTCGTGAAATGATGATGACTTATTACCCTACATCGCTAGTTTCTCCA
CylA-S GGACAAATTGATGCTCGTGAAATGATGATGACTTATTACCCTACATCGCTAGTTTCTCCA
*****
CylA-P CTAGGCAAAGCTGCTGACTTTCCAGATGGTTATACACTTTCTTTTGGAAACAAGTTTAGCA
CylA-S CTAGGCAAAGCTGCTGACTTTCCAGATGGTTATACACTTTCTTTTGGAAACAAGTTTAGCA
*****
CylA-P ACTCCAGAAGTAAGCGCAGCTTTAGCAGC
CylA-S ACTCCAGAAGTAAGGCGCAGCTTTAGCAGC
*****

```

Figure 4. Results of Multiple sequence Alignment. CylA-P was published sequence; CylA-S was target DNA sequence; the underline part means Primer Sequence; the blackbodies means Mutation nucleotides.



Biology of *Macrolophus caliginosus* (Heteroptera: Miridae)
Predator of *Trialeurodes vaporariorum* (Homoptera: Aleyrodidae)

Mohd Rasdi, Z., Fauziah, I. & Wan Mohamad, W.A.K

Faculty of Applied Science, Universiti Teknologi MARA, 40450, Shah Alam, Selangor, Malaysia

Tel: 60-9-490-2000 E-mail: dddpim@pahang.uitm.edu.my

Syed Abdul Rahman, S.R

Malaysian Agricultural Research and Development Institute (MARDI)

Cameron Highlands, 39000 Pahang, Malaysia

Tel: 60-5-491-1255 E-mail: syedar49@gmail.com

Che Salmah, M.R.

School of Biological Sciences, Universiti Sains Malaysia

11800 Pulau Pinang, Malaysia

Tel: 60-4-653-4061 E-mail: csalmah@usm.my

Kamaruzaman, J. (Corresponding author)

Department of Forest Production, Universiti Putra Malaysia

Serdang, 43400 Selangor, Malaysia

Tel: 60-3-8946-7176 E-mail: kamaruz@putra.upm.edu.my

This project is funded by Ministry of Higher Education, Malaysia (Sponsoring information)

Abstract

Macrolophus caliginosus Wagner (Heteroptera: Miridae) is a highly polyphagous predatory bug, which has proven to be effective in controlling many insect pests of greenhouse vegetables (eggplant, tomato, and cucumber) especially whiteflies, aphids, and thrip. It is mainly used as a biological control auxiliary against *T. vaporariorum* Westwood (Homoptera: Aleyrodidae). The greenhouse whitefly, *Trialeurodes vaporariorum* is particularly harmful to tomato plants grown under the greenhouse. It has become prevalent whenever crops are frequently sprayed with insecticides. Biological control is becoming important for controlling this insect pest. A mirid bug management programme has been developed for an Integrated Pest Management (IPM) in tomato. The objective of the programme was to keep the predator population densities high enough in order to maintain *T. vaporariorum* and other insect pest populations below the economic threshold. In this study, it was very important to determine the biology of predator in term of its life cycle, behaviour at different stages, fecundity, longevity and searching abilities, in order to provide detail data for formulating the means of control against whitefly. Results of this study indicated that *Macrolophus caliginosus* adults fed on whitefly larvae of all stages from the first larval stage to the pupal stage. The predator consumed the preys at almost similar daily rates (average of 5.94 per day). The study implies that *M. caliginosus*, with its life cycle, predation, longevity and fecundity and host preference, is a beneficial insect to combat against whitefly.

Keywords: *Macrolophus caliginosus*, Predator, Life cycle, Fecundity, Longevity

1. Introduction

Macrolophus caliginosus Wagner (Heteroptera: Miridae) is a highly polyphagous predatory bug (Carapezza, A., 1995), which has proven to be effective in controlling many insect pests of greenhouse vegetables (eggplant, tomato, and cucumber) especially whiteflies (Maulana, J.C., 1996), aphids, and thrips (Berengere, C., 1996). It is mainly used as a biological control auxiliary against *T. vaporariorum* Westwood (Homoptera: Aleyrodidae) (Maulana, J.C., 1987). The greenhouse whitefly, *Trialeurodes vaporariorum* is particularly harmful to tomato plants grown under the greenhouse. It has become prevalent whenever crops are frequently sprayed with insecticides. Biological control is becoming important for controlling this insect pest. A mirid bug management programme has been developed for an Integrated Pest Management (IPM) in tomato. The objective of the programme was to keep the predator population densities high enough in order to maintain *T. vaporariorum* and other insect pest populations below the economic threshold (Alomar, O., 1996 and Albajes, R., 1999). In this study, it was very important to determine the biology of predator in term of its life cycle, behaviour at different stages, fecundity, longevity and searching abilities, in order to provide detail data for formulating the means of control against whitefly. In Malaysia, the predator *M. caliginosus* was first reported by Syed Abdul Rahman et al. (2000) (Albajes, R., 1999) on tomatoes in Cameron Highlands. Studies include biology (life cycle, predation, longevity and fecundity) and host preference of *M. caliginosus*.

2. Methods and materials

2.1 Life cycle of predator, *Macrolophus caliginosus*

This experiment was carried out at the Crop Protection Laboratory, Malaysian Agricultural Research and Development Institute (MARDI), the Cameron Highlands at Tanah Rata, Pahang, starting from February until August 2003. The predator, *M. caliginosus* were collected from brinjal (*Solanum melongena*) and tomato (*Lycopersicum esculentum*) plants grown around MARDI station. From the stock culture, a pair of predator adults were selected and placed in an oviposition container (15 cm x 8 cm) filled with fresh single brinjal leaf. A healthy, 14-day-old brinjal plant was selected and placed together with the male and female predators in the container. Female and male adults were allowed to mate in 24 hours period. The female predators laid the eggs in the stem of leaf. After five days, all the adults were removed from the oviposition container and placed back into the stock culture (50 cm x 45 cm x 60 cm). A total of 10 oviposition containers were prepared for this experiment. Some of the eggs of predators were deeply embedded in the ribs or stems of brinjal plants. No observation was carried out during the egg stage. The development of different stages from nymph to adult was observed daily. The data were recorded at different stages of life cycle and analysed with calculated means of days. The data on body length (mm), antennae, budding of different stages were also recorded and analysed.

2.2 Predation of *Macrolophus caliginosus* on Whitefly immatures

A total of 50 *T. vaporariorum* larvae of various stages on the under surface of a brinjal leaf were selected and marked. They were taken from whitefly stock culture and placed in a plastic container. Then an adult predator of *M. caliginosus* was randomly taken from the culture cage and introduced into the plastic container with the whitefly larvae. The experiment was replicated ten times (PC₁ - PC₁₀). The whitefly larvae killed by predators which had an opening at the centre of its empty body were counted and recorded. A total of 50 whitefly larvae were replaced at every two days until 10 days. Exuviae from successful emergence of whiteflies were not counted. The numbers of larvae killed by the predator were counted daily under microscope for ten days. The daily mortality of preys was regressed to generate the consumption rate of the predator. The experimental design (plastic containers) was arranged in CRD (Complete Randomised Design).

2.3 Adult longevity of *Macrolophus caliginosus*

Five plastic containers (PC1, PC2, PC3, PC4, and PC5) were prepared in this experiment. Five different treatments were used namely T0 (no treatment - no food provided), T1 (only single leaf plant), T2 (honey), T3 (single leaf plant and infested leaf with whitefly larvae), and T4 (moisturised cotton wool). No food was provided in T0 in order to determine the predator that could survive without food. Treatment T1 was to determine duration of the predator could survive on the plant without larvae or any source of food. Treatment T2 was to determine how long the predator could survive with honey, while treatment T3 consisted of predator which was provided with single leaf plant and larvae of whitefly to determine how long it could survive when it was served with sufficient food. Finally, treatment T4 consisted of predator which was served with water only. The whitefly larvae were placed in T3 for every two days. The adult predator was placed individually in the plastic container. The experiment was replicated three times and the plastic containers were arranged in CRD (Complete Randomised Design). Due to limitation of adults, these experiments randomly used adult male or female predators. In this experiment, the adults were reared by feeding them with various foods to observe how long they could survive by given those foods. One treatment was used as a control whereby no food was given to the predator.

2.4 Adult fecundity of *Macrolophus caliginosus*

Prior to the experiment, six *M. caliginosus* adults from the stock culture were randomly chosen, anaesthetised and sexed under a dissecting microscope. Following that, a pair of predators was placed in a cylindrical cage provided with a brinjal plant for oviposition. They were fed with new batch of 20 to 30 whitefly larvae of various stages every two days until the end of the experiment. The experiment was repeated three times and the plastic containers were arranged in CRD (Complete Randomised Design). The observation was carried out at the end of 30 days during adult life span, due to the longevity of predator (previously ranging between 32 to 35 days) and to avoid the second generation emergence of predator.

2.5 Data analysis

The data were recorded at different stages of life cycle and analysed with calculated means of days. The data on body length (mm), antennae, budding of different stages were also recorded and analysed. The daily mortality of preys was regressed to generate the consumption rate of the predator, number of days in the longevity of predator adult, number of predator's progeny of on fecundity of predator. Data collected was subjected to Analysis of Variance (One way ANOVA) in order to determine the significance differences among treatment means and Regression analysis using SAS Programme (Syed Abdul Rahman, 2000).

3. Results and discussion

3.1 Life cycle of predator, *Macrolophus caliginosus*

Observations on the life cycle showed that the females started to lay eggs approximately two days after mating. The eggs were embedded deeply into the stem making them unavailable for observation. Table 1 summarizes the results of the developmental stages in the predator's life cycle. After 8.6 days the eggs hatched and the first instar nymph lasted for 3.3 days before it moulted into the second instar. A total of four nymphal instars were observed in this study and the duration for third and fourth instars were 4.4 and 7.3 days, respectively. The total mean of developmental period for predators from egg to adult was 27.6 days.

<<Table 1: The mean number of days (mean \pm S.E) for each life cycle stage of the predator *Macrolophus caliginosus*>>

Table 2 and show the size of body length from head to end of abdomen measured at every stages of life cycle. The mean body length of first instar was 0.504 ± 0.0002 mm, second instar was 1.249 ± 0.0016 mm, third instar, was 2.12 ± 0.0057 mm, and fourth instar, was 3.021 ± 0.0023 mm, and adult, was 3.482 ± 0.0002 mm.

Table 2 is also summarizes the results of antennae lengths which were recorded at every stages in the predator's life cycle. For the first instar, the length of antennae was 0.34 mm, second instar was 0.71 mm, third instar was 1.27 mm, fourth instar was 1.79 mm, and adult was 2.31 mm. The development of antennae seemed to be almost constantly linear at every stage in the predator's life cycle. Table 3 and also show the length of predator's wings measured at every developmental stage of life cycle. There was no wing bud observed during the first instar stage. The bud started to develop in the second instar with a mean length of 0.304 mm. In the third instar, the wing bud increased to 1.035 mm, and in the adult, it was 2.52 mm. Results from the study demonstrated that the morphological characteristics and the immature stage of four nymphal instars were clearly noticeable.

<<Table 2: The length (mean \pm S.E.) of body, antennae and wing bud of various life cycle stages of *Macrolophus caliginosus*>>

The developmental period of oligophagus predators varies due to factors such as host plants, temperature, relative humidity (RH), habitat and most importantly the predators' species. The temperature for example, could influence the growth rate of an insect significantly. In this study, *M. caliginosus* spent 27.6 days at temperature of $24 \pm 0^\circ\text{C}$ to complete its life cycle. At 22°C , Berengere et al., (1996) found that *M. caliginosus* completed its life cycle (tomato) within 35-40 days with a preoviposition period of about 5 days. Although the temperature difference was only 2°C , the life cycle of *M. caliginosus* showed a variation of 8-13 days. The optimum temperature for species development is extremely important as insect shows maximum growth rate at such temperature. Besides temperatures, host plants influence insects' growth and life cycles of oligophagus heteropteran predator quite tremendously. Nutrients provided by the host plants are important for the egg and nymphal developments before predatory activity is intensified in the adult stage. The turgidity of the leaf ribs and midribs was extremely critical during embryonic development especially for *M. caliginosus* as it affected the hatchability of their eggs (Berengere, C., 1996). Taksdal (1963) (Sandra, D.S., 1987), Evans (1976) and Fauvel et al., (1987) had proven some plants were better hosts for certain predators. Brinjal is one of the good hosts for *M. caliginosus* as its development is relatively short in this study. Nutrients in various host plants also influence insects' mortality. *Macrolophus caliginosus* had shown variable mortality rates when fed on different host plants (Fauvel, G., 1987). Other studies showed significant difference in developmental period of *M.*

caliginosus on *Nicotiana tabacum* and *Pelargonium peltatum* which indicate that some plants are better hosts, as has been reported for several Heteroptera (Sandra, D.S., 1987; Taksdal, G. 1963 and Evans, 1976).

3.2 Predation of *Macrolophus caliginosus* on Whitefly immature

Macrolophus caliginosus ate whitefly larvae by inserting its proboscis into their bodies. Daily predation rate of *M. caliginosus* has been enumerated from the number of empty larvae with mean ranges of 5.5 to 6.8 larvae per day. The predators were found to attack the larvae of whitefly randomly regardless of larval stages and larval distribution on the leaves. Result from the studies demonstrated that the total mean of whitefly larvae killed by predators' adults was 5.94 per day. However, from the linear regression, it was found that the number of whitefly consumed by *M. caliginosus* was not significantly influenced by the number of days.

Macrolophus caliginosus adults fed on whitefly larvae of all stages from the first larval stage to the pupal stage. Within a 10-day observation, the predatory habit did not show any feeding trend. The predator consumed the preys at almost similar daily rates (average of 5.94 per day). Therefore, one predator was capable of decimating approximately 60 larvae in a period of 10 days. This capacity was relatively similar to an earlier study whereby Lucas and Alomar (2002) recorded a predation rate of 5 to 5.3 larvae per day. However when only the second and fourth larval stages whiteflies were offered to the predator, the predation rate dropped to only 2.7 larvae per day (Lucas, E., 2002). Coincidentally these larvae were reared on tomatoes. The host plant of the prey could also be a determining factor. The plant nutrient might affect the taste of the preys making them either more tasteful or less desirable to the predators. In this case brinjal might produce better tasting preys as compared to tomatoes. The feeding of *M. caliginosus* was obviously more active in the presence of various prey life stages although all individuals were randomly consumed. They were probably more alerted by different sizes and movements of the preys. *Macrolophus caliginosus* usually attacked the preys nearest to them. Alomar et al., (2002) found that this predator was more abundant in outer crop rows closer to the source of the predator. They also concentrated on plants with higher whitefly densities. Therefore in the field situation the density and location of the whiteflies on the crop plants as well as the direction and distance of predator source or reservoir influence the predation rate of *M. caliginosus* on their preys. Previous study (Barnadas, I., 1998), in the greenhouse, predators attacked the whitefly nymphs as their food source. *Macrolophus caliginosus* was more abundant in outer rows, particularly in fields close to predator sources, which were concentrated on plants with higher whitefly densities (Alomar, O., 2002). Furthermore, Castane et al. (2004) found that *M. caliginosus* was an important source of pupal mortality since no other predators were consistently found in the surveys. The role of the surrounding vegetation in the colonisation is poorly known. Although, the predator *M. caliginosus* was a good biological control agent but the predatory effect it was better when it combined with other natural enemies such as *Encarsia formosa*. For further study, researchers should take advantage of the presence of this predatory complex and consider its interactions with other biological control agents in controlling whitefly. It should also assess the movement of the greenhouse whitefly and its predators especially *M. caliginosus* between greenhouses and the surrounding habitats.

3.3 Adult Longevity of *Macrolophus caliginosus*

Results from the study showed that the predators could survive for 3.67 days without any food source (Table 3). There was a significant ($F=515.6$; $df=4,10$; $P<0.05$) in longevity of predator among the treatments. Longevity of predator was significantly ($P<0.05$) on brinjal plant with the presence of the whitefly preys and brinjal plant alone than on other treatment. There was no significance ($p>0.05$) difference in longevity when the predators lived on water alone as compared to those without eating any food. The predators lived longer when they were provided with preys (whiteflies). However, since they are polyphagous insect, predators survived quite well on brinjal without prey. When *M. caliginosus* were fed with honey, the longevity slightly improved (live longer) as compared to living on water alone. It was also observed that no food treatment gave the lowest mean days (3.67 ± 0.33), followed by supplied with water alone (4.33 ± 0.33), honey (6.33 ± 0.33) and young brinjal single leaf plant alone (25.67 ± 2.33). Finally, treated predators together with brinjal single leaf and whitefly showed the highest mean days (33.67 ± 2.33) of longevity.

The brinjal plant served as an alternative feeding source to predators, *M. caliginosus*. The ability of predators to survive was significantly different ($p<0.05$) with no food treatment. Treatment with cotton wool moisturised with water did not significantly affect the longevity of the predator. However, they could also live for quite a long time on brinjal plants in the absence of the preys. Single leaf brinjal plant and whitefly larvae show significant ($p<0.05$) influence on the longevity of predators. This was evident that the presence of whitefly larvae in the plastic containers as predators' food supply could increase the survival rate or life span of the predators. *Macrolophus caliginosus* is a relatively hardy insect that survived without food for almost 4 days. In the presence of water, the predator could live slightly longer. Water from moisturised cotton wool did not seem to directly contribute to the longevity of predators. They depend on the plant sap and their preys. Furthermore, *M. caliginosus* has piercing sucking mouthparts and need the food from the plant or their preys based on their acceptance or rejection phenomenon. Although incomparable to host plant and prey, honey prolonged the predator's life even longer (6 days) than living on water alone. This information is useful for emergency cases such as during an experiment whereby the food for this insect is not available. They can be starved up to 3 days

without fearing them dead. In situation where the food supply in the field is cut off due to harvesting of crops or destruction of habitats as well as its preys, the predator could live for a few days before supplementary food is critically required.

Nevertheless, in field conditions, there may be different results in longevity due to their behaviour in searching for food which are also affected by the environmental factors such as photo period, humidity, and temperature (Castane, C., 2004). *Macrolophus caliginosus* thrived better and live longer on host plants with a lot of whiteflies. This longevity was significantly longer than when the predator was denied of preys. As an oligophagus feeder it enjoyed food from plant and animal sources for a longer life. Feeding on mixed diet was found to improve the performance of the predator as compared to living on single-prey diets [19]. In the presence of more than one prey species, *M. caliginosus* often exhibited the tendency to choose varieties of them. When preys, *Trialeurodes vaporariorum* and *Bemisia tabaci* were available, the predator fed on both species, shifting from one to the next as availability changes (Dean, 1995). This behavioural plasticity enabled the predator to exploit alternative food when prey populations are low or temporarily absent.

<<Table 3: The survival period (days) of the predators, *Macrolophus caliginosus* with various food>>

3.4 Adult Fecundity of *Macrolophus caliginosus*

The reproduction of the predators was observed for a month. The total mean number of predators in each cage was 51, indicating that each female could produce an average of 51 progenies within 30 days. The eggs of the predators were not clearly seen. At the end of 30 days, some of the eggs had developed into adults. There were four nymphal instars with the mean period of 11.7, 14.7, 16 and 5.7 days for the first, second, third and fourth instars respectively. Therefore, the life cycle of *M. caliginosus* was completed within slightly less than a month (Table 4).

<<Table 4: Total number of predators, *Macrolophus caliginosus* after 30 days>>

In this study, it was found that a female *M. caliginosus* fed with whitefly immatures produced 51 nymphs in 30 days on brinjal plant. Unfortunately the eggs of the predators could not be observed because they were deeply embedded in the ribs of the leaves. Assuming that eggs hatchability was 100%, the hatching rate was at an average of 1.7 eggs per day. The difference in the number of progenies produced by a female was very much determined by the host plant characteristics (Gerling, D., 2001) such as hardness of the leaf petioles and midribs. Berengere et al., (1996), recorded hatching rates of *M. caliginosus* at 3 and 1.6 eggs per female per day on tobacco and a medium with *Inula viscose* extract respectively. Should hatching be approximately 100% in their study, hatchability would be of the same rates on each medium. Comparing the present result to these two records, the oviposition and eventually the hatchability rates of *M. caliginosus* eggs were closer to that of artificial substrate. Structurally, brinjal leaves are harder than tobacco leaf although both of them have a lot of hairs. It is obvious that tobacco was a much preferred host for oviposition. Therefore, the hardness, thickness and possibly the moisture content of the host plant influence the number of eggs laid by females on specific hosts. Based on previous study (Evans, H. F., 1976), the diet of the predator was very important for the fecundity of *M. caliginosus*. When the predator was fed with the eggs of *Ephestia kuehniella* (Zeller) (Lepidoptera: Pyralidae) and allowed to oviposit on *Pelagonium peltatum*, a female predator produced 268 eggs at 20°C in 35 days. The hatchability rate increased from 3 to 5.67 nymphs per day after 10 days. It peaked on day 15th to 16 nymphs per day before dropping 11.7 nymphs per day on day 25th. Feeding on whitefly larvae such as in this study, only 51 progenies were produced by a female *M. caliginosus* over a period of one month. However, if this study were prolonged until the female died, the number of eggs and offspring could be different or higher. In the life cycle structure recorded after 30 days, there were approximately 13% (11.7 nymphs) of first instar larvae. The tendency was that more eggs were hatching and more young larvae would add to the total number of the offsprings should the period of study be extended. The comparison to the previous data would then be more meaningful. Nevertheless, the aspect of environment should be taken into account as it might affect the fecundity of a female predator. In the laboratory study, caging might affect the fecundity of predators. Fecundity of *M. caliginosus* was also studied by Van Schelt et al. (1995), who placed one female and one male in a Petri dish (8 cm diam. X 3 cm) with *T. vaporariorum*. Result of the study were not comparable to the present study as the types of cages used was a cyclinder cage (15 cm diam. X 30 cm) which were less suitable for fecundity of *M. caliginosus*. However, the study of *M. caliginosus* fecundity in Petri dishes does not seem to be the best approach as females can easily escape from the dishes (Van Schelt, 1995). Interestingly, *M. caliginosus* was commercialized in Europe a biological control agent for greenhouse pests such as whiteflies. At the moment, egg laying and subsequent developments to the adult stage have been initiated on artificial substrates (Berenger et al., 1996). The predator can be mass produced to meet the need of greenhouse farmers. Nevertheless, more researches are required for cheaper and more efficient production of this predator.

4. Conclusion

It can be concluded from this study that *M. caliginosus* contribution in managing whitefly is significant. However, *M. caliginosus* alone is insufficient to restrain whitefly. Good farming practices are needed to complement the effects of

M. caliginosus in controlling whitefly. Future work should be carried out on other beneficial crops, large scale production of solanaceae crops and low land area to determine its effects.

References

- Albajes, R., and Alomar, O. (1999). Current and Potential Use of Polyphagous Predators. Integrated Pest and Disease Management in Greenhouse Crops, Kluwer Academic Publisher, Dordrecht. 265-275.
- Albajes, R., and Alomar, O. (1999). Current and Potential Use of Polyphagous Predators. Integrated Pest and Disease Management in Greenhouse Crops, Kluwer Academic Publisher, Dordrecht. 265-275.
- Alomar, O., and Albajes, R. (1996). Greenhouse Whitefly (Homoptera: Aleyrodidae) Predation and Tomato Fruit Injury by the Zoophytophagous Predator *D. tamaninii* (Heteroptera: Miridae). In: Zoophytophagous Heteroptera: Implication for Life History and Integrated Pest Management, Thomas Say Publ. Entomol. Lanham, MD. 155-177.
- Alomar, O., Goula, M. and Albajes, R. (2002). Colonisation of Tomato Fields by Predatory Mirid Bugs (Hemiptera: Heteroptera) in Northern Spain. pp. 105-115.
- Barnadas, I., Gabarra, R., and Albajes, R. (1998). Predatory Capacity of Two Mirid Bugs Preying on *Bemisia tabaci*. Entomol. Exp. Appl. 86 (1998). 215-219.
- Berengere, C., Grenier, S., and Bonnot, G. (1996). Artificial Substrate for Egg Laying and Embryonic Development by the Predatory Bug *Macrolophus caliginosus* (Heteroptera: Miridae). 20 Avenue Albert Einstein, 69621, Villeurbanne Cedex, France. Volume 7, Issue 2. 140-147.
- Carapezza, A. (1995). The Specific Identities of *Macrolophus melanotoma* (Costa, A. 1853) and *Stenodema curticolle* (Costa, A. 1853) (Insecta Heteroptera, Miridae). Natural. Siliciano S. IV 19 (1995). 295-298.
- Castane, C., Alomar, O., Goula, M. and Gabarra, R. (2004). Colonization of Tomato Greenhouses by the Predatory Mirid Bugs *Macrolophus caliginosus* and *Dicyphus tamaninii*. Department de Biologia Animal, Spain. Science direct, Biological Control 30. pp. 591-597.
- Constant, B., Grenier, S., Febvay, G., and Bonnot, G. (1996). Host plant hardness in oviposition of *Macrolophus caliginosus* (Hemiptera: Miridae). J. Econ. Entomol. 89: 1446 - 1452.
- Dean, D.E., and Schuster, D.J. (1995). *Bemisia argentifolii* (Homoptera: Aleyrodidae) and *Macrosiphum euphorbiae* (Homoptera: Aphididae) as prey for two species of Chrysopidae. Environ. Entomol. 24. 1562-1568.
- Evans, H. F. (1976). The effect of prey density and host plant characteristics on oviposition and fertility in *Anthocoris confusus* (Reuter). Ecol. Entomol. 1, 157-161.
- Fauvel, G., Malausa, J. C., and Kaspar, B. (1987). Etude en laboratoire des principales caractéristiques biologiques de *Macrolophus caliginosus* (Heteroptera: Miridae). Entomophaga 32(5), 529-543.
- Gerling, D., Alomar, O., and Arno, J. (2001). Biological Control of *Bemisia tabaci* using Predators and Parasitoids. Department of Zoology, Israel. Crop Protection 20 (2001). 779-799.
- Hansen, D.L., Brødsgaard, H.F., and Enkegaard, A. (1999). Life Table Characteristics of *Macrolophus caliginosus* Preying Upon *Tetranychus urticae*. Entomol. 269-275.
- Lenteren, J.C., and Noldus, L.P.J.J. (1990). Whitefly Plant Relationships: Behavioural and Ecological Aspects. In: Whiteflies: Their Bionomics, Pest Status and Management, D. Gerling (ed). Intercept, Hants, United Kingdom. 47-90.
- Lucas, E., and Alomar, O. (2002). Impact of the Presence of *Dicyphus tamaninii* Wagner (Heteroptera: Miridae) on Whitefly (Homoptera: Aleyrodidae) Predation by *Macrolophus caliginosus* (Wagner) (Heteroptera: Miridae). Biol. Control. 123-128.
- Malausa, J.C., and Trottin, C.Y. (1996). Advances in the Strategy of Use of the Predaceous Bug *Macrolophus caliginosus* (Heteroptera: Miridae) in Glasshouse Crops. Thomas Say Publ. Entomol., Lanham, MD (1996). 178-189.
- Malausa, J.C., Drescher, J. and Franco, E. (1987). Perspectives For the Use of A Predaceous Bug *Macrolophus caliginosus* Wagner (Heteroptera: Miridae) on Glasshouses Crops. Bull. OILB/SROP, 10(2). 106-107.
- Richard, J.E. (1990). Fundamentals of Entomology. Fifth Edition. Prentice Hall, Upper Saddle River, New Jersey 07458. 495 p.
- Root, R.B. (1973). Organization of A Plant-Arthropod Association in Simple and Diverse Habitat: The Fauna of Collards (*Brassica oleracea*). Ecol. Monogr. 43. 95-124.
- Sandra, D.S. and Ramon, C.L. (1987). SAS System for Elementary Statistical Analysis. SAS Institute Inc. 418 p.

Syed Abdul Rahman, S.A.R., Sivapragasam, A., Loke, W.H. and Ruwaida, M. (2000). Whiteflies in Malaysia. Paper Presented at University of Malaya, Kuala Lumpur. (Unpublished Report). 6 pp.

Taksdal, G. (1963). Ecology of plant resistance to the tarnished plantbug, *Lygus lineolaris*. *Ann. Entomol. Soc. Am.* 56, 69–74.

Van Schelt, J., Klapwijk, J., Letard, M., and Aucouturier, C. (1995). The use of *Macrolophus caliginosus* as a whitefly predator in protected crops, *In* D. Gerling and R. T. Mayer (eds.), Bemisia: 1995. Taxonomy, Biology, Damage, Control and Management. Intercept, Andover. 515-522.

Table 1. The mean number of days (mean \pm S.E) for each life cycle stage of the predator *Macrolophus caliginosus*

Stages	Means (day) mm \pm (S.E.)	Range (days)
Eggs	8.6 \pm (0.31)	7 – 10
First Instar	3.3 \pm (0.15)	3 – 4
Second Instar	4.0 \pm (0.26)	3 – 5
Third Instar	4.4 \pm (0.16)	4 – 5
Fourth Instar	7.3 \pm (0.3)	6 – 9
Total	27.6 days	-

Table 2. The length (mean \pm S.E.) of body, antennae and wing bud of various life cycle stages of *Macrolophus caliginosus*

Stages	Length mean (mm) \pm S.E.		
	Body	Antennae	Wing Bud
First Instar	0.50 \pm 0.000 (0.48 – 0.52)	0.34 \pm 0.016 (0.3 – 0.4)	0
Second Instar	1.25 \pm 0.002 (1.20 – 1.30)	0.71 \pm 0.031 (0.6 – 0.8)	0.30 \pm 0.008 (0.27 – 0.34)
Third Instar	2.12 \pm 0.006 (2.00 – 2.20)	1.27 \pm 0.026 (1.2 – 1.4)	0.51 \pm 0.008 (0.48 – 0.55)
Fourth Instar	3.02 \pm 0.002 (2.96 – 3.10)	1.79 \pm 0.023 (1.7 – 1.9)	1.04 \pm 0.024 (0.9 – 1.11)
Adult	3.48 \pm 0.000 (3.46 – 3.50)	2.31 \pm 0.023 (2.2 – 2.4)	2.52 \pm 0.020 (2.40 – 2.60)

Table 3. The survival period (days) of the predators, *Macrolophus caliginosus* with various food

Treatments	Mean days survival + S.E.
No food (T0)	3.67 \pm 0.33 d
Young brinjal single leaf plant (T1)	25.67 \pm 2.33 b
Honey (T2)	6.33 \pm 0.33 c
Brinjal single leaf plant + whitefly larvae (T3)	33.67 \pm 2.33 a
Water (T4)	4.33 \pm 0.33 d

Means with the same letters are not significantly different at $P = 0.05$ based on Duncan Multiple Range Test (DMRT).

Table 4. Total number of predators, *Macrolophus caliginosus* after 30 days

Stages\Cylinder Cages	CC 1	CC 2	CC3	Total	Means \pm S.E
Eggs	0	0	0	0	0
First Instar	14	9	12	35	11.7 \pm 6.3
Second Instar	16	13	15	44	14.7 \pm 2.3
Third Instar	15	14	19	48	16.0 \pm 7.0
Fourth Instar	5	6	6	17	5.7 \pm 0.3
Adult	2	3	4	9	3.0 \pm 1.0
Total Number of Predators	52	45	56	153	51.0 \pm 31.0

Note: CC - Cylindrical cage (CC1, CC2, and CC3)



Molecular Cloning and Characterization of a Putative *BnHEC3* Gene in Oilseed Rape (*Brassica Napus*)

Xiaoli Tan (Corresponding Author)

Institute of Life Sciences, Jiangsu University

Zhenjiang 212013, China.

Tel: 86-511-8291-4326 E-mail: xltn@ujs.edu.cn

Lili Zhang & Zongwei Xia

Institute of Life Sciences, Jiangsu University

Zhenjiang 212013, China.

E-mail: zhanglily0511@163.com

The research is financed by the National High Technology Research and Development Program (863 projects) of China (No. 2003AA222101) and Postdoctoral Foundation of Jiangsu Province (No. 060101).

Abstract

HECATE3 (HEC3) is an important transcription factor involved in regulating the carpel and transmitting tract development in *Arabidopsis thaliana*. The homologous gene of *HEC3* in *Brassica napus* (designed as *BnHEC3*) was obtained by *in silico* cloning and rapid amplification of cDNA end (RACE) method. *BnHEC3* obtained from cDNA is of 748 bp, containing an open reading frame (ORF) of 546bp and coding a peptide of 181 amino acid residues. Sequence alignment revealed that *BnHEC3* is highly homologous to *HEC3* in *Arabidopsis thaliana*, especially in bHLH region, which is sharing nearly 100% identity, and the polygenetic analysis indicated that *BnHEC3* belongs to atypical bHLH protein family. RT-PCR results showed that *BnHEC3* is mainly expressed in young leave. Southern blotting analysis indicated that *BnHEC3* has at least three copies in *Brassica napus* genome. The transient expression of *BnHEC3-sGFP* in onion epidermic cells showed that *BnHEC3* localized in nuclei. These features implied that *BnHEC3* functions as *HEC3*, and may be involved in the development of female reproductive tissues in *Brassica napus*.

Keywords: *Brassica napus*, Transmitting tract development, bHLH protein, Transcription factor, Subcellular localization

1. Introduction

Properly coordinated development of female reproductive tissues, including stigma, style, septum and transmitting tract, is essential to the successful fertilization. Much of the recent progress has come from studies of model plant *Arabidopsis thaliana*. Rapeseed (*Brassica napus* L.) is an important oil and vegetable crop. However, the mechanism of reproductive development in rapeseed remains elusive. The *Brassica napus* gynoeceium, like that of *Arabidopsis*, is a complex organ specialized for seed production and dispersal. It also arises from two congenitally fused carpels and at maturity consists of an apical stigma for pollen capture, a short intervening style and a large central ovary where ovule and seed development occurs. The ovary is divided into two compartments by the septum (Hill and Lord et al., 1989; Okada et al., 1989; Smyth et al., 1990; Sessions and Zambryski et al., 1995; Gremski et al., 2007). The transmitting tract, a specialized tissue which coincides with the path of pollen tubes in the gynoeceium, develops in the center of both the style and the septum to increase fertilization efficiency.

During fertilization, pollen grains germinate on the stigma, and then form a tube to deliver the sperms towards the awaiting ovules. The elongation of the pollen tube during pollination is facilitated by differentiation of the transmitting tract tissue, which is composed of highly secretory cells characterized by an extensive extracellular matrix (ECM). And the transmitting tract cells are also undergoing a program of developmentally controlled cell death (Lennon et al., 1998;

Wang et al., 1996; Crawford et al., 2007; Gremski et al., 2007). In the absence of proper transmitting tract differentiation, pollen tube growth is limited and fertility is reduced (Crawford et al., 2007; Gremski et al., 2007).

Through studying on the model plant *Arabidopsis*, a number of genes, including *SPATULA* (*SPT*), *STYLISH1* (*STY1*), *STYLISH2* (*STY2*) and *ETTIN* (*ETT*), have been proved to be involved in patterning the stigma, style, septum and transmitting tract. In recent years, three new genes, *HECATE1* (*HEC1*), *HECATE2* (*HEC2*) and *HECATE3* (*HEC3*), have been identified as important factors for patterning the transmitting tract, which are necessary in the complex program of gynoecium's development. All of these three genes encode closely related basic helix-loop-helix (bHLH) transcription factors with overlapping function. Loss of HEC function leads to defects in the development of the transmitting tract, septum and stigma, and a decrease in fertility. HEC proteins and SPT, another transcription factor belonging to the bHLH family which plays an important role in the septum and stigma development, are likely to cooperatively interact in controlling development (Gremski et al., 2007).

In this study, we cloned the cDNA of putative *BnHEC3* gene (748 bp) from cultivated *B. napus* cv. *Ningyou12* by *in silicon* cloning and the rapid amplification of cDNA ends (RACE) method (Frohman, 1993). And we showed that *BnHEC3* were homologous to *HEC3* with nearly 100% identity in bHLH sequence. Our data suggested that *BnHEC3* may function in the process of transmitting tract development in *Brassica napus*.

2. Materials and methods

2.1 Plant materials and DNA, RNA extractions

B. napus cv. *Ningyou12* was used in this study. Roots, stems, leaves, floral buds, and siliques (35d after pollination) were harvested at the indicated stages. RNA and DNA were extracted immediately. Total RNA was isolated with Trizol (Invitrogen) reagent according to the manual. Mature leaves were harvested for genomic DNA extracted with CTAB extraction method.

2.2 Cloning of the full-length cDNA of *BnHEC3*

50µg total RNA from flower buds of *Ningyou12* was reverse-transcribed into first-strand cDNAs with the PrimeScript Reverse Transcriptase (Takara) in a 50 µl reaction volume. For screening of the *BnHEC3* from *Brassica*, the cDNA sequence of *HEC3* (NM_121012.1) was used as a query to blast against *Brassica* database in the TAIR (www.arabidopsis.org), and a putative *BnHEC3* EST and a genomic DNA BAC were obtained. The PCR primers (E1/E2, P1/P2 and P3/P4) were designed according to the sequences above.

Primers are as follows:

E1: 5'-CAC TAC TCT TTT CTC CGG AG-3',

E2: 5'-AGC TTG ATC TTG CGG CGG-3',

P1: 5'-ATC ATC ATA ACG ATC CAA TCG G-3',

P2: 5'-ATT GCA CCA TTA CTC ACA CTT TAT-3',

P3: 5'-ATG GCC ATG GAC CAA CAC AC-3',

P4: 5'-TTA AAT CAG TTC ACC TCC TCC TCC-3'

The PCR thermocycling conditions were as follows: 94 °C for 5 min, followed by 35 cycles of 94 °C for 1min, 60 °C for 30 sec, and 72 °C for 1 min, and a final extension at 72 °C for 10 min. The *BnHEC3*-EST and partial *BnHEC3* genomic DNA fragments were purified and cloned into pMD18-T vector (Takara) and sequenced. The 5' and 3' FULL RACE Kits (Takara) were used to clone 5' and 3' flanking sequence of the cDNA.

2.3 Bioinformatic analysis of *BnHEC3*

DNA and amino-acid sequences manipulation were performed with DNASTar 5.0 software. Homology analysis was also performed using Blastx, Genedoc, and BLAST Network Service in TAIR (<http://www.arabidopsis.org>) and BLAST Network Service in NCBI (<http://www.ncbi.nlm.nih.gov/>). Expasy database (<http://www.expasy.org/>) was used to analyze the profile of *BnHEC3* protein. The sequences alignment was performed using the program Multalin with the default parameters (<http://prodes.toulouse.inra.fr/multalin/multalin.html>) (Corpet, 1988), and GeneDoc were used for editing sequence alignment. Neighbor-Joining Phylogenetic Tree with bootstrap values was constructed using Mega 3.1.

2.4 Southern hybridization analysis

Six restriction enzymes (*Bam*H I, *Eco*R I, *Kpn* I, *Sac* I, *Xba* I, *Xho* I) were used for Southern blotting. About 10 µg of genomic DNA was digested with 20 unit of restriction enzyme in a final volume of 100 µl at 37°C for 18 h. The cleaved DNA fragments were run on a 0.8% (w/v) agarose gel and transferred to Hybond-N + membranes (Amersham Pharmacia). The *BnHEC3*-EST (360bp) was amplified with E1/E2 by PCR and purified as a probe for southern blotting hybridization. The membranes were hybridized following the standard protocols (Chomczynski, 1992), and then was washed with 2×SSC plus 0.1% (w/v) SDS at 65°C for 30 min and exposed to X-ray film at -70°C.

2.5 Analysis of *BnHEC3* expression

Five micrograms of the total RNA isolated from roots, stems, young leaves (before pollination), mature leaves (35 days after pollination), flowers, and pods of the cultivar *Ningyou12* were reverse-transcribed into first strand cDNA with the PrimeScript Reverse Transcriptase (Takara), respectively. The first strand cDNA mix was used as template and P3/P4 were used as primers for RT-PCR. The PCR were performed as follows: 94 °C for 5 min, followed by 35 cycles of 94 °C for 1min, 60 °C for 30 sec, and 72 °C for 45 sec, and a final extension at 72 °C for 10 min. *BnActin* gene amplified with primers β - Actin F (5'-ATG GCC GAT GGT GAG GAC ATT C-3') and β - Actin R (5'-GGT GCG ACC ACC TTG ATC TTC-3'), was used as an internal control in the experiments.

2.6 Subcellular localization of *BnHEC3*

Motif Scan (http://myhits.isb-sib.ch/cgi-bin/motif_scan) was used to predict the subcellular localization of *BnHEC3* and *HEC3*. *sGFP* vector, which have a multiple cloning site (MCS) between 35S promoter and *sGFP* gene, was used for constructing *BnHEC3-sGFP*. Briefly, ORF of *BnHEC3* without stop coding (TAG) was amplified with two primers containing *Xba* I and *Bam*H I restrict sites respectively as follows: 5'-tct aga ATG GCC ATG GAC CAA C-3' and 5'-gga tcc AAT CAG TTC ACC TCC T-3'. The PCR thermocycling conditions were as follows: 94 °C for 5 min, followed by 35 cycles of 94 °C for 1min, 58 °C for 45 sec, and 72 °C for 1 min, and a final extension at 72 °C for 10 min. The PCR product was purified, ligated to pMD18-T-vector, and sequenced. Then the correct plasmid was digested with *Xba* I and *Bam*H I, and the fragment was gel purified, ligated into the *Xba* I/ *Bam*H I predigested *sGFP* vector to construct *BnHEC3-sGFP*.

The recombination plasmid was transformed into the onion epidermal cells using gene-gun. Then, the onion epidermal cells was cultured under 25 °C and observed under fluorescence microscope after 16-24 hr.

3. Results

3.1 Cloning and structural analysis of *BnHEC3*

HEC3 gene was used as a query to search against the *Brassica* database, thus an EST and a partial genomic DNA were obtained, which are 360bp (AT002234.1) and 848bp (DU105139) in length, respectively. The EST sequence is same to the corresponding region in the partial BAC sequence, so it is named as the *BnHEC3*-EST. A complete open reading frame (ORF) indicated by DNASTar was 546bp. Fragments obtained by PCR from cDNA and genomic DNA are uniform, indicating that *BnHEC3* has no introns (Fig. 1.).

To get the complete sequence of *BnHEC3*, RACE method was used. Two sequences with different lengths in 3' ends were obtained by 3' RACE. The length of the longest sequence amplified from cDNA of *BnHEC3* is of 748 bp with a 23 bp of incomplete 5'-leader sequence and 219 bp of 3'-untranslated region (Fig. 2.). The putative ORF of 546 bp from *BnHEC3* encodes a peptide of 181 amino acids with a predicted molecular weight of 20.3 kDa and a calculated isoelectric point of 5.88 (Protparam: [http:// www.expasy.ch](http://www.expasy.ch)).

Using SMART program (Simple Modular Architecture Research Tool: [http:// smart.embl-heidelberg. de](http://smart.embl-heidelberg.de)), a bHLH domain (amino acid 89-137) was identified in the *BnHEC3*, and an alanine residue (A) was also found at site 9 within the basic region of the *BnHEC3*, indicating that *BnHEC3* is an atypical bHLH protein, whereas typical bHLH proteins have a glutamic acid residue (E) at that site instead (Fisher and Goding, 1992; Buck and Atchley, 2003; Toledo-Ortiz et al., 2003) (Fig. 2.). The extensive protein sequence similarity between *BnHEC3* and *HEC3* was a 30 amino acid N-terminal extension of the region of the bHLH domain. This led to *BnHEC3* being grouped as a subfamily of bHLH proteins (Heim et al., 2003; Gremski et al., 2007). The conservation was primarily restricted to the bHLH region, and the other regions showed also a high degree of similarity among the bHLH proteins comparing (Fig.3.). The bHLH domain of *BnHEC3* shared extremely high similarities (nearly 100%) with that of *HEC3* (Fig. 3.). Sequence alignment of the *BnHEC3* with *HECs* and another related bHLH factor INDEHISCENT (IND) revealed that the *BnHEC3* also lack a conserved glutamate at position 13 of the basic domain (Fig.3.). This glutamate has been shown to be important for DNA binding (Ellenberger et al., 1994; Ma et al., 1994; Gremski et al., 2007). The phylogenetic tree showed that *BnHEC3* belongs to the atypical bHLH proteins group with *HEC3*, and also strongly supported the high identity between *BnHEC3* and *HEC3* (Fig. 4.).

3.2 Genomic structure of the *BnHEC3* gene

The genomic DNA was digested by six restriction enzymes, respectively, and subjected to Southern analysis. The 360bp *BnHEC3*-EST was used as a probe. The result was illustrated in Fig. 5. It can be seen that there were three bands (one visible band and two weaker bands) in the first, second and fourth lane. The third lane had only one band but the fifth and sixth lanes had three bands with one weak band and two bright ones. The result of the Southern Blotting suggested that there were at least three copies of *BnHEC3* in the genome of *B. napus*.

3.3 Analysis of the *BnHEC3* expression

The result of RT-PCR showed that the expression of *BnHEC* was in young leaves, mature leaves, floral buds and

siliques rather than in roots or stems, and most strongly in young leaves (Fig. 6.). Flowers are abnormal organs of the leaves, and they are the essential origin of the fruits in many plants including oilseed rape. The expression profiles of *BnHEC3* suggested that *BnHEC3* may be involved in regulating the growth and development of leaves and the formation of flower tissues. It may have similar function as *HEC3*, which can regulate the carpel formation and transmitting tract development in *Arabidopsis*.

3.4 Subcellular localization of *BnHEC3*

As a possible transcription factor, *BnHEC3* may be localized in nuclei, however, there was no nuclear localization sequence detected in *BnHEC3* by Motif Scan. Whereas, a putative nuclear localization sequence containing Arginine-rich region (RRREISEKIRILKR) was predicted in *HEC3* in *Arabidopsis*. Based on the sequence alignment of *HEC3* and *BnHEC3*, *BnHEC3* also contains a motif (RRRISERIRILQR) corresponding to the putative nuclear localization sequence of *HEC3*, which may be the putative nuclear localization sequence of *BnHEC3* (Fig. 2). Further investigate the cellular localization of *BnHEC3*, transient expression of *BnHEC3*-sGFP fusion protein in onion epidermal cells was performed. Two kinds of plasmids for transient expression were constructed (Fig.7.A) and transferred into onion epidermal cells respectively. Fluorescence microscopy showed that green fluorescence was observed all over the cells carrying sGFP plasmid, whereas green fluorescence was observed clearly in nuclei of the cells carrying *BnHEC3*-sGFP plasmid, indicating that *BnHEC3* localized in nuclear (Fig. 7.B).

4. Discussion

The bHLH transcription factors, such as *HEC1*, *HEC2* and *HEC3*, play essential roles in development of female reproductive tissues in model plant *Arabidopsis thaliana*. But their function in Rapeseed (*Brassica napus* L.) is still unknown. In this study, we successfully identified a novel gene, named as *BnHEC3*, which may be involved in similar process in Rapeseed.

We obtained the partially complete cDNA of *BnHEC3* from *Brassica napus* using *in silico* cloning and RACE method. Sequence and phylogenetic analysis indicated that *BnHEC3* is highly homologous to *HEC3* and belongs to atypical bHLH family. We performed transient expression of *BnHEC3*-sGFP in onion epidermal cells, and found it is localized in nuclear, which further prove it to be a possible transcription factor as *HEC3*. Southern blotting of *BnHEC3* showed that *BnHEC3* has at least three copies, suggesting that *BnHEC3* plays an important role in the development process of female reproductive tissues in oilseed rape. Our RT-PCR analysis showed that the *BnHEC3* is mainly expressed in young leaves, indicating it may be involved in the specification of floral organs. And it is also expressed in flowers and fruits, suggesting it may have function in regulating the specification of subsequent different cell types in female reproductive tissues.

Before reaching ovules, pollen tubes must travel through several distinct tissues, including the stigma, the stylar transmitting tract and the septum transmitting tract (Crawford et al., 2007; Gremski et al., 2007). Coordinated development of these tissues is crucial for successful fertilization, and the transmitting tract differentiation, is one of the most important process affecting the pollen tube development (Crawford et al., 2007; Gremski et al., 2007). In *Arabidopsis*, three related bHLH transcription factors, *HEC1*, *HEC2* and *HEC3*, are identified to be required for this process (Gremski et al., 2007). An RNA-null mutant of *HEC3* displayed a loss of fertility and defects in transmitting tract tissue in both septum and style (Gremski et al., 2007). Over-expression of *HEC3* led to the ectopic production of stigmatic tissue, consistent with its requirement for stigma development (Gremski et al., 2007).

Therefore, *BnHEC3*, as the homologous gene of *HEC3* in *Brassica napus*, may also play essential roles in the development of female reproductive tissues. Our study paved the way for subsequent research on *BnHEC3* in *Brassica napus*. By further study on it, we may finally get much more understanding about the fertility mechanism in rapeseed, and the knowledge may be useful to the agricultural production.

Acknowledgments

This work was supported by the National High Technology Research and Development Program (863 projects) of China (No. 2003AA222101) and Postdoctoral Foundation of Jiangsu Province (No. 060101). We thank Dr. Xinyu Wang for technical helps in *BnHEC3* subcellular localization.

References

- Buck, M.J., and Atchley, W.R. (2003). Phylogenetic analysis of plant basic helix-loop-helix proteins. *J Mol Evol* 56, 742-750.
- Chomczynski, P. (1992). One-hour downward alkaline capillary transfer for blotting of DNA and RNA. *Analytical Biochemistry* 201, 134-139.
- Corpet, F. (1988). Multiple sequence alignment with hierarchical clustering. *Nucleic Acids Res* 16, 10881-10890.
- Crawford, B.C.W., Ditta, G. and Yanofsky, M.F. (2007). The NTT Gene is required for transmitting tract development in

carpels of *Arabidopsis thaliana*. *Curr.Biol.*17, 1101-1108.

Ellenberger, T., Fass, D., Arnaud, M. and Harrison, S.C. (1994). Crystal-structure of transcription factor E47-E-box recognition by a basic region helix-loop-helix dimer. *Genes Dev.*8, 970-980.

Fisher, F., and Goding, C.R. (1992). Single amino acid substitutions alter helix-loop-helix protein specificity for bases flanking the core CANNTG motif. *Embo J* 11, 4103-4109.

Frohman, M.A. (1993). Rapid amplification of complementary DNA ends for generation of full-length complementary DNAs: thermal RACE. *Methods Enzymol* 218, 340-356

Grandori, C., Cowley, S.M., James, L.P., and Eisenman, R.N. (2000). The Myc/Max/Mad network and the transcriptional control of cell behavior. *Annu Rev Cell Dev Biol* 16, 653-699.

Gremski, K., Ditta, G. and Yanofsky, M.F. (2007), The HECATE genes regulate female reproductive tract development in *Arabidopsis thaliana*, *Development* 134, 3593-3601

Heim, M. A., Jakoby, M., Werber, M., Martin, C., Weisshaar, B. and Bailey, P. C. (2003). The basic helix-loop-helix transcription factor family in plants: A genome-wide study of protein structure and functional diversity. *Mol.Biol.Evol.* 20, 735-747.

Hill, J.P. and Lord, E.M. (1989). Floral development in *Arabidopsis thaliana*: a comparison of the wild type and the homeotic pistillata mutant. *Can.J.Bot.* 67, 2922-2936.

Lennon, K.A., Roy, S., Hepler, P.K. and Lord, E.M. (1998). The structure of the transmitting tissue of *Arabidopsis thaliana* (L.) and the path of pollen tube growth. *Sexual Plant Reprod.*11, 49-59.

Liljegren, S.J., Roeder, A.H., Kempin, S.A., Gremski, K., Ostergaard, L., Guimil, S., Reyes, D.K., and Yanofsky, M.F. (2004). Control of fruit patterning in *Arabidopsis* by INDEHISCENT. *Cell* 116, 843-853.

Ma, P.C.M., Rould, M.A., Weintraub, H. and Pabo, C.O. (1994). Crystal structure of MyoD bHLH domain-DNA complex-perspectives on DNA recognition and implications for transcriptional activation. *Cell* 77, 451-459.

Massari, M.E., and Murre, C. (2000). Helix-loop-helix proteins: regulators of transcription in eucaryotic organisms. *Mol Cell Biol* 20, 429-440.

Okada, K., Komaki, M.K. and Shimura, Y. (1989). Mutational analysis of pistil structure and development in *Arabidopsis thaliana*. *Cell Diff.Develop.* 28, 27-38.

Sessions, R.A. and Zambryski, P.C. (1995). *Arabidopsis* gynoecium structure in the wild type and in ettin mutants. *Development* 121, 1519-1532.

Smyth, D.R., Bowman, J.L. and Meyerowitz, E.M. (1990). Early flower development in *Arabidopsis*. *Plant Cell* 2, 755-767.

Toledo-Ortiz, G., Huq, E., and Quail, P.H. (2003). The *Arabidopsis* basic/helix-loop-helix transcription factor family. *Plant Cell* 15, 1749-1770.

Wang, H., Wu, H.M. and Cheung, A.Y. (1996). Pollination induces mRNA poly(A) tail-shortening and cell deterioration in flower transmitting tissue. *Plant J.*9, 715-727.

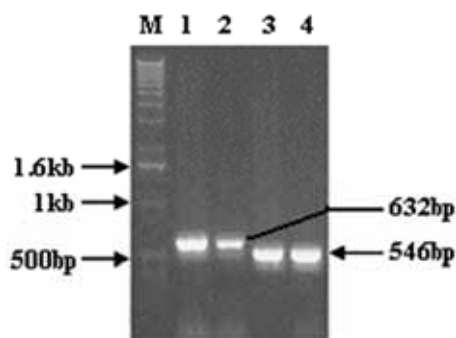


Figure 1. The fragments are amplified by PCR (P1/P2, P3/P4) from cDNA and genomic DNA of *BnHEC3*, respectively.

M: DNA marker; 1 and 3: fragments amplified from genomic DNA of *BnHEC3*. 2 and 4: fragments amplified from cDNA of *BnHEC3*.

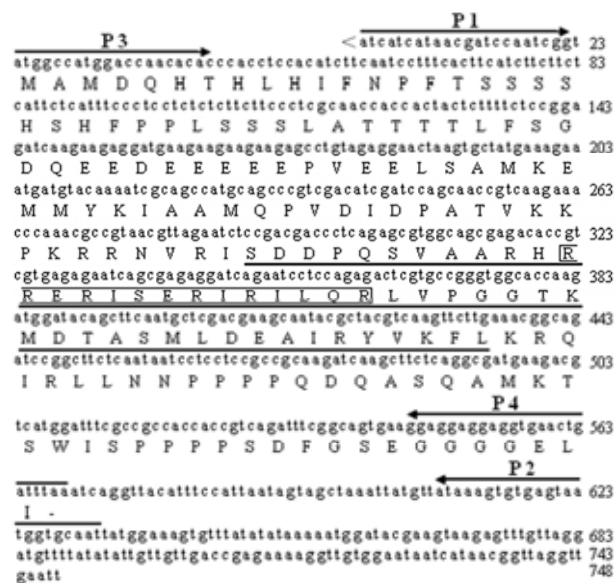


Figure 2. cDNA sequence of the *BnHEC3* gene and deduced amino acid sequence.

“<” in front of cDNA sequence showed that the incomplete 5'- end sequence of cDNA of *BnHEC3*. bHLH domain signature region of *BnHEC3* is underlined. A putative nuclear localization sequence was marked with rectangular box. Primers (P1/P2 and P3/P4) were indicated with the arrows.



Figure 3. Multiple sequence alignment of the bHLH region from *BnHEC3* and other bHLH family proteins from *Arabidopsis*.

The proteins aligned are: *BnHEC3*, *HECATE3* (*HEC3*), *HECATE2* (*HEC2*) and *HECATE1* (*HEC1*) (Gremski et al., 2007) and *INDEHISCENT* (*IND*) (Liljegren et al., 2004). The black arrow head marks an alanine that replaces the conserved glutamate carried by most other *Arabidopsis* bHLH proteins. Different grey level represents the different percentage of similarity.

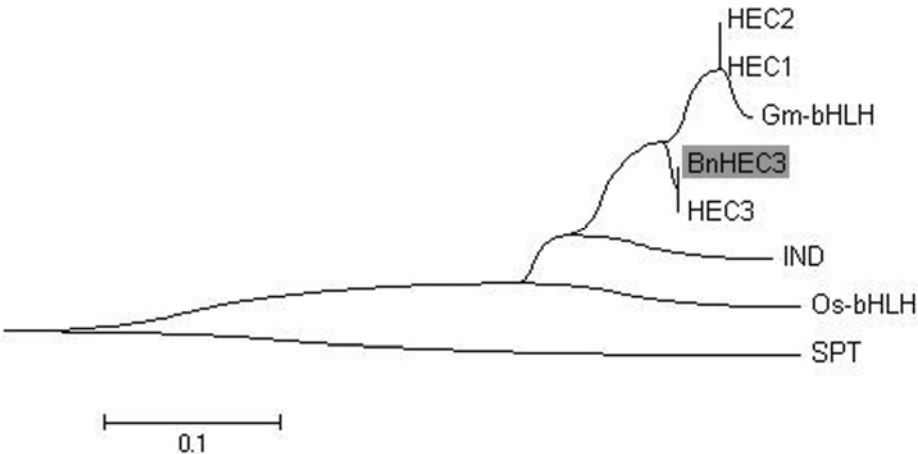


Figure 4. Neighbor-Joining Phylogenetic Tree of the bHLH Domains of bHLH family proteins.

The Phylogenetic Tree showed the phylogenice relationship among the bHLH family proteins, including *BnHEC3*, *HECATE3* (*HEC3*), *HECATE2* (*HEC2*), *HECATE1* (*HEC1*), *SPATULA* (*SPT*), *INDEHISCENT* (*IND*), *Gm-bHLH* (*Glycine max-bHLH*) and *Os-bHLH* (*Oryza sativa Japonica Group-bHLH*). It is obvious that *BnHEC3* and *HEC3* are highly homologous.

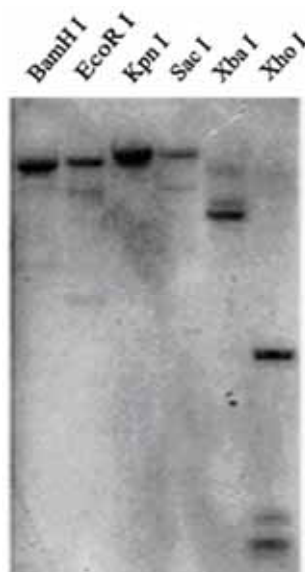


Figure 5. Southern blotting of *BnHEC3* gene in *Brassica napus* genome.

Genomic DNA was digested with *Bam*H I (line 1), *Eco*R I (line 2), *Kpn* I (line 3), *Sac* I (line 4), *Xba* I (line 5) and *Xho* I (line 6), respectively, followed by hybridization with the probe of *BnHEC3*-EST.

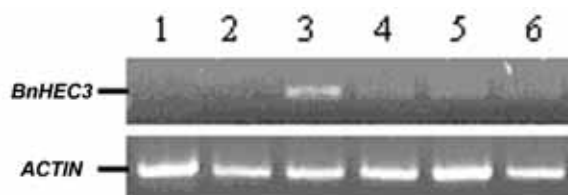


Figure 6. Expression profile of *BnHEC3* was analyzed by RT-PCR.

1: roots; 2: stems; 3: young leaves; 4: mature leaves; 5: floral buds s; 6: siliques (35d after pollination). β -ACTIN was used as control.

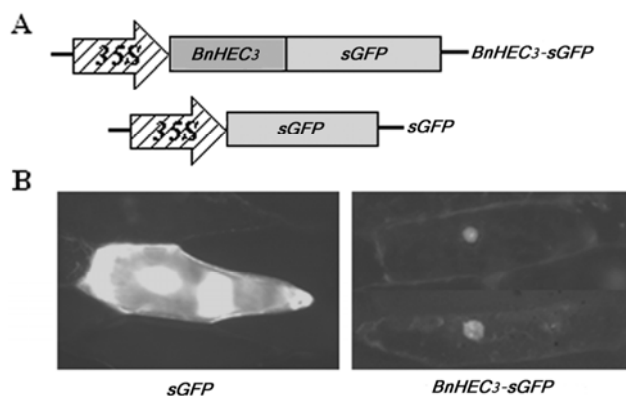


Figure 7. Subcellular localization of *BnHEC3* in onion epidemic cell.

(A) Schematic diagram of recombination plasmid. (B) Fluorescent microscopy analysis of subcellular localization of *BnHEC3*. It shows the onion epidemic cells that carrying *sGFP* plasmid (left) and carrying *BnHEC3* –*sGFP* plasmid (right).



A New Species of *Aspergillus*

Zongzhou Zhang

School of Life-Science and Chemistry, Tianshui Normal University

Tianshui 741000, Gansu, China

Tel: 86-938-836-7716 E-mail: tshzzz66@163.com

The research is financed by Ministry of Science and Technology Support Program No.2007BAD89B17

Abstract

A new species of *Aspergillus* was isolated from the hill meadow soil in Tianzhu, Gansu. On the Czapek's medium at 20°C it produced branching conidiophores, heads pure yellow, hypha septate, footcell not inflating. Sterigmas were in two series and primary sterigmas were approximately triangle on which 4 bottle structure second sterigmas were present. At 25°C colony was white and produced abundant sclerotia instead of branching conidiophores. According to the morphological and culture characters, it should belong to *Aspergillus*. Through compared with similar species; here it was considered as a new species of *Aspergillus*. Therefore, it was named *Aspergillus racemosus* sp.n. Type specimens of the new species are deposited in the microbiological lab of Tianshui Normal University.

Keywords: *Aspergillus*, Branching conidiophores, *Aspergillus racemosus*

The Jing-qiang River in Tianzhu lies to the northwest of Wushao Mountain, the annual average, temperature is -0.3°C. The annual rainfall is 416mm. Soil is hill meadow soil. A strain of *Aspergillus* was isolated from the soil. Optimum growth temperature was 20°C. On the Czapek's medium, it formed milky white colony 10 days, colonial diameter 1.5cm, height 1.0cm, hyphae close and produce orange water soluble pigment in the medium. Hyphae have septum, diameter 2-3µm, footcell not inflating, and shape as Fig.1. 15 days, it began to produce pure yellow conidial heads in the centre of the colony. The branching conidiophores conidiophore hyaline, surface smooth, length 3-4 mm, diameter 5.6-6.5µm, bifurcate and no septate, as Fig.2. The conidial heads were close globose, radiate, outer diameter 150-250 µm. Vesicle was globe, diameter 54.5-55.0 µm. The primary sterigms were approximately triangles, length 7 µm, 4 bottle structure second sterigms were present, size 7.6×1.5-2.0µm. Two series sterigma were pure yellow or yellow brown. Conidia were approximate globose, diameter 2.3 µm, surface rough (fig.3). Incubated in the Czapek's liquid medium 10 days, detected with FeCl₃, there was not aspergillus acid.

On the Czapek's medium, incubated at different temperature the growth state was as Table 1. It could be seen that the best state was at 20°C, hyphae vigorous. Above 20°C though hyphae spread fast, it was relatively thin and weak as table 1.

At 25°C it could grow on different mediums: the Czapek's medium, malt extract medium and potato agar medium. On the malt extract medium it grew faster than on the others, 10 days the colonial diameter was 2.5 cm, milky white, close and thriving. The back of colony was white grey and radial winkle, sclerotia were relatively abundant. Only on the Czapek's medium it could produce orange water soluble pigment. On the potato agar medium, colony was close, growth was slower than that on the malt extract medium. The colonial and colour morphological characters were similar to that on the malt extract medium.

The strain had the outstanding characters of *Aspergillus* and was identical with the characters of *Aspergillus ochraceus* group. But it was apparently different to the species of the group that had been reported. According to the morphological and culture characters, it should belong to *Aspergillus*. Through compared with similar species as table 2, it was considered as a new species of *Aspergillus*. It was named *Aspergillus racemosus* sp.nov.

References

- K.B.Rer. *Aspergillus* Genus. 196
- K.H.Domsch, W. Gams. (1970). *Fungi in Agricultural soils*, p27-30
- Shen, Ping. (2001). *Microbiology*. Beijing: Higher Education Press, p364-369
- Zhou, De-qing. (2006). *Microbiology* second edition. Beijing, Higher Education Press, p59-62

Table 1. Morphological Characters at Different T. on Czapek's Medium*

T. °C	Colonies (diameter) cm	Colour	Heads	characters of the colonies	Sclerotia
8	0.8	pure yellow	+	close and high	—
12	1.0	pure yellow	+	close and high	—
15	1.2	pure yellow	+	close and high	—
20	1.2	pure yellow	+	close and high	—
25	2.2	milky white	—	disperse and flat	+
30	1.6	milky white	—	disperse and flat	+
37	1.3	milky white	—	disperse and flat	+

*15days. relative humidity 70%.

Table 2. Comparisom of Simillar Species *

Name	Colong	Sterigs	Conidiophores heads	Sclerotia	Conidium
<i>A. sulphureus</i>	4.2	two series	milky white, disperse d.<400µm	milky white, light yellow	spindie young, globe in age 2.0~2.5µm
<i>A. sclerotioru s</i>	4.6	two series	light yellow, semiglobose d.55~0µm	white oryage, globose	globose, smooth 2.0~3.0µm
<i>A. alliaceus</i>	6.5	two series	brown yellow, globose d.100~1000µm	black, oval d.500~700µm	oval, smooth 3.7×2.0 µm
<i>A. auricomus</i>	2.6	two series	globose, radiative d.350~500µm	black, globose d.500~700µm	oval, smooth 2.75~3.5µm
<i>A. melleus</i>	2.6	two series	globose, pillar in age, pure yellow d.350~400µm	brown, globose d.400µm	globose, smooth 3.0~3.5µm
<i>A. ochlanceus</i>	3.6	two series	globose, pillar in age d.200~500µm	purplish red, globose d.900~1000µm	globose, smooth 2.5~3.5µm
<i>A. elegans</i>	2.7	two series	globose, pillar in age d.200~500µm	yellow brown, globose b.600~700µm	oval smooth 3.2~4×2.5~3.2µm
<i>A. ostianus</i>	2.9	two series	globose, pillar in age d.400~500 µm	black, globose d.500~1000µm	oval, rough 4.0~4.5×1.3~3.5µm
<i>A. petrakii</i>	3.3	two series	globose, radiative d. <100µm	no	euipital smooth 2.5~4.0µm
<i>A. flavus</i>	3.3	one or two series	globose, radiative d.250~300µm	brown, globose d.800~1000µm	globose rough 3.5~5.0µm
<i>A. racemosus</i> (20°C)	2.0	two series	pure yellow, globose, radiative, d.250~300µm	no	flat globose 2.4µm
<i>A. racemosus</i> (25°C)	3.5		no	grey beck, oval d.600~1500×400 ~800µm	no

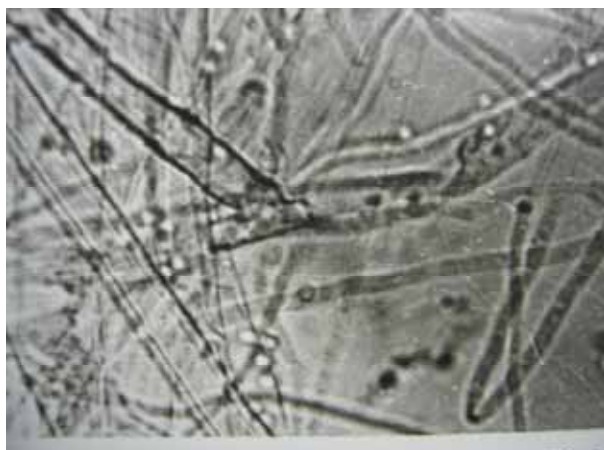


Figure 1. Footcell not Inflating



Figure 2. Branching Conidiophores

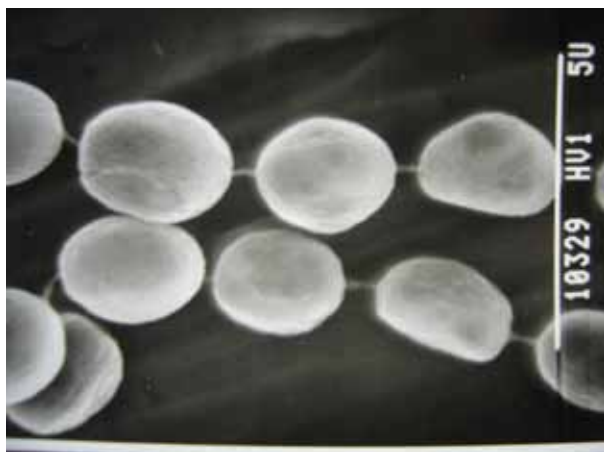


Figure 3. Conidia



Transcription and Expression of Major VP Gene of *Bombyx Mori* Parvo-like Virus

Jinsong Cheng & Qin Yao (Corresponding author)

Institute of Life Sciences, Jiangsu University

301 Xuefu Road, Zhenjiang 212013, China

Tel: 86-511-8879-1923 E-mail: yaoqin@ujs.edu.cn

Meng Lv, Chen Sun, Yuanqing He & Keping Chen

Institute of Life Sciences, Jiangsu University

301 Xuefu Road, Zhenjiang 212013, China

The research is financed by the Program of the National Natural Science Foundation (30871826) and the National High Technology Research and Development Program of China (2008AA10Z145).

Abstract

The *Bombyx mori* parvo-like virus (China Zhenjiang isolate), termed as *BmDNV-Z*, replicates only in host's midgut columnar cells and causes flacherie disease. The viral genome is composed of two sets of different single-stranded linear DNA molecules, Viral DNA 1 (VD1) and Viral DNA 2 (VD2). Here we cloned the major VP gene from the plasmid contained viral DNA fragments. The gene consists of 1500 nucleotides and the deduced protein has 499 amino acid residues, with the predicted molecular weight of 54934.24Da, isoelectric point of 6.73. The coding sequence was inserted into expression plasmid vector pET-30a and expressed in *Escherichia coli* BL21 (DE3) under the inducible promoter LacZ. The expressed product was detected by Western blotting with anti-His antibody. Interestingly, there are four ladder band instead of one. We speculated that this virus may use leaky scanning mechanism to express four proteins in one ORF. And we investigated the major VP gene transcriptional time phase in susceptible silkworm through real time quantitative PCR (qPCR). The result showed that the mRNA level of VP gene increased greatly after 24 hours post inoculation.

Keywords: *Bombyx mori* parvo-like virus, Major VP protein gene, Transcription, Expression, qPCR

1. Introduction

Bombyx mori is not only an economic insect but also a model in life sciences. *Bombyx mori* parvo-like virus, termed as *BmDNV-2* (Yamanashi isolate) or *BmDNV-Z* (China Zhenjiang isolate), is one of the most disastrous viruses in cocoon production. Similar to the typical symptom in the host of silkworm infected by the *BmDNV-1* (Ina Isolate) (Bando H, 1987, 553-560), the *BmDNV-2* also infected the columnar cells of midgut epithelium and caused flacherie disease of silkworm (Bando H, 1992 187-193). The most obvious characteristic in the genome of *BmDNV-2* is that it has 2 sets of DNA molecular (VD1, VD2), and each of them is encapsidated respectively in the form of single-stranded liner DNA (+VD1, -VD1, +VD2, -VD2) so the *BmDNV-2* has 4 kinds of virions. Furthermore the sequence of *BmDNV-2* is able to encode DNA polymerase itself (Bando, H., 1992 187-193; Bando, H. 1995 1147-11; Hayakawa Tohru et al 2000 66 101-108). *BmDNV-2* has six structural proteins comprising four smaller structural proteins (VP1, 2, 3, and 4) with molecular weights around 50 kDa, and two larger ones with molecular weights around 110 kDa. The four smaller structural proteins are the major structural proteins, and amino acid sequencing and peptide mapping have revealed that VP1 to 4 are encoded in VD1. VP5 and 6 are rather minor components found in some purified virion fractions (Hayakawa Tohru, et al 2000 66 101-108). These unusual properties for a parvo-like virus imply an infection and replication mechanism different from parvovirus.

In 2005, the genome analysis of *BmDNV-Z* was completed by our laboratory (GenBank accession no. DQ017268 and

DQ017269). Sequence analysis showed that VD1 genome consists of 6,543 nts and VD2 genome consists of 6,022 nts. Comparison of the complete genome sequence between *BmDNV-Z* and *BmDNV-2* showed an identity of 98.4% in VD1 and 97.7% in VD2, with a total number of 228 bp substitutions, 11 bp deletions and 3bp insertions found in *BmDNV-Z* (Wang et al., 2007, 35:103–108). The VP-ORF is located on the VD1 of *BmDNV-Z* ranging from 1417 nts to 2916 nts. *BmDNV-Z* has a high homology with *BmDNV-2*. It implicated that *BmDNV-Z* may share the same mechanism in gene expression and virion packaging with *BmDNV-2*. Very little is known about the Transcription and Expression of Major VP Proteins of *Bombyx mori* Parvo-like Virus.

In this paper, we investigated the major VP gene transcriptional time phase in susceptible silkworm through real time quantitative PCR (qPCR). The major VP gene of *BmDNV-Z* was expressed in *Escherichia coli* BL21 (DE3) and the fusion protein was detected by Western blotting with anti-His antibody. The result showed that the mRNA level of VP gene increased greatly after 24 hours post inoculation. The expression of recombinant VP tagged with 6 histidines was confirmed by Western blotting and there were four clearly distinct polypeptide bands. In light of above, we infer that this virus may use leaky scanning mechanism to express four proteins in one ORF.

2. Materials and methods

2.1 Cloning of VP gene and Construction of expression plasmid

ORF region of the major VP gene of *BmDNV-Z* was amplified by PCR using the forward primer

5'GCGGATCCATGGGTAGAGTACTTGGCTCATT3' and the reverse primer 5'GCAAGCTTTTAT

GAAAACCAACAAGCCT3' containing *Bam*HI and *Hind*III restriction sites (underlined) respectively. PCR reaction was carried out for 35 amplification cycles (94°C /30 sec, 58°C /30 sec, 72°C /1.5 min). The PCR product was ligated into pMD19-T (TaKaRa, Dalian) vector using T4 DNA ligase (TaKaRa, Dalian) and then transformed into *E. coli* (TG1 strain). Sequencing was performed in Shanghai Sangon Bio-technology Corporation using the plasmid pMD19-vp.

2.2 Expression of VP fusion protein in *E. coli*

After digestion with *Bam*H I and *Hind* III from the plasmid pMD19-vp, the purified DNA fragment was ligated into expression vector pET-30a (Novagen) and introduced into *E. coli* BL21 (DE3) by transformation. The vector pET-30a can express fusion protein with both the N-terminal and C-terminal His-tag. We deleted the stop codon of the CDS of the VP and allowed the fusion protein has both N-terminal and C-terminal His-tag. So the fusion protein can be purified through His purification system. The expression of recombinant VP was induced overnight at 28°C by the addition of isopropyl-β-D-thiogalactopyranoside (IPTG) to a final concentration of 1.0 mM when the optical density of the culture at 600 nm reached 0.5. A 10% sodium dodecyl sulfate-polyacrylamide gel electrophoresis (SDS-PAGE) was performed to analyze the fusion protein.

2.3 Western blot analysis

To identify the fusion protein, the western blotting was performed using anti-His-tag antibody (TIANGEN, Beijing) following the standard protocol.

2.4 Transcriptional time phase of VP gene by qPCR

The total RNA was extracted from infected midgut tissue of susceptible silkworm strain HUABA35 at 12 time points (2, 4, 6, 12, 24, 28, 36, 40, 48, 52, 66, 72 h post inoculation) using a Trizol reagent (Invitrogen, Carlsbad, CA), according to the manufacturer protocol. The total RNA subjected to messenger polyA RNA isolation using the Oligo Tex mRNA Mini Kit (QIAGEN Inc. Valencia, CA). Finally, the RNA was dried and resuspended in DEPC-H₂O containing 1% RNase inhibitor and stored at -80°C. The first-strand cDNA synthesis was performed SYBR RT-PCR Kit A (TaKaRa) at 37°C for 1h in a final volume of 20 μl reaction buffer.

QPCR was conducted on an MX3000P thermal cycler amplification and detection system (Stratagene). QPCR amplification of the cDNA was performed using the SYBR RT-PCR Kit B (TaKaRa). Specific primers for virus gene vp is: the forward primer 5'GGTACGATGTTGACCCAG3' and the reverse primer 5'ACTCCACCAGCAAAGAC3'. Each reaction was performed in a 20μl reaction volume which contained 10μl of SYBR Premix Ex Taq; 1μM of each upstream and downstream primer and 1μl cDNA templates diluted first-strand cDNA (1/10). Preincubation was performed for 30s at 95°C to denature the template DNA and to activate Taq-polymerase. DNA was amplified for 40 cycles of 10s at 95°C, 20s at 56 °C, and 20s at 72°C.

The primers' design was based on the complete genome sequence of *BmDNV-Z* (GenBank accession no. DQ017268). Primers were designed by using the software Primer Premier 5. Two pairs of primers were located on the ORF3 region of the *BmDNV-Z* VD1 genomic sequence. *BmactinA3* gene was used as an internal control for normalization. Actin A3 was amplified using the forward primer 5'GCGCGGCTACTCGTTCACTACC3' and the reverse primer 5'GGATGTCCACGTCGCACTTCA3'. The specificity of the primers was confirmed by using NCBI BLAST (BLASTN) algorithms.

3. Results and Discussion speculation

The transcriptional time phase analysis of VP gene by qPCR indicated that transcription of VP gene start at 24 hours after inoculation in midgut tissue of susceptible silkworm (figure 5). After 52h the transcriptional level of VP gene increased greatly. This profile is consistent with the most of viral gene expression process. As a late gene the transcriptional level of VP gene is fairly low at the beginning, because the virus needs to save energy for perform viral DNA replication. After 52h pi the virus prepares for packaging.

The limited complexity of parvovirus genome means that the virus must put its genes into full play. This strategy is implemented and orchestrated by a few multifunction viral regulatory protein (FeÂ dieÂ re, 2004, 181– 189) or adapts some kind of mechanism to generate more protein through less content of genome. The strategy of VP gene expression for most parvovirus including Densovirus (e.g. *Bombyx mori* Densovirus 1, *Casphalia extranea* Densovirus, *Galleria mellonella* Densovirus) is leaky scanning mechanism, which was confirmed through western blotting. (Sotoshiro H, 1995,66 :60 – 67, Hayakawa T, et al, 2000, 101-108. G. FeÂ dieÂ re, & Y. Li 2002, 299-308; P. Tijssse & Y. Li, 2003, 10357–10365). By the Leaky scanning model the virus can generate about four structural proteins from a single transcript. Each additional peptide extension is thought to fulfill at least one unique function in the viral cycle. These strategies also allow the virus to express the different domains to different optimal amounts. The reason why the virus uses leaky scanning is that the virus must put its genes into full play with one mRNA to produce one wholesome protein and three N-terminal truncated proteins. The expression level suggested a 2-5 fold increase in leaky scanning (Byung-Sik Shin, 2002, 1015-1025).

In this experiment the viral VP protein was expressed in prokaryotic and analyzed by SDS-PAGE and detected by using Western blotting (figure 4). Four clearly distinct polypeptide bands were witnessed with protein molecular mass approximately 64 kDa (VP1), 55 kDa (VP2), 41 kDa (VP3), 34 kDa (VP4) respectively. The open reading frame starts at nucleotide 1 (1AUG), 115(115AUG), 486(486AUG), 657(657AUG) on the ORF sequence of VP gene. Predictions of the molecular masses of the four structural proteins from the first four in-frame AUGs in the VP ORF corresponded well with the values seen in SDS-PAGE analysis. These results implied that the *Bombyx mori* parvo-like virus (China Zhenjiang isolate) may use leaky scanning mechanism to generate four N-terminal truncated VP proteins. As the vector pET-30a can express fusion protein with both the N-terminal and C-terminal His-tag. We reserved the C-terminal His-tag sequence through deleting the stop codon of the CDS of the VP. In this way, the fusion protein VP1 has both N-terminal and C-terminal His-tag, and the VP2, VP3 and VP4 have C-terminal His-tag. So all of them can be detected by Western blotting with His-tag antibody.

The results also showed that the VP1 and VP3 are the main components of the viral structural protein and the VP2 and VP4 are much less than VP1 and VP3 in amount. This phenomenon indicated that the initiation codons of VP1 and VP3 were preferentially expressed. The genome of plum pox virus contains a single open reading frame that is translated into a large polyprotein. Although the open reading frame starts at nucleotide 36 (36AUG), it is translated from the second, 147AUG, which is in a more favorable context for translation initiation. When the cryptic 36AUG was placed in a favorable context, it turned into an efficient initiation codon in vitro. Furthermore, AUGs that were placed in a favorable context, initiating short intraleader open reading frames, repressed translation initiation from the 147AUG in vitro and in vivo. These results pointed to leaky scanning as the mechanism of translation initiation of plum pox virus RNA. Nevertheless, it is a peculiar leaky scanning where the initiation of translation does not require a cap structure at the 5' end. (Simón-Buela L, Guo HS, García JA.1997 2691-9.). Western blotting revealed that translation of these VP transcripts of *Casphalia extranea* Densovirus was not restricted to the first AUG but that it also led to recognition of downstream initiation codons to yield all structural proteins contained in the expressed transcript. Initiation codons 3 and 3' were the least leaky (G. FeÂ dieÂ re, 2002, 292 299±308). Two years later G. FeÂ dieÂ re et al showed that the denonucleosis virus of *Mythimna loreyi* use the same expression strategy to generate VP3 and VP4 yielded background products that were smaller than VP4 but reacted with the virus-specific antiserum. It appeared that the VP4 codon became somewhat leaky in the absence of the VP1 and VP2 initiate codon. (G. FeÂ dieÂ re, 2004, 181– 189) by bioinformatics analysis. The short untranslated 5' leader sequence and the less favorable contexts of VP2 and VP4 AUG initiation codons were found in VP gene of *BmDENV-Z*.

It is the first time that the leaky scanning mechanism of major VP gene of *BmDENV-Z* was witnessed by western blotting. Nevertheless, it would be possible that the set of VPs is generated by proteolysis of the largest VP (VP1), translation downstream of (an) internal ribosome entry site(s), or ribosomal shunting. As an economic and model insect of Lepidoptera, research for *B.mori* and related genes has attracted more and more attention. Specially, the VP gene may have some unknown functions. The transcription and expression analysis can help us to do further study about this gene. The details of capsid assembly mechanism and the interactions between VP and silkworm cell protein is in progress.

References

Bando H, Kusuda J, Gojobori T, Maruyama T, & Kawase S. (1987). Organization and nucleotide sequence of a densovirus genome imply a host-dependent evolution of the parvoviruses. *Journal of virology Feb*; 61(2):553-560.

- Bando, H., Choi H., Ito, Y., Nakagaki, M., & Kawase, S. (1992). Structural analysis on the single-stranded genomic DNAs of the virus newly isolated from silkworm: the DNA molecules share a common terminal sequence. *Arch. Virol.* 124: 187–193.
- Bando, H., Hayakawa, T., Asano, S., Sahara, K., Nakagaki, M., & Iizuka, T. (1995). Analysis of the genetic information of a DNA segment of a new virus from silkworm. *Arch. Virol.* 140: 1147–11
- Byung-Sik Shin, David Maag, Antonina Roll-Mecak, M. Shamsul Arefin, Stephen K. Burley, Jon R. Lorsch, & Thomas E. Dever. (2002). Uncoupling of Initiation Factor eIF5B/IF2 GTPase and Translational Activities by Mutations that Lower Ribosome Affinity Cell, Volume 111, Issue 7, 27 December, Pages 1015-1025
- G. FeÂ dieÁ re, M. El-Far, Y. Li, M. Bergoin, & P. Tijssen. (2004). Expression strategy of densovirus from *Mythimna loreyi* *Virology* 320 181– 189
- G. FeÂ dieÁ re, Y. Li, Z. ZaÂ dori, J. Szelei, & P. Tijssen. (2002). Genome Organization of *Casphalia extranea* Densovirus, a New *Iteravirus* *Virology* 292, 299-308.
- Li Y, Zadori Z, Bando H, R. Dubuc, G. FeÂ dieÁ re, J. Szelei & P. Tijssen. (2001). Genome organization of the densovirus from *Bombyx mori* (BmDNV-1) and enzyme activity of its capsid. *The Journal of general virology* Nov; 82 (Pt 11):2821-2825.
- Hayakawa T, Kojima K, & Nonaka K, et al. (2000). Analysis of proteins encoded in the bipartite genome of a new type of parvo-like virus isolated from silkworm structural protein with DNA polymerase motif. *Virus Res* Jan., 66 (1):101-108.
- P. Tijssen, Y. Li, M. El-Far, J. Szelei, M. Letarte, & Z. Za'dori. (2003). Organization and Expression Strategy of the Ambisense Genome of Densovirus of *Galleria mellonella* *JOURNAL OF VIROLOGY*, 19, 10357–10365.
- Simón-Buela L, Guo HS, & García JA. (1997). Cap-independent leaky scanning as the mechanism of translation initiation of a plant viral genomic RNA. *J Gen Virol.* Oct;78 (Pt 10):2691-9.
- Sotoshiro H, Kobayashi M1. (1995). Identification of viral structural polypeptides in the midgut and feces of the silkworm *Bombyx mori*, infected with *Bombyx* Densovirus Type 2 *J Invertebr Pathol*, 66 :60 – 671
- Wang, Yongjie, Yao, Qin, Chen, Keping, Wang, Yong, Lu, Jian, & Han, Xu. (2007). Characterization of the genome structure of *Bombyx mori* densovirus (China isolate) *Virus Genes* 35:103–108 DOI 10.1007/s11262-006-0034-3

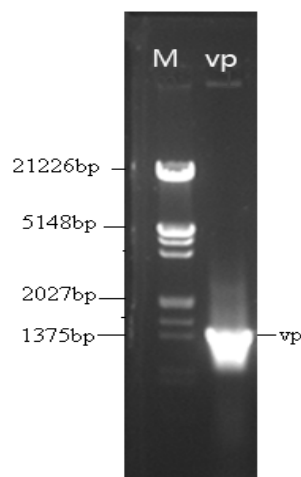


Figure 1. The result of PCR for vp. Lane M, DNA molecular mass maker; Lane vp, PCR product of vp (1500bp).

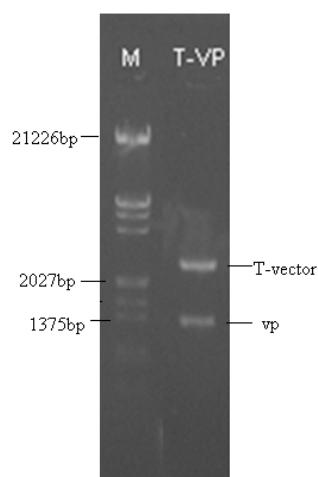


Figure 2. Identification of the recombinant plasmid pMD19-T/*vp*. Lane M, DNA molecular mass maker. Lane T-*vp*, pMD19-T/ *vp* digested with *Bam*HI and *Hind*III generated two fragments: pMD19-T (2.6 Kbp) and *vp* (1500 bp);

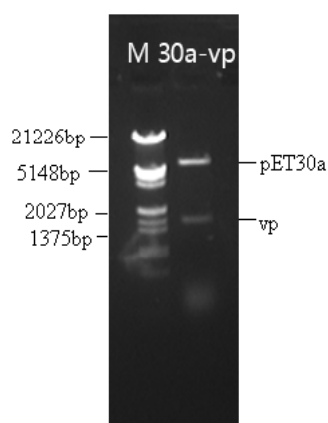


Figure 3. Identification of the expression vector His-*vp*-pET30a. Lane M, DNA molecular maker. Lane 30a-*vp*, His-*vp*-pET30a digested with *Bam*HI and *hind*III generated two fragments: His-pET30a (5.4Kbp) and *vp* (1500 bp).

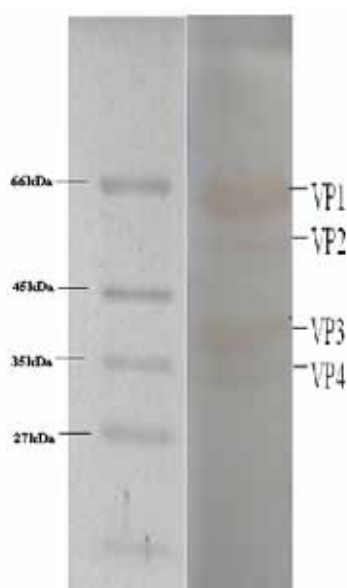


Figure 4. Western blotting analysis. Protein of *E. coli* BL21 contained His-pET30a induced by IPTG; Protein of *E. coli* BL21 contained His-GlcAT-S-pET30a induced by IPTG Western blot results of His-VP fusion protein. The four fusion protein bands were indicated by arrows.

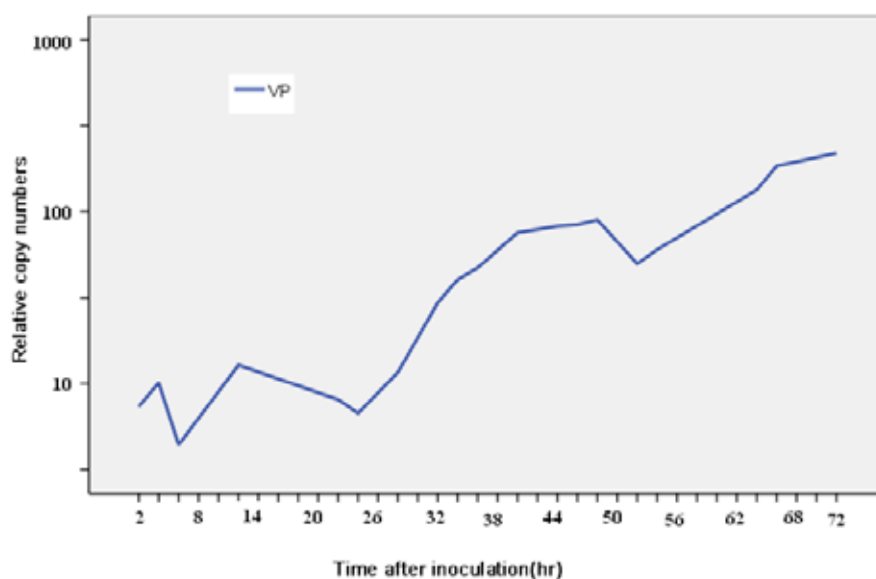


Figure 5. The mRNA level of *BmDNV-Z* VP protein. The copy numbers of vp mRNA increase considerably after 24hrs. *BmactinA3* gene was used as an internal control for normalization.



Effects of Waterlogging on Growth and Physiology of *Hopea odorata* Roxb

Hazandy Abdul-Hamid, Nor Aini Ab. Shukor, Sapari Mat & Abdul Latib Senin
Department of Forest Production, Faculty of Forestry, Universiti Putra Malaysia
43400 Serdang, Selangor, Malaysia.

Tel: 60-3-89-467-585 E-mail: hazandy@putra.upm.edu.my

Kamaruzaman Jusoff (Corresponding author)
Department of Forest Production, Universiti Putra Malaysia
Serdang, 43400 Selangor, Malaysia
Tel: 60-3-8946-7176 E-mail: kamaruz@putra.upm.edu.my

This research is funded by Fundamental Research Grant Scheme (FRGS/5523233), Ministry of Higher Education, Malaysia (sponsoring information)

Abstract

This study examines the growth and physiological characteristics of *Hopea odorata* growing under waterlogging condition. *H. odorata* was selected as it is widely planted as urban landscape tree species which experienced some growth stresses. Two waterlogging treatments and a control were designed. Forty 5-year old saplings each were subjected to waterlogged condition for 30 days which were then allowed to recover for a further 30 days as Treatment 1 (T1) and waterlogged condition for 60 days as Treatment 2 (T2). Aboveground and belowground biomass including leaf area was determined before and at 30 and 60 days of study. The net photosynthesis (A_{net}), stomatal conductance (G_s), transpiration rate per unit leaf area (E_L) and leaf to air vapour pressure deficit (ΔW) were assessed weekly for 60 days. The results showed that there were no significant differences between treatments for all growth attributes. There were also no significant reductions of these attributes found within treatments throughout the experimental period. Furthermore, no significant effects were observed in gas exchange variables. The results demonstrate that severe waterlogged condition did not affect the physiology of *H. odorata*. These findings add to the increasing evidences that *H. odorata* is a flood as well as a pollution tolerance species that ensuring it to survive and grow well in urban areas by regulating the partitioning strategies.

Keywords: Waterlogging, *Hopea odorata*, Gas exchange, Growth, Physiology

1. Introduction

Urban forests can play a critical role in helping to reduce increasing levels of atmospheric CO₂, as well as provide a wide variety of ecological services and amenities to communities. Trees store carbon (C) derived from CO₂, the major gas contributing to global climate change, reduce peak cooling and heating loads on power plants, thereby reducing C emissions. They can also reduce the higher ambient air temperatures which occur in urbanized areas due to large amounts of heat-absorbing materials. However, plants planted in urban areas are frequently exposed to a variety of environmental stresses that occur concurrently. These compounding stresses can be more detrimental to plant growth and survival than either stress when encountered alone. The ability of a plant to resist stresses can be an important factor in plant growth and survival. Overall, the wide variety of stresses that plants are exposed to elicit relatively similar responses from plants (Lichtenhaler, 1996). However, when the stress is severe enough to overwhelm the preconditioned defense of the plant, long term damage can occur.

In urban areas, one of the common stresses is waterlogging. Waterlogging is defined as ponding of water over an area of crop land (Scott and Batchelor, 1979). It can be induced by an abundance of rainfall or supraoptimal irrigation, especially in areas where land is poorly leveled. Waterlogging reduces plant growth rate by replacing the soil's air with water, therefore depriving of oxygen in the roots. Since oxygen diffuses slower through water than air, the roots soon become deprived of oxygen which then unable to maintain normal respiration. Although several abnormalities result from this rapid oxygen deprivation by soil microbe, yield loss appears linked most closely to reduced nitrogen uptake (Bacanamwo and Purcell, 1999 and Kozłowski, 1984).

Plants become affected in a number of ways when soil becomes flooded. Air within the soil pore spaces has oxygen content similar to that of the atmosphere (about 20%) (Pezeshki, 1994). When soil becomes flooded, the ordinary air in the pore spaces of the soil is replaced with water, greatly restricting the flow of oxygen through the soil. The small amount of oxygen left in the soil is quickly depleted by root and soil microorganisms' respiration. Soil oxygen depletion is accelerated under warmer soil temperatures, because oxygen becomes less soluble in water as temperature rises. Pezeshki (1994) stated that once the soil becomes anaerobic, adverse effects on plants occur such as chlorosis, reduced growth rate, disruption of cell membranes, adverse effects on mineral uptake, altered growth regulator relationships, stomatal closure, leaf wilting and epinasty, reduced photosynthesis and respiration, altered carbohydrate partitioning, and potentially death. To date, with few exceptions (Thomson *et al.* 1992; Malik *et al.* 2001) most experiments investigating the effects of waterlogging on plant growth have evaluated responses during waterlogging, or, in cases when recovery was assessed, only the effects on final yield were considered (Watson *et al.* 1976; Belford *et al.* 1985; Meyer *et al.* 1985; Meyer & Barrs, 1988; Melhuish *et al.*, 1991). Knowledge of the physiology of recovery after varying durations of waterlogging is scanty. Here, we assess the effects of waterlogging on growth and physiology caused by two durations of exposure and also the basis of recovery from this stress. The present study evaluates some growth attributes, and photosynthetic capacity and efficiency during waterlogging as well as during subsequent recovery when the soil was drained. The study attempts to examine the relative tolerance of an indigenous dipterocarp species, i.e. *Hopea odorata* to waterlogging. *H. odorata* was chosen since it is widely planted as urban tree in Malaysia. Eventhough it originated from natural forest, this species seems to be adapted well in urban areas. In this paper, an attempt was made to explain a few mechanisms which the species utilize to tolerate or to avoid harmful effects of the applied stress.

2. Materials and methods

2.1 Plant materials and experimental design

A total of 60 saplings aged five years were obtained from Mantin Nursery, Negeri Sembilan, Malaysia. They were transplanted into 10-litre polyethylene bags potted with mixture of 2: 1: 1 of soil, peat and sand, and they were then supplied with slow-release fertilizer. These saplings were then divided into three groups (two treatment groups and a control). There were 20 saplings assigned to each treatment utilizing a Randomized Complete Block Design (RCBD) with two concrete frames sized 1 m X 4 m laid with high durable plastic sheets which were then filled to volume with water. Each frame was divided into six subframes and each subframe comprised of five saplings. Two replicates were assigned randomly for each treatment. The water was added and maintained periodically at 4 cm above the soil surface for waterlogged condition while saplings for the control subframe were being watered daily until the end of experiment.

2.2 Growth attributes measurement

Each treatment with five saplings were selected randomly and were then destructed in every time of measurements. The destructed saplings were divided into three parts, i.e. root, stem and branch (if any), and shoot (leaf). All the leaves were excised from the destructed saplings and total leaf area was determined using LI-3100 leaf area meter (LiCor Inc, Lincoln, Nebraska, USA). These leaves were then dried in an oven at 60°C for four days. Meanwhile, masses of the root and the stem were measured immediately after they were cleaned and oven dried at 70°C for four days or until constant weight was achieved.

2.3 Gas exchange measurement

The gas exchange measurement of all saplings was compared between treatments together with a control. The measurements were conducted on a random subframe-by-subframe basis on sunny days between 8:00 AM and 12:00 PM using LiCor 6400 portable photosynthesis system (LiCor Inc, Lincoln, Nebraska, USA) at initial stage and every week for duration of eight weeks. The gas exchange measurements were made on fully expanded leaves from the uppermost part of each sapling. Since the frames were placed under shading mesh, all plants were exposed to 15 minutes of full sunlight to allow for stomatal opening prior to taking measurements. The sample leaf was then placed in the cuvette that was maintained at 27°C and exposed to 1200 $\mu\text{mol.m}^{-2}\text{s}^{-1}$ PAR and CO₂ concentration was set to 360 $\mu\text{mol.m}^{-2}\text{s}^{-1}$. Once stomatal conductance and CO₂ assimilation stabilized, data were recorded. When inside the cuvette, all sampled leaves were exposed to identical environmental conditions. Three sequential measurements were made within 1 to 4 minutes, and the average values were used for analyses.

2.4 Data analyses

The data obtained from repeated measurements were summed and averaged for each individual tree prior to any data analysis. If necessary, data transformations (normalised) were applied to stabilise error variance. These data were then analysed using one-way analysis of variance (ANOVA) and general linear model (GLM) for balanced and unbalanced data among treatments respectively. All the statistical analyses were performed using Statistical Analysis System version 9.0 (SAS Institute Inc. 2002) and the significance level was set at 0.05.

3. Results and discussion

3.1 Growth attributes

Table 1 shows the summary of ANOVA. There were no significant effects of waterlogging found between treatments for all the growth attributes taken. However, significant differences between treatments for all the parameters were only observed over time.

<<Insert Table 1 here>>

The mean values for all the growth attributes were plotted in Figure 1. Regardless of insignificant effects of waterlogging throughout the experimental period, the growing trends were observed in aboveground biomass ($M_{\text{stem+branch}}$ and M_{leaf}) as shown in Figure 1A and Figure 1C. In contrast, no growing trends were observed in belowground biomass (M_{root}) for all the treatments (Figure 1B). The growing trends of leaf area (A_L) were more apparent in T2 which is shown the highest value at 60 days (Figure 1D). In both waterlogging treatments, there were substantial increasing trends as compared to control.

<<Insert Figure 1 here>>

3.2 Gas exchange attributes

Similar results were also observed in gas exchange attributes. There were no significant differences between treatments and the interaction between treatment and time (Table 2) for net photosynthesis (A_{net}), stomatal conductance (G_s), transpiration rate per unit leaf area (E_L) and leaf to air vapour pressure deficit (ΔW). In contrast, significant differences were only found over time.

<<Insert Table 2>>

The mean values of each gas exchange parameter for every measurement were summarized in Figure 2. Similar trends were observed for A_{net} , G_s and E_L throughout the experimental period. The steep decreasing patterns observed in week 2 and 3 for A_{net} (Figure 2A) and G_s (Figure 2B) were associated with leaf to air vapour deficit (ΔW) as shown in Figure 2D.

Data on responses of this species to waterlogging is almost non-existent or new. The data with regard to stress available for this species were related to nutrient and water stresses (Siti Rubiah and Ahmad Husni 2007). Hence, we demonstrated here the responses of *H. odorata* within 60 days waterlogged by measuring growth and physiological attributes. In this study, insignificant effects of waterlogging on biomass or even on net photosynthesis rate (A_{net}), stomatal conductance (G_s) and transpiration rate per unit leaf area (E_L) were found. From this, the physiological variables were not changed dramatically and the changes were only associated with changes of leaf to air vapour pressure deficit (ΔW). However, the increasing trends were observed in aboveground parts for stem and branch ($M_{\text{stem+branch}}$), and leaf (M_{leaf}).

<<Insert Figure 2>>

The results clearly indicated that *H. odorata* can tolerate well with stress imposed by long term (60 days) waterlogging treatment through controlling the carbon partitioning. The regulation of allocation of carbon was more pronounced in aboveground in waterlogged saplings. The extent to which newly acquired carbon was allocated to the production of new leaf area and this has contributed to the growing of aboveground parts. The functional equilibrium model introduced by Thornley (1976) and Brouwer (1983) has successfully described how leaf area might be preferentially expanded under low irradiances. The allocation to leaf area is clearly a subset of more general problem such as stress imposed by low irradiance. This principle can also be applied in these findings. The strategies that imposed by this species to avoid severe damage by increasing leaf area and mass in 60 days immersed in the water. By taking the value of leaf area and leaf mass in this study, the specific leaf area (SLA) which is leaf area to leaf mass ratio also increased in T2. In contrast, the low watering treatment was effective in inducing similar adaptive morphological changes such as reduced SLA as reported by Grace and Russell (1977). Judging from substantial increasing patterns of leaf area and mass, the plants were forced to expand the leaf area and accumulate mass in leaves rather than in stems, branches or roots. This could be it strategies to drain the water from the bottom by increasing leaf area and mass. During the growth of plants, water is removed from the soil by transpiration. The rate of transpiration is proportional to the leaf area. Trees have a large leaf area and deep roots encouraging a high transpiration rate and the transpiration by plants helps to dry out soils.

During rain, water will infiltrate more readily into a dry soil and the removal of water by transpiration allows more water to enter soils during rain and this will reduce water runoff and lower flooding or waterlogging.

The adaptive responses of this species have brought it up to survive well in urban areas. The present study clearly demonstrated that the growth and photosynthesis rate or other gas exchange attributes of *H. odorata* were unaffected by waterlogging. Responses of *H. odorata* to waterlog were invariable, and to some extent it was unexpected. The tolerance of the *H. odorata* to short and long-term waterlogging was quite surprising. In particular, this species tried to avoid severe damage to its system or dying off by increasing the partitioning of carbon and dry weight to leaf. Judging from both growth and physiological aspects, the effects of waterlogging were only seen on the partitioning strategies as discussed above.

References

- Bacanamwo, M. & L.C Purcell. (1999). Soybean Root Morphological and Anatomical Traits Associated with Acclimation to Flooding. *Crop Science* 39: 143-149.
- Belford, R.K., R.Q. Cannell & R.J. Thomson. (1985). Effects of single and multiple waterloggings on the growth and yield of winter wheat on a clay soil. *Journal of the Science of Food and Agriculture* 36: 142–156.
- Brouwer, H. (1983). Functional equilibrium: sense or nonsense? *Netherlands Journal of Agricultural Science*, 31: 335-348.
- Grace, J. & G. Russell. (1977). The effect of wind on grass. III. Influence of continuous drought or wind on anatomy and water relations in *Festuca arundinacea* Schreb. *Journal of Experimental Botany*, 28: 268–278.
- Kozlowski, T.T. (1984). Responses of woody plants to flooding. In *Flooding and plant growth*. Ed. T. T. Kozlowski. Academic Press, New York. Pp. 120.
- Lichtenthaler, H.K. (1996). Vegetation stress: an introduction to the stress concept in plants. *Journal of Plant Physiology* 48:4-14.
- Malik A.I, T.D. Colmer, H. Lambers & M. Schortemeyer. (2001). Changes in physiological and morphological traits of roots and shoots of wheat in response to different depths of waterlogging. *Australian Journal of Plant Physiology*, 28: 1121–1131.
- Melhuish, F.M., E. Humphreys, W.A. Muirhead & R.J.H. White. (1991). Flood irrigation of wheat on a transitional red-brown earth. I. Effect of duration of ponding on soil water, plant growth, yield and N uptake. *Australian Journal of Agricultural Research*, 42: 1023–1035.
- Meyer, W.S. & H.D. Barrs. (1988). Response of wheat to single, short-term waterlogging during and after stem elongation. *Australian Journal of Agricultural Research*, 39: 11–20.
- Meyer, W.S., H.D. Barrs, R.C.G. Smith, N.S. White, A.D. Heritage & D.L. Short. (1985). Effect of irrigation on soil oxygen status and root and shoot growth of wheat in a clay soil. *Australian Journal of Agricultural Research*, 36: 171–185.
- Pezeshki, S.R. (1994). Responses of baldcypress seedlings to hypoxia: leaf protein content, ribulose-1,5-bisphosphate carboxylase/oxygenase activity and photosynthesis. *Photosynthetica*, 30:59--68.
- Scott, H.D. & J.T. Batchelor. (1979). Dry weight and leaf area production rates of irrigated determinate soybeans. *Agronomy Journal*, 71: 776-782.
- Siti Rubiah, Z. & M.H. Ahmad Husni. (2007). Physiological response of *Hopea odorata* Roxb. and *Mimusops elengi* Linn. seedlings under combined nutrient and water stresses. *The Malaysian Forester*, 70(1): 41-48.
- Thomson, C.J., T.D. Colmer, E.L.J. Watkin & H. Greenway. (1992). Tolerance of wheat (*Triticum aestivum* cvs. Gamanya and Kite) and triticale (*Triticosecale* cv. Muir) to waterlogging. *New Phytologist*, 120: 335–344.
- Thornley. (1976). Mathematical models in plant physiology. Academic, London.
- Watson, E.R, P. Lapins and R.F.W. Barron. (1976). Effect of waterlogging on growth, grain and straw yield of wheat, barley and oats. *Australian Journal of Experimental Agriculture and Animal Husbandry*

Table 1. Analysis of variance (ANOVA) for growth characteristics of *H. odorata* exposed to waterlogging treatments.

Source of Variation	Parameter			
	F Value			
	M_{root}	$M_{\text{stem+branch}}$	M_{leaf}	Total A_L
Treatment	0.125 ^{ns}	0.101 ^{ns}	1.288 ^{ns}	1.498 ^{ns}
Time	0.317 ^{ns}	9.363 ^{***}	2.566 ^{ns}	7.289 ^{**}
Treatment x Time	0.506 ^{ns}	1.119 ^{ns}	0.721 ^{ns}	1.33 ^{ns}

Note: * significant difference at $p < 0.05$

** significant difference at $p < 0.01$

*** significant difference at $p < 0.001$

^{ns} Not significant

Table 2. Analysis of variance (ANOVA) for gas exchange attributes of *H. odorata* exposed to waterlogging treatments.

Source of Variation	Parameter			
	F value			
	A_{net} ($\mu\text{mol CO}_2 \cdot \text{m}^{-2} \cdot \text{s}^{-1}$)	G_s ($\text{mol H}_2\text{O} \cdot \text{m}^{-2} \cdot \text{s}^{-1}$)	E_L ($\text{mmol H}_2\text{O} \cdot \text{m}^{-2} \cdot \text{s}^{-1}$)	ΔW (kPa)
Treatment	0.504 ^{ns}	1.076 ^{ns}	0.459 ^{ns}	1.006 ^{ns}
Time	4.001 ^{***}	4.429 ^{***}	3.267 ^{**}	10.539 ^{***}
Treatment x Time	1.033 ^{ns}	0.8 ^{ns}	0.632 ^{ns}	1.297 ^{ns}

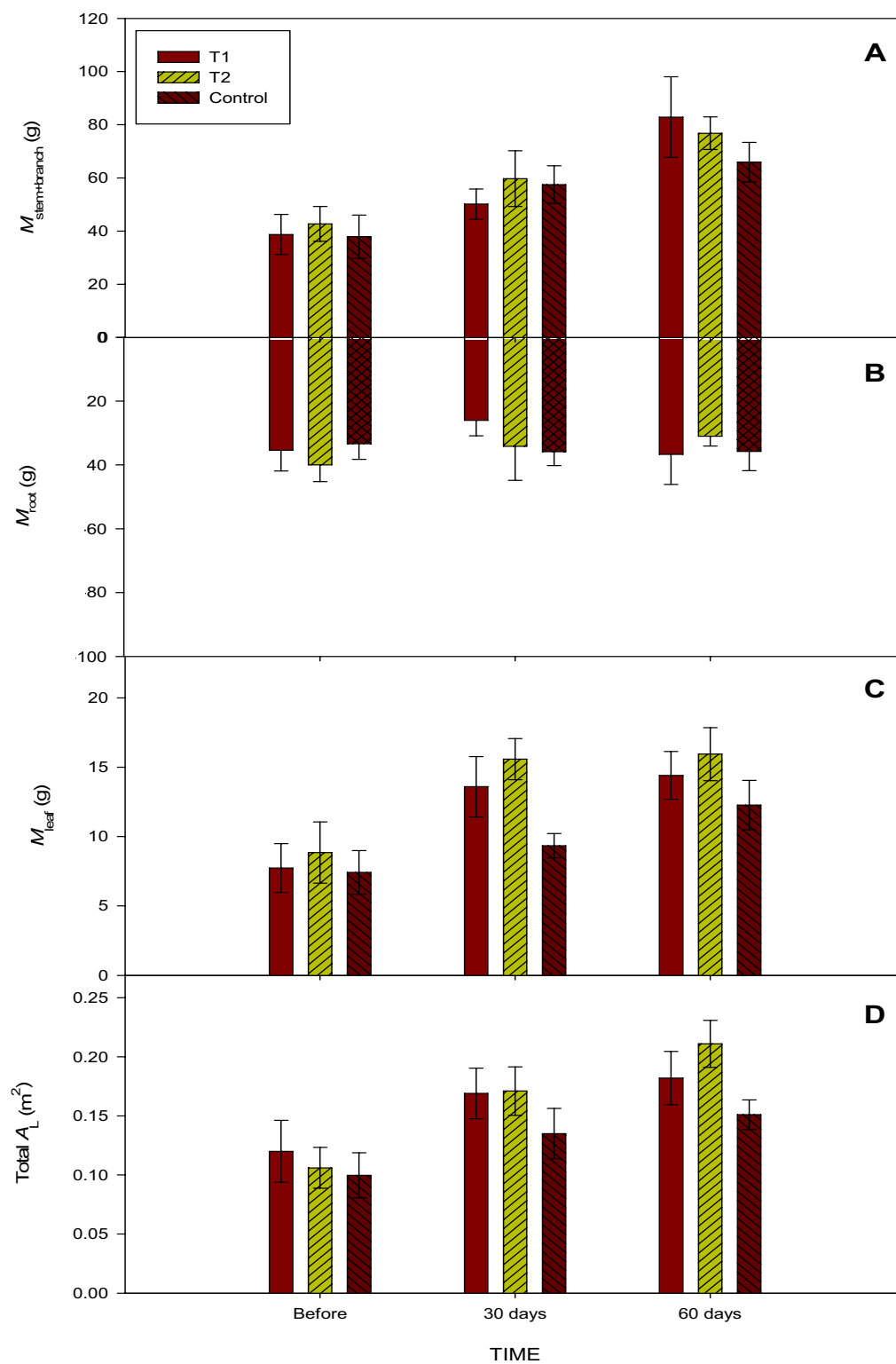


Figure 1. The mean values of stem and branch mass (A), root mass (B), leaf mass (C) and total leaf area (D) for each treatment.

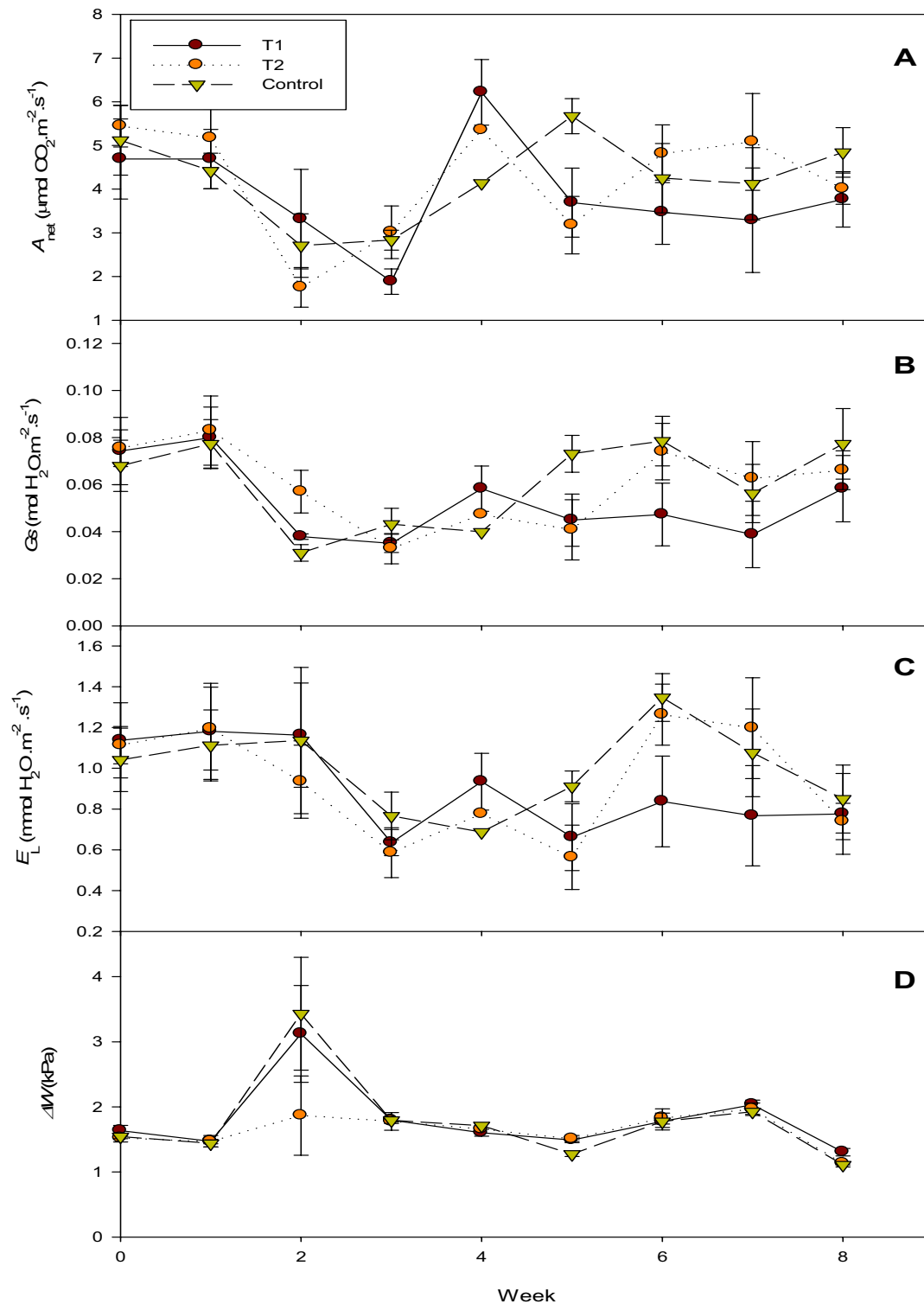


Figure 2. The mean values of net photosynthesis (A), stomatal conductance (B), transpiration rate per unit leaf area (C) and leaf to air vapour pressure deficit (D) for each treatment.



Preliminary Study on the Mechanism for Adaptation of Stipagrosits Pennata to Desert

Baohua Gong, Jianbo Zhu & Hongying Zhao

National Key Laboratory of Agricultural Biotechnology, College of Life Science

Shihezi University, Shihezi, Xinjiang 832003, China

E-mail: javaxsun@163.com

Yuxing Zhang (Corresponding author)

National Key Lab of Tropical Biotechnology Institute

Chinese Academy of Tropical Agricultural Sciences, Haikou, Hainan 571101, China

E-mail: zyx2027193@163.com

The research is funded by Doctoral Foundation of the XPCC (Xinjiang Production and Construction Corps). No. 2006jc07 (Sponsoring information)

Abstract

Psammophyte can resist drought through different mechanism, such as small and thin leaves, leaves covered with wax, well developed roots. As typical psammophyte, stipagrosits pennata' root form entwined structure with sand, therefore shows excellent drought tolerance. This paper describes the mechanism of the adaptation of stipagrosits pennata to desert from different aspects such as morphology, anatomical structure and stress simulation.

Keywords: Stipagrosits pennata, Drought tolerance, Desert, Entwined root

1. Introduction

In severe circumstances, such as drought, salinity, extreme temperature, plants activate all their physiological and metabolic defense systems to respond abiotic stress. Tolerance and susceptibility are complex matters of abiotic stress adaptation. Abiotic stress is the major cause of yield reduction of plant. Annual reduction caused by abiotic stress amounts more than 50% (Boyer J S, 1982, p. 443-448; Bray E A, 2000, p. 1158-1249). Therefore, study on the adaptation of plant to severe circumstances has positive and practical significance. Among abiotic stresses globally, drought is the main reason causing yield reduction. Plants in drought activate their physiological changes and developmental changes during growth process (Wang W, 2003; Vinocur B, 2005; Chaves M M, 2004; Shinozaki K, 2003; Yamaguchi-Shinozaki K, 2005). Plants in severe circumstances exhibit not only physiological and biochemical changes, but also morphological and structural changes.

Growing in the above-described severe environment, psammophyte forms special morphological structures, such as small and curling leaves, leaves covered with vegetable wax, short stems, entwined roots, all for the adaptation to the desert climate. Stipagrosits pennata, evolved in desert climate for long time, exhibits a form excellent in resisting drought, wind erosion and sand burying.

Stipagrosits pennata genera, including about 150 species, are found widely in extratropical and subtropical drought area. There are total 11 species in China, 3 species in Xinjiang, mainly in the Gurban Tongut Desert in North Xinjiang. With excellent tolerance to drought, wind erosion and sand burying, stipagrosits pennata is a perfect sand-fixing plant. Together with C.leucocladum, C. henopodiaceae and other plants with good sand tolerance and sand adaptation, it forms sand-tolerant plant community (Mamat, Yiti, 1990, p. 51-56).

2. Materials and methods

2.1 Studied samples

Stipagrosits pennata and their seeds come from Moguanchu, 148 Corps of Shihezi, Xinjiang, China.

2.2 Observation on ecology of stipagrosits pennata and effects of temperature on its stomatal conductance

The effects of temperature on stomatal conductance of stipagrosits pennata are investigated in field by LICOR LI-6400 V4.0.1.

2.3 Anatomic experiment on the structure of entwined root

Wash the seeds by tap water for 3 times, then rinse the seeds by distilled water for 3 times. In an aseptic container, disinfect the seeds with 75% alcohol for 45 s under a bacteria-free environment, then with 0.1% mercuric chloride for 8 min (Mao, Weiguang, 2006, p. 116-118). Keep the sterilized seeds in culture medium (1/2MS+2.0 mg/L GA3) for germination, and change to MS+0.3 mg/L NAA after 25 days (Zhou, Jiyuan, 1997, p. 77-82; Chen, Xuesen, 1997, p. 373-377). Seedlings' root will grow bigger and thicker, and also grow out lateral roots. With about 20 days more, seedlings will grow up with their roots extending out from 0.2 mm to 1 mm. The entwined structure of root is obvious visible. On this occasion, however, this may not happen to every seedling. At this moment, the size of seedling's root is nearly same as the one in wild. With further growth, the root grows longer but thicker.

2.4 Simulation experiment on the stress adaptation to desert

Collect 1-year old stipagrosits pennata from Mosuowan Desert of Shihezi of Xinjiang in China and plant them in a plant pot with 5 kg sand per pot. Simulate the drought stress at different concentration of PEG6000 after two-week domestication in laboratory. Assuming 3 gradients of PEG stress processes: 0, 10% and 30% with 8 pots per gradient (non-stress gradient is taken as the Control Group). Use the saturated weighing method to maintain their water content. Specifically the procedure is as following: take weigh measurement on each pot at 19:00 every day; refill the lost water to keep the same water content; collect the samples within 72 hours of stress process; choose 3 pots of seedlings with same growth condition as the studied materials; take 3 parallel samples from each pot.

2.4.1 Effects of PEG6000 on membrane permeability

Conductivity process (Hao, Zaibin, 2004).

(1) Rinse the leaves of both the Treatment Group and the Control Group with deionized water, use clean filter paper to absorb water from leaves' surface, cut leaves into segments of 2 mm, and then keep them in clean scaled test tubes.

(2) Introduce 10 mL deionized water into leaf-contained tubes.

2.4.2 The effects of PEG on the content of soluble protein

Coomassie Brilliant Blue method (Hao, Zaibin, 2004) is applied. Weigh 0.5 g fresh stipagrosits pennata leaves, grind them together with 2 mL distilled water into paste, centrifuge at 4,000 r/min for 20 minutes, take 1.0 mL supernatant and drop it into a tube, add 5 mL Coomassie brilliant blue solution (G-250) and thoroughly mix them. After 2 minutes, measure the absorbance at 595 nm by colorimetric method. Find the protein content from the specification curve, calculate the content of soluble protein in sample with the following formula (1).

$$Cs=(C \times VT)/(V1 \times FW \times 1000) \quad (1)$$

Here, Cs (mg/g) represents the content of soluble protein; C (μg) represents the content of soluble protein out of the specification curve; VT (mL) represents the total amount of extracted sample; V1 (mL) represents the amount of measured sample; FW (g) represents the fresh weight of sample.

3. Results

3.1 Adaptation of stipagrosits pennata to drought

The boundary region of desert, where Stipagrosits pennata grows, belongs to continental temperate zone and drought desert climate. The annual average precipitation is about 117.2 mm, and the potential evaporation is up to 1942.1 mm. The annual average temperature is 5-11 °C, the lowest temperature recorded is -42.6 °C and the highest temperature is 62.2 °C. In the desert, the surface temperature can be as high as 60 °C. High temperature leads to the amount of water evaporation more than the amount of precipitation. It demands stipagrosits pennata having a fully developed water-absorption and water-storage system, and meanwhile a structure minimizing water evaporation. Stipagrosits pennata's root grows deep into earth for 4 to 5 meters to absorb water from deep underground. It has an average of more than 80 well-developed entwined lateral roots of 5 to 15 meters in length, radially extended into sand layers 6 to 35 centimeters below the ground, which can absorb water from the distant place without competing with other plants. Moreover, stipagrosits pennata's root will develop new tiller buds at places with relatively sufficient water supply. As a result, stipagrosits pennata clusters together at desert and has powerful vitality. These are the reasons that stipagrosits pennata can grow without obvious suffering even when the water content is only 0.22%-4.33% in sand layers of 0-30

cm depth.

Stipagrostis pennata, perennial herbaceous, has the following features: smooth sheath, mostly shorter than internodes; dwarf membranous ligule with extremely short cilia; vertically winded needle-shaped leaves up to 20 cm in length; thickly growing stalks with smooth branches, up to 50 cm in height. For adaptation to the windy climate during its growth period from May to June, its tenuous and flexible stems and leaves swing in wind and are not susceptible to break, meanwhile, its strongly curling leaves can prevent water from excessive evaporation (Mamat, Yiti, 1990, p. 51-56).

The lateral root of *stipagrostis pennata* has an entwined structure, which holds a thick layer of sand and increases the friction between the sand and roots. The structure has a function of preventing sand flow and insulating the root from the overheated sand surface to prevent the root from heat damage as sand has relatively low thermal conductivity. From figure 1 (microstructure of root), we can see that, different from the root of other plants with which root hairs are found only at 2-3 cm over root tip, root hairs grow over the entire root surface to increase its hygroscopic capacity. In addition, the tight attachment between root hairs and sand can effectively stabilize the root into mobile dunes. From figure 2 and figure 3 (anatomic structure of root), we can see that root hairs are closely connected to epidermal cells, and there is a hollow airtight chamber between epidermal cells and parenchyma cells. The chamber is as a vacuole in plant, with many cabins separated by connection belt. Its cell wall is thicker than that of parenchyma cell at 3-4 times, and thicker than that of epidermal cell at 2-3 times, which provides better pressure resistance for water storage. Three or more drapes linked between epidermal cell and chamber cell wall facilitate the water absorption from sand to root hairs and the water transportation from root hairs into root chamber. As in a reservoir, the chamber generally stores water, and releases until the plant needs. In this way, *stipagrostis pennata* adapts well to the intermittent rainfall in desert. The chamber, with 3 root hairs and 2-4 pellicular cells inside (figure 2), is so large that water therein can be easily transported to the well-developed tube in root, which in turn ensures the long distant transportation of water to the other parts of plant.

3.2 Adaptation of *stipagrostis pennata* to cold climate

It is the well-developed root that ensures perennial herbaceous *stipagrostis pennata* to live in the desert with annual average temperature of 5-11 °C and the extremely low temperature at -42.6 °C. The sand layer tightly held on the root can insulate the root from outside cold hardness and keep the winter bud warmed; on the other hand, there is no water in the root chamber in winter, such hollowed structure can protect the root from frostbite.

3.3 Nutrient absorption process of *stipagrostis pennata* for adaptation to desert

No matter what kinds of roots they are and which directions the roots extend into, the well-developed roots of *stipagrostis pennata* not only absorb water and nutrient from long distance, but also extend along a certain direction to a proper site to tiller for reproduction and further enhancing vitality. With drift of sand, *stipagrostis pennata* can absorb nutrients from new sand. The root of *stipagrostis pennata* can extend outward more than 15 m in sand because the viscosity of sand is much less than that of soil. All these make *stipagrostis pennata* well adapted to live in desert. Although the precipitation in desert is very little and the water content in top layer sand is only 0.22%-4.33%, the absorbed nutrients therein is much more concentrated.

3.4 Stoma changes of *stipagrostis pennata* for adaptation to desert

Temperature affects stomata conductance drastically. Average stomata opening is very small around 24 °C, increases with the rise of temperature, decreases however when temperature is over 35 °C, but maintains at about 2 times of that at 24 °C (figure 5 and figure 6). It indicates that the evaporation rate of *stipagrostis pennata* reaches the maximum at 35 °C, and stays stable after that to prevent excessive evaporation resulted in withering.

3.5 Simulate the adaptation to desert by PEG6000 simulated stress experiment

Observe the differences among samples processed with 3 different concentrations of PEG. At the beginning, three different types of samples maintain the same. After 36 hours, membrane permeability increases in accordance with the concentration of PEG. This is because the samples don't need this much water. It increases the membrane permeability to absorb water only under the stress of drought. After 72 hours, all the samples still show healthy outlook, while cotton samples processed by 25% PEG died for lack of water after 48 hours.

Figure 7 and figure 8 show that the concentration of soluble protein in *stipagrostis pennata* is increased in accordance with the concentration of PEG. The content of soluble protein stressed with 20% and 30% PEG is 20% higher than that stressed with 10% PEG. It is 50% higher than that of the Control Group. It indicates that the content of soluble protein inside *stipagrostis pennata* is very low under stress-less circumstance, however gradually increases against the high osmotic potential caused by drought stress in order to keep absorbing water from its surroundings.

4. Discussion

There are two kinds of reproduction mechanisms for *stipagrostis pennata*: one is asexual propagation, namely, the

tillered root grows up into a independent young plant, this mechanism is an effective way to reproduce in drought desert; the other one is sexual propagation, namely, stipagrosits pennata flowers and bears fruit from June to August, then its seeds germinate from March to April next year. Very small number of seeds has a chance to grow up due to rather limited amount of matured seeds, high temperature, drought in desert, and likely consumed by birds and insects, etc.

The root stipagrosits pennata presents itself as a long and slender entwined sand mass and with no entwined structure on the tip of root. It is difficult to investigate the structure, especially the microstructure of the entwined root directly from wild stipagrosits pennata. Cultivation of aseptic seedling can solve this issue. Cell membrane of root hair is similar to the membrane of thin wall cell. Water can easily pass through the thin wall of cell into epidermal cell of root hair. The entwined root can fix stipagrosits pennata onto sand tightly. Moisture sand itself is sticky. Entangled with the moisture sands, the roots will better fasten to the sand. In summer, the surface temperature can go up to 60 °C. Aged roots are often exposed to the shallow layer of sand due to wind erasure. Entwined effectively protects the root with a layer thermal insulator. Entwined root has strong physical and chemical properties, and is able to remain its original form even under long-term contact with cellulose, pectase or 6 mol/L hydrochloric acid. Polysaccharide secreted from the self-formed entwined root of stipagrosits pennata makes the entwined structure sticky (M Sridhara Murthy, 1975, p. 243-249; Ma, Wei, 2007, 55-56). The formation of entwined root shows important ecological function and significance. The root of rice stays in oxygen-short water in general, so the chamber in rice root is used for respiration. However, the chamber in stipagrosits pennata's root is used to store water against the drought in desert where water is in constant shortage expect when snow accumulated in winter melts and few plants can survive in such environment.

Besides the special structure of entwined root (Pathan M S, 2004, p. 525-569; Serraj R, 2002, p. 333-341), stipagrosits pennata exhibits different metabolic strategies for adaptation to drought stress (Tabaeizadeh Z, 1998, p. 193-247). Stipagrosits pennata is proved to be an excellent resource for drought resistance genes with excellent tolerance to drought, good resistance to high and low temperature fluctuation, etc. Through the investigation of this special plant, revelation of mechanism for adaptation to desert, and research on its genetic basis, and screening and cloning of drought resistance genes, we can acquire its potential gene resource for crop improvement. The research in this area has huge academic and economic value. Currently, there is very limited research on stipagrosits pennata in the world, especially on drought resistance genes and relative biomacromolecule.

Acknowledgements

The study is completed in the National Key Lab of Agricultural Biotechnology, College of Life Science, Shihezi University. I hereon thank Dr. Yuxing Zhang and Dr. Jianbo Zhu for their guidance.

References

- Boyer J.S. (1982). Plant productivity and environment. *Science*, 218, 443-448.
- Bray E. A, Bailey-Serres J & Weretilnyk E. (2000). Responses to abiotic stresses in biochemistry and molecular biology of plants. In Gruissem W, Buchannan B & Jones R (Eds.), *American Society of Plant Physiologists*, pp. 1158-1249.
- Chaves M M & Oliveira M M. (2004). Mechanisms underlying plant resilience to water deficits: prospects for water-saving agriculture. *J Exp Bot*, 55, 2365-2384.
- Chen, Xuesen, Deng, Xiuxin & Zhang, Wencai. (1997). Effects of medium and culture environment on flavonoid production of ginkgo biloba callus. *Journal of gardening*, 4, 373-377.
- Hao Zaibin, Cang Jing & Xu Zhong. (2004). *Plant physiology experiment*. Harbin: Publisher of Harbin Institute of Technology.
- M Sridhara Murthy & R Ravindra. (1975). Allelopathic effects of a ristida adscensionis. *Oecologia Berl*, 18, 243-249.
- Ma, Wei & Li, Chunjian. (2007). Root sheath of plant and its ecological significance. *World Agriculture*, 4, 55-56.
- Mamat, Yiti. (1990). Ecological and biological characteristics of stipagrosits pennata and evaluation on them. *Arid Zone Research*, 4, 51-56.
- Mao, Weiguang, Weng, Mangling, Wu Zhen & Li Shijun. (2006). The influence of different processes to the germination characteristics of leaf beet seeds. *Jiangsu Agricultural Sciences*, 3, 116-118.
- Pathan M S, Subudhi P K, Courtois B & Nguyen H T. (2004). Molecular dissection of abiotic stress tolerance in sorghum and rice. In Nguyen H T & Blum A (Eds.), *Physiology and biotechnology integration for plant breeding*. Marcel Dekker Inc. p. 525-569.
- Serraj R & Sinclair T R. (2002). Osmolyte accumulation: can it really help increase crop yield under drought conditions? *Plant Cell Environ*, 25, 333-341.
- Shinozaki K, Yamaguchi-Shinozaki K & Seki M. (2003). Regulatory network of gene expression in the drought and cold stress responses. *Curr Opin Plant Biol*, 6, 410-417.

Tabaeizadeh Z. (1998). Drought-induced responses in plant cells. *Int rev cytol*, 182, 93-247.

Vinocur B & Altman A. (2005). Recent advances in engineering plant tolerance to abiotic stress: achievements and limitations. *Curr Opin Biotechnol*, 16, 123-132.

Wang W, Vinocur B & Altman A. (2003). Plant responses to drought, salinity and extreme temperatures: towards genetic engineering for stress tolerance. *Planta*, 218, 1-14.

Yamaguchi-Shinozaki K & Shinozaki K. (2005). Organization of cis-acting regulatory elements in osmotic and cold stress responsive promoters. *Trends Plant Sci*, 10, 88-94.

Zhou, Jiyuan & Dai, Jungui. (1997). Effects of plant growth regulators on callus formation and organogenesis of *astragalus chinensis* l. *Journal of Central China Normal University (Natural Sciences)*, 1, 77-82.



Figure 1. Wild stipagrostis pennata and roots set

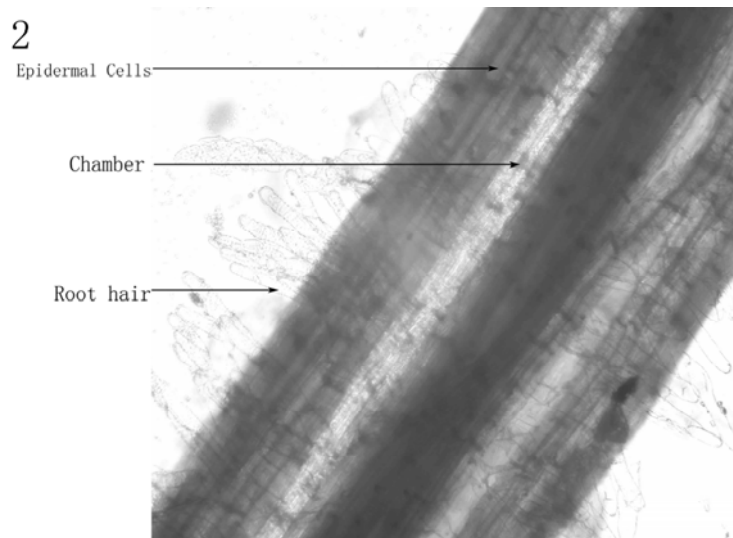


Figure 2. Root hair in medium

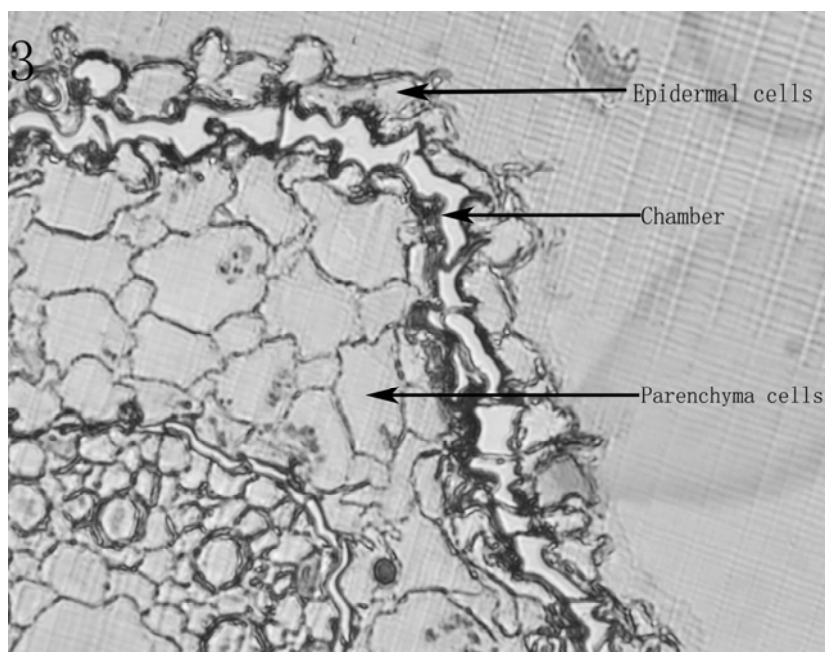


Figure 3. Dyeing of safranin and fast green

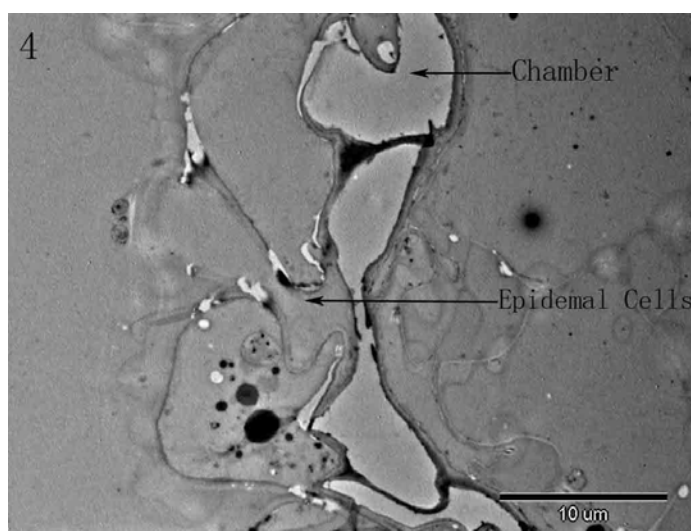


Figure 4. Roots set structure by electron microscope

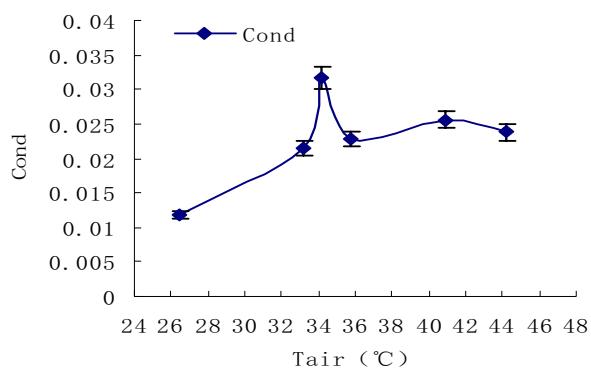


Figure 5. Effects of air temperature on conductivity

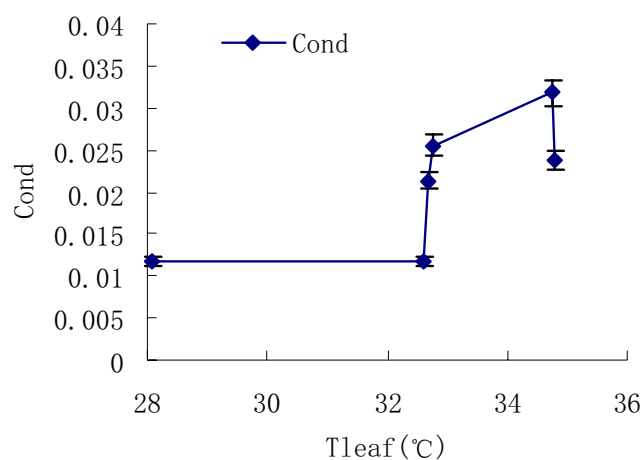


Figure 6. Effects of leaf temperature on conductivity

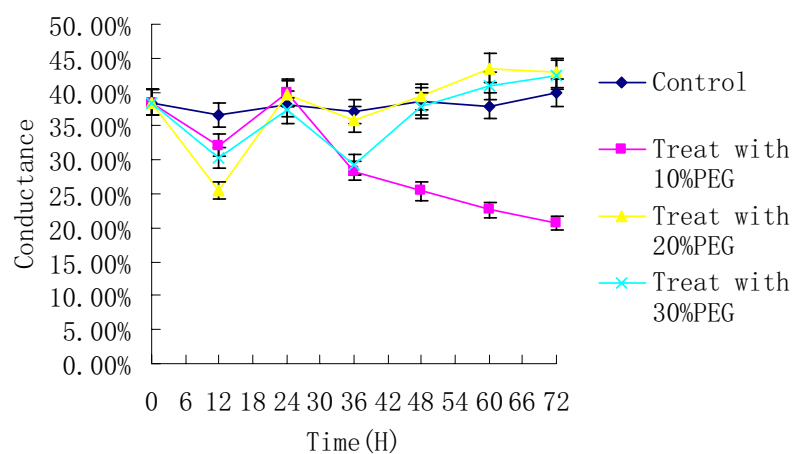


Figure 7. Effects of PEG6000 on membrane permeability

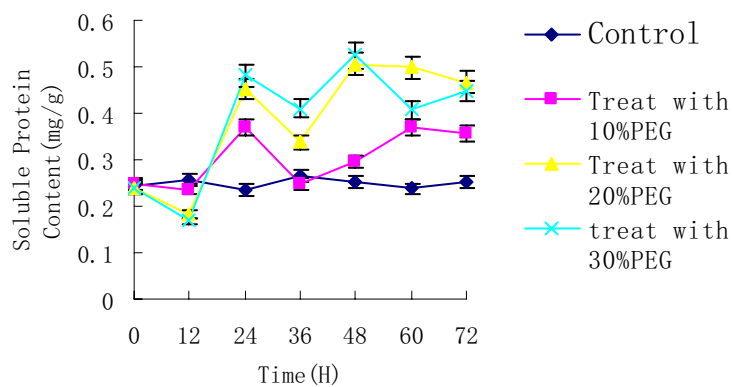


Figure 8. Effects of PEG6000 on soluble protein content



Isolation and Characterization of a Silkworm cDNA Encoding a Protein Homologous to the 14kDa Protein of Bovine Ubiquinol-cytochrome C Reductase

Guangwei Xing (Corresponding author)

Department of Health chemistry, Jiangsu University

301 Xuefu Road, Zhenjiang, 212013, China

Tel: 86-511-8503-8449 E-mail: xgw_123@163.com

Jinghong Xing

Clinical Laboratory, NO. 454 hospital of PLA, Nanjing, 210002, China

Tel: 86-25-8454-5559 E-mail: xjh88@163.com

Suhua Wang

Department of Health chemistry, Jiangsu University

301 Xuefu Road, Zhenjiang, 212013, China

Tel: 86-511-8503-8425 E-mail: wsh1673@yahoo.com.cn

Abstract

In this study, we characterized the small subunit of ubiquinol-cytochrome C reductase (*Bmuccr*) of the silkworm *Bombyx mori*, a model insect of Lepidopteron species. The *Bmuccr* gene covers a 1.4 kb genome region and contains 3 exons. The ORF contained 354bp and encoded 117 amino acid residues, which shares 69% overall amino acid sequence identities with the subunit VII of ubiquinol-cytochrome C reductase from bovine. Phylogenetic tree showed *Bmuccr* had high homology with *T. castaneum* homologous. The multiple sequence alignment of 16 subunit VII homologues shows that *Bmuccr* is very hydrophilic, has a characteristic charge distribution, and has a high helical content. Expression analysis indicated that *Bmuccr* was highly expressed in larva stage and was down-regulated in embryos stage and adult stage of silkworm. The tissue-specific expression indicated *Bmuccr* had high-expression level in tissues that consume oxygen. The analysis of domain structure of this protein suggested that it might be involved in correct assembly of the cytochrome bcl complex. Definition of the homologous of bovine subunit VII of ubiquinol-cytochrome C reductase should facilitate further analysis of structure/function relationships of silkworm cytochrome bcl complex.

Keywords: *Bombyx mori*, Ubiquinol-cytochrome c reductase, Multiple sequence alignment, Subunit VII, Mitochondria

1. Introduction

The cytochrome bcl complex (commonly known as ubiquinol-cytochrome c reductase or Complex III) is a segment of the mitochondrial respiratory chain that catalyzes reduction of Cyt c by the oxidation of ubiquinol (Hatefi et al., 1967, p. 235; Bechmann et al., 1992, pp.199). Coupled to this reaction is the translocation of protons across the inner membrane of mitochondria in eukaryotic organisms and across the cytoplasmic membrane in many bacteria. The bcl complex of these prokaryotes consists of 3 or 4 subunits (Trumpower, 1990, p.101), while those from eukaryotes may consist of up to 11 subunits (Schägger, et al., 1986, p.224). Two large "core" proteins, three respiratory proteins that directly participate in electron transport (Cyt b, Cyt cl, and the "Rieske" iron sulfur protein), and four to six small proteins with molecular masses of less than 20 kDa.

Since bacterial bcl complexes that contain only the respiratory subunits have the same activity as the eukaryotic enzymes (Trumpower, 1990, p.101), the role of the small subunits is not quite understood. In the 11 different

polypeptide subunits of bovine ubiquinol-cytochrome C reductase complex, 7.2kDa protein (subunit X) maintains contact with cytochrome c1 and iron sulfur protein (Schagger et al., 1983, p. 307). Both subunits VII and VIII (14 kDa and 11 kDa, respectively) of *S. cerevisiae* are thought to be in close association with cyt b (Berden et al., 1988. P.195). Disruption of these subunits showed that both are essential for correct assembly of the complex (Braun et al., 1995. p.1217; Boumans et al., 1995. p.105). So these small subunits may play an essential role in the proper assembly of the bc1 complex.

Here, we report the isolation, tissue expression, and *in vitro* expression of a novel silkworm cDNA which encodes 117 amino acids that share 69% sequence identity with subunit VII of the bovine bc1 complex.

2. Materials and methods

2.1 Silkworm strain

The silkworm *B. mori* (Strain DaZao P50) were used. All larva were fed with mulberry leaves three times a day at 25 ± 2 °C under a 12 h light/12 h dark cycle.

2.2 Isolation and DNA sequencing of a cDNA clone

We have been determinate the nucleotide sequences of cDNA clones randomly selected from a silkworm cDNA library. By comparing the DNA sequences of these cDNA clones with known DNA sequences in the database, we identified a clone that encoded a protein highly homologous to the bovine ubiquinol-cytochrome C reductase, 14kDa protein (GenBank accession: NP_001029969).

Midgut tissues were collected from the larva of 3rd day old 5th instar. Total RNA was isolated with the Trizol method. The synthesis of first-strand cDNA was catalyzed by MMLV. The specific primers: '5 ATGGCTTTTAGAGCAACTGC 3' and '5 ATATTCCTTCTCCCACTGCTC 3', were designed for the *Bmuccr* based on the predicted coding sequences and were used for the amplification of total length cDNAs. The amplicons were then cloned into the vector pMD18-T (Takara) for sequencing.

2.3 Bioinformatics

The *Bmuccr* cDNA sequence was compared with the silkworm genomic sequences using SIM4 (<http://pbil.univ-lyon1.fr/sim4.php>). Translation into amino acid sequence was done with SwissProt database ExPASy Translate tool (<http://au.expasy.org/tools/dna.html>). Homology searches were performed using Clustal w Network Service (www.ebi.ac.uk/clustalw). The secondary structure prediction was carried out using the HNN secondary structure prediction method in PBIL (<http://pbil.univ-lyon1.fr/>). We submitted the *Bmuccr* sequence to the Swiss-Model homology modeling server (<http://swissmodel.expasy.org/SWISS-MODEL.html>) to predict its three-dimensional model using the automatic modeling mode. The sequencing results were processed using Molecular Evolutionary Genetic Analysis (MEGA) version 3.1. The neighbor joining (NJ) method was used to construct phylogenetic trees.

2.4 Expression analysis of target gene

Total RNA were isolated from embryos 3 day before hatching, larva of 1st instar, 3rd instar, 5th instar, 5 day old pupae, and 1 day old adults using the Trizol reagent kit (invitrogen,USA). Total RNA samples from the following tissues were extracted and used to synthesize first-strand cDNA: midgut, haemolymph, fat body, silk gland, ganglion, epidermis, testis, ovary, tuba Malpighii. First-strand cDNA was synthesized using oligod(T)18, followed by PCR using the specific primers. *BmActin A3* was amplifying as housekeeping gene.

2.5 In Vitro Expression and Western blot

The *Bmuccr* cDNAs without any mismatch nucleotides were cloned into the expression vector PET30a (Novagen) and were transformed into the *E. coli* expression strain BL21 (DE3). The induced *E. coli* cells were collected and lysed by lysozyme on ice. The fusion proteins present in the supernatant were subjected to electrophoresis on 12% SDS-polyacrylamide gels. Then western blot was operated. Blotted proteins were incubated with corresponding 6×HIS tag antibodies at room temperature for 2 h, followed by washing with TBST (TBS, 0.05% Tween-20). After incubation for 1 h with horseradish peroxidase conjugated secondary antibody (IgG-HRP), the nitrocellulose membrane was rinsed extensively with TBST. Immunodetection was carried out using a substrate of DAB.

3. Results

3.1 Isolation and sequencing of cDNA, chromosomal localization, and genomic structure

The nucleotide and deduced amino acid sequences of the novel silkworm gene, termed *Bombyx mori* ubiquinol-cytochrome C reductase 14kDa subunit (*Bmuccr*), are shown (Figure 1). The cDNA sequence consists of 553 nucleotides with an open reading frame of 354 nucleotides encoding a 117-amino-acid peptide of approximately 14kDa (GenBank accession No. NP_001038957). An in-frame termination codon (TGA) is located 12 nucleotides upstream of the first methionine (ATG), and the polyadenylation signal, AATAAA, begins 16 bases upstream of the polyadenylation site.

A homology search, using the BLASTN programs, revealed that the nucleotide sequences of the cDNA were identical to parts of the genomics DNA sequence Dazao Contig002343 (AADK01002343), which had been assigned to silkworm chromosome 5. A comparison of cDNA and genomic DNA sequences defined the genomic structure, which appears to span a genomics region of about 1.4kb and consists of three exons.

3.2 Protein sequence alignments and homology modeling

A FASTA search for homologies between the predicted amino acid sequence and archived proteins revealed 50~70% identity with several other the equivalent proteins from other species, the closest of them being the 14kDa protein of *T. castaneum* (XP_975188) (Figure 2A). The crystal structure of subunit VII of bovine cytochrome bcl complex is available in PDB (PDB ID: 1bccF) and it was used as the template to build the model of *Bmuccr* protein (Figure 2B). The apparent structural similarity indicated two proteins also share functional similarities.

3.3 Phylogenetic analyses

The multi-sequence alignment was performed using Clustal W to identify *Bmuccr* protein sequence distances between 16 species. The phylogenetic tree showed that the *B.mori* branched with *T. castaneum* at a level of 71% identity and with 57% bootstrap support, which indicated they were homology protein and belonged to a protein family. The similarity of *Bmuccr* with *D. melanogaster*'s and *A. aegypti*'s subunit VII of cytochrome bcl complex reached 57% and 61%, respectively, but low genetic relationship to *S. pombe*. *D. melanogaster* was closely related to *A. aegypti*, *H. sapiens* showed high genetic relationship to *B. Taurus* (Figure. 3). The results indicated that *Bmuccr* of *B. mori* was close in genetic relationship to Coleoptera species.

3.4 Bmuccr expression pattern

The tissue distribution of the *Bmuccr* mRNA was assessed by RT-PCR using the primer specific. As illustrated (Figure 4A), the mRNA were detected in all silkworm tissues. There was no sex difference in expression levels of the mRNA (data not shown). But expression was significantly abundant in tuba Malpighii, intestinal, epidermis, silk gland, testis and ovary, tissues that consume oxygen at high level.

The expression profile of *Bmuccr* throughout development was further analyzed from embryos to adult by RT-PCR (Figure 4B). The results showed that expression of *Bmuccr* was much lower in embryos stage. *Bmuccr* expression increased slowly in larva stage, and peaked at the 3rd stage larvae. Subsequently, *Bmuccr* transcription decreased to lower levels in pupa stage and adult stage. These observations strongly suggest that *Bmuccr* plays a specific role during larval growth and development.

3.5 Prokaryotic Expression, SDS-PAGE, and Western blotting of the Bmuccr proteins

The Pet30a expression vector was used to transform to competent *E. coli* BL21. The results of SDS-PAGE and Western blotting analysis of the *Bmuccr* protein is shown in Fig. 5. The expressed fusion protein Bmuccr-HIS had a molecular weight of 20.6 kDa and it was soluble in the supernatant, as detected by SDS-PAGE. Western blotting confirmed that its molecular weight was about 20.6 kDa (Figure 5)

4. Discussion

In this study, we have isolated a gene from *B. mori* and identified it as the *Bmuccr* gene encoding subunit VII of the bcl complex based on sequence identity with the bovine subunit VII. It seems to be essential for correct assembly of the complex.

Because the function of the 14-kD subunit in electron transport and/or proton translocation is rather unclear, it is difficult to discuss domain-like structures of the protein. However, Molecular features of the 14-kD subunit of Cyt c reductase were very characteristic. The conserved amino acids, indicated by a black box in Fig.2, are not distributed over the entire protein, are predominantly found in the central domain and C-terminus. The N-terminus is highly variable, both in amino acid composition and in length. But The Nterminal part (corresponding to amino acids 1-36 from) has a surplus of positive charges (human and bovine 6+/1—; fruit fly 5+/0—). Most of these proteins are rather small. Import of proteins with cleavable presequences was shown to depend on the positive charge of the N-terminal extensions and on the membrane potential across the inner mitochondrial membrane with the negative side facing the matrix (Schleyer et al., 1982. p.109) This postulated N-terminal part (amino acids 1-36) of the 14-kD protein from silkworm has typical features of a mitochondrial presequence: it comprises 6 positively charged amino acids, only 1 negative residue, and 4 Ser residues. Alternatively, one of the internal amphiphilic helices may be involved in import of the 14-kD subunit into mitochondria.

The C-terminal half of this 14-kD protein contains a large number of both acidic and basic residues, and comprises five conserved Arg residues (at positions 54, 64, 67, 70, and 110 in the protein from silkworm). This 14-kD protein is predicted to have a high helical content, a feature which is confirmed by the sequence alignment. A previous study on this C-terminus in *S. cerevisiae* showed the importance of this part of the protein ((hydrophilicity and charges) for correct assembly of the bcl complex, but not for electron transport (Hemrika et al., 1994. p. 569).

Of all cell organelles, the mitochondria play a primary role in the pathogenesis of peroxidative damage, because mitochondria consume about 90% of inhaled oxygen, and reactive oxygen species such as superoxide, hydrogen peroxide, and the hydroxyl radical are formed in the mitochondria as physiologic metabolites of the respiratory chain (Richter et al., 1995. p. 67). If malfunction, generation of reactive oxygen species results in disturb homeostasis and cellular death (Marcelo et al., 2002. p.537). Silkworm is model insect of Lepidoptera species. More detailed analysis of other subunits of cytochrome bc1 complex from silkworm is needed for production of silk fibers and control of pest.

References

- Bechmann, G., Schulte, U., Weiss, H. (1992). Mitochondrial ubiquinolcytochrome c oxidoreductase. In L Ernster, ed, *Molecular Mechanisms in Bioenergetics*. Elsevier, Amsterdam, The Netherlands, pp. 199-216
- Berden, J.A., Schoppink, P.J. and Grivell, L.A. (1988). In: F. Palmieri and E. Quagliariello, Editors, *The Molecular Basis of Biomembrane Transport*. Elsevier. *Amsterdam*, pp. 195-208.
- Boumans, H., Berden, J.A., Grivell, L.A. (1995). Identification of additional homologues of subunits VII and VIII of the ubiquinol-cytochrome c oxidoreductase enables definition of consensus sequences. *FEBS Letters*, 368. 105-109
- Braun, H.P. and Schmitz, U.K. (1995). Molecular Features and Mitochondrial Import Pathway of the 14-Kilodalton Subunit of Cytochrome c Reductase from Potato. *Plant Physiol*, 107. 1217-1223
- Hatefi Y. and Rieske J.S. (1967). Preparation and properties of DPNH-coenzyme Q reductase (complex I of the respiratory chain). In: R.W. Estabrook and M.E. Pullman, Editors. *Methods in Enzymology*, 10. pp.235-239.
- Hemrika, W., De Jong, M., Berden, J.A. and Grivell, L.A. (1994). The C-terminus of the 14-kDa subunit of ubiquinol-cytochrome-c oxidoreductase of the yeast *Saccharomyces cerevisiae* is involved in the assembly of a functional enzyme. *Eur J Biochem*, 220 (2). 569-576
- Marcelo, H.L. and Tania, Z.S. (2002). Animal response to drastic changes in oxygen availability and physiological oxidative stress. *Comp. Biochem. Physiol. C*, 133. 537-556.
- Richter, C., Gogvadze, V., Laffranchi, R. (1995). Oxidants in mitochondria: from physiology to diseases. *Biochim Biophys Acta*, 1271. 67-74.
- Schägger, H., Link, Th. A., Engel, W. D. and Jagow, G. von. (1986). Isolation of the eleven protein subunits of the bc1 complex from beef heart. *Methods Enzymol*, 126. 224-237.
- Schagger, H., Von Jagow, G., Borchart, U. and Machleidt, W. (1983). Amino acid sequence of smallest protein of the cytochrome c1 subcomplex from beef heart mitochondria. *Hoppe Seylers Z Physiol Chem.*, 364. 307-311
- Schleyer, M., Schmidt, B., Neupert, W. (1982). Requirement of a membrane potential for the posttranslational transfer of proteins into mitochondria. *Eur J Biochem*, 125. 109-116
- Trumpower, BL. (1990). Cytochrome bc, complexes of microorganisms. *Microbiol. Rev* 54. 101-129



Figure 1. The complete nucleotide and deduced amino acid sequence of *Bombyx mori* ubiquinol-cytochrome C reductase, 14kDa subunit. The start, stop codons and polyadenylation signal of *Bmuccr* are indicated by bold boxes. The primers used for the amplification of total length cDNAs and RT-PCR are underlined

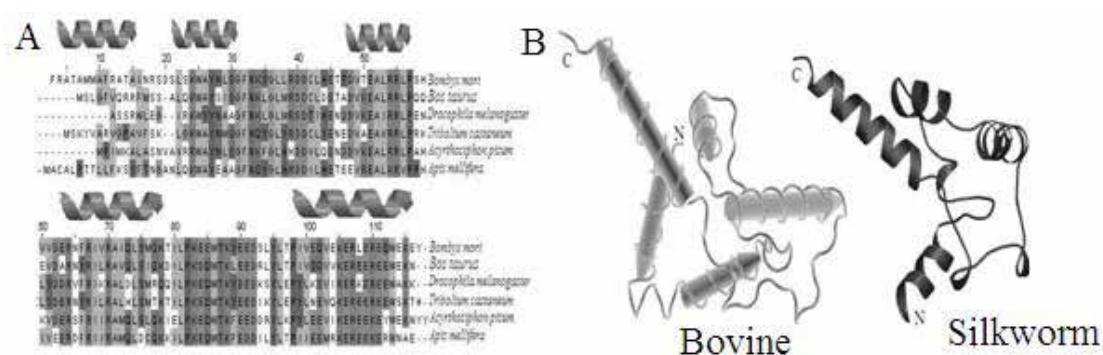


Figure 2. (A) Alignment of sequences of several ubiquinol-cytochrome C reductase 14kDa subunits. Residues that are identical in all six proteins are shaded. Five corresponding helices are indicated. (B) 3D model of ubiquinol-cytochrome C reductase 14kDa subunit VII. Bovine subunit VII protein and silkworm *Bmuccr* protein share the same fold. N and C denote the N-terminus and C-terminus, respectively.

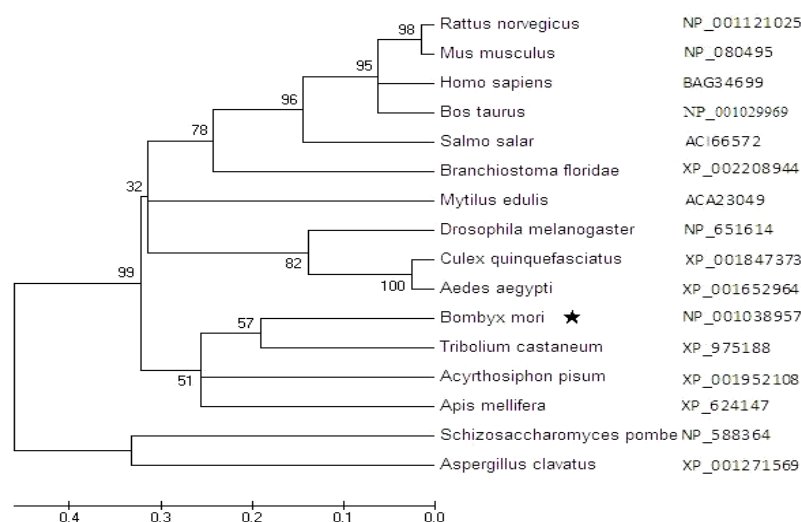


Figure 3. Phylogenetic tree showing the relationship of *Bmuccr* to other species homologous protein. The phylogenetic tree was generated based on the entire amino acid sequences and the tree-drawing software mega 4.0.

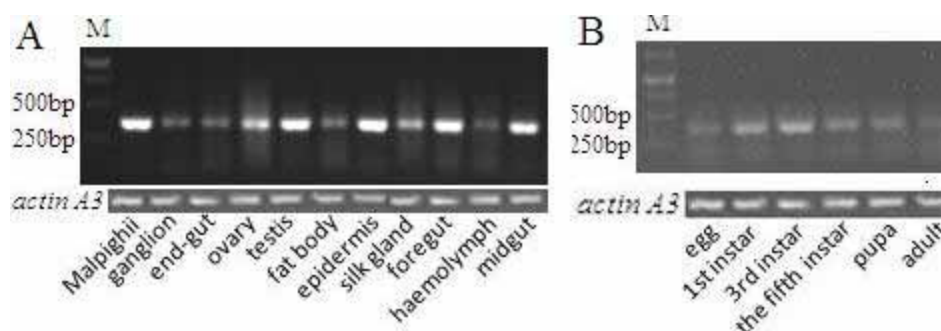


Figure 4. (A) Distribution of *Bmuccr* in different tissues of the strain Dazao. (B) RT-PCR analysis for expression of mRNAs for *Bmuccr* and *actin A3* in different development stage, whose cDNA sizes amplified are 354 and 289 base pairs.

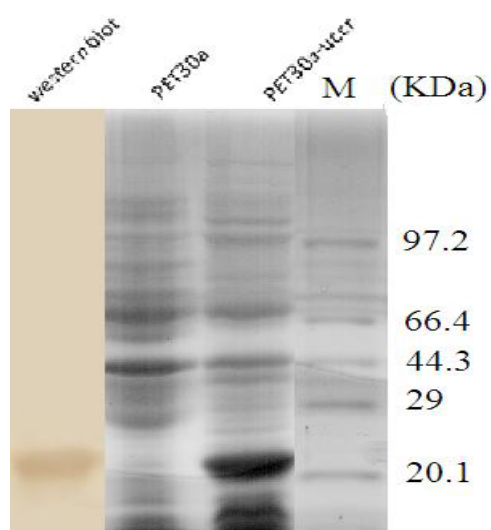


Figure 5. Expression and western blotting analysis of the pET 30a-*Bmucrr* protein.



Expression of Cocoonase in Silkworm (*Bombyx mori*) Cells by Using a Recombinant Baculovirus and Its Bioactivity Assay

Jianjun Yang

Institute of Life Sciences, Jiangsu University

301 Xuefu Road, Zhenjiang 212013, China

Tel: 86-511-8292-7891 E-mail: lirongrong_1986@163.com

Wenbing Wang (Corresponding author)

Institute of Life Sciences, Jiangsu University

301 Xuefu Road, Zhenjiang 212013, China

Tel: 86-511-8292-7891 E-mail: wenbingwang@ujs.edu.cn

Bing Li & Yudan Wu

Institute of Life Sciences, Suzhou University

199 Renai Road, Suzhou 215300, China

Huiling Wu

Institute of Life Sciences, Jiangsu University

301 Xuefu Road, Zhenjiang 212013, China

Weide Shen

Institute of Life Sciences, Suzhou University

199 Renai Road, Suzhou 215300, China

The research is financed by the Six-Field Top programs of Jiangsu Province, National Natural Science Foundation of Jiangsu Education Community (06KJD180043) and the 973 National Basic Research Program of China (2005CB121005).

Abstract

In this research, the cocoonase gene was cloned by RT-PCR as an 860 bp fragment, including the signal peptide and the core sequence of cocoonase gene. In order to investigate the function of signal peptide, recombinant transfer vector pBacPAK8-Cocoonase-EGFP were constructed by fusing with enhanced green fluorescent protein (EGFP) gene to observe under fluorescence microscope. The purified pBacPAK8-Cocoonase-EGFP DNA was co-transfected with linear virus Bm-BacPAK6 DNA into BmN cells. The homologous recombination occurred in the cells and then the recombinant virus Bm-BacPAK8-Cocoonase-EGFP was obtained. BmN cell was infected with the recombinant virus Bm-BacPAK8-Cocoonase-EGFP, and fluorescent signal was detected in most of the cells under fluorescence microscope at 72 hrs postinfection. Then BmN cells were harvested. Both SDS-PAGE and Western-blotting analysis indicated that the cocoonase was expressed successfully in silkworm (*Bombyx mori*) baculovirus expression vector system. Furthermore, referred to Astrup methods, used fibrin plate process confirmed that expression product in vitro had cellulolytic activity. We conclude that silkworm expression system can be used successfully to express functional cocoonase.

Keywords: Cocoonase, *Bombyx mori*, Recombinant baculoviruses, Expression product

1. Introduction

Cocoonase is a protease produced by silk moths during adult development and used for hydrolyzing and softening the end of the cocoon to permit exit of the adult moth. Studies on the cocoonase have significance not only in the understanding of the physiological process of the silkworm's escape from cocoon, but also in the exploitation of silk protein. The full-length sequence of the cocoonase gene has released in the National Center for Biotechnology Information (GenBank accession No. EF428980) and the full-length cDNA of the cocoonase gene from *Bombyx mori* is 1047 bp with an ORF of 780 bp, 54 bp nucleotide sequence in 5'UTR (untranslated region), 210 bp nucleotide sequence in 3'UTR and termination codon TAA. The protein which was encoded by the cocoonase gene contains 260 amino acids. The protein molecular weight is about 27.6 kDa and its isoelectric point is 8.89. An alignment of the cDNA sequence with the silkworm genome sequences revealed that there were 4 introns and 5 exons within the open reading frame in the cocoonase gene from *B. mori*.

The baculovirus expression vector system (BEVS) is an effective recombinant protein production system which utilizes the recombinant virus carrying the gene of interest to infect cultured cells or host larvae (Wu *et al.*, 2004, 155 462–466). In this paper, recombinant pBacPAK8-Cocoonase-EGFP was expressed very well using *B. mori* nuclear polyhedrosis baculovirus expression vector system. Infected BmN cell with recombinant virus, and fluorescent signal was detected in most of the cells by fluorescent microscope showing the successful expression of cocoonase-EGFP fusion protein in BmN cells. Then BmN cells were harvested at 72 hrs postinfection. Protein from the cells was analysed by SDS-PAGE and Western-blotting, indicated that the cocoonase was expressed successfully in silkworm (*B. mori*) baculovirus expression vector system. More importantly, we have confirmed that expression product in vitro had cellulolytic activity.

2. Materials and methods

2.1 Materials

The silkworm *B. mori*, *E. coli* (strain TG1) and *B. mori* nuclear polyhedrosis virus were inbred in our lab. Transfer vector (pBacPAK8-EGFP vector) was supplied by our lab. Restriction enzyme, T4 DNA ligase, PCR reagents and pMD18-T were obtained from TaKaRa Company (Dalian); primer and other reagents were obtained from Shanghai Sangon Bio-technology Corporation.

2.2.1 RT-PCR

A pair of specific primers was designed based on the sequence we obtained. The forward primer (5'-GCAGGATCCATGGAAAAGTTGTATCTGTTTAT-3') contained a *Bam*H I restriction enzyme site (underlined), and the reverse primer (5'-TATGGTACCTAGGCCCGCCGTTGATTTTAT-3') contained a *Kpn* I restriction enzyme site (underlined). cDNA was prepared from midgut RNA with M-MLV reverse transcriptase and an oligodT primer. PCR reaction was carried out with Taq polymerase for 35 amplification cycles (94°C for 45 sec; 58°C for 45 sec; 72°C for 1min). PCR product was examined by electrophoresis in 1% agarose gel with the ethidium bromide staining.

2.2.2 Cloning and sequencing

The PCR product was ligated into pMD18-T vector using T4 DNA ligase and then transformed into *E. coli* (TG1 strain). Plasmid was purified with MiniBEST Plasmid Purification Kit (Takara). The sequencing was performed using an automatic sequence: CEQ8000 (Beckman company).

2.2.3 Construction of transfer vector

The plasmid pMD18-T/Cocoonase was digested with *Bam*H I and *Kpn* I, and then purified. The purified fragment was ligated with the *Bam*H I-*Kpn* I digested pBacPAK8-EGFP vector and transformed into *E. coli* (TG1 strain). The transformants harboring the recombinant plasmid were confirmed by restriction enzyme analysis (Fig. 1).

2.2.4 Generation of recombinant baculoviruses

The lipofection technique was used to cotransfect into monolayers of BmN cells with the recombinant transfer vectors, all generated as described above, and *Bsu*36I triple-cut *B. mori* nuclear polyhedrosis virus DNA (Felgner *et al.*, 1987, 84 7413-7417). Recombinant baculoviruses were selected on the basis of their LacZ-negative phenotypes, plaque purified, and propagated as described elsewhere (Kitts *et al.*, 1993, 14 810-817).

2.2.5 Detection of the expression of Cocoonase-EGFP fusion protein

BmN cells transfected with recombinant baculoviruses were examined under fluorescent microscope for expression of Cocoonase-EGFP 72 hrs post transfection.

2.2.6 Protein analysis

Confluent monolayers of BmN cells in 35-mm tissue culture dishes were infected with recombinant baculovirus at a multiplicity of infection (MOI) of 5. At 48 hrs post infection, cells were harvested and lysed in 150 µl of lysis buffer (50

mM Tris-HCl, pH 8, 200 mM NaCl, 1% Triton X-100). Twenty microliters of the protein samples were boiled for 6 min in 5× sample buffer [2.3% sodium dodecyl sulfate (SDS), 2.5% (vol/vol) glycerol, 5% (vol/vol) β-mercaptoethanol, 62.5 mM Tris-HCl, pH 6.8, 0.01% bromophenol blue], and proteins were separated by 10% SDS-polyacrylamide gel electrophoresis (PAGE) and stained with Coomassie blue.

2.2.7 Western blot analysis

Western blot analysis of proteins was performed following the standard protocol as described previously (Kar *et al.*, 2004, 324 387-399).

2.2.8 Assay for cellulolytic activity of expression product in vitro

Referred to *Astrup* methods (Park *et al.*, 1999, 32 239-246; Lee *et al.*, 2001, 11 845-852), used fibrin plate process to measure cellulolytic activity of expression product. Collected BmN cells were added lysis buffer solution and sonicated by ultrasonic wave while ice bathed. After centrifugated, took 20 μl and 40 μl supernatant into the hole of nutrient medium and incubated at 37°C for 48 hrs.

3. Results

3.1 Cloning and identification of cocoonase

PCR amplification of the midgut cDNA was performed using the two specific primers. After electrophoresis in 1% agarose gel, we obtained a band about 860 bp, which was consistent with the expected molecular mass. The PCR product was ligated into pMD18-T vector and confirmed by restriction endonuclease digestion and DNA sequencing. The cocoonase fragment could be isolated from the pMD18-T vector after the recombinant plasmid was digested with *Bam*H I and *Kpn* I (Fig. 2).

3.2 Construction of recombinant transfer vector

The plasmid pMD18-T/Cocoonase was digested with *Bam*H I and *Kpn* I and ligated with pBacPAK8-EGFP which was also digested with the same restriction enzymes to generate pBacPAK8-Cocoonase-EGFP. The cocoonase fragment could be isolated from the pBacPAK8-Cocoonase-EGFP vector after the recombinant plasmid was digested with *Bam*H I and *Kpn* I (Fig. 3, lane 1). The EGFP fragment could be isolated from the pBacPAK8-Cocoonase-EGFP vector after the recombinant plasmid was digested with *Kpn* I and *Eco*R I (Fig. 3, lane 2). The recombinant plasmid pBacPAK8-Cocoonase-EGFP was successfully constructed (Fig. 3).

3.3 Expression of Cocoonase-EGFP fusion protein

BmN cells transfected with recombinant baculoviruses showed cytopathic effect at 72 hrs post transfection. To detect the expression of Cocoonase-EGFP fusion protein, these cells were examined by fluorescent microscope. Fluorescent signal was detected in most of the cells (Fig. 4), showing the successful expression of Cocoonase-EGFP fusion protein in BmN cells.

3.4 SDS-PAGE and Western blotting analysis

BmN cells were infected with recombinant baculoviruses BacPAK8-Cocoonase-EGFP and virus BacPAK6 as a control, and cells were harvested at 72 hrs post infection. Protein from the cells was analysed by SDS-PAGE. Recombinant baculoviruses BacPAK8-Cocoonase-EGFP includes a 57 kDa band that is absent from virus BacPAK6 (compared lanes 1 and 2). This corresponds to the size expected for the Cocoonase-GFP fusion protein. Immunoblot analysis with antiserum specific for GFP confirmed that this band includes EGFP and cocoonase (Fig. 5).

3.5 Assay for cellulolytic activity of expression product in vitro

Used fibrin plate process to measure cellulolytic activity of expression product, the protein of BmN cells which infected with pBacPAK8-Cocoonase-EGFP had apparently dissolved plaque, however, the protein of BmN cells which infected with BacPAK6 had not yet dissolved phenomenon (Fig. 6). It confirmed that expression product in vitro had cellulolytic activity.

4. Discussion

The baculovirus expression system has been proven to be a most effective and versatile eukaryotic expression tool (Maeda, 1989, 34 351-371) and it has been used to express many recombinant proteins using insects as bioreactors (Sehgal *et al.*, 2003, 27 27-34). Recombinant proteins are functional properties similar to those of their native counterparts. Baculovirus-infected insect cells perform many of the posttranslational modifications higher eukaryotes do, and this advantage makes this expression system become a valuable tool for production of biologically active proteins.

Cocoonase is an important protease produced by silk moths during adult development and used for hydrolyzing and softening the end of the cocoon to permit exit of the adult moth. In this study, we successfully cloned cocoonase gene and constructed recombinant transfer vector pBacPAK8-Cocoonase-EGFP. After infected BmN cell with the

recombinant virus, we observed BmN cells by a fluorescence microscope and detected fluorescent signal in most of the cells. Both SDS-PAGE and Western-blotting indicated that the Cocoonase was expressed successfully in silkworm (*Bombyx mori*) baculovirus expression vector system. Furthermore, we successfully confirmed that expression product in vitro had cellulolytic activity. To further study of the cocoonase both in the understanding of the physiological process of the silkworm's escape from cocoon and in the exploitation of silk protein to lay the foundation.

References

- Felgner, P. L., T. R. Gadek, M. Holm, R. Roman, H. W. Chan, H. Wenz, J. P. Northrop, G. M. Ringold and M. Danielson. (1987). Lipofectin: a highly efficient, lipid-mediated DNA-transfection procedure. *Proc. Natl. Acad. Sci USA* 84, 7413–7417.
- Kar, A. K., M. Ghosh and P. Roy. (2004). Mapping the assembly of Bluetongue virus scaffolding protein VP3. *Virology* 324, 387–399.
- Kitts, P.A. and R. D. Possee. (1993). A method for producing recombinant baculovirus expression vectors at high frequency. *BioTechniques* 14, 810–817.
- Lee, S. K., D. H. Bae, T. J. Kwon, S. B. Lee, H. H. Lee, J. H. Park, S. Heo and M. G. Johnson. (2001). Purification and characterization of a fibrinolytic enzyme from *Bacillus* sp. KDO-13 isolated from soybean paste. *Microbiol Biotechnol*, 11, 845 - 852.
- Maeda, S. (1989). Expression of foreign genes in insects using baculovirus vectors. *Annu. Rev. Entomol.* 34, 351–371.
- Park, Y. S., M. H. Cha, W. M. Yong, H. J. Kim, I. Y. Chung and Y. S. Lee. (1999). The purification and characterization of *Bacillus subtilis* tripeptidase (PepT). *J. Biochem. Mol. Biol.* 32, 239 - 246.
- Sehgal, D., P. S. Malik and S. Jameel. (2003) Purification and diagnostic utility of a recombinant hepatitis E virus capsid protein expressed in insect larvae. *Protein Expr. Purif.* 27, 27–34.
- Wu, X. F., C. P. Cao, V. Shyam Kumar and W. Z. Cui. (2004). An innovative technique for inoculating recombinant baculovirus into the silkworm *Bombyx mori* using lipofectin. *Res. Microbiol.* 155, 462–466.

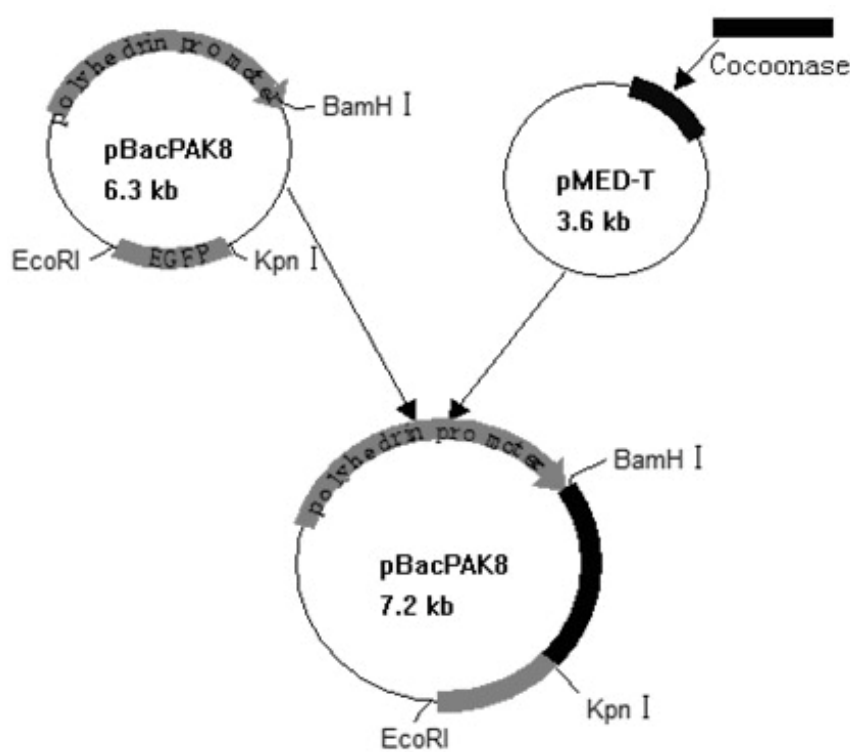


Figure 1. The construction of pBacPAK8-Cocoonase-EGFP.

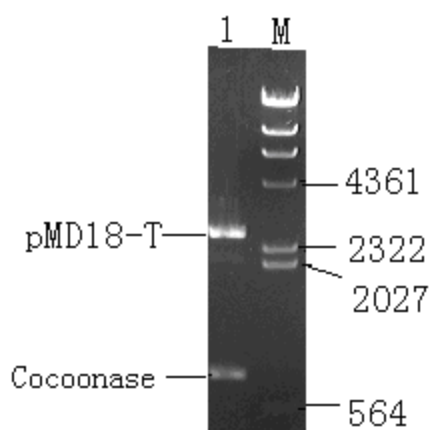


Figure 2. Identification of the recombinant plasmid pMD18-T/Cocoonase. Lane 1, pMD18-T/Cocoonase digested with *Bam*H I and *Kpn* I generated two fragments: pMD18-T (2.6 Kbp) and cocoonase (860 bp); M, DNA molecular mass maker.

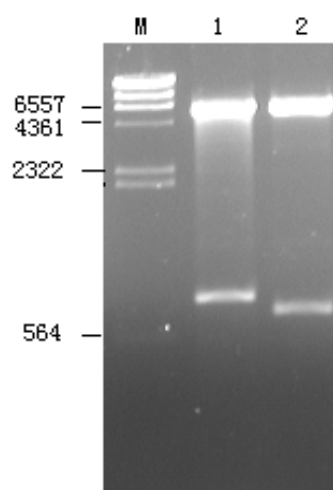


Figure 3. Identification of the transfer vector pBacPAK8-Cocoonase-EGFP. Lane 1, pBacPAK8-Cocoonase-EGFP digested with *Bam*H I and *Kpn* I generated two fragments: pBacPAK8-EGFP (6.3 Kbp) and cocoonase (860 bp); Lane 2, pBacPAK8-Cocoonase-EGFP digested with *Kpn* I and *Eco*R I generated two fragments: pBacPAK8-Cocoonase (6.36 Kbp) and EGFP (800 bp); M, DNA molecular mass maker.

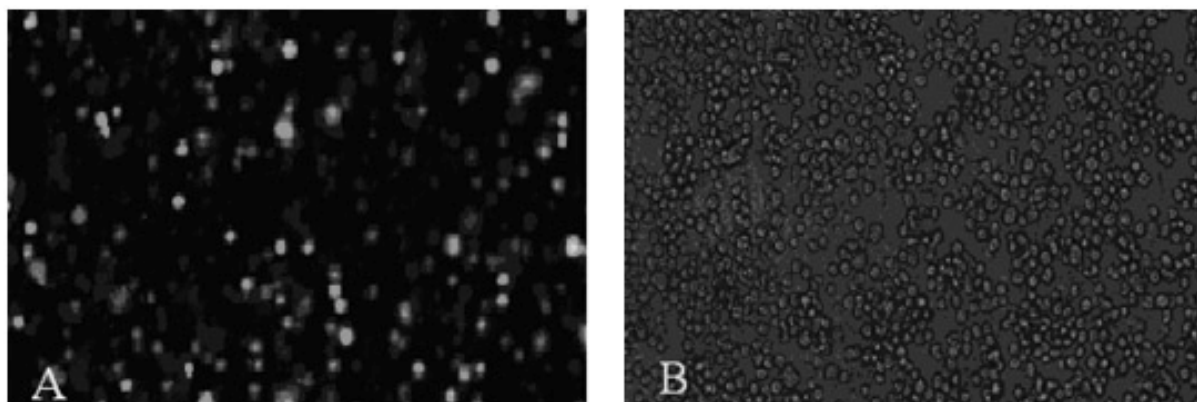


Figure 4. Detection of the expression of cocoonase-EGFP fusion protein. BmN cells were infected with recombinant baculovirus expressing the Cocoonase-EGFP fusion protein and EGFP fluorescence was detected with fluorescence (A) and light (B) microscope.

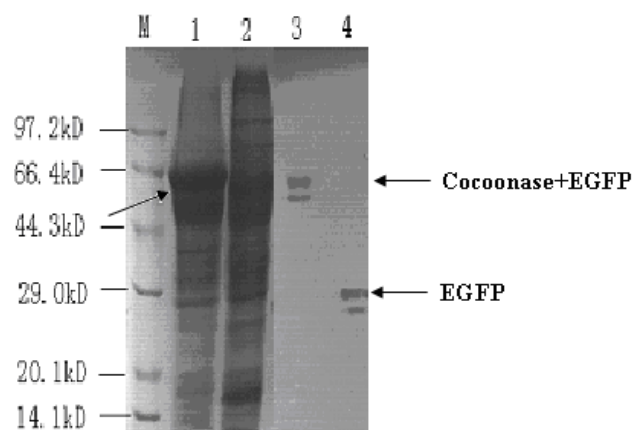


Figure 5. SDS-PAGE and Western blotting analysis. M, Protein marker; Lane 1, BmN cells infected with recombinant baculoviruses Bm-BacPAK8-Cocoonase-EGFP; Lane 2, BmN cells infected with Bm-BacPAK8-EGFP; Lane 3, Western blot results of Cocoonase-EGFP fusion protein; Lane 4, Western blot results of EGFP protein. The fusion protein bands were indicated by arrows.

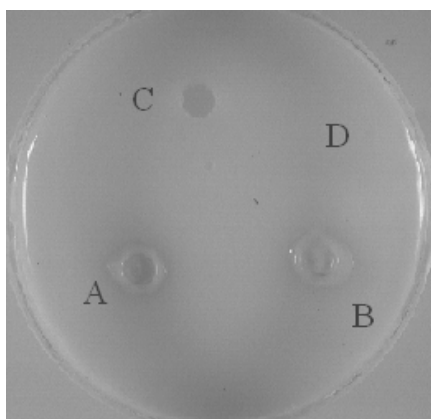


Figure 6. Assay for cellulolytic activity of expression product in vitro. (A) 20 μ l of expression product of BmN cells infected with Bm-BacPAK8-Cocoonase-EGFP. (B) 40 μ l of expression product of BmN cells infected with Bm-BacPAK8-Cocoonase-EGFP. (C) 40 μ l of expression product of BmN cells infected with Bm-BacPAK6. (D) Non-treatment.



IGF-1 Gene Polymorphism and Weight-Related Analysis

Wei Li

College of Animal Science and Technology of Shihezi University

Shihezi, 832003, China

E-mail: lwi-xyz@126.com

Fangqun Li

College of pharmacy of Shihezi University

Shihezi, 832003, China

E-mail: lfq003@126.com

Daquan Li

College of Animal Science and Technology of Shihezi University

Shihezi, 832003, China

E-mail: lidaquan37@163.com

Abstract

The PCR-RFLP technology, Rose crown chicken broiler red cards, the new Roman layer, hybrid chicken (reciprocal cross) of the 50 insulin-like growth factor-I (IGF-I) gene regulation and control of the 5-end Genetic Polymorphisms of areas, the control region of the PCR products digested by PstI after "-/-" "+/-" "+/+" 3 genotypes, experimental through hybridization chicken (orthogonal and Anti-settlement), Rose chicken crown, the new pro-Roman red cards in this and the pro-IGF-1 to the PstI-RFLP. Genotype frequency, there "+/+>+/->-/-" trend, but in 12 weeks, body weight, the whole "-/->+/->+/+" trend. Which rose crown hybrid chicken and chicken "-/-" ">+/-", orthogonal portfolio significantly different ($P < 0.05$).

Keywords: Chicken, Insulin-Like Growth Factor-I, Weight, PCR-RFLP

1. Introduction

Rose giant crown Chickens in China's age-old chicken breeds, the red mulberry-like crown shaped like Xinjiang's Tianshan snow lotus, the colorful, rough-resistant and have fed, cold-resistant and heat resistant and strong, and other biological characteristics of the fine. The existing 2,000 rose only crown chicken meat with delicious, aroma, delicate and delicious, such as quality, this is our country and the world's poultry valuable germplasm resources and breeding material (Liao he rong, 2004, p. 176).

In this experiment, in order to crown the Rose chicken, red cards broilers, layers of the new Roman, red cards and the new hybrid of the Roman chicken (after referred to as the hybrid chicken) for the study to IGF-1 gene as a candidate gene using PCR-RFLP method, The detection of chicken IGF-1 gene polymorphism PstI, aimed at IGF-1 gene PstI restriction site polymorphism in the chicken and weight-related analysis, for further study IGF-1 gene polymorphism and growth The speed of molecular genetic markers to establish a foundation.

2. Materials and Methods

2.1 Experimental Materials

2.1.1 Experimental populations

Rose chicken Canopy test chickens, chickens red cards, the new Roman laying hens, chickens hybrid (cross-positive and negative) of 50, keeping a unified stand in the trial, immunization procedures and keeping management in

accordance with the general management, as far as possible to ensure that subjects chicken Keeping the same management conditions. 0-3 wk age, 4-8 wk age and 8-12 wk age feeding stage.

2.1.2 Primer

Primers used in reference to the Nagaraia (2000, p.150) provided by the sequence, the following sequence:

Forward 5'-GACTATACAGAAAGAACCCAC-3', Reverse 5'-TATCACTCAAGTGGCTCAAGT-3'. Primed by the Shanghai Biological Engineering Co., Ltd. synthesis.

2.2 DNA polymorphism analysis

2.2.1 Genomic DNA extraction

Wing vein blood 0.3mL Add 1 × STE 470μl, 10% SDS 25μl, adding to the concentration of 0.1mg/ml of Proteinase k 5.25μl, 55 °C water bath for the night, to fully digest protein and RNA; such as adding the volume of saturated phenol (about 550μl), Gently shaken 10min, centrifugal (12000rpm) 15min, to draw the DNA-containing supernatant; adding 500μl phenol, chloroform, isoamyl alcohol (25:24:1) mixture, Gently shaken 10min, centrifugal (12000rpm) 15min, Learned of the DNA-containing supernatant, with chloroform, isoamyl alcohol (24:1) and then extract 1, adding 1 /10 the size of NH₄AC (about 60μl), blending, add twice the size of the pre-cooling Ethanol, gently mixing, flocculation sediment can be seen, 4 °C precipitation 1 hour, centrifugal (10000rpm) 10min, to abandon after the supernatant. Precipitation will be placed 20-30min, to make ethanol volatile clean, and then adding 100μl TE₄ °C refrigerator to preserve back-up.

2.2.2 Genomic DNA concentration and quality of Determination

Take DNA solution 10μl, adding two-Stream 2.999ml of the water, fully dissolved by ultraviolet spectrophotometer determination of 260nm and 280nm wavelength ultraviolet light absorption value of the Department, the nucleic acid absorption in the UV wavelength 260nm, The protein in the UV absorption peak 280nm, if a more complete removal of protein, samples The OD_{260nm}/OD_{280nm} should be between 1.6-1.8. DNA concentration formula: DNA solution concentration

= OD_{260nm} × multiple of diluted × 50 (ng / μl). According to the determination of the post-genomic DNA sample concentration, the genomic DNA into a diluted 200ng/μl, 4 °C refrigerator to preserve back-up.

2.2.3 PCR amplification and PCR-RFLP

In order to get the best PCR amplification effect on the PCR reaction conditions are optimized, according to the main PCR Factors that affect the order of importance, in order to optimize the annealing temperature, concentration of magnesium and primer concentration(Hertzel AV,2002,p.2106

), and optimize the results are as follows: 25ul reaction system, 10xBuffer 2.5μl, MgCl₂ (25mmol / L) 1μl, dNTPs (2.5mmol / L) 1.5μl, before and after the primer (5pmol / L) of all 1μl, TaqDNA polymerase (2.5U/μl) 0.5μl, template DNA1μl, deionized water 16.5μl. PCR conditions were 94°C for 5min, 34 cycles at 94°C for 60s, 56°C for 120s, 72°C for 90s, and an extension at 72 °C for 8min, 4°C preservation. PCR amplification products by 1% agarose gel electrophoresis, PCR products by adding 7μl, at the same time adding a total of DNAMarker Beach, for an estimated molecular weight, ethidium bromide staining after the detection results of the expansion. Miscellaneous not with the kind of in order to carry out the next steps.

PCR product of taking 12μl, PstI enzyme (10U/μl) 1.5μl, 10xBuffer1.5μl, plus double-distilled water to 20μl, 37°C overnight digestion, the product of the enzyme by 2% agarose gel electrophoresis, EB stained gel Photo imaging analysis system for detecting genotyping.

2.3 Statistical analysis

All data are used spss11.0 statistical analysis software, the distribution of genotypes with x² test.

3. Results

3.1 PCR-RFLP analysis

According to the chicken IGF-I gene sequence leading projection, the target for the amplified fragment length 621bp. This study was amplified by the fragment length by 0.8% agarose gel electrophoresis detection in line with, and not with miscellaneous can be further enzyme digestion (Figure 1).

3.2 Gene frequency and genotypic frequency

Product of the enzyme by 2% agarose gel electrophoresis, EB staining, see the pictures (Figure 2). Map can be seen from a point mutation PstI digestion, that is, a pair of alleles, can not be digested are marked PstI "-" (621 bp), who tags can be digested marked PstI "+" (364bp +257 bp); Combination of the three bands, that is, the three genotypes ("++" "-/-" "+/-"). S. C. Nagaraia (2000,p.154) this report the results.

pair of Rose chicken Canopy (to the table in place of MM), red cards broiler (to the table in place of AA), the new Roman layer (the table in order to replace the XX), the chicken cross the orthogonal (to the table in place of AX), Anti-pay (in the table in order to replace the XA) PstI digested by the combination of genotypes and their frequency and the weight difference in table 2.1.

Based on the above test, in Table 3.1 are listed in a different IGF-1 chicken Genotype and the relationship between body weight, can be seen from the table, the effect of different varieties of genotypic to show inconsistencies in the law: IGF-1 by enzyme PstI The emergence of the three genotypes in the hybrid chicken, Rose chicken Canopy, the new Roman parents and red cards parents on the birth weight is no significant difference. In the anti-settlement, "-/-">"+/+>"-/-"; portfolio in the combination of orthogonal and red cards in this pro-, "-/-">"-/-">"+/+"; In the Rose and Crown and the new chicken in this pro-Roman, "-/-">"-/-">"+/+"; In the 6-week-old body weight, the chicken cross the new Roman parents, parental red cards and Rose chicken Canopy are the trends "-/-">"-/-">"+/+". But also in the chicken cross the orthogonal combination of Rose and Crown in chicken, "-/-" significantly higher than "+/+" (P < 0.05). In the 9-week-old body, this new pro-Roman and red cards parents still "-/-">"-/-">"+/+" a continuation of the trend; 12 weeks after the chicken cross the combination of orthogonal, "-/-">"-/-">"+/+", And "-/-" "+/-" and + / + significant difference (P < 0.05); the chicken cross the anti-cross combination, "+ / -">"-/-">"+/+", Three no significant difference (P > 0.05); in the Rose chicken Canopy in, "-/-">"-/-">"+/+", "-/-" And + / + significant difference (P < 0.05).

In Table 2.2, an analysis of the chicken cross (orthogonal and anti-cross), Rose chicken Canopy, the new Roman parents and parents of red cards, rooster and hen of the IGF-1 enzyme PstI by the three genotypes And the frequency of gender differences in body weight between. One rooster and hen, after digestion of the three genotypes in "-/-" have shown that the growth speed advantage.

4. Discussion

From the above we can see the results: The genotype frequencies, "+/+>"-/-">"-/-" trend, but in the 12-week weight, there is a whole "-/-">"-/-">"+/+". Rose and Crown in which the chicken cross the chicken orthogonal portfolio "-/-" >"+/+", significant difference (P < 0.05). On the IGF-1 gene PstI restriction sites of the relationship between genotype and weight analysis has been done, WANG Zhi-yue (2004,p.11) reported: New Yangzhou chicken "-/-" type than + / + 7.8% high. Gender differences between the cumulative growth significant genotype effect sex investigation and the findings of a similar merger. Ouyang Jianhua (2003,p.528) reported: in Nanjing are Sanhuang, "-/-" genotype in the 3-month-old chicken weight trends higher than that of other genotypes, which are similar to the experimental results, but he also reported in million Leisure contained in the yellow loci showed heterozygosity advantage. Seo (2001,p.920) has studied the report: local chickens in South Korea KNOC cock, "+/+" genotypes in body weight in 30-week-old chickens were significantly higher than "-/-" type, in the 20-60 week period, greater than the trend of other genotypes.

The results are inconsistent, on the one hand may be due to sampling method and determination of the object due to a difference, such as chicken KNOC is measured body weight after 20 weeks of age, while the yellow Leisure Wanzai only hens were studied; on the other hand, probably because the number of trait loci sit (QTL) expression to a large extent by environmental conditions and genetic background influence on the possibility of using a gene markers as well as any how to make use of feeding and management should be as specific conditions and characteristics of the species.

By this test hybrid chicken (orthogonal and anti-cross), Rose chicken Canopy, the new Roman parents and red cards in this pro-IGF-1 for the PstI-RFLP. Experimental chickens, including laying hens, chickens, local chickens are hybrid chickens, a more comprehensive comparison of the IGF-1 enzyme PstI by the genotype associated with body weight. The results show that the genotype "-/-" as a positive correlation with the weight of good sites for future breeding chickens to provide a reference.

References

- Hertzel AV, et al. (2002). Increased lipolysis in transgenic animals overexpressing the epithelial fatty acid binding protein in adipose cells. *J. Lipid Res.* 43(12): 2105-2111
- Liao, herong, Zhao, zong sheng, Li, Yan, Sun, Jie. (2004). Rick tournament. Rose crown chicken and chicken meat quality of different types of comparative study. *China's poultry*, 8 (1):176-178.
- S. C. Nagaraia, S. E. Aggreyetc. (2000). Trait Association of a Genetic Marker in Egg-Laying Chickens. *Heredity*:91(2)150-156.
- Seo D S, Yun J S, Kang W J. (2001). Association of insulin-like growth factor-1 gene polymorphism with serum IGF-1 concentration and body weight in Korean Native Ogo chicken Asian-Aust. *J Anita Sci*, 14 (7): 915-921.
- Wang, Zhiyue, Fan, Ganglong, Yang, Haiming, Wang, Zhanggui, Sheng, Dongfeng, Liu, Guiqiong. (2004). New Yangzhou chicken IGF-1 gene polymorphism and early study on the relationship between growth rate. *China's poultry*, 26 (24):9-12

Yang, Jianhua, Sun, Han, Lin, Shumao et al. (2003). Chicken insulin-like growth factor -1 genetic polymorphism and its relationship between body weight *Journal of Animal Husbandry and Veterinary Medicine*. 34 (6):525-529

Table 1. Different chicken IGF-1 by digestion Pst1 three genotype frequency and weight differences

	genotype	frequency	birthweight	Six week body weight	twelve week body weight
XA	"-/-"	20.97%	38.77+0.378	661.38+38.898	1714.69+61.432
	"+/-"	32.26%	38.05+0.473	642.75+18.427	1720.50+56.166
	"+/+"	46.77%	38.66+0.489	629.10+14.700	1663.62+43.279
AX	"-/-"	30.00%	47.11+0.851	807.89+20.385 ^a	2382.94+66.718 ^a
	"+/-"	30.00%	47.72+0.976	804.33+24.390 ^a	2221.50+74.914 ^a
	"+/+"	40.00%	46.88+0.581	723.88+14.777 ^b	1931.08+41.558 ^b
MM	"-/-"	22.00%	36.73+1.251	464.09+12.344 ^a	882.82+44.742 ^a
	"+/-"	36.00%	36.50+0.768	422.56+18.978	819.50+35.429
	"+/+"	42.00%	35.71+0.662	407.86+11.102 ^b	767.38+27.154 ^b
XX	"-/-"	22.45%	34.55+1.139	504.55+14.542	916.45+34.483
	"+/-"	38.78%	33.79+0.538	475.00+9.258	841.84+24.718
	"+/+"	38.78%	33.63+0.685	473.11+11.324	830.58+28.503
	genotype	frequency	birthweight	Six week body weight	nine week body weight
AA	"-/-"	20.97%	37.38+0.756	1519.69+48.871	2257.08+79.811
	"+/-"	32.26%	38.05+0.634	1508.10+53.832	2210.75+86.695
	"+/+"	46.77%	37.07+0.438	1506.21+34.177	2175.07+49.872

means significant difference at $P < 0.05$ in the same column with different superscripts

Table 2. Different chicken IGF-1 by digestion Pst1 three different genotype frequency and gender differences in body

	Sex	genotype	frequency	Birth weight	Six week body weight	twelve week body weight
MM	♂	“-/-”	23.08%	37.00±0.964	513.63±18.049	944.00±66.775
		“+/-”	40.38%	37.25±1.830	478.30±16.926	872.73±47.787
		“+/+”	36.54%	35.70±1.309	441.69±14.505	799.33±45.926
	♀	“-/-”	20.83%	35.83±0.491	426.73±24.855	809.40±43.025
		“+/-”	31.25%	36.20±0.712	419.40±15.452	735.86±35.442
		“+/+”	47.92%	36.00±0.831	392.72±10.891	747.50±28.550
AX	♂	“-/-”	42.86%	48.00±1.066	803.92±23.323 ^b	2473.33±58.355 ^a
		“+/-”	32.14%	49.44±1.334	873.89±26.848 ^a	2451.22±81.915 ^a
		“+/+”	25%	44.71±0.918	734.86±23.962 ^b	2068.71±79.540 ^b
	♀	“-/-”	18.75%	45.33±1.202	815.83±42.733 ^a	2202.17±83.579 ^a
		“+/-”	28.14%	46.00±1.236	734.78±24.451	1991.78±62.835
		“+/+”	53.13%	44.94±0.745	719.35±18.712 ^b	1874.41±42.893 ^b
XA	♂	“-/-”	18.92%	38.86±0.634	744.29±42.556	1768.71±98.500
		“+/-”	40.54%	38.07± 0.581	660.47±20.043	1720.87±66.979
		“+/+”	43.24%	38.94±0.766	668.81±15.559	1652.00±64.549
	♀	“-/-”	21.74%	38.60±0.510	579.40±49.613	1692.40±39.747
		“+/-”	21.74%	38.00±0.837	589.60±35.942	1719.40±113.282
		“+/+”	56.52%	38.31±0.570	580.23±19.788	1677.92±57.519
XX	♂	“-/-”	31.03%	34.33±1.394	519.78±12.033	1175.56±35.294
		“+/-”	41.38%	33.75±0.676	501.50±6.232	1086.50±21.214
		“+/+”	27.59%	33.75±1.013	516.00±16.592	1150.00±53.775
	♀	“-/-”	10%	35.50±0.500	436.00±26.000	915.00±55.00
		“+/-”	35%	33.86±0.962	429.57±5.588	853.14±20.767
		“+/+”	55%	33.55±0.966	441.91±5.234	911.45±20.348
Sex	genotype	frequency	birth weight	Six week body weight	nine week body weight	
AA	♂	“-/-”	18.92%	37.43±1.251	1638.43±59.920	2465.71±68.139
		“+/-”	35.14%	38.00±0.641	1619.15±51.489	2433.31±60.437
		“+/+”	45.95%	37.41±0.659	1570.94±35.827	2293.00±42.566
	♀	“-/-”	24%	37.33±0.882	1381.17±16.298	2013.67±67.940
		“+/-”	28%	38.14±1.455	1301.86±73.926	1797.43±83.109
		“+/+”	48%	36.58±0.499	1414.50±56.888	2008.00±85.077

weight

means significant difference at P<0.05 in the same column with different superscripts

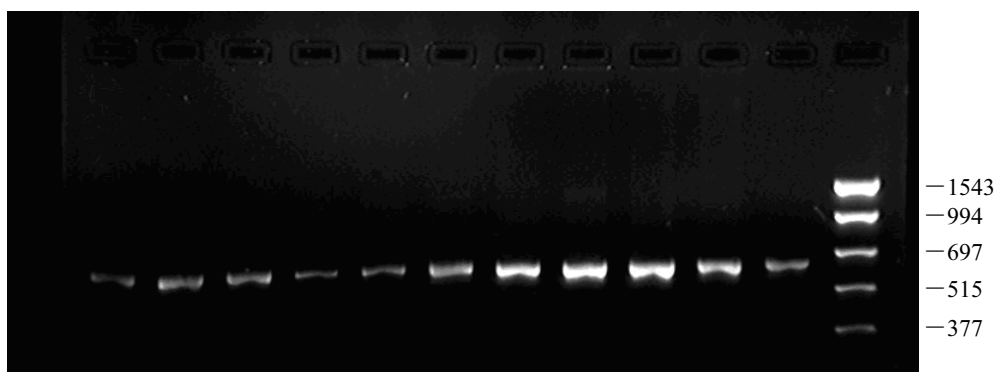


Figure 1. IGF-I gene regulatory region PCR products M: pBR322 DNA/Pst I

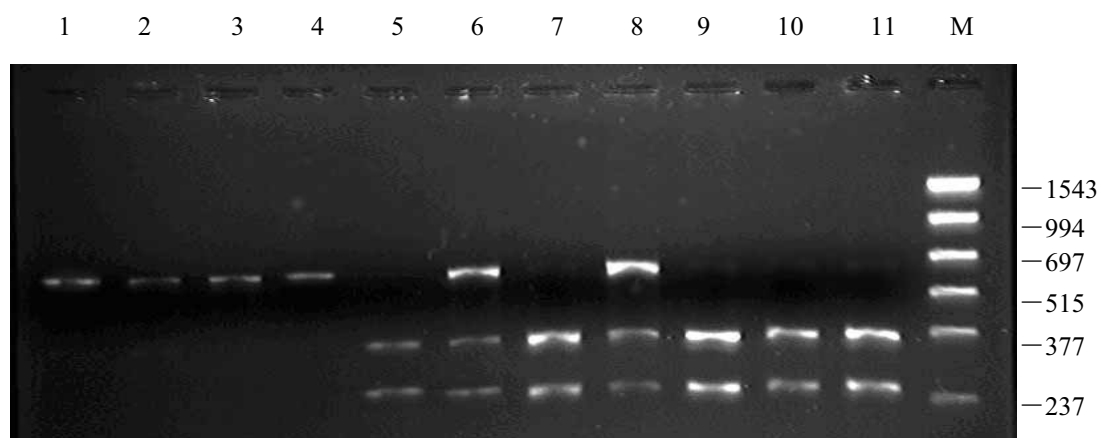


Figure 2. IGF-I gene PCR-RFLP results 5,7,9,10,11: +/+; 6,8: +/-; 1,2,3,4: -/-; M: PCR DNA Markers



Bioinformatics of NS3 Gene and Inverted Terminal repeats (ITR) of *Bombyx Mori* Parvo-like Virus (China Zhenjiang Isolate)

Chen Sun

Institute of Life Sciences, Jiangsu University
301 Xuefu Road, Zhenjiang 212013, China
E-mail: boystrong001@163.com

Qin Yao (Corresponding author)

Institute of Life Sciences, Jiangsu University
301 Xuefu Road, Zhenjiang 212013, China
Tel: 86-511-879-1923 E-mail: yaoqin@ujs.edu.cn

Huijuan Yin

Institute of Life Sciences, Jiangsu University
301 Xuefu Road, Zhenjiang 212013, China

Yuanqing He

Institute of Life Sciences, Jiangsu University
301 Xuefu Road, Zhenjiang 212013, P. R. China
E-mail: yqhe@ujs.edu.cn

Keping Chen

Institute of Life Sciences, Jiangsu University
301 Xuefu Road, Zhenjiang 212013, China
E-mail: kpchen@ujs.edu.cn

The research is financed by the National Natural Science Foundation of China (30871826), China National "863" Project (No. 2008AA10Z145) and grants from Jiangsu Sci-Tech Support Project – Agriculture (No. BE2008379).

Abstract

Bombyx mori Parvo-like virus (China Zhenjiang isolate) had termed as *BmDNV-Z*. NS3 is one of the three nonstructural proteins that is responsible for the replication of virus DNA. To explore the nature of NS3 and determine how it differs from other NS3 sequence, we extracted amino acid sequences of NS3 from four sequenced DNV genomes, and carried out sequence-based phylogenetic and structural analyses. In addition, to investigate the importance of the ITR as a signal for some viral and /or cellular factors further, we performed a computer analysis for prediction of secondary structure. We found that Comparisons of protein sequence with those of the databases showed low homologies with NS-3 of JcDNV (30% identity), GmDNV (26% identity), MIDNV (26% identity). But zinc-finger motifs appear to be conserved greatly. Further the structural importance of the terminal sequence (CTS) common to VD1 and VD2 was also predicted by a DNA folding web.

Keywords: *BmDNV-Z*, NS3, Bioinformatics, ITR

1. Introduction

The family Parvoviridae includes two subfamilies: the Parvovirinae, members of which infect vertebrates, and the Densovirinae, members of which infect invertebrates (Berns 1990). Similar to other parvoviruses, densoviruses (DNVs) are small, nonenveloped particles of 18–26 nm diameter. Each virion contains two 4–6.5 kb single-stranded complementary DNA molecules, which are termed plus and minus strands, respectively. These strands will anneal when it is extracted in buffers under high salt concentrations. DNVs can infect a wide range of insect tissues and lead to death of the host in most cases; however, they cannot infect tissues of vertebrates, thus making them potential biological agents for controlling main agricultural pests (El-Far, Li et al. 2004).

Six DNV isolates have been obtained from silkworm and these six isolates are classified into two groups designated as Bombyx DNV type I and II (*BmDNV* I and *BmDNV* II) on the basis of their serological characteristics and genome structure (Lü 1998). *BmDNV* I, such as Ina isolate, has a monosense genome of a little over 5 kb. *BmDNV* II (Saku isolate, Yamanashi isolate and China isolate *BmDNV*-Z), has two sets of genome (VD1 VD2) which are enveloped in different virions, respectively (Tijssen P 1995). Both DNAs of *BmDNV* II have imperfect inverted terminal repeats, i.e. 270 nts for VD1 and about 530 nts for VD2, surprisingly; both are unable to form terminal hairpins. These unusual properties imply a unique replication mechanism different from the rolling circle replication of other densoviruses or vertebrate parvovirus. Furthermore, the genome of *BmDNV* II is able to encode DNA polymerase itself (Bando, Kusuda et al. 1987; Bando, Kusuda et al. 1987; Bando, Choi et al. 1992; Bando, Hayakawa et al. 1995).

The terminal sequences of these viral genomes are believed to be important for specific interactions between the viral genome and the viral RNA polymerase and/or contribute to the encapsidation of the genome by the nucleocapsid protein. Furthermore, this structural feature has been observed in single stranded DNA virus, parvovirus, though the significance of the structure is still obscure. It must be noted here that all of parvovirus genomes which have been reported so far contain a terminal palindromic sequence of 50 to 70 nucleotides which play important roles during replication. However, the terminal palindrome could not be found in VD1 and 2.

Our groups had completed the genome analysis of *BmDNV*-Z in 2005 (Genbank Accession Number: DQ017268; DQ017269). Sequence analysis showed that VD1 genome consisted of 6,543 nts and VD2 genome consisted of 6,022 nts (Wang, Yao et al. 2007). However, effects of the gene and replication mechanisms are still unclear. In this study, we collected amino acid sequences from five DNV genomes, followed by systematical analysis at three different levels with the GENEDOC and MEGA tools, including their overall phylogeny, domain structures, and identifiable motifs. After that, we predicted the secondary structure of ITR by (<http://frontend.bioinfo.rpi.edu/applications/mfold/cgi-bin/dna-form1.cgi>). The aim of this study is to infer the features and evolution of the NS3 of densoviruses using a phylogenetic approach, to provide information that could render some insights regarding NS3 and ITR functions during viral DNA replication.

2. Materials and methods

2.1 Protein sequence and Phylogenetics analysis

We used Inter Proscan (<http://www.ebi.ac.uk/InterProScan/index.html>) to analysis amino acid sequence. GENEDOC tool was also used to align amino acid sequence of NS3 from five DNV. We used the deduced amino acid sequences to reconstruct phylogenetic trees. The trees were constructed by using the neighbor-joining method (NJ) with JTT distances. The reliability of internal branches was assessed by using 1,000 bootstrap replicates, and sites with gaps were ignored in this analysis. NJ searches were conducted by using the computer program MEGA3.

2.2 Secondary structural analysis of ITR

We predicted the secondary structure of ITR by:

(<http://frontend.bioinfo.rpi.edu/applications/mfold/cgi-bin/dna-form1.cgi>.)

3. Results

3.1 Characterization of ORF2

ORF2 was found to span from nt 4761 to nt 5429, and the coding sequence of NS3 consisted of 222 aa residues starting at the ATG initiation codon at position 4761 and ending at the TAA stop codon at position 5429. This sequence presents some interesting features including two zinc-finger motifs [C:(X)2:C:X3:C (aa 152 to 173) and C:(X)2:C:H:X:C (aa 198 to 214)], six putative N glycosylation sites (NWSK/NRTT/NLST/NDSN/NNSN/NDSN, aa 74 to 77, 100 to 103, 130 to 133, 137 to 140, 164 to 167 and 219 to 222), and four putative phosphorylation site SvFD, TypD, SteE, SinD (aa 68 to 71, 103 to 106, 132 to 135 and 217 to 220). Comparisons of this sequence with those of the databases showed low homologies with NS-3 of MIDNV (26% identity), GmDNV (26% identity) and *Diatraea saccharalis* DNV (26% identity) (Fig. 1). Curiously, the DsDNV NS3 and *BmDNV*-Z NS3 sequence is truncated of the 34 C-terminal amino acid sequence common to NS3 of JcDNV, MIDNV, and GmDNV. No further significant homologies could be detected with NS polypeptides of Densovirinae and Parvovirinae or with any protein of the data banks.

3.2 Phylogenetic analysis

To analyse the NS3 evolution in virus, we tried several methods (neighbor-joining, minimum evolution, and maximum parsimony) to assess the phylogeny of NS3 and achieved similar results. Based on the phylogenetic analysis, GmDNV, JcDNV and MIDNV, clustered together, indicating a common origin. However, *BmDNV-Z* also showed a low of relatedness to other. These results suggested a possible different origin for NS3.

3.3 Secondary structural analysis of ITR

Assuming that both virus DNAs (VD1 and 2) are necessary to complete replication of *BmDNV-Z*, it is not difficult to explain that VD1 and 2 share a common terminal sequence of 53 nucleotides(CTS)[Bando 1992], since all of the segmented genomic DNAs must contain the signals for recognition by a replication and /or for encapsidation by the viral componets. To investigate the importance of the CTS as a signal for some viral and /or cellular factors further, we performed a computer analysis for prediction of secondary structure (<http://frontend.bioinfo.rpi.edu/applications/mfold/cgi-bin/dna-form1.cgi>.) Figure 3 shows the predicted structure of the terminal 150 nucleotides of VD1 and VD2 as their most stable secondary form. In the predicted structure (Fig. 3), CTS seems to be divided into 4 structural domains, A, B, C, and D. The structural importance of CTS was emphasized by the predicted localization of a Sp1-binding consensus motif as an exposed element on the stem-loop constituted by C and D. Moreover, D containing a Sp1-binding consensus motif also fold into a stem structure with a sequence out of the CTS which contains another Sp1-binding consensus motif, and the stem structure was also conserved in both VD1 and VD2

4. Discussion

The high level of sequence conservation of NS3 protein among the members of the Densovirus (Fig. 1) suggests that the biological function(s) of this protein is essential for the accomplishment of their life cycle. Zinc-finger motifs indicated the involvement of NS3 in the viral DNA replication. Our results constitute a first step toward the understanding of NS3 function(s) during the *BmDNV-Z* life cycle. However, the precise level at which this polypeptide acts and its specific biological function(s) remain to be elucidated. The lack of significant homology between the NS3 amino acid sequence and proteins of the data banks, including NS proteins of parvoviruses, implies that its function is either specific to this type of virus, i.e., of the genus *Bidensovirus*, or that it is somehow related to function(s) of the host cell necessary for their replication. At present, it is not possible to decide in favor of one of these hypotheses, which are not exclusive of one another. These differences might reflect specific requirements for cellular proteins functioning in partnership with NS and (or) VP proteins in order to achieve the viral replicative cycle, as has been recently demonstrated for vertebrate parvoviruses.

The representative of the genus *Iteravirus*, *BmDNV-1*, which lacks NS3, shares with the members of the genus *Densovirus* the property of having as natural hosts exclusively lepidopteran insects. His genome was only 5 kb in length, with J-shaped ITRs of 230bp. Moreover, the NS and VP genes were located on the same strand, as in the vertebrate parvoviruses. VP was located downstream of the NS ORF(Li, Zadori et al. 2001). *BmDNV-Z* VD1 genome consisted of 6 543 nt, including inverted terminal repeats (ITRs) of 224 nt. In the viral genome, three open-reading frames (NS ORF and VP) in the plus strand and one major ORF (ORF4) codes for DNA polymerases in the complementary strand were identified(Wang, Yao et al. 2007). The essential difference between *BmDNV-1* and *BmDNV-Z* VD1 at the genome level lies in ORF4 DNA polymerases. Computer analysis suggests that VD2 has not enough information to produce progeny virions by itself. So we predicted *BmDNV-Z* VD1 might have diverged from *BmDNV-1* and it obtained DNA polymerases from host cell during further evolution. VD2 come from other parvo-like maybe help infection and replication of VD1, while VD1 can provide necessary nonstructural proteins and VP proteins. Whether the *BmDNV-Z* is the mixture of two parvo-like viruses or a virus with a multipartite genome need further identification.

References

- Bando, H., H. Choi, et al. (1992). Structural analysis on the single-stranded genomic DNAs of the virus newly isolated from silkworm: the DNA molecules share a common terminal sequence. *Arch Virol*, 124(1-2): 187-93.
- Bando, H., T. Hayakawa, et al. (1995). "Analysis of the genetic information of a DNA segment of a new virus from silkworm. *Arch Virol* 140(6): 1147-55.
- Bando, H., J. Kusuda, et al. (1987). Organization and nucleotide sequence of a densovirus genome imply a host-dependent evolution of the parvoviruses. *J Virol*, 61(2): 553-60.
- Bando, H., J. Kusuda, et al. (1987). Molecular cloning and characterization of Bombyx densovirus genomic DNA. Brief report. *Arch Virol* 93(1-2): 139-46.
- Berns KI. (1990). Parvoviridae and their replication. *Virology*, Volume 2. New York: Raven Press, pp.1743–1763.
- El-Far, M., Y. Li, et al. (2004). Lack of infection of vertebrate cells by the densovirus from the maize worm *Mythimna loreyi* (MIDNV). *Virus Res*, 99(1): 17-24.

Lü, H. (1998). Molecule Biology of Insect Virus, *China Agriculture Science and Technology Publishing Company Press*.

Li, Y., Z. Zadori, et al. (2001). Genome organization of the densovirus from *Bombyx mori* (BmDNV-1) and enzyme activity of its capsid. *J Gen Virol* 82(Pt 11): 2821-5.

Tijssen P, B. M. (1995). Densonucleosis Viruses Constitute an increasingsy diversified subfamily among the parvoviruses. *Virology* 6: 347-355.

Wang, Y. J., Q. Yao, et al. (2007). Characterization of the genome structure of *Bombyx mori* densovirus (China isolate). *Virus Genes* 35(1): 103-8.

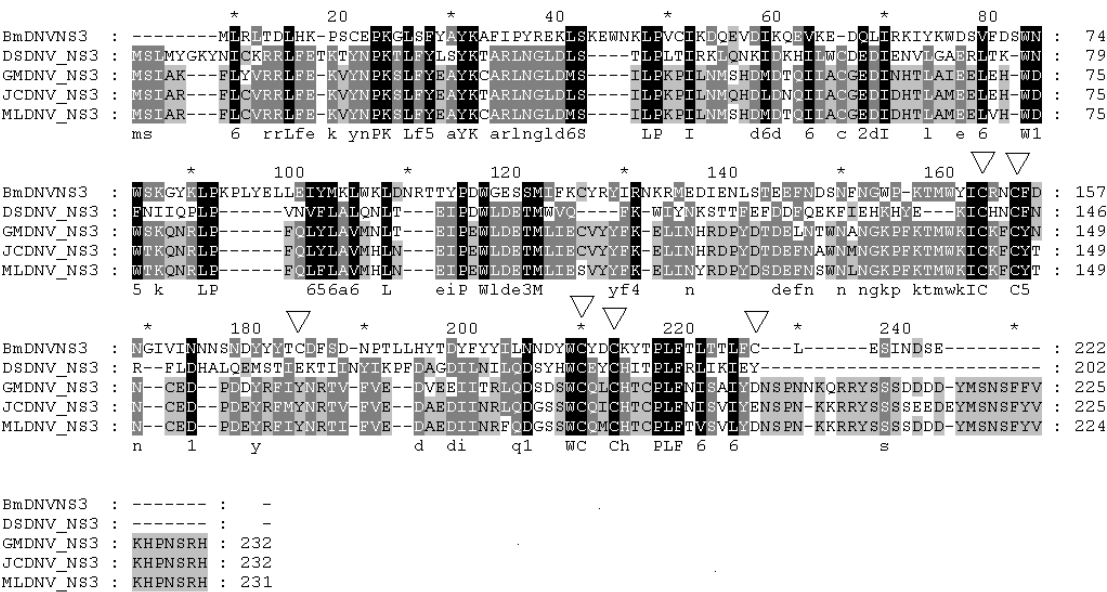


Figure 1. Alignment of amino acid sequence of NS3 from five DNV by using the Gene doc program Amino acid numbers begin with the start codon. Identical amino acids among the NS3s are marked by asterisks (*). Putative zinc-finger motifs are marked by ▽. Abbreviations: BmDNV-Z(GenBank accession number DQ017269), *Bombyx mori* densovirus (China isolate); JcDNV(GenBank accession number NP_694826), *Junonia coenia* densovirus; GmDNV (GenBank accession number NC_004286), *Galleria mellonella* densovirus; And DsDNV (GenBank accession number NC_001899), *Diatraea saccharalis* densovirus; MIDNV(GenBank accession number NP_958098), *Mythimna loreyi* densovirus

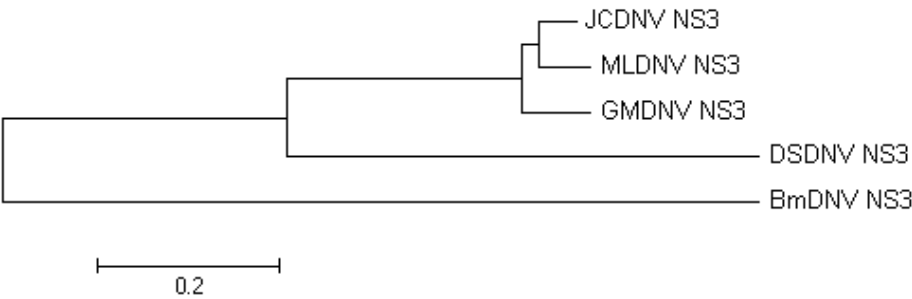


Figure 2. Phylogenetic relationship of the NS3 groups. Numbers in bootstrap consensus tree indicated degree of confidence. Sequences above are from GenBank

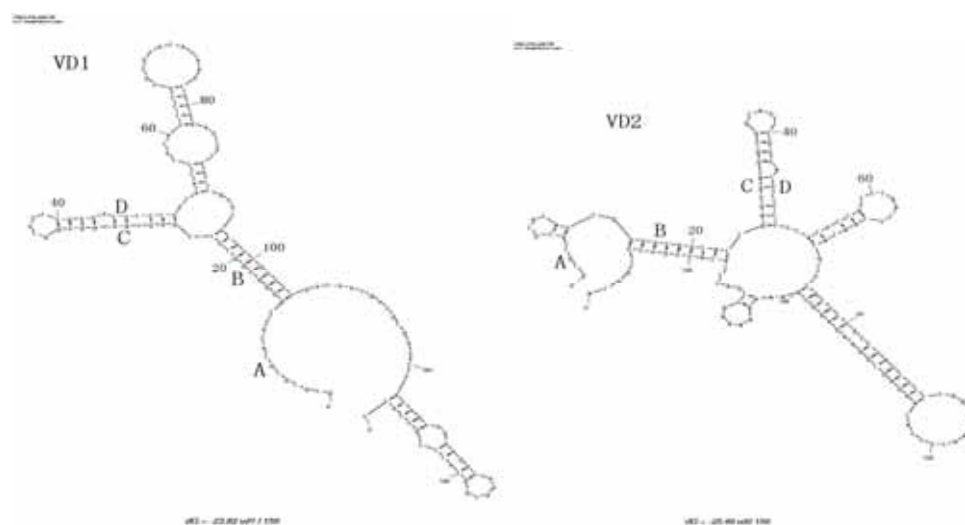


Figure 3. Predicted secondary structure of the terminal regions of VD1 and VD2.

A journal archived in Library and Archives Canada

A journal indexed in Canadiana

A journal indexed in AMICUS

A journal included in Ulrich's

A journal indexed in Google Scholar

A journal indexed in Genamics JournalSeek

A journal indexed in DOAJ

A journal included in PKP Open Archives Harvester

International Journal of Biology

Semiannual

Publisher Canadian Center of Science and Education

Address 4915 Bathurst St. Unit # 209-309, Toronto, ON. M2R 1X9

Telephone 1-416-208-4027

Fax 1-416-208-4028

E-mail ijb@ccsenet.org

Website www.ccsenet.org

Printer William Printing Inc.

Price CAD.\$ 20.00

